PNNL-24200
53451-RPT21, Rev. 0

Pacific Northwest
NATIONAL LABORATORY
Proudly Operated by Battelle Since 1965

Evaluation of Settler Tank Thermal Stability during Solidification and Disposition to ERDF

DE Stephenson
CH Delegard
AJ Schmidt

March 2015

U.S. DEPARTMENT OF ENERGY

Prepared for the U.S. Department of Energy
under Contract DE-AC05-76RL01830

DISCLAIMER

PACIFIC NORTHWEST NATIONAL LABORATORY
operated by
BATTELLE
for the
UNITED STATES DEPARTMENT OF ENERGY
under Contract DE-AC05-76RL01830

Printed in the United States of America

Available to DOE and DOE contractors from the
Office of Scientific and Technical Information,
P.O. Box 62, Oak Ridge, TN 37831-0062;
ph: (865) 576-8401
fax: (865) 576-5728
email: reports@adonis.osti.gov

Available to the public from the National Technical Information Service,
U.S. Department of Commerce, 5285 Port Royal Rd., Springfield, VA 22161
ph: (800) 553-6847
fax: (703) 605-6900
email: orders@ntis.fedworld.gov
online ordering: http://www.ntis.gov/ordering.htm


This document was printed on recycled paper.
(9/2003)

Evaluation of Settler Tank Thermal Stability during Solidification and Disposition to ERDF

DE Stephenson
CH Delegard
AJ Schmidt

March 2015

Prepared for the U.S. Department of Energy
Under Contract DE-AC05-76RL01830

Pacific Northwest National Laboratory
Richland, Washington 99352

Revision History

Rev. #	Effective Date	Description of Change
0	March 2015	Initial issue.

Executive Summary

This report presents an analysis of the thermal stability of the contents of the settler tanks during planned grouting through the subsequent handling and packaging operations for disposition of the settler tanks to the Environmental Restoration Disposal Facility (ERDF).

Background

Ten 16-foot-long and 20-inch diameter horizontal tanks currently reside in a stacked 2×5 (high) array in the ~20,000-gallon water-filled Weasel Pit of the 105-KW Fuel Storage Basin on the US-DOE Hanford Site. These ten tanks are part of the Integrated Water Treatment System used to manage water quality in the KW Basin and are called "settler" tanks because of their application in removing particles from the KW Basin waters. Based on process knowledge, the settler tanks are estimated to contain about 124 kilograms of finely divided uranium metal, 22 kg of uranium dioxide, and another 55 kg of other radioactive sludge. The Sludge Treatment Project (STP), managed by CH2MHill Plateau Remediation Company (CHPRC) is charged with managing the settler tanks and arranging for their ultimate disposal by burial in ERDF.

The presence of finely divided uranium metal in the sludge is of concern because of the potential for thermal runaway reaction of the uranium metal with water and the formation of flammable hydrogen gas as a product of the uranium-water reaction. Thermal runaway can be instigated by external heating.

The STP commissioned a formal Decision Support Board (DSB) to consider options and provide recommendations to manage and dispose of the settler tanks and their contents. Decision criteria included consideration of the project schedule and longer-term deactivation, decontamination, decommissioning, and demolition (D4) of the KW Basin. The DSB compared the alternatives and recommended *in-situ* grouting, size-reduction, and ERDF disposal as the best of six candidate options for settler tank treatment and disposal.

It is important to note that most grouts contain a complement of Portland cement as the binding agent and that Portland cement curing reactions generate heat. Therefore, concern is raised that the grouting of the settler tank contents may produce heating sufficient to instigate thermal runaway reactions in the contained uranium metal sludge.

Report Summary

The STP engaged the Pacific Northwest National Laboratory (PNNL) to evaluate the chemical and physical outcomes of the grouting and disposal operations based on its experience in analyzing K Basin sludge and characterizing the reactions occurring in the sludge, particularly the reactions between water and the contained uranium metal and the reactions of uranium metal in various grouts.

The following report describes the settler tank sludge genesis, quantities, and expected properties and analyzes the longitudinal distribution of the sludge within the ten settler tanks based on the radiological surveys conducted by the STP. The settler tank and Weasel Pit configurations are described and the decision-making process by the STP and DSB for settler tank disposition briefly outlined. Results of

laboratory testing at PNNL and elsewhere, which show that grouting has practically no impact on the rates of uranium metal corrosion compared with the rates in water alone, are summarized. Prior Hanford Site process experience in grouting uranium metal chips and fines from fuel fabrication operations also is described.

The general composition of the K East Discharge Chute grout, which includes Portland Type I/II cement, Class F fly ash, and water (as well as rheological modifiers and anti-washout additives), is examined as an appropriate formulation for use in the settler tanks based on its previous use and the commonality of data quality objectives established for its development (i.e., good flow properties, low heat generation rate, sufficient set strength to allow its size-reduction without undue crumbing). The thermodynamics and kinetics of Portland cement and fly ash hydration reactions (setting or curing) then are examined to help forecast heat generation rates as functions of reaction temperature and time.

With inputs established for geometry (settler tanks, uranium metal particle size and depth, and waste box dimensions), heat sources (e.g., uranium metal reaction and decay heat, grout hydration, and solar heating), and physical properties, heat transport finite element analyses were applied to evaluate the thermal stability of various process steps associated with the solidification and subsequent handling of the settler tank material. For the modeling assessment, thermal instability was defined/declared when the temperature in the uranium-rich sludge bed exceeded 100 °C. At this temperature, water vapor voids form in the sludge, drastically diminishing thermal conductivity, while uranium metal reaction with water continues unabated, thus engendering thermal runaway conditions. Key observations and recommendations from the modeling are summarized below.

Underwater grouting of the settler tanks. The first step in the D4 sequence is to fill the settler tanks with grout and then allow the grout to cure for a minimum of about 28 days. Grouting is done while the settler tank array is submerged in pool water, which has historically been maintained at less than 20 °C. The pool water conducts and convects heat from grout curing within the settler tanks and also provides a substantial heat sink.

- The Weasel Pit water provides a heat sink sufficient to allow simultaneous grouting of all settler tanks. *Basis: An adiabatic calculation showed that the simultaneous grouting and instantaneous curing of all 10 settler tanks and 100% reaction of the contained uranium metal would raise the temperature of the water within the Weasel Pit by only 5.5 °C.*

- The 2-dimensional model set up to examine thermal stability of grouting of the settler tanks ran cases at the greatest depth of sludge (a depth of 2.3 cm in Tank 5 of the South array, or tank S-5.)

- With the temperature of the settler tank wall equal to the water temperature, the grouting operation is thermally stable at all reasonable water/basin pool temperatures [i.e., pool temperature 79 °C (174 °F) or less] and at a uranium metal reaction rate multiplier of 3×.
    - Confirmation of model validity: Under adiabatic conditions (i.e., heat rejection at the settler tank wall arbitrarily set to zero), temperature instability in the sludge layer will be reached in less than 8 h due to heat of hydration from grout curing, leading to the uranium metal reaction runaway. This simulation verified correct model functioning and underscored the importance of the surrounding water as a heat sink.

- The baseline thermal conductivity of uranium metal particles in water (fuel piece sludge) is set at 3.9 W/(m·K) in the Sludge Databook (Johnson 2014). However, if the thermal conductivity of the sludge layer is degraded by an order of magnitude (postulated reduction from worst-case gas bubble retention with particle bed dry-out), thermal instability could be encountered at basin pool temperatures of >40 °C (104 °F) at a reaction rate enhancement factor of 3× or if the sludge depth inside the worst-case settler tank is doubled.

Behavior of post-grouted settler tank array during Weasel Pit D4 activities. After grouting the settler tanks (and after nominal 28-day cure time), debris on the Weasel Pit floor *may* be encapsulated by pouring a 6- to 14-inch-thick layer of grout.

- If the grout is poured to a depth of 14 inches (to encapsulate debris on the pit floor), the bottom 2 inches of settler tanks N-5 and S-5 (which are separated from the pit floor by a distance of 12 inches) will be bathed in grout. The resulting grout curing heat will cause thermal instability in the bottom two settler tanks, N-5 and S-5.
- If grout is poured to a depth of 6 inches, allowing 6 inches of water between the top of the grout pour and bottom of tanks N-5 and S-5, thermal instability is highly unlikely when including the heat convention term for the pool water.
- To summarize, if grout is used to encapsulate the Weasel Pit floor, controls should be implemented to keep the top of the pour well below the bottom two settler tanks.

Draining of the KW pool and backfilling the Weasel Pit with dry/wet Sand (5 days). The KW Basin will be emptied of water, the tanks will be briefly exposed to air, and the settler tanks will be covered with a backfill material. While covered, the settler tanks will be sectioned by a mechanical shear, and the sections will be lifted out and loaded into waste disposal boxes. The STP project estimates that draining, backfill, shearing, and removal of the sections will be completed in 4-days' time. Backfill materials that were considered included a controlled-density fill (a low-strength grout), dry sand, and wet sand. For modeling, PNNL examined a 5-day window of thermal stability for this work evolution.

- A series of simulations of the settler tanks exposed to boundary condition of convective cooling with air at a constant temperature was performed to examine stability behavior after pool water drainage, or while awaiting load-in into a waste box. The convective heat transport was evaluated with heat transfer coefficients of 7.9 and 3 $W/m^2 \cdot K$, which are typical for the steel in air at low flow (10 $W/m^2 \cdot K$) to free convection (5 $W/m^2 \cdot K$). Under these conditions, with a uranium reaction rate multiplier of 1× and the baseline sludge thermal conductivity (3.9 W/m·K), thermal stability is maintained if the air temperature is <46 °C (115 °F). At a reaction rate multiplier of 3×, thermal instability can be incurred at air temperatures > 29 °C (84 °F).

- Controlled-density fill (CDF) is a self-compacting cementitious material. Because of the heat of hydration associated with cement constituents and the inability to reject sufficient heat from the grouted settler tanks, use of CDF in not recommended.

- The thermal conductivity of dry sand may be as low as 0.13 W/(m·K); consequently, dry sand can serve as a thermal insulator. In this case, the settler tank array will be thermally unstable within 5 days if the initial dry sand temperature exceeds 44 °C (111 °F).
- The thermal conductivity of water-saturated sand (~1.3 W/m·K) is an order of magnitude higher than that of dry sand. Increasing the conductivity and heat capacity by addition of water leads to stability of 56 °C (133 °F) at 1× and 39 °C (102 °F) at 3× uranium reaction rate multipliers, respectively, for a five-day period.

In summary, it is recommended that the dewatering, backfilling, shearing, and waste box loading operations be scheduled for the cooler months of the year because of the limited ability to reject heat from grouted settler tanks after the KW basin is drained of water. Exposure to warm air or warm dry sand must be avoided. Wet or damp sand is recommended for the backfill material. If exposure to warm air cannot be avoided, active cooling with sprinklers should be considered.

Waste Disposal Box. After sectioning, segments of the settler tank will be loaded into waste disposal boxes for transport to and disposal at ERDF. In consultation with ERDF staff, STP estimated that the time between box loading at KW and box burial at ERDF will be on the order of 30 days. For most modeling of the waste box thermal stability, the worst-case 1.25 ft long section from tube S5 was considered. However, a final case was developed to model a 4.25 ft long section at the worst-case uranium loading.

- Based on consultation with STP staff and after evaluation of a number of alternatives, the following configuration is suggested to provide long-term and robust thermal stability.
    - Box: Size: 4(L) × 6(W) × 4 (H) ft steel box, painted white to maximize solar reflectance.
    - Internals: Lower half of box should be fitted with ~20-inch to 21-inch inside-diameter heavy-wall carbon steel half-pipe that is 1 to 2 inches in wall thickness and 3.25 to 5 ft long to act as a cradle, heat conductor, and particularly as a heat sink. The 1-in wall thickness is sufficient to maintain thermal stability of the worst-case sludge depth at a 1× uranium reaction rate multiplier. A 2-inch cradle thickness will provide additional margin for a 3× uranium reaction rate multiplier.
    - The half-pipe and its support structure should be embedded in high-thermal-conductivity grout [thermal conductivity ≥ 1.0 W/(m·K)] to extend the heat sink and to provide shielding from radioactivity. The high-thermal-conductivity grout will be added to depth of 2 feet. The waste box, with half-pipe and high-thermal-conductivity grout, should be made up well in advance of use to allow the grout a cure time of 28 days or more and thus dissipate the curing heat.
    - To provide good thermal connectivity between settler tank section and half-pipe, a non-curing thermal conductivity paste/grease should be placed on the half-pipe before the settler tank section is lowered into place. As the section is lowered, the paste will fill gaps between the half-pipe and tank section. The thermal conductivity of the paste/grease must be ≥0.67 W/(m·K). Thermal stability was examined with a paste thickness of up to 1/4 inch.

  - After the settler tank section is in place, the upper half of the disposal box should be filled with cool, dry sand. The sand will provide shielding and insulate the settler section from solar heating while the box is awaiting burial at ERDF.
  - For this configuration to be effective, the settler tanks must be marked such that they are oriented in the box with the uranium sludge layer on the bottom of the tank and in contact with the heat sink. Such alignment should be readily observed because of the presence of strengthening ribs on the bottom length of the settler tanks.

- Concern exists about whether the shapes of the sheared settler tank sections with stiffening ribs can be made to conform to the half-pipe contours and thus guarantee the requisite maximum tolerable ¼-inch gap. Tolerance in thermal stability for a gap size wider than ¼ inch with a higher-thermal-conductivity paste (e.g., greater than 1 W/m·K) may be possible. However, additional modeling would be required to determine the sensitivity among the other critical parameters (including thickness of cradle, reaction rates, etc.).
- At the baseline uranium metal reaction rate (1×), simulations with initial outside ambient and interior temperatures of 50 °C (122 °F) show that with the recommended waste disposal box configuration thermal stability will be maintained for a 4.25 ft worst-case section with a 1-inch-thick cradle, during severe top and side solar heating. This configuration remains stable even with an air gap of $^{1}/_{16}$ inch between the tank and half-pipe.
- At a rate multiplier of 3× and a 2-inch-thick cradle, thermal stability is maintained for the worst-case 1.25-ft section with initial outside ambient and interior temperatures of 50 °C (122 °F). However, with a 4.25-ft section and solar heating from the top, thermal stability was not demonstrated, even with 4-inch-thick cradle and 1/8-inch gap.

In conclusion, the suggested waste box configuration is sufficiently robust to handle to a 4.25-ft settler tank section loaded with uranium metal at the maximum depth estimated for a single location with a conservative treatment of solar heating. However, when additional conservatism was stacked on (e.g., reaction rate multiplier of 3×), thermal stability was not shown when the length of tube section was increased from 1.25 to 4.25 ft. Additional modeling would be required to better determine the stability envelope of a setter tank section with the 3× rate multiplier.

Acknowledgements

The authors would like to acknowledge Mike E. Johnson and Mike Davis of CH2MHill Plateau Remediation Company for their technical and programmatic support and contributions to this effort.

Acronyms and Abbreviations

ALARA	as-low-as-reasonably-achievable
BNFL	British Nuclear Fuels Limited
CDF	controlled-density fill
CHPRC	CH2M Hill Plateau Remediation Company
CFR	Code of Federal Regulations
D4	deactivation, decontamination, decommissioning, and demolition
DSB	Decision Support Board
ECRTS	Engineered Container Retrieval and Transfer System
ERDF	Environmental Restoration Disposal Facility
ETB	Engineer Tool Box
FEA	finite element analysis
H	height
IWTS	Integrated Water Treatment System
J	joule
K	kelvin (unit of absolute temperature measurement)
KOP	Knock-Out Pot
KE	K East
KW	K West
L	length
m	meter
MCO	multi-canister overpack
NAFEMS	International Association for the Engineering Modelling, Analysis and Simulation Community (founded as the National Agency for Finite Element Methods and Standards)
OPC	ordinary Portland cement
PC	Portland cement
PDE	partial differential equation
PIGCO	Pacific International Grout Company
PNNL	Pacific Northwest National Laboratory
PSI	pounds per square inch
QA	quality assurance
STP	Sludge Treatment Project
W	width or watt, depending on context
WAC	Waste Acceptance Criteria or Washington (State) Administrative Code, depending on context

Contents

Executive Summary iv
Acronyms and Abbreviations xi
1.0 Introduction 1.1
2.0 Settler Tank Sludge 2.1
2.1 Description of Material Within the Settler Tanks 2.1
2.2 Axial Distribution of Uranium Within the Settler Tanks 2.6
3.0 Settler Tank and Weasel Pit Configuration 3.1
4.0 Management and Disposition of the Settler Tanks 4.1
5.0 Prior Hanford Experience in Grouting Uranium Metal 5.1
6.0 Portland Cement Grout Formulations 6.1
7.0 Portland Cement Thermodynamics 7.1
8.0 Modeling of Thermal Behavior of Settler Sludge 8.1
8.1 Approach 8.1
8.1.1 COMSOL Model 8.1
8.1.2 COMSOL QA Approach 8.1
8.1.3 Overview of Cases 8.2
8.2 Model Input Parameters 8.3
8.2.1 Heat Sources 8.3
8.2.2 Geometry of Settler Tanks, Weasel Pit, and Disposal Boxes 8.6
8.2.3 Values for Physical Properties Used for Modeling 8.7
8.3 Modeling Results 8.11
8.3.1 Underwater Grouting of Highest U-Content Tank Section (Case 1) 8.11
8.3.2 Grouted Settler Tanks Backfilled with Sand (Case 2) 8.15
8.3.3 Grouted Settler Tank Underwater + 14 Inches of Grout Added to Floor of Weasel Pit (Case 3) 8.18
8.3.4 Grouted Settler Tank Underwater + 6 Inches of Grout Added to Floor of Weasel Pit (Case 4) 8.21
8.3.5 Settler Tank Section in IP2 Waste Box (Case 5) 8.24
8.3.6 Settler Tank Section in 4-ft × 6-ft × 4-ft Box with Carbon Steel Cradle Surrounded by Sand (Case 6) 8.27
8.3.7 Settler Tank Section in 4-ft × 6-ft × 4-ft box with Carbon Steel Cradle Embedded in High-Conductivity Grout, with Top Filled with Sand (Case 7) 8.30
8.3.8 Settler Tank Section in Box with Cradle Embedded in High-Conductivity Grout, Top Filled with Sand, with Solar Heating and Convective and Radiative Cooling (Case 8) 8.35

8.3.9 Case 9 is Case 1 with Substitution of Convective Cooling for the Constant-Temperature Boundary Conditions with Long-Term Grout Heat Generation Being Used 8.41
8.3.10 Longer Settler Tank Section (4.25 ft) in Box (Case 10) 8.44
9.0 Conclusions and Recommendations 9.1
10.0 References 10.1
Appendix A 10.1
Appendix B 10.1

Figures

2.1. Particles Found in the KOPs 2.3
2.2. Estimate of Settler Tank Dry Non-Uranium Sludge Mass 2.4
2.3. Uranium-Bearing Sludge Depth Profile in the South Settler Tanks 2.9
2.4. Uranium-Bearing Sludge Depth Profile in the North Settler Tanks 2.9
3.1. IWTS Settler Tank Array 3.1
3.2. Settler Tank Array Layout in the KW Basin Weasel Pit, End and Side Views 3.2
5.1. Uranium Metal Corrosion Rate Data in Liquid Water and in BNFL Portland Cement Grouts and PNNL Portland Cement and Magnesium Phosphate Grouts 5.1
5.2. Fines and Chips Mixing with Masonry Cement and Casting into 27-Liter Steel Billet Cans 5.3
5.3. Masonry Cement Castings of Uranium Machining Chips and Fines after First Auto-Ignition Incident, August 1977 ..... 5.4
5.4. Temperature Curves for Test Castings That Underwent Thermal Runaway. 5.5
6.1. Some of the Grout Mixtures Tested and the Mix Ultimately Used in the KE Discharge Chute Grouting, PIGCO C25 ..... 6.3
6.2. Analysis of Mojave Class F Fly Ash, April 2004 ..... 6.4
6.3. KE Discharge Chute Grout Pour Card 6.6
7.1. Nominal Portland Cement Hydration Heat Generation Rates 7.1
7.2. Type I and Type II Portland Cement Hydration Enthalpies 7.2
7.3. Specific Power of Curing Portland Cement at 20-21°C as a Function of Time 7.3
7.4. Arrhenius Plots of Specific Powers of Portland Cements 7.4
7.5. Volumetric Grout Heat Generation Rates as Functions of Time and Temperature 7.6
8.1. Two Dimensional Cross Section (2-D) of a Tank Modeled in Comsol Multiphysics 8.11
8.2. 2D Cross Section of Grouted Tank Seven Hours After Initial Grouting with Adiabatic Tank Wall Boundaries 8.13
8.3. Maximum Uranium Sludge Temperature in Centigrade Plotted versus Time for Adiabatic Boundary Conditions 8.13
8.4. 2D Cross Section of Grouted Tank 72 Hours After Initial Grouting with Tank Wall Boundary Set to 25° C 8.14
8.5. Maximum Uranium Sludge Temperature in Centigrade Plotted versus Time with Tank Wall Boundary Set to 25° C 8.14
8.6. Sensitivity of Thermal Stability of Grouted Tank as a Function of Sludge Thermal Conductivity, Rate Multiplier and Sludge Depth 8.15
8.7. Weasel Pit Temperature Prediction After Five Days from Backfilling with Dry Sand 8.17
8.8 Maximum Temperature in Centigrade of the Uranium Sludge for the Dry Sand versus Time in Seconds 8.17
8.9. Maximum Temperature in Centigrade of the Uranium Sludge for the Wet Sand Plotted versus Time in Seconds 8.18

8.10. 2D Cross Section of the Weasel Pit That Shows the 10 Tanks Plus the 14 Inches of Grout 8.19
8.11. Weasel Pit with 14 Inches of Grout and Constant Temperature Wall Boundary Conditions at a 1X Uranium Sludge Heating Rate 8.20
8.12. Weasel Pit Maxium Uranium Sludge Temperature versus Time for the Constant Temperature Boundary Conditions with 1X Uranium Sludge Heating 8.20
8.13. 2D Cross Section of the Weasel Pit That Shows the 10 Tanks Plus the 6 Inches of Grout 8.21
8.14. Weasel Pit with 6 Inches of Grout and Constant Temperature Wall Boundary Conditions at a 1X Uranium Sludge Heating Rate After 416 days 8.22
8.15. Weasel Pit Maxium Uranium Sludge Temperature versus Time for the Constant Temperature Boundary Conditions with 1X Uranium Sludge Reaction Rate 8.23
8.16. Weasel Pit Maxium Uranium Sludge Temperature versus Time for the Adiabatic Boundary Conditions with 1X Uranium Sludge Heating 8.24
8.17. Moist Sand-Filled IP2 Box with Uranium Sludge Reacting at 1× Rate and Constant-Temperature Boundary Conditions 8.25
8.18. IP2 Waste Box with 1X Uranium Sludge Reacting Rate with Dry Sand Surrounding the Tank Section 8.26
8.19. Maximum Temperature Profile of the Uranium Sludge Over Time for the Dry Sand 1X Uranium Rate Case 8.27
8.20. Settler Tank Section Fitted into a Steel Cradle with Some Thermally Conductive Paste in Between, with the Waste Box Filled by Dry Sand 8.28
8.21. 1 Inch Cradle Thickness with 1/8th Inch Paste Thickness at 1× Uranium Reaction Rate 8.29
8.22. Maximum Uranium Sludge Temperature with Time for 1 Inch Cradle Thickness with 1/8th Inch Paste Thickness at 1× Uranium Reaction Rate 8.30
8.23. Tank Section Fitted Into a Steel Cradle with Some Thermally Conductive Paste In Between, with Bottom Half of Box Filled with Grout and Top Half Filled with Dry Sand 8.31
8.24. 3× Uranium Sludge Rate with 1/8th Inch Thermally Conductivity Paste with 1 Inch of Cradle Thickness 8.32
8.25. Maximum Sludge Temperature with Time for 3× Uranium Sludge Rate with 1/8th Inch Thermally Conductivity Paste with 1 Inch of Cradle Thickness 8.33
8.26. Temperature Profile for ½ Inch Cradle Thickness with 1/8th Inch Gap Filled with Air at 1× Uranium Sludge Rate 8.34
8.27. Uranium Temperature with Time for ½ Inch Cradle Thickness with 1/8th Inch Gap Filled with Air at 1× Uranium Sludge Rate 8.34
8.28. Settler Tank Section with 2 Inch Cradle Thickness with Solar Radiation and Convective and Radiative Cooling at Steady State without Uranium Reactions 8.36
8.29. Temperature Profile of Waste Box with Solar Heating 8.37
8.30. Maximum Sludge Temperature and Maximum Waste Box Temperature with Time 8.38
8.31. Isosurface Plot of Waste Box After Temperature Dependent Heating is Turned On 8.38
8.32. Temperature Profile of Waste Box with Solar Heating Before Uranium Sludge Heating 8.39
8.33. Maximum Sludge Temperature (blue line) and Maximum Waste Box Temperature with Time. 8.40
8.34. Isosurface Plot of Waste Box with Solar Heating After Uranium Sludge Heating 8.40

8.35. Sensitivity of Thermal Stability of Grouted Tube as a Function of Sludge Thermal Conductivity, Rate Multiplier and Sludge Depth for Case 9, with Heat Transfer Coefficient of 7.9 W/(m^2×K) 8.42
8.36. Sensitivity of Thermal Stability of Grouted Tube as a Function of Sludge Thermal Conductivity, Rate Multiplier and Sludge Depth for Case 9, with Heat Transfer Coefficient of 3 W/(m^2×K) 8.42
8.37. 2D Cross Section of Grouted Tube 30 Days After Removal From Weasel Pit with Convective Tube Boundaries 8.43
8.38. Maximum Uranium Sludge Temperature in Centigrade Plotted versus Time for Convective Boundary Conditions After Removal From Weasel Pit 8.44
8.39. Temperature Profile for 4.25 ft Section with 1-Inch Cradle Thickness and 1/4th Inch Gap Filled with Paste at 1X Uranium Sludge Rate 8.45
8.40. Isosurface Plot of Waste Box with Solar Heating After Uranium Sludge Heating 8.46
8.41. Maximum Sludge Temperature in Centigrade and Maximum IP2 Box Temperature With Time for 4.25 ft Section. 8.47
8.42. Maximum Sludge Temperature and Maximum IP2 Box Temperature With Time. 8.48
8.43. Temperature Profile of IP2 Box With Solar Heating From Top and the Right Side. 8.49
8.44. Isosurface Temperature Profile of Box With Solar Heating 50% From Top and 50% From Side. 8.50
8.45. Maximum Sludge Temperature and Maximum IP2 Box Temperature With Time for Waste Box With 50% Top and 50% Side Heating. 8.51
8.46. Isosurface Temperature Profile of Waste Box With Solar Heating 100% From Top and 50% From Side. 8.52

Tables

2.1. Settler Tank Sludge Quantities 2.5
2.2. Dose Rates at the Settler Tank Bottoms (taken from Tables 1 and 2 of Landsman 2014) 2.6
2.3. Dose-Rate Pro-Rated Uranium-Bearing Sludge Inventories in Settler Tank Segments 2.7
2.4. Uranium-Bearing Sludge Maximum Depths in Settler Tank Segments 2.8
8.1. Overview of Cases Modeled 8.2
8.2. Parameters for Development of Heat Source Term from Uranium Metal 8.4
8.3. Component Dimensions used in Modeling 8.6
8.4. Depth of Uranium Metal Sludge in Settler Tanks 8.7
8.5 Thermal Conductivity, Density, and Specific Heat Values for Modeling 8.8
8.6. Calculation of KE Discharge Chute Grout Specific Heat by the Sum-of-Fractions Method 8.10
8.7. Option and Properties of Thermally Conductive Pastes 8.11
8.8. Thermal Properties of Sand Used for Backfill 8.16

1.0 Introduction

Ten 16-foot-long and 20-inch-diameter horizontal tanks currently reside in a stacked 2×5 (high) array in the ~20,000-gallon water-filled Weasel Pit of the 105-KW Fuel Storage Basin on the US-DOE Hanford Site. These ten tanks are part of the Integrated Water Treatment System (IWTS) used to manage water quality in the KW Basin and are called "settler" tanks because of their application in removing particles from the KW Basin waters. Based on process knowledge, the settler tanks are estimated to contain about 124 kilograms of finely divided (i.e., less than 600-µm) uranium metal, 22 kg of uranium dioxide, and another 55 kg of other radioactive sludge.

The presence of finely divided uranium metal in the sludge is of concern because of the potential for thermal runaway reactions of the uranium metal with water and the formation of flammable hydrogen gas as a product of the uranium-water reaction. The thermal runaway reactions can be instigated by heating. In an untreated/unstabilized form, the settler sludge could be considered pyrophoric.

The Sludge Treatment Project (STP) manages the settler tanks for the US DOE and commissioned a formal Decision Support Board (DSB) to consider options and provide recommendations to manage and dispose of the settler tanks and their contents. Decision criteria included worker and public safety, and consideration of the project schedule and longer-term deactivation, decontamination, decommissioning, and demolition (D4) of the KW Basin. The DSB compared the alternatives and recommended *in-situ* grouting, size-reduction, and burial in the Hanford Site Environmental Restoration Disposal Facility (ERDF) as the best of six candidate options for settler tank treatment and disposal. In Section 4.3.5 of the ERDF Waste Acceptance Criteria, (Casbon 2014), the following type wastes are prohibited from disposal (*partial listing*):

- Ignitable or reactive dangerous waste unless treated prior to disposal such that the resultant mixture no longer exhibits the ignitable or reactive characteristic, except for waste disposed of as a labpack in accordance with Washington Administrative Code (WAC) 173-303-161. (40 CFR 264.312)
- Incompatible wastes or materials shall not be placed in close proximity to each other in the same landfill cell unless such action is done in a manner that prevents adverse reactions that could result in generation of extreme heat, flames, violent reactions, gases, toxic fumes, dusts, or gases; pose a fire or explosion risk; damage the structural integrity of the facility; or through other like means threaten human health or the environment. (40 CFR 264.313)
- Pyrophoric waste, unless treated, prepared, and packaged to be nonflammable prior to being disposed. (10 CFR 61.56)

In consideration of these prohibitions the STP engaged the Pacific Northwest National Laboratory (PNNL) to evaluate the chemical and physical outcomes of the settler tank grouting and packaging options that would result in thermally stable configurations. This engagement is based on PNNL's experience in analyzing K Basin sludge and characterizing the reactions occurring in the sludge, particularly the reactions between water and the contained uranium metal and the reactions of uranium metal with water in various grouts.

The following report describes the settler tank sludge genesis, quantities, and expected properties and analyzes the longitudinal distribution of the sludge within the ten settler tanks based on the radiological surveys conducted by the STP. The settler tank and Weasel Pit configurations are described and the decision-making process by the STP and DSB for settler tank disposition briefly outlined. Results of laboratory testing at PNNL and elsewhere, which show that grouting has practically no impact on the rates of uranium metal corrosion compared with the rates in water alone, are summarized. Prior Hanford Site process experience in grouting uranium metal chips and fines from fuel fabrication operations also is described. It is important to note that most grouts contain a complement of Portland cement as the binding agent and that Portland cement curing reactions generate heat. Therefore, concern is raised that the grouting of the settler tank contents may produce heating sufficient to instigate thermal runaway reactions in the contained uranium metal sludge.

The general composition of the K East Discharge Chute grout, which includes Portland Type I/II cement, Class F fly ash, and water (as well as rheological modifiers and anti-washout additives), is examined as an appropriate formulation for use in the settler tanks based on its previous use and the commonality of data quality objectives established for its development (i.e., good flow properties, low heat generation rate, sufficient set strength to allow its size-reduction without undue crumbing). The thermodynamics and kinetics of Portland cement and fly ash hydration reactions (setting or curing) then are examined to help forecast heat generation rates as functions of reaction temperature and time.

With inputs established for geometry (settler tanks, uranium metal particle size and depth, and waste box dimensions), heat sources (e.g., uranium metal reaction, radiolytic decay heat, and grout hydration reactions), and physical properties, heat transport finite element analyses were applied to evaluate the thermal stability of various process steps associated with the solidification and subsequent handling of the settler tank material. For the modeling assessment, thermal instability was defined and declared when the temperature in the uranium-rich sludge bed exceeded 100 °C (i.e., the onset of thermal runaway). A finite element model, which includes analysis, solver, and simulation, was used to perform the thermal modeling.

The thermal modeling examined the thermal stability of the following steps, in the following order, in the D4 process for the KW Settler tanks:

- Grouting of the worst-case (from a reactivity perspective) settler tank cross section during the grout curing period.
- Grouted settler tank array in air and while covered with fill material in the Weasel Pit.
- Grouted settler tank sections while loaded into waste disposal boxes.

Conservative modeling input values and boundary conditions were used to generate models that were robust and reasonably bounding. Both nominal and safety basis parameter values from the Sludge Databook (Johnston 2014) were evaluated. Results from the modeling are presented in Section 8.0 and Appendix A and summarized in the Executive Summary.

2.0 Settler Tank Sludge

This section describes the settler tank sludge genesis, quantities, and expected properties and analyzes the longitudinal distribution of the sludge within the ten settler tanks based on the radiological surveys conducted by the STP.

2.1 Description of Material Within the Settler Tanks

The settler tanks are part of the Integrated Water Treatment System or IWTS in the 105-KW Fuel Storage Basin (KW Basin) and are located in the Weasel Pit of the KW Basin. During previous fuel washing and packaging operations, water from the KW Basin was routed through screens to remove irradiated metallic uranium particles larger than 0.25 inch in diameter. These >0.25-inch particles were considered to be fuel. The material that passed the 0.25-inch screens was directed to Knock-Out Pots (KOPs) and 600-µm or 500-µm strainers. The <0.25-inch but >600- or 500-µm particles that were removed by the KOPs and strainers are referred to as KOP material. The water that contained the <600- or <500-µm particles that passed the strainers then was routed through the settler tanks. Because the 20-inch-diameter settler tanks markedly decreased velocity compared with the 1.5-inch-diameter input transfer lines, the larger and denser solids (e.g., uranium metal and uranium oxide) collected in the settler tanks by sedimentation. The clarified decanted water then was routed from the settler tanks through garnet and sand filters before return to the KW Basin.

The ten settler tanks collected about 3.5 m^3 of the <600- or <500-µm settler sludge during the KW Basin fuel washing and packaging operations. In 2010, after the fuel handling operations were completed, about 99.7% of the settler tank contents were transferred into the engineered container SCS-CON-230. However, 5.9 liters of sludge remained in the settler tanks as judged by borescope inspection (Leshikar 2010). The sludge in SCS-CON-230 was sampled and analyzed (Johnson 2014; Shimskey et al. 2013). The mean results for these analyses show a settled density of 2.0 kg/liter, 22 g uranium metal/liter, and 610 g total uranium/liter (i.e., 610 – 22 = 588 g uranium, as oxide, per liter as derived from Tables 4-1, 4-4, and 4-3, respectively, of Johnson 2014). Other major sludge components include aluminum (33 g/liter), iron (73 g/liter), silicon (98 g/liter), and 73 volume% water (Tables 4-38 and 4-2, respectively, of Johnson 2014). Given the settled sludge density and the interstitial water concentration, there are (2.0 – 0.73 =) 1.27 kg of solids per liter of sludge or 7.49 kg of solids total in the 5.9 liters of residual sludge in the settler tanks. Based on the uranium concentration analyses, the 5.9 liters of sludge contains 0.13 kg of uranium metal and 3.47 kg of uranium as oxide (i.e., 3.94 kg UO_2, the most likely uranium oxide). Therefore, there are (7.49 – 0.13 – 3.94 =) 3.42 kg of non-uranium solids (dry basis) in the residual sludge within the settler tanks from the KW Basin fuel packaging operations. These solids likely are comprised largely of aluminum hydroxide, $Al(OH)_3$, ferric hydroxide, $Fe(OH)_3$, and silica sand, SiO_2.

In 2011, the irradiated uranium metal particle material that had been gathered in the KOPs and strainer baskets from fuel washing operations underwent a density separation process and ensuing size-reduction process in the “KOP Pretreatment” campaign. Aluminum metal wires from the canisters,

aluminum hydroxide nodules, and Grafoil®[1], which had been present in the original KOP materials (see Figure 2.1), were removed by hydrodynamic methods (i.e., elutriation). The aluminum wire and much of the aluminum hydroxide and Grafoil were collected for discard, based on radiometric assay, as low-activity waste. After 600-µm screening, uranium metal fines, uranium oxide, some aluminum hydroxide and Grafoil, but no aluminum metal, were dispatched to the settler tanks (Sloughter 2011). The dry mass of solids in these materials was estimated to total 122.8 kg with 62.6 kg present as uranium metal particles, 13.2 kg as the uranium oxide UO_2, and 47.0 kg as non-uranium aluminum hydroxide and Grafoil (Table 6-3 of Sloughter 2011). The non-uranium solids as settled sludge from KOP Pretreatment occupy 42.99 liters (on a dry basis) and have a combined particle density of 1.88 g/mL (Table 4-2 of Sloughter 2011). If the interstitial water volume (void fraction) is 0.4 of the total (as assumed for sludge; Table 5-1 of Sloughter 2013), the settled non-uranium sludge density is 1.37 g/mL.[2]

[1] Grafoil® is a registered trademark of GrafTech International Holdings Inc., Lakewood, Ohio.

[2] The solids in 47 kg of non-uranium sludge occupy (47 kg/(1.88 kg/liter) =) 25 liters. Based on 0.4 void (water) volume in settled sludge, the density of the settled non-uranium sludge is:

$$\frac{47 \text{ kg solids} + 0.4 \times 25 \text{ liters} \times 1.0 \text{ kg } H_2O/\text{liter}}{25 \text{ liters solids} + (0.4/0.6) \times 25 \text{ liters } H_2O} = 1.37 \text{ kg/liter}$$

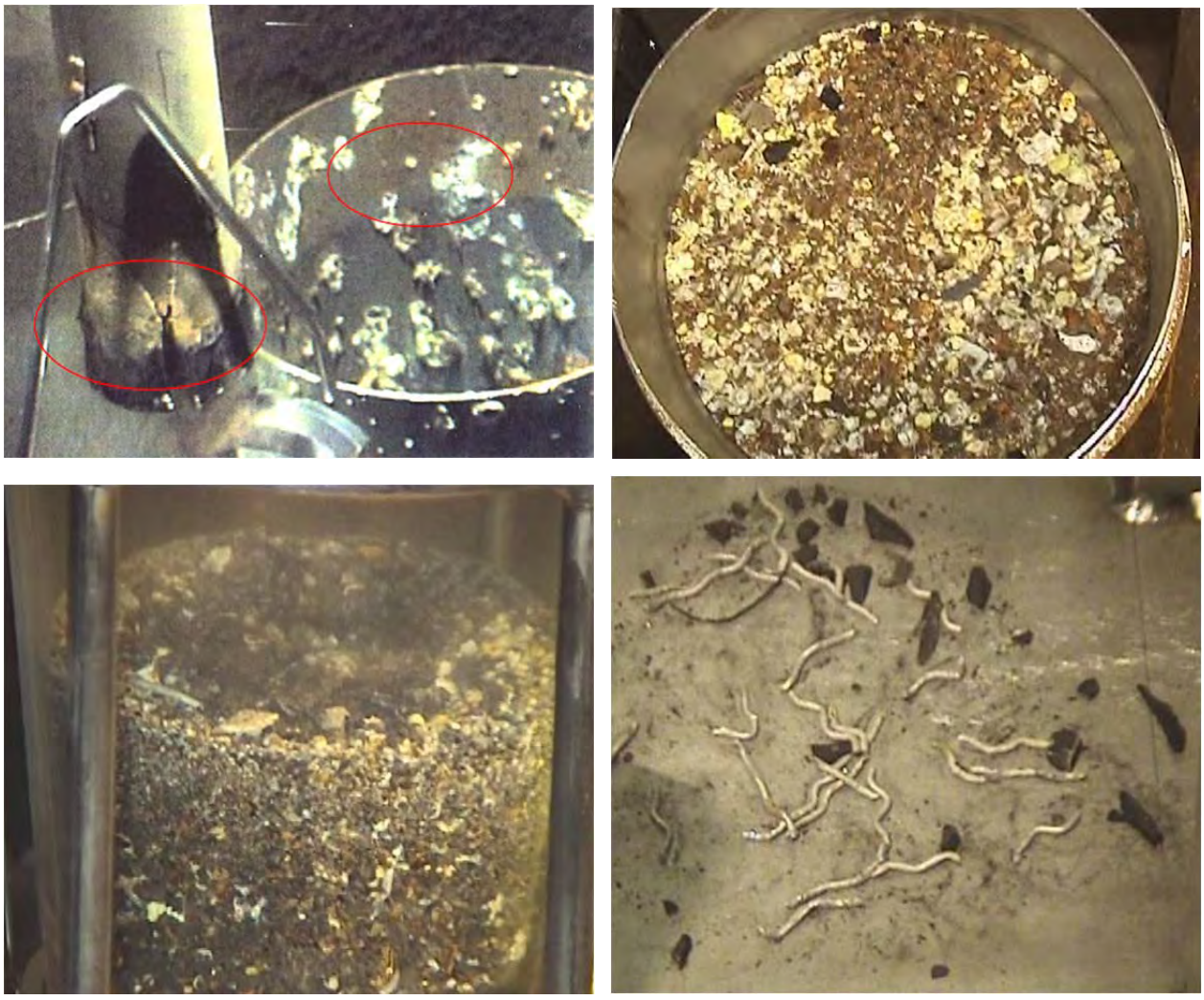

Figure 2.1. Particles Found in the KOPs (Sloughter and Pottmeyer 2013)

Top left – $Al(OH)_3$ nodules on fuel and aluminum canisters
Top right – white and yellow-tinted particles of $Al(OH)_3$
Bottom left – Grafoil flakes
Bottom right – aluminum wires (up to 1.25 inches long and 0.0625 inch or ~1.6 mm diameter) broken from fuel canisters, and black irradiated uranium metal particles

The KOP contents underwent further processing in 2012 to remove additional materials that were not uranium metal. Under these "KOP Processing" operations, the remaining material was further refined. The resulting largely metallic uranium particles larger than 600-µm that had been present in the KOPs were loaded into specially designed multi-canister overpack (MCO) basket inserts constructed of copper to facilitate heat removal. The baskets were loaded into MCOs and the MCO contents dried under cold vacuum in the Cold Vacuum Drying Facility and shipped for storage at the Canister Storage Building in the 200 East Area (Sloughter 2013). During KOP Processing, additional fine (<600-µm) material was removed from the KOPs during underwater operations and dispatched to the settler tanks by use of the IWTS. In this operation, the KOP contents were placed in a thin layer on a 600-µm screened surface and the material agitated by water jets. The <600-µm material that passed through the screen was collected in

the IWTS and directed to the settler tanks. The mass of uranium metal particles going to the settler tanks is estimated to be 61.2 kg with a further estimated 5.5 kg as UO_2 (Tables 5-3 and 6-1 of Sloughter 2013). Although no explicit estimate of the quantity of (dry) non-uranium aluminum hydroxide and Grafoil was provided by Sloughter (2013), the quantity, 4.4 kg, can be derived based on values provided in Tables 5-3 and 6-1 of Sloughter (2013) as shown in Figure 2.2.

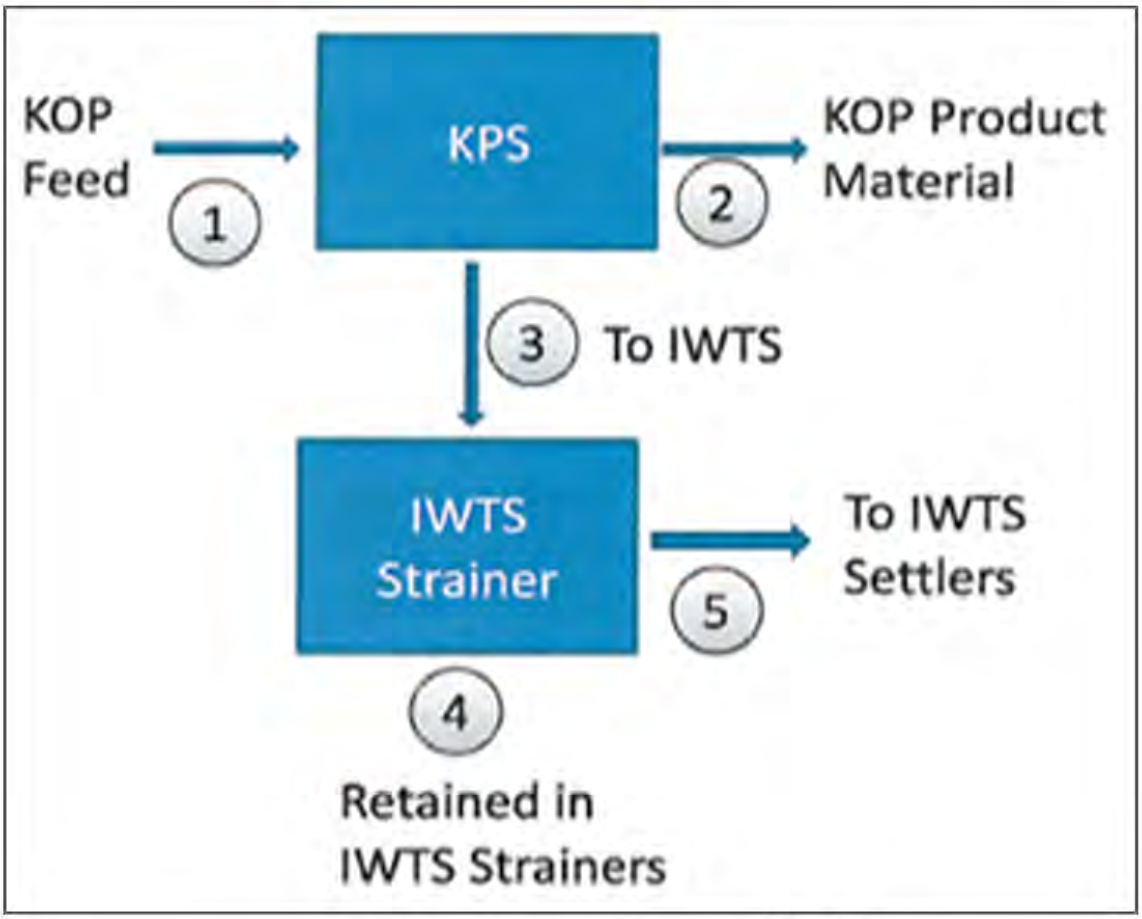

	Mass, kg			
	Total	**U_{metal}**	**UO_2**	**Non-Uranium**
Data Source (Sloughter 2013)	Table 6-1	Table 6-1	Table 5-3	= Total - U_{metal} - UO_2
KOP Feed - Stream 1	519.5	470.8	7.4	41.3
KOP Product - Stream 2	423.4	388.1	0.6	34.7
Retained in IWTS Strainers - Stream 4	25.0	21.5	1.3	2.2
Data Source	Calculation: Stream 5 = Stream 1 - Stream 2 - Stream 4			
To IWTS Settlers - Stream 5	71.1	61.2	5.5	4.4

Figure 2.2. Estimate of Settler Tank Dry Non-Uranium Sludge Mass (based on Sloughter 2013)

The settler tanks thus contain materials from three sources – the residual material from incomplete transfer of KW Basin fuel washing sludge to the engineered container SCS-CON-230 in 2010, solids washed from KOP uranium metal fragments in the KOP Pretreatment operations in 2011, and solids

washed from KOP fragments in KOP Processing operations in 2012. The total quantity of <600-µm uranium metal particles from these sources is (0.13 + 62.6 + 61.2 =) 123.9 kg. The three streams also contain (3.47 + 13.2 + 5.5 =) 22.2 kg of UO_2 and (3.42 + 47.0 + 4.4 =) 54.8 kg of non-uranium solids such as aluminum hydroxide and Grafoil.

Based on a bulk density for uranium metal particles of 8.0 kg uranium/liter (Section 5.2 of Landsman 2014; see also Section 5.1 of Sexton 2011 which pertains to KOP material), the bulk volume of the uranium metal particles is 15.5 liters. If the 22.2 kg of UO_2 is added to the uranium metal and the uranium within the UO_2 credited as uranium metal to calculate the total volume (as was done by Landsman 2014; see Section 5.2.1), the amount of additional uranium present as oxide would be (22.2 × 0.8815 =) 19.6 kg, the total uranium would be (123.9 + 19.6 =) 143.5 kg, and the total volume of the uranium metal (plus UO_2) bed would be 17.9 liters at 8.0 kg U/liter density. However, a more conservative concentration of the uranium within the uranium metal and UO_2 bed is 9.2 g/cm^3 (within a sludge bulk density of 9.6 g/cm^3) based on the practical limit achieved in the final processing of KOP materials (Table 4.1 of Sloughter 2013). The uranium metal plus UO_2 bed volume thus is [143.5 kg U/(9.2 kg U/liter) =] 15.6 liters.

By density and settling rates, it is anticipated that the uranium-bearing materials, dominated by the uranium metal, would lie at the bottom of the settler tanks. The dense uranium phases would be present with 54.8 kg, dry basis, of less-dense and slower-settling non-uranium $Al(OH)_3$ and Grafoil particles plus likely trace amounts of SiO_2 and $Fe(OH)_3$ from the initial settler tank heel that pre-existed the KOP Pretreatment and Processing operations. Based on the settled density of the non-uranium sludge of 1.37 kg/L (shown in Footnote 2, above), 40 liters of non-uranium sludge are present in the settler tanks and this sludge likely overlies the denser uranium-bearing sludge but also is present further downstream in the settler tanks because of its slower settling rate. The mass and volume inventories of the sludge constituents in the settler tanks are summarized in Table 2.1.

Table 2.1. Settler Tank Sludge Quantities

Sludge Component	Mass, kg	Volume, L	Bulk Density, kg/L
Uranium metal	123.9	15.6	9.6
Uranium oxide as UO_2	22.2		
Non-uranium[(a)]	54.8	40.0	1.37

[(a)] Non-uranium includes Grafoil, $Al(OH)_3$, and traces of iron oxides and sand.

Based on the 600-µm upper particle size cut-off and postulated smoothly diminishing size distribution below this threshold, the Sauter mean diameter of the uranium metal in the settler tank material is estimated to be 450 µm (radius = 0.0225 cm), i.e., 3/4 that of the largest particle (pages B-20,21, Schmidt and Sexton 2009). Assuming spherical (or, equally, cubic) particle shape, the specific surface area of the KOP fines is 7.02 cm^2/g U metal.[(3)] Thus, the overall surface area of the 123.9 kg of settler tank uranium metal (density = 19.0 g/cm^3) is 8.70×10^5 cm^2.

[(3)] For spherical <600-µm KOP fines,

$$\text{Specific Surface Area} = \frac{4\times\pi\times(0.0225\text{ cm})^2}{\frac{4}{3}\times\pi\times(0.0225\text{ cm})^3\times19.0\text{ g/cm}^3} = 7.02\text{ cm}^2/\text{g}\ .$$

2.2 Axial Distribution of Uranium Within the Settler Tanks

The distribution of the uranium-bearing sludge within the settler tanks has been estimated based on systematic gamma dose rate measurements of the settler tanks (Landsman 2014). Six dose rate measurements were made along the lengths of each settler tank at the tank bottoms. Dose rate measurements at the floor below the tanks, in the Weasel Pit as background, and in the inlet tank also were made. The measurements were more closely spaced at the entry end of the tanks in anticipation that more of the dense uranium would be located near these entry points. The south bank of settler tanks was measured 24 September 2014 and the north bank on 7 October 2014.

It was assumed that the amount of uranium-bearing sludge in each settler tank is proportional to the total dose rate in that tank, pro-rated by the total dose rates measured for all 60 tank positions (10 tanks × 6 positions per tank). The background dose rates were found to be negligible compared with the dose rates at the settler tank bottoms and, therefore, were neglected. Thus, amounts of uranium-bearing materials within each segment were determined by their segment dose rates divided by the total dose rate for the 60 measurements taken for all ten tanks.

The 60 dose rate results for the settler tanks are shown in Table 2.2. The positions are measured from the entrance points. The dose rates had to be corrected at the B position for the South tanks because of unanticipated structural dunnage (Landsman 2014). The dose rates shown in Table 2.2 provide the corrected position B values.

Table 2.2. Dose Rates at the Settler Tank Bottoms (taken from Tables 1 and 2 of Landsman 2014)

South Tanks							
Position[(a)]	**A**	**B**	**C**	**D**	**E**	**F**	**Sum**
Distance, feet	1.5	2.5	4.0	4.5	8.0	14.0	
Tank	**Dose Rate, R/h**						
S1	66.0	12.0	25.0	29.0	7.6	5.4	145.0
S2	79.0	22.0	12.0	20.0	6.5	5.0	144.5
S3	65.0	27.0	11.0	13.0	6.0	1.6	123.6
S4	11.0	37.0	11.0	12.0	5.5	4.9	81.4
S5	47.0	72.0	1.0	8.0	8.0	5.1	141.1
North Tanks							
Position	**G**	**H**	**I**	**J**	**K**	**L**	**Sum**
Distance, feet	1.5	4.0	5.0	8.0	9.0	12.0	
Tank	**Dose Rate, R/h**						
N1	34.2	24.3	14.6	8.3	6.5	6.4	94.3
N2	20.5	4.5	10.3	7.2	5.8	5.3	53.6
N3	13.1	8.0	8.0	5.3	5.1	4.5	44.0
N4	15.7	9.3	7.6	4.8	4.7	4.2	46.3
N5	10.6	11.3	7.2	5.5	5.0	4.5	44.1

[(a)] Position from settler tank entrance.

According to Section 5.2.1 of Landsman (2014), the total uranium present in the settler tanks is 123.8 kg as metal and 18 kg as UO_2 (i.e., 15.87 kg of contained uranium). These values are only slightly different than those provided by better, later estimates (123.9 kg uranium metal and 22.2 kg UO_2) as

shown in Table 2.1. The Landsman (2014) values, used in the following calculations of uranium distribution for consistency, showed 123.8 + 15.87 = 139.67 kg of total uranium in the settler tanks. At an assumed uranium concentration within the sludge of 9.2 kg/liter, the total volume of dense uranium-bearing sludge in the ten settler tanks is 15.18 liters. Based on the working assumption that the uranium distribution throughout the tanks is proportional to the measured gross dose rates (Section 2.1.1 of Landsman 2014), the volumetric sludge allocation for each of the measured segments is shown in Table 2.3. This allocation assumes that the tank segments at the ends are bounded by the ends of the tanks (i.e., for positions A, F, G, and L) and by their neighboring segments at the midpoints between the adjacent measurement positions.

Table 2.3. Dose-Rate Pro-Rated Uranium-Bearing Sludge Inventories in Settler Tank Segments

South Tanks							
Position	**A**	**B**	**C**	**D**	**E**	**F**	**Sum**
Distance	0-2.0	2.0-3.25	3.25-4.25	4.25-6.25	6.25-11.0	11.0-16.0	
Length, feet	2.00	1.25	1.00	2.00	4.75	5.00	
Tank	**Inventory at Position, liters**						
S1	1.092	0.198	0.413	0.480	0.126	0.089	2.398
S2	1.307	0.364	0.198	0.331	0.108	0.083	2.391
S3	1.075	0.447	0.182	0.215	0.099	0.026	2.044
S4	0.182	0.612	0.182	0.198	0.091	0.081	1.346
S5	0.777	1.191	0.017	0.132	0.132	0.084	2.333
						Sum South Tanks	10.512
North Tanks							
Position	**G**	**H**	**I**	**J**	**K**	**L**	**Sum**
Distance	0-2.75	2.75-4.5	4.5-6.5	6.5-8.5	8.5-10.5	10.5-16.0	
Length, feet	2.75	1.75	2.00	2.00	2.00	5.50	
Tank	**Inventory at Position, liters**						
N1	0.566	0.402	0.241	0.137	0.108	0.106	1.560
N2	0.339	0.074	0.170	0.119	0.096	0.088	0.886
N3	0.217	0.132	0.132	0.088	0.084	0.074	0.727
N4	0.260	0.154	0.126	0.079	0.078	0.069	0.766
N5	0.175	0.187	0.119	0.091	0.083	0.074	0.729
						Sum North Tanks	4.670
						Sum	15.182

The depth of the dense uranium-bearing sludge within each segment was estimated assuming that the sludge volume within each segment (from Table 2.3) lay flat at the bottom of the 50.27-cm (19.79-inch; DOE 2000) maximum diameter settler tank over the entire length of the particular segment. The maximum depths are shown in Table 2.4 and the depth profiles for the South and North banks of tanks plotted in Figure 2.3 and Figure 2.4, respectively. The maximum depth of the uranium-bearing sludge, 2.235 cm, is found in the B segment of tank S5. What this depth appears like in profile is shown in the Figure 2.3 inset. The non-uranium sludge containing primarily $Al(OH)_3$ and Grafoil totals ~40 liters and is expected to overlie but also be somewhat downstream of the much denser uranium-bearing sludge based on settling characteristics of the less dense material.

Table 2.4. Uranium-Bearing Sludge Maximum Depths in Settler Tank Segments

South Tanks						
Tank	**A**	**B**	**C**	**D**	**E**	**F**
Distance	0-2.0	2.0-3.25	3.25-4.25	4.25-6.25	6.25-11.0	11.0-16.0
Length, feet	2.00	1.25	1.00	2.00	4.75	5.00
Tank	**Depth at Position, cm**					
S1	1.547	0.686	1.271	0.888	0.183	0.136
S2	1.746	1.004	0.790	0.704	0.162	0.128
S3	1.530	1.149	0.748	0.530	0.153	0.061
S4	0.472	1.433	0.748	0.501	0.143	0.126
S5	1.218	2.235	0.128	0.373	0.191	0.130
North Tanks						
Position	**G**	**H**	**I**	**J**	**K**	**L**
Distance	0-2.75	2.75-4.5	4.5-6.5	6.5-8.5	8.5-10.5	10.5-16.0
Length, feet	2.75	1.75	2.00	2.00	2.00	5.50
Tank	**Depth at Position, cm**					
N1	0.986	1.071	0.892	0.384	0.162	0.154
N2	0.716	0.345	0.718	0.345	0.149	0.134
N3	0.533	0.524	0.610	0.272	0.135	0.118
N4	0.602	0.581	0.589	0.252	0.127	0.113
N5	0.459	0.660	0.568	0.280	0.133	0.118

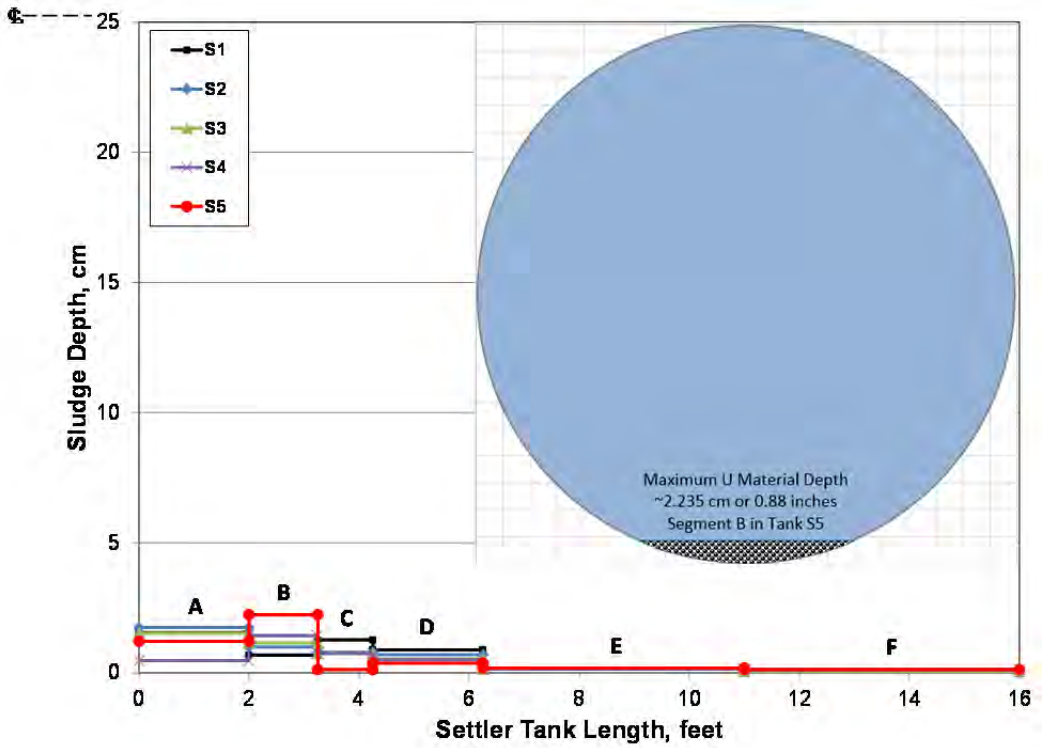

Figure 2.3. Uranium-Bearing Sludge Depth Profile in the South Settler Tanks (inset illustrates the maximum sludge depth, found in the B segment of Tank S5)

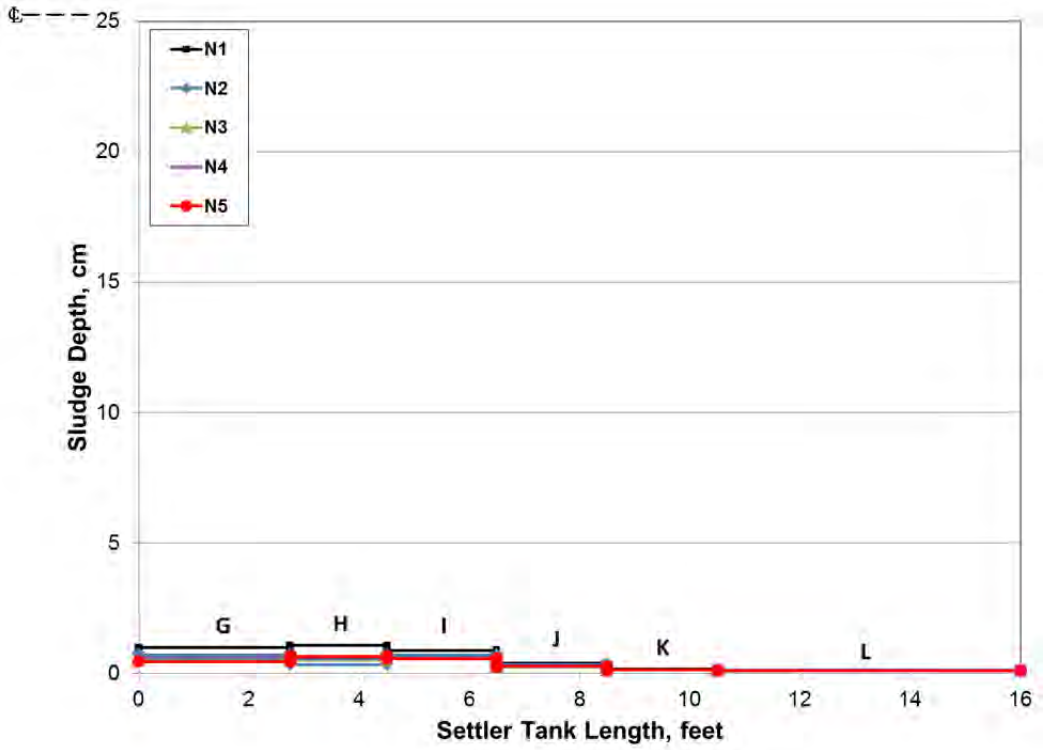

Figure 2.4. Uranium-Bearing Sludge Depth Profile in the North Settler Tanks

3.0 Settler Tank and Weasel Pit Configuration

The settler tank system array is part of the IWTS and is located in the Weasel Pit of the 105-KW Fuel Storage Basin. The settler tank array is shown in Figure 3.1.

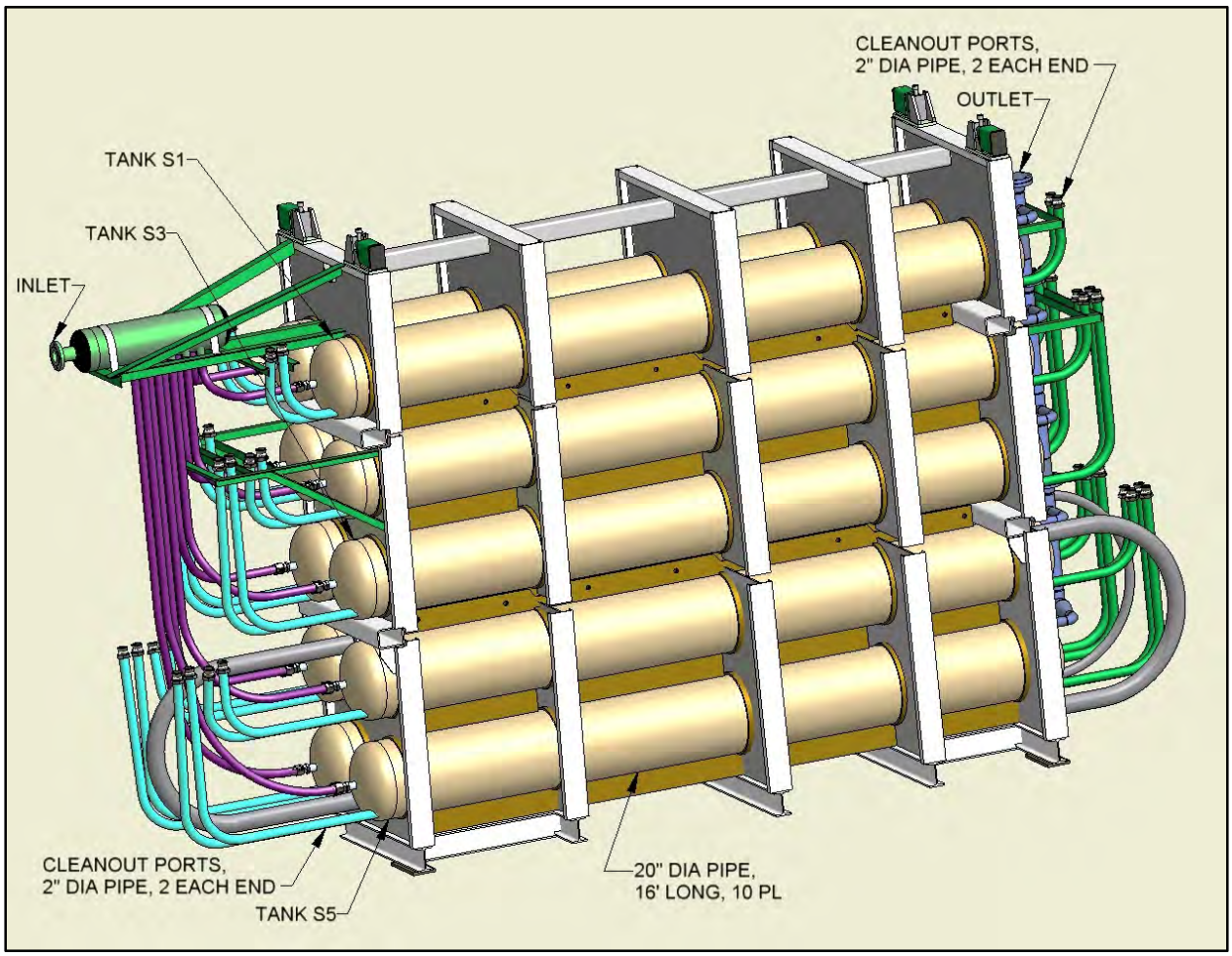

Figure 3.1. IWTS Settler Tank Array

The placement of the Settler Tank array within the KW Basin Weasel Pit is shown in Figure 3.2. As seen in Figure 3.2, the KW Weasel Pit has a truncated right trapezoidal cross-section at this point with width, at the bottom, of 53 inches and width at the waterline, 16 feet above the bottom, of 63 inches, with a total length of about 32-feet 3-inches as it opens into the rest of the KW Basin. However, the right-trapezoid cross-section is maintained only for the middle 12-foot 6-inch length of the Weasel Pit. The beginning and end segments of that side are straight-walled, about 10-feet 9-inches long and 9 feet long, respectively, with distance to the opposite rectangular wall of 66 inches. The nominal water volume of the Weasel Pit absent any Settler Tank apparatus thus is 2721 cubic feet or 77,050 liters.

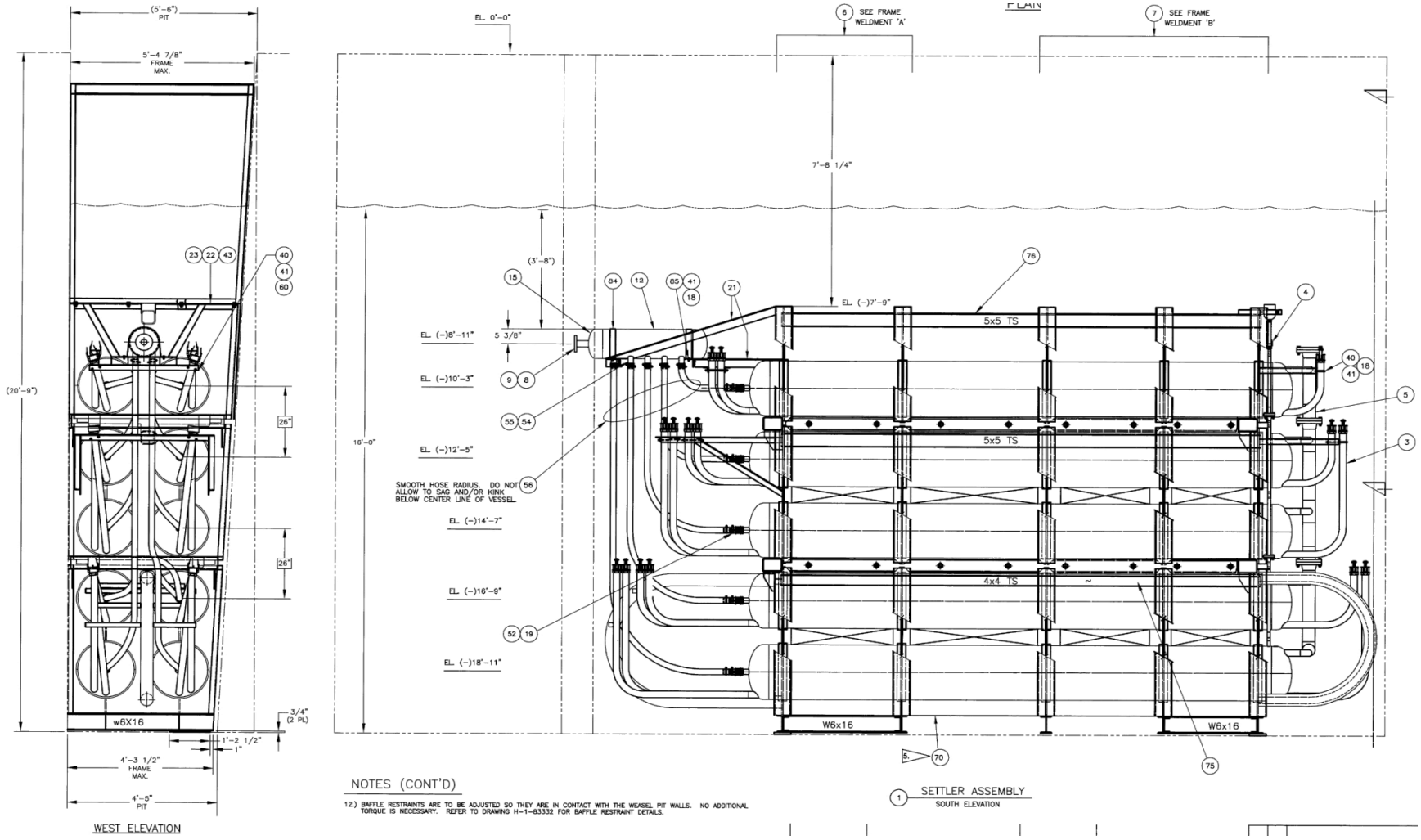

Figure 3.2. Settler Tank Array Layout in the KW Basin Weasel Pit, End and Side Views (excerpt of sheet 1 of DOE 2000)

As shown in Figure 3.1 and Figure 3.2, the Settler Tank array contains ten tanks constructed of Type 304 stainless steel. Each tank is 16 feet long and has a maximum inside diameter of 19.79 inches using 20-inch diameter schedule 10 pipe (DOE 2000). The tanks are slightly rounded at each end with the radius of curvature not specified. Assuming a right circular cylindrical geometry at the specified 16-foot length and the maximum inside diameter, each tank's capacity is 34.18 cubic feet (968 liters) or 9677 liters total enclosed volume in the ten tanks. The Inlet Tank, shown in green on the left side of Figure 3.1, was used to receive the materials destined for the Settler Tanks. The Inlet Tank is constructed of 10-inch diameter (10.42-inch inner diameter) schedule 10 Type 304 stainless steel pipe and is 32 inches long (DOE 2000). Assuming 10.42-inch inner diameter and a right circular cylinder that is 32-inches long, the contained volume of the Inlet Tank is 1.579 cubic feet or 44.7 liters.

4.0 Management and Disposition of the Settler Tanks

The STP commissioned a formal Decision Support Board (DSB) to consider options and provide recommendations to manage and dispose of the settler tanks' contents (Honeyman 2013). The two overall options were either to retrieve the settler tank contents for subsequent processing and disposal or to grout the settler tank contents in-place for subsequent processing and disposal. Decision criteria included consideration of the near-term Engineered Container Retrieval and Transfer System (ECRTS) project schedule in handling the balance of the sludge currently held in the five KW Basin engineered containers and the longer-term deactivation, decontamination, decommissioning, and demolition (D4) of the KW Basin. An STP team, further expanding the options to consider whether long-term D4 benefits might offset the near-term cost, schedule, and worker exposure in retrieval, arrived at six alternative options, four with no preliminary sludge retrieval and two with retrieval. The DSB compared the alternatives and recommended a preferred alternative in a structured, facilitated process based on defined outcome criteria.

The DSB found no significant benefit accrued by either of the preliminary sludge retrieval options aside from source term reduction under as-low-as-reasonably-achievable (ALARA) principles. Options including a second settler tank retrieval campaign also were judged to be more costly and require longer performance time. Of the four remaining options, the preferred alternative was to stabilize the residual sludge in the settler tanks by grouting, size-reduce the grouted settler tanks *in-situ*, and dispose of the settler tank segments, with the balance of the KW Basin structure, as debris at the ERDF disposal site. This option was judged to be technically feasible and produce a product waste form expected to meet the ERDF Waste Acceptance Criteria (WAC). The DSB judged this option to be among the top for almost all criteria and weightings considered even as the two retrieval options scored higher in the ALARA criterion. Because the *in-situ* grouting, size-reduction, and ERDF disposal option had the best balanced score of all options, it was recommended for implementation.

5.0 Prior Hanford Experience in Grouting Uranium Metal

Uranium metal corrodes in anoxic liquid water according to the following reaction to form flammable hydrogen gas, H_2, and uranium dioxide, UO_2 (Delegard and Schmidt 2009):

$$U + 2\ H_2O \rightarrow UO_2 + 2\ H_2.$$

This reaction is highly exothermic ($\Delta H_{reaction,\ 298}$ = -513.2 kJ/mole of uranium) and continues under anoxic conditions at practically the same rate (i.e., largely within a factor of ±3 of the nominal rate) irrespective of whether the uranium metal is in liquid water, saturated water vapor, wet sludge, or even within grout over wide varieties of grout composition or dryness (Delegard and Schmidt 2009). The corrosion rates of non-irradiated uranium metal observed in liquid water and grout (mostly Portland cement but also magnesium phosphate) systems are shown in Figure 5.1. The testing by British Nuclear Fuels Limited (BNFL) and the Pacific Northwest National Laboratory (PNNL) with various grout formulations, including many with intentionally "dry" water-starved compositions, showed uranium metal corrosion rates virtually indistinguishable from rates in anoxic liquid water. Corrosion rates for irradiated uranium metal are more scattered but, in general, may be lower by a factor of ~2-3 than the trends shown in Figure 5.1 even though corrosion rates higher than those of non-irradiated uranium metal sometimes also are observed for irradiated uranium metal (Figure 5.3 of Delegard and Schmidt 2009).

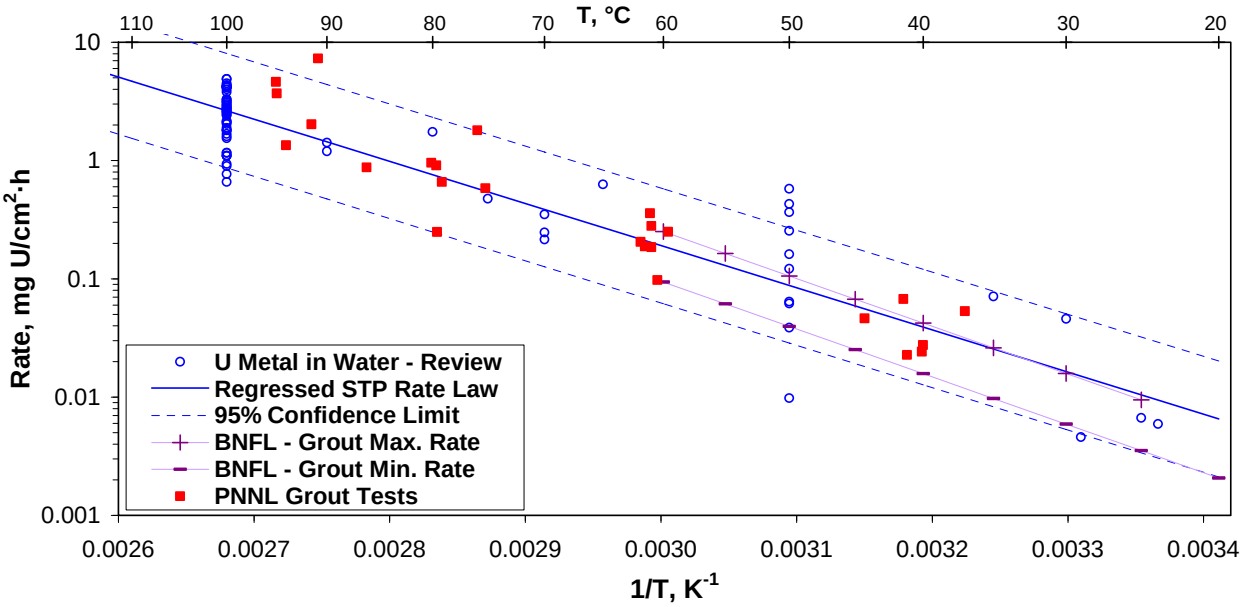

Figure 5.1. Uranium Metal Corrosion Rate Data in Liquid Water and in BNFL Portland Cement Grouts and PNNL Portland Cement and Magnesium Phosphate Grouts (Delegard and Schmidt 2009)

Hanford Site experience with grouting of Zircaloy-clad uranium metal fuel fabrication machining chips and saw fines from 1971 until 1982 also has been surveyed for insights relevant to the proposed uranium metal grouting operations in the settler tanks (Schmidt 2013 and references within). Until 1971,

the chip and fines metal scrap was ignited to their oxides, U_3O_8 and ZrO_2, within open-air incinerator barrels in the 303-L Building. The product oxide then was shipped to National Lead Company in Fernald, Ohio, for uranium recovery (Everett Weakley, personal communication, October 2003). Burning of uranium and Zircaloy chips/fines resumed in 1984 in the 303-M building, the "Uranium Oxide Facility," built for this purpose (Weakley 1982; Gydesen 1982) and continued until N Reactor fuel production ceased in 1987.

The unirradiated uranium metal fuel fabrication scrap grouting was done in Hanford Site operations in an attempt to stabilize the pyrophoric uranium metal for its safe shipment to Fernald. The fines and chips were generated at weekly rates of 550 pounds and 1280 pounds (~30 wt% fines and 70 wt% chips), respectively, with the fines being 60-70 wt% uranium (U) and 4.5 wt% zirconium (Zr) and the chips 96 wt% U and 2.8 wt% Zr (Weakley 1980). The chips and fines were estimated to have respective specific surface areas of 5.8 and 31 cm^2/g (Schmidt 2013). At nominal loadings of 18 kg metal per 27-liter capacity grouted billet can, the uranium metal surface area was ~1.79×10^5 cm^2 or ~6.6×10^3 cm^2 of uranium metal surface area per liter of grout.(4) This compares with 8.7×10^5 cm^2 of uranium metal surface area in the 9677-liter capacity of the settler tanks or ~90 cm^2 of uranium metal surface area per liter of grout, on average. The uranium metal scrap grouting was conducted manually at Hanford both in the mixing of the fines and chips with masonry cement and filling of the cans with the grout mixture (Figure 5.2). In the grouting process employed in the 304 Concentration Building, the wet collected metals were mixed with masonry cement (47% limestone, 3% gypsum, and 50% Type II Portland cement) and water using an ordinary tilting-drum rotating ~3-cubic-foot cement mixer at a nominal per-charge weight ratio of 18 kg metal/54 kg masonry cement/30 kg water where the metal represents the machining chips and saw fines containing both uranium metal and Zircaloy cladding (based on Weakley 1980). When it was subsequently found that the fines segregated to the bottom of this style of mixer and not mix uniformly with the wet cement and chips, a paddle-type cement mixer was used instead (Weakley 1980). The grouted mixtures were cast in ~27-liter (~7¼-gallon) thin-walled steel cans called "billets" (Weakley 1980); similarly-dimensioned polyethylene cans also were used (Weakley 1982). Relative dimensions, derived from photos (e.g., Figure 5.3) of the slightly tapered steel cans (known to nest when empty) and knowledge of their stated capacities, allows estimation of the average billet can diameter (29.9 cm, ~11.8 inches) and height (38.4 cm, ~15.1 inches).

(4) $\frac{18\text{ kg metal}}{\text{billet can}} \times \left(0.3\text{ kg fines} \times \frac{0.65\text{ kg U fines}}{\text{kg fines}} \times \frac{3.1\times10^4\text{cm}^2}{\text{kg U fines}} + 0.7\text{ kg chips} \times \frac{0.96\text{ kg U chips}}{\text{kg chips}} \times \frac{5.8\times10^3\text{cm}^2}{\text{kg U chips}}\right) = 1.79 \times 10^5\text{ cm}^2$.

Figure 5.2. Fines and Chips Mixing with Masonry Cement and Casting into 27-Liter Steel Billet Cans (photo number 86201-21cn, 304 Building, April 3, 1979)

At National Lead, the thin (0.010-inch or ~2 mm) steel cans were cut and peeled from the cast billets, the castings broken into 6 to 8 chunks, and the chunks charged to a gas-fired oven where the cement decomposed and crumbled from calcination of the contained limestone ($CaCO_3$) to release carbon dioxide gas and water vapor while the uranium metal and Zircaloy burned to U_3O_8 and ZrO_2. The fired product was removed from the oven and passed through an 8-mesh screen. The materials not passing the 8-mesh screen were crushed further and re-burned. The crushed and fired materials then were transferred to a facility for acid dissolution and solvent-extraction purification of the dissolved uranium (Weakley 1973; Figure 6 of Weakley 1976).

However, thermal runaway was observed for production castings in three separate incidents, the first two of which occurred during the hotter summer months. At the time of the first incident, it was postulated that the Portland cement hydration heat, aided by summertime temperatures, and the poor grout thermal conductivity were sufficient to cause the uranium metal within certain of these production cylindrical castings to undergo thermal runaway. The thermal runaway was manifest in split metal containers and crumbled cement. The appearances of the six burst metal containers and crumbled cemented uranium castings following the first production casting incident in August 1977 are shown in Figure 5.3.

Figure 5.3. Masonry Cement Castings of Uranium Machining Chips and Fines after First Auto-Ignition Incident, August 1977 (from original color negative after Figure 1 of Weakley 1980)

The second auto-ignition incident occurred in July 1979 in the 3712 Building warehouse. In this event, the wooden shipping boxes in which the billets were packed also ignited and 21 concreted billets were damaged or destroyed. In these first two auto-ignition incidents, the crumbled uranium-bearing materials were simply swept up and cast again in masonry cement. However, concern over the safety of storing and shipping the U/Zr metal-bearing product billets led to suspension of the grouting and shipping practice in August 1979 (Fuels Production Department 1979).

To address the growing backlog of fines and chips, an experimental program was rapidly implemented in 1979 to determine the causes of the runaway reactions and identify processing techniques to eliminate the risk of auto-ignition. Curing times and temperatures, uranium/Zircaloy granularity (fines, chips) and loading, and drying and long-term storage/curing temperatures for the cast billets were varied within the test program. Billets prepared under nominal process conditions and taken from production were used in six of the test conditions while specially prepared billets were used in the remaining tests. In addition to the 22 test conditions examined in parametric testing, separate test billets were prepared under varied hydration conditions but without U/Zr fines/chips with the objective of determining the masonry cement curing temperatures and properties.

The experimental studies showed that hydrogen was released during auto-ignition events, indicating that the reaction of uranium metal with water occurred and was a key source of heat. Under intentionally extreme conditions, numerous thermal runaways were observed within the parametric tests, some resulting in complete crumbling and others in expansion of the grout and splitting of the cans (see overview; Schmidt 2013). Centerline temperatures up to 803 °C were found in the parametric tests for

which thermal runaway occurred. The limited reported temperature/time data also showed that sharply accelerating rates occurred once the boiling temperature of water was reached as shown in Figure 5.4.

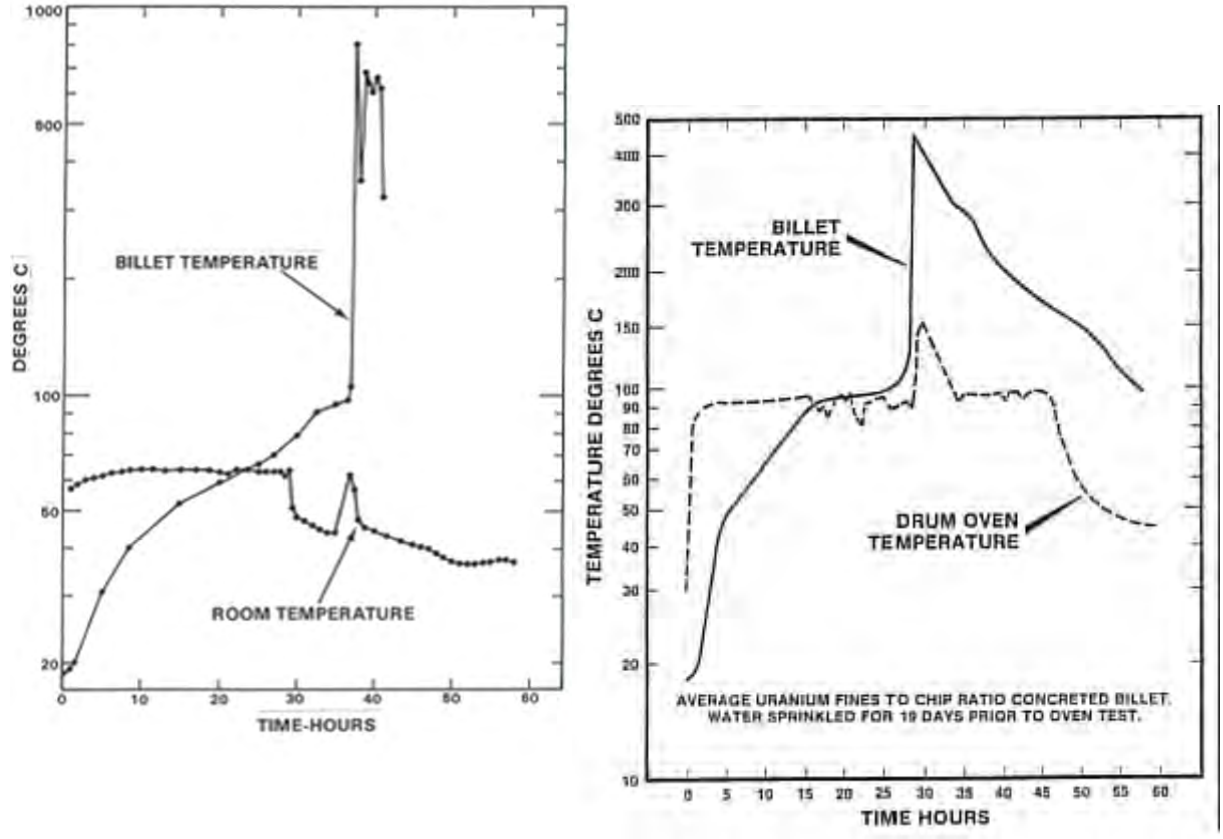

Figure 5.4. Temperature Curves for Test Castings That Underwent Thermal Runaway. (Left: Test II-4. Heavy uranium fines-to-chip ratio concreted item containing additional 0.9 kg of unmixed fines in the center. Water was sprinkled for 3 days before ~63 °C heating. From Figure B-4 of Weakley [1980]. Right: Test III-1. Average uranium fines-to-chip ratio concreted item. Water was sprinkled for 19 days before ~97 °C drum oven heating. From Figure B-6 of Weakley [1980]).

At the conclusion of these parametric studies, the authors concluded that the risk of auto-ignition could be eliminated by implementing a careful drying and high-temperature curing protocol. This sequence was judged to be equivalent to a "burning test" (or proof-test) at temperatures exceeding those the billets might reach during shipment (Weakley 1980). Preparation and shipment of grouted billets resumed according to the modified protocols based on the experimental findings.

However, a subsequent concreted billet auto-ignition occurred in March 1982 during the high-temperature curing cycle and before shipment. Renewed concerns with auto-ignition during storage and particularly during shipment, with the additional potential involvement in fiery in-transit road accidents, led the Department of Energy to call for investigation of alternative means to transport uranium for recycle (Weakley 1982). As a result, the grouting process was abandoned and the prior practice of

stabilizing the chips and fines, before shipment to Fernald for recovery, by ignition to U_3O_8 and ZrO_2 was reinstated in a new specially-designed facility.

Thus, the lab testing at BNFL and PNNL shows that grouting provides no significant change in the uranium metal corrosion rate. More importantly, the uranium metal fuel fabrication scrap grouting experience at Hanford shows that elevated temperatures caused by grout curing, sometimes aided by high summertime temperatures and imposed high-temperature curing, can lead to thermal runaway. Therefore, implementation of *in-situ* grouting of the uranium metal-bearing sludge in the settler tanks requires considering whether slow and controlled corrosion can be maintained by limiting temperature excursions during the grouting operations and subsequent retrieval and disposal operations, or would more rapid oxidation under thermal runaway conditions occur instigated by Portland-cement-based grout hydration reactions and/or self-heating of the uranium metal particle bed by the corrosion reaction, radiolytic processes, and external heating (e.g., insolation).

6.0 Portland Cement Grout Formulations

The formalized decision-making process engaged to determine the best method for stabilizing and disposing the KW Basin settler tanks is outlined in Section 4.0. The decision process outcome was the recommendation that *in-situ* grouting (i.e., filling the settler tanks with grout) be done. Time would then be allowed for the grout to strengthen by curing before size-reduction and ERDF disposal of the settler tanks and their contents (Honeyman 2013).

Grouting has been implemented in prior K Basin stabilization operations as a method to fix radioactive contamination during subsequent D4 operations. Once cured, the grouted materials must be of sufficient strength during rubblization that handling can be done without undue crumbling during loading and transport to ERDF. In the case of grouting the settler tanks, an additional concern arises in that the heating caused by curing the grout might be sufficient to instigate thermal runaway reactions within the uranium metal particle bed on the settler tank bottoms.

Preservation of sufficient grout set strength for rubblization while minimizing curing heat also was a key consideration in grouting of the KE Basin Discharge Chute (Yanochko et al. 2005) as revealed in investigation of prior K Basin grouting operations. For the discharge chute application, extensive grout testing was undertaken to arrive at a mix engineered to meet goals of wet and dry density, compressive strength, self-leveling, fluidity, and limited heat of hydration (to prevent steam generation or steam bursts within the massive pour required for the KE Basin Discharge Chute). The wet grout had to be pumpable and suitable for underwater placement with sufficient fluidity to encapsulate debris and leave no water pockets. The cured grout had to have minimal expansion or shrinkage. The favorable attributes of the grout mix designed for the KE Basin Discharge Chute and its acceptance and implementation in K Basin operations thus commend it for consideration in settler tank grouting.

The K Basin Project engaged the grout development lab and vendor Pacific International Grout Company, Incorporated, PIGCO, Bellingham, Washington, to propose and test candidate grout formulations to minimize temperature within massive castings and still have acceptable cured compressive strength while being flowable and self-leveling and being suitable for both dry and underwater placement (Yanochko et al. 2005). The proposed proprietary grout mixes consisted of water, Portland cement, and fly ash. As would be expected, the testing showed that increase of the fly ash proportion at the expense of Portland cement decreased heating and also decreased the grout set strength. Fly ash improves fluidity for placing, attributed to the roughly spherical shapes of the fly ash particles (Massazza 1998), and retards early stage Portland cement hydration (Thomas 2007). It is known that although fly ash hydration ultimately is slightly exothermic, the contribution of fly ash to the heat at early ages (when most of the heat is generated by Portland cement) is no more than 15 to 35% of the heat from an equal weight of Portland cement (ACI 2002a) and is observed to be negligible in other tests of early hydration enthalpy (i.e., within the first three days at ambient cure temperatures; Table 4 of Langan et al. 2002; Figure 3.13 of Kim 2010; Figure 3 of Bentz et al. 2013). The benefit of fly ash substitution in decreasing hydration heat increases by decreasing the complement of calcium oxide, CaO, in the fly ash (Thomas 2007).

Thus, substitution of fly ash for Portland cement delays the hydration heat generation rate, decreasing the internal grouted casting temperatures by allowing time for the hydration heat to dissipate. Substitution of fly ash for Portland cement also lowers the overall hydration enthalpy by dilution because of the much lower hydration enthalpy of fly ash than Portland cement, particularly if the fly ash has low CaO content.

PIGCO tested various proportions of Type I/II Portland cement, Class F fly ash, and water and also proposed and tested additives to improve flowability and decrease washout and water turbidity during placement for the KE Basin Discharge Chute application. The dry grout formulation ultimately used in September 2004 for the KE Basin Discharge Chute was the one found in test C25 (Muller 2015), 26 wt% Lehigh Type I/II Portland cement and 74 wt% Boral Mojave Class F fly ash mixed with water at a 0.425 water:dry ingredient mass ratio (Figure 6.1). The Mojave Class F fly ash analysis that was produced about the time of acquisition for use in grouting the KE Discharge Chute grout has 9.72 wt% CaO (Figure 6.2) is no longer available. Its composition is also at the high end of CaO concentration for Class F fly ash (Figure 5 of Thomas 2007). Class F fly ash with CaO concentrations as low as 6.40 wt% are available from the same vendor and fly ash with even lower CaO concentrations is available elsewhere. Substitution of fly ash with different CaO concentrations or from different sources may alter the grout strengths, setting characteristics, and placing (Stephens 2015).

Thompson Mechanical | Submittal 23362-8-E-AFW-ENG | FH Contract 23362

Base Mix Design (Range)

	% Cement	Cement Type	% Fly Ash	Fly Ash Type	Water/Cement Ratio	Design Strength - PSI at 28 Days	Design Density - ASTM C138 - PCF	Flow Cone - ASTM C939 - Sec	Admixtures		
Base Mix Design	24 to 28	Lehigh Type I/II	72 to 76	Boral Mohave F	0.4 to 0.5	250	100 to 120	11 to 90	Rheomax UW-450 0 to 30.0 oz/cwt	Glenium 3030NS 0 to 20 oz/cwt	Delvo 0 to 4 oz/cwt

Tested Mixes

PROCUREMENT / CONTRACT SUBMITTAL
ACC ☐ AFW ☑ APP ☐
A(✓) Conforms to the Contract Requirements
B( ) Minor Comments-Approved With Exceptions
Re-submittal Required YES ☐ NO ☐
C( ) Revise and Re-submit
Date: 7/25/05

Mix #		% Cement	Cement Type	% Fly Ash	Fly Ash Type	Water/Cement Ratio	Design Strength - PSI at 28 Days	Design Density - ASTM C138 - PCF	Flow Cone - ASTM C939 - Sec	Admixtures		
PIGCO	C25	26	Lehigh Type I/II	74	Boral Mohave F	0.425	1400	105.93	20.2	Rheomax UW-450 30.0 oz/cwt	Glenium 3030NS 2 oz/cwt	Delvo 6 oz/cwt
PIGCO	C4	50	Lehigh Type I/II	50	Boral Mohave F	0.50	2500	106.5	11	None		
PIGCO	C5	40	Lehigh Type I/II	60	Boral Mohave F	0.50	2500	108.1	11	None		
PIGCO	C6	50	Lehigh Type I/II	50	Boral Mohave F	0.35	2500	110.5	90	Rheomax UW-450 7.0 oz/cwt	Glenium 3030NS 5.8 oz/cwt	Delvo TBD
PIGCO	C7	50	Lehigh Type I/II	50	Boral Mohave F	0.35	2500	110.5	90	None		
PIGCO	C8	60	Lehigh Type I/II	40	Boral Mohave F	0.40	2500	110.4	69	Rheomax UW-450 10.85 oz/cwt	Glenium 3030NS 5.0 oz/cwt	Delvo TBD
PIGCO	C9	60	Lehigh Type I/II	40	Boral Mohave F	0.40	2500	110.4	69	None		
PIGCO	C10	50	Lehigh Type I/II	50	Boral Mohave F	0.40	2500	110.3	64	Rheomax UW-450 11.0 oz/cwt	Glenium 3030NS 5.0 oz/cwt	Delvo TBD
PIGCO	C11	50	Lehigh Type I/II	50	Boral Mohave F	0.40	2500	110.3	64	None		
PIGCO	C12	50	Lehigh Type I/II	50	Boral Mohave F	0.45	2500	110.0	32	Rheomax UW-450 10.0 oz/cwt	Glenium 3030NS 5.0 oz/cwt	Delvo TBD
PIGCO	C13	50	Lehigh Type I/II	50	Boral Mohave F	0.45	2500	110.0	32	None		

Sub 08, Ver 4 - Mix Design Rev 3 | 7/15/2005

Figure 6.1. Some of the Grout Mixtures Tested and the Mix Ultimately Used in the KE Discharge Chute Grouting, PIGCO C25 (Muller 2015)

Boral Material Technologies BORAL™

ENTERED

REPORT OF FLY ASH ANALYSIS

Project Name:	**Mohave Unit 1 & 2**	**Date Received:**	**06-Jul-04**
Sample ID #:	**3429-01**	**Tested By:**	**Mark/Steve/Johnn**
Sample Date:	**April, 2004**	**Report Date:**	**24-Aug-04**

CHEMICAL TESTS	RESULTS	ASTM C 618 CLASS F/C	AASHTO M 295 CLASS F/C
Silicon Dioxide (SiO_2), %	54.28		
Aluminum Oxide (Al_2O_3), %	21.63		
Iron Oxide (Fe_2O_3), %	5.43		
Sum of SiO_2, Al_2O_3, Fe_2O_3, %	81.34	70.0/50.0 min.	70.0/50.0 min.
Calcium Oxide (CaO), %	9.72		
Magnesium Oxide (MgO), %	1.98		
Sulfur Trioxide (SO_3), %	0.76	5.0 max.	5.0 max.
Sodium Oxide (Na_2O), %	2.60		
Potassium Oxide (K_2O), %	0.68		
Total Alkalies (as Na_2O), %	3.18		
Available Alkalies (as Na_2O), %	1.33		

PHYSICAL TESTS	RESULTS	ASTM C 618 CLASS F/C	AASHTO M 295 CLASS F/C
Moisture Content, %	0.03	3.0 max.	3.0 max.
Loss on Ignition, %	0.57	5.0 max.	5.0 max.
Amount Retained on No. 325 Sieve, %	26.05	34 max.	34 max.
Specific Gravity	2.33		
Autoclave Soundness, %	0.07	0.8 max.	0.8 max.
Strength Activity Index with Portland Cement at 7 days, % of Control	92.0	75 min.*	75 min.*
Strength Activity Index with Portland Cement at 28 days, % of Control	98.8	75 min.*	75 min.*
Water Required, % of Control	98.3	105 max.	105 max.
Loose Bulk Density, lbs/ft^3			

Meets ASTM C 618 and AASHTO M 295, Class F

*Meeting the 7 day or 28 day strength activity index will indicate specification compliance.

Date: 24-Aug-04

By: Diana Benfield

Diana Benfield
Quality Specialist

By:

Zhaozhou Zhang
Manager, Analytical Services and Development

45 NE LOOP 410, SUITE 700 SAN ANTONIO, TEXAS (210) 349-4059

Figure 6.2. Analysis of Mojave Class F Fly Ash, April 2004 (courtesy Boral Material Technologies)

The finalized mix also contained three additives per 100 lbs of grout mix: 30 ounces of Rheomac UW-450 (an anti-washout agent), 2 ounces of Glenium 3030 NS (a water-reducing agent), and 6 ounces of Delvo Stabilizer (a water-reducing agent). The order of addition of these additives and the general procedure used to prepare the C25 and KE Discharge Chute grouting mixtures are proprietary and vital to successful implementation (Stephens 2015).

The candidate KE Discharge Chute grout compressive strengths were measured after 28 days of curing to ensure that they exceeded the agreed-upon lower limit of 250 (design) + 1000 (margin) pounds per square inch (PSI) (Yanochko et al. 2005; beginning page A-33). The selected C25 test formula produced a 1400 PSI compressive strength at 28 days (Figure 6.1), above the 1250 PSI requirement. The flowability of the wet grout also met the design goal based on the ASTM C939 flow cone test. Good flowability was necessary to allow the wet grout to encompass debris in the KE Discharge Chute and eliminate water pockets. The test C25 product density was 105.93 pounds/ft^3 or 1.697 kg/liter and the pour density of the actual KE Discharge Chute grout of the same formula was 105.5 pounds/ft^3 or 1.690 kg/liter (Figure 6.3). This compares well with the 1.72 kg/liter density projected based on the densities of the constituent Portland cement (3.25 kg/liter), fly ash (2.10 kg/liter), and water (1.00 kg/liter) by the law of mixtures (Bentz et al. 2011). The lower observed density likely is an effect of entrained air (the effects of the grout additives being relatively small and thus ignored). The wet grout mixture temperature measured for the KE Discharge Chute application was 77 °F (25 °C) as described in the pour card (Figure 6.3) and the ambient temperature at the time of the pour (9 AM, on 3 September 2004) was ~62 °F or ~17 °C. [(5)]

[(5)] Weather Underground, Weather History for KPSC, Friday, September 3, 2004: http://www.wunderground.com/history/airport/KPSC/2004/9/3/DailyHistory.html?req_city=Richland&req_state=WA&req_statename=Washington&reqdb.zip=99354&reqdb.magic=1&reqdb.wmo=99999

Grout Pour Card

Grout Design Information (FH Responsibility)		
Project No. A 22 B	Location 105 KE DISCHARGE CHUTE	Date: 9-1-04
Campaign No. 2 Pour No. 1	☒ Max. Pour Depth 6' – 4 ½" (Temp. Control)	Elev. of Completed Pour (-) 5'-9" Depth of Completed Pour 5.99'
☒ Grout Campaign 1 Final set Test Cylinder/Strength 580.0 psi > 36.0 psi REF. SUBMITTAL NO. 16 VERSION 1, 8-31-04	☒ TSR Limit not exceeded – ___ 1st Campaign < 9' – 2" (elev. (-) 11'-7") X 2nd Campaign < 16' – 0" (elev. (-) 4'-9") ___ 3rd Campaign < 18' – 0" (elev. (-) 2'-9")	Projected Grout/Concrete: Quantity (Cu. Yd) 214 Projected Water Volume: Quantity (Gallons) 43,325
Basin Water Level 16'10 5/16" (1" = 6,174 gal. = 30.5 c.y.) Max. water level 17' – 6"	☐ Basin water space needed 7.68 7.74 7.74 9/3/04 ☒ Basin water space available 7.68"	Mix Initial Temp. 40-90° F Grout/Concrete Type G
Top of Barrier Door Elev. (-)2' – 9" Weir Opening Invert (-) 4'–7 1/16"	☒ Do not overflow Weir Door Opening or top of Barrier Door with grout/concrete	Compressive Strength 250 (psi) Density 100 – 120 pcf

43,325 / 6174 = 7.02" ☒ DO NOT EXCEED 17'6" BASIN WATER LEVEL

Special Instruction

43,325 / 5,600 = 7.74"

Pre-Pour Approvals

Signature: R.M. Yanochko Date: 9-1-04 Cognizant Engineer	Signature: [signature] Date: 9/3/04 Design Authority
Signature: [signature] Date: 9/3/04 Quality Assurance	Signature: [signature] Date: 9/3/04 Construction
Signature: N/A 09/9/3/04 Date: Other	Signature: [signature] Date: 9/1/04 Operations

Actual Grout Data (TMC Responsibility)

Placement Date: 9.3.04	Placement Time: 9:00 AM	Quantity (Cu. Yd): 216.0
Flow Cone 36.4 Ave sec.	Grout Mix Temp. 77°F	Wet Density: 105.5 Ave
No. of Test Specimens: 36	Depth of Grout Pour 9-3-04 0930 216. 6.22'	Elev. of Completed Pour 15' – 2 3/4"
Signature: [signature] Date: 9-3-04 Contractor	Signature: [signature] Date: 9-3-04	

Completed Grout Pour Card identifying requirement compliance and approvals.

Figure 6.3. KE Discharge Chute Grout Pour Card (from page A-25 of Yanochko et al. 2005)

Given the favorable experience in grouting the KE Basin Discharge Chute, the grouting of the settler tanks is modeled here based on the same grout recipe. The modeling is undertaken using the following additional simplifying assumptions:

1. To a first approximation, the grout hydration enthalpy (heat generation) is assumed to be proportional to the Portland cement complement with negligible enthalpic contribution by the fly ash. This assumption is slightly non-conservative because, as noted, fly ash contributes perhaps 15% as much heat as an equal mass of Portland cement (ACI 2002; Table 4 of Langan et al. 2002; Figure 3.13 of Kim 2010; Figure 3 of Bentz et al. 2013) and the amount of heat decreases with the complement of calcium oxide in the fly ash, which is generally lower for Class F fly ash (Thomas 2007). Furthermore, the heat contribution by fly ash occurs much later than that of Portland cement so it does not add to the thermal power generation maximum for Portland cement that occurs at room temperature about 8 to 12 hours after mixing with water.
2. It is also assumed that the heat generation in the Portland cement/fly ash mixture occurs at the same rate as for a pure Portland cement paste. This assumption is made because heat generation rate data are much better known for pure Portland cement pastes than for cement/fly ash mixtures. This assumption is conservative in that fly ash and the water-reducing agents generally retard the setting of Portland cement and so will decrease the heat generation rate (Massazza 2001; Thomas 2007; Kumar et al. 2012).
3. Finally, it is assumed that the Portland cement/fly ash hydration reactions follow an Arrhenius kinetic dependence; i.e., that the logarithm of the rate is inversely proportional to the inverse absolute temperature in the same manner as pure Portland cement.

Portland cement thermodynamics is considered in more detail in the following section.

7.0 Portland Cement Thermodynamics

Portland cement hydration reactions are exothermic, showing an initial heat generation rate spike upon mixing at room temperature of perhaps 2 mW/g cement due to dissolution of the contained calcium hydroxide, $Ca(OH)_2$. This spike is sufficiently rapid that it occurs within the grout mixer upon introduction of water to the dry components. The initial heat spike is followed by a brief induction time of low heat generation rate before an increasing heat rate occurs, peaking at ~4 mW/g after 8 to 12 hours at ~20 °C temperatures. After this heat generation maximum, the heat generation rate slowly diminishes, taking years to complete. The nominal Portland cement heat generation curve in Figure 7.1 illustrates the early heat generation behavior.

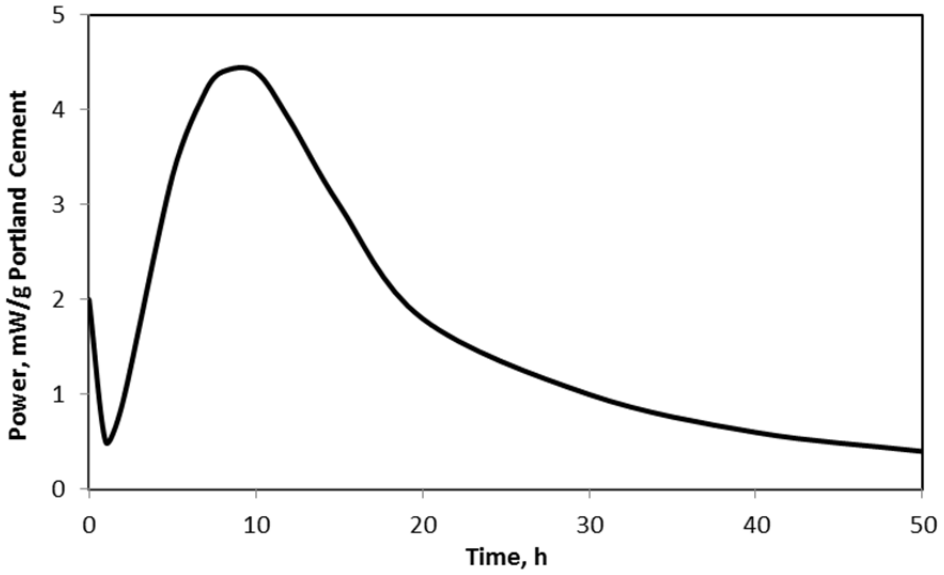

Figure 7.1. Nominal Portland Cement Hydration Heat Generation Rates (based on Lawrence 1998)

The total heats generated in curing of Portland Type I and Type II cements for extended curing times at 21 °C are shown in Figure 7.2 (derived from Table 9 and Figure 10 of Copeland et al. 1960; enthalpy data are averages of eight different Type I and five different Type II Portland cements). The rapid early heat evolution is illustrated by the fact that about half of the total curing heat arises in the first three days. However, heat continues to evolve at ever-diminishing rates even after more than 6½ years of curing. The "final" enthalpies, simple extrapolations that are 2% higher than the final data taken at 13 years, are -504 and -430 J/g for Type I and II Portland cement, respectively.

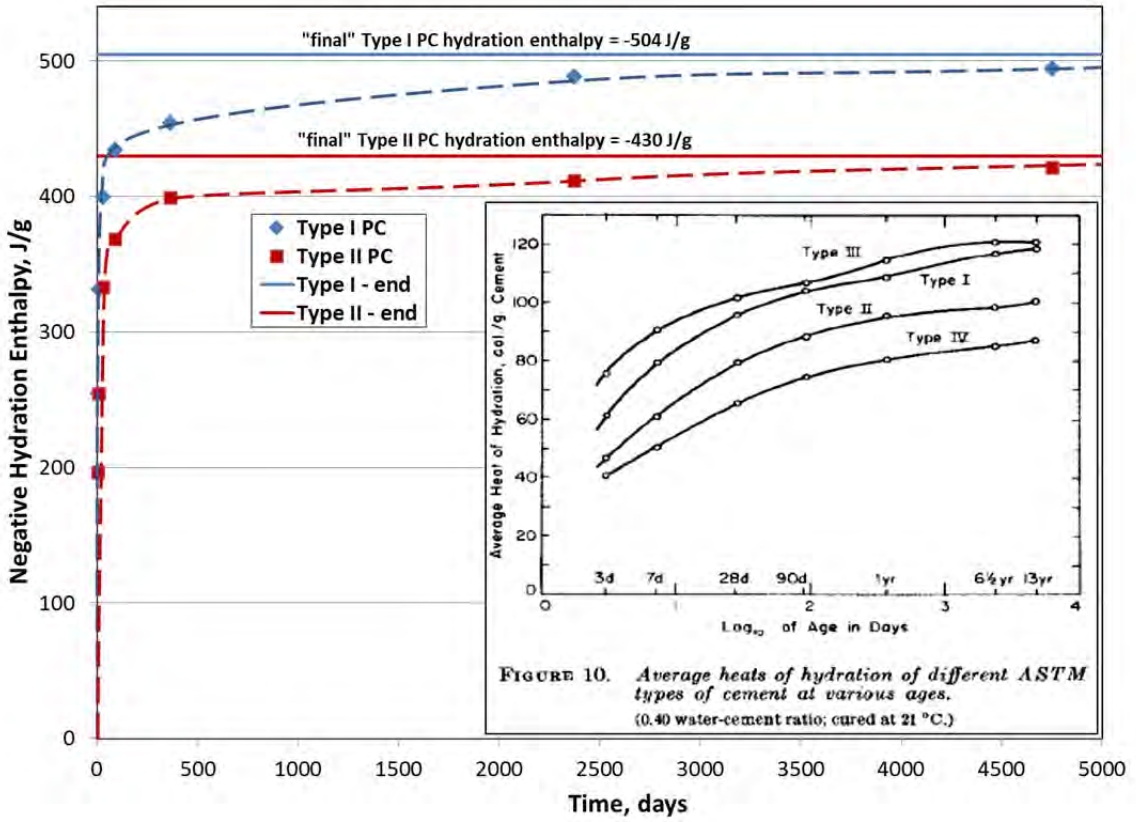

Figure 7.2. Type I and Type II Portland Cement Hydration Enthalpies (derived from values taken from Table 9 and Figure 10 of Copeland et al. 1960, inset)

To help in modeling the heat-generation behavior of the Type I/II-based grout to be used in the settler tanks, the Portland cement hydration heat generation rates were plotted for early times for the maximum heat generation rate at ~8-12 hours and at 50 hours at 20 °C (from Figures 8.1 through 8.3 of Lawrence 1998) and more extended times, ranging from 3 days to 13 years at 21 °C (with rates derived by taking slopes from plots similar to Figure 7.2 based on data found in Table 9 and Figure 10 of Copeland et al. 1960 and their studies of Type I and II Portland cements).

The data for these two disparate studies were found to be remarkably consistent and showed predictable thermal power for Portland cement curing at and after the initial thermal power peak at ~10 hours. The data presented in Figure 7.3 show that the specific power in curing Portland cement at 20-21 °C as a function of time at and after the peak rate at ~10 hours may be represented by the following equation:

$$\text{Specific power, mW/g Portland cement} = 1.176 \times (\text{time, days})^{-1.277}$$

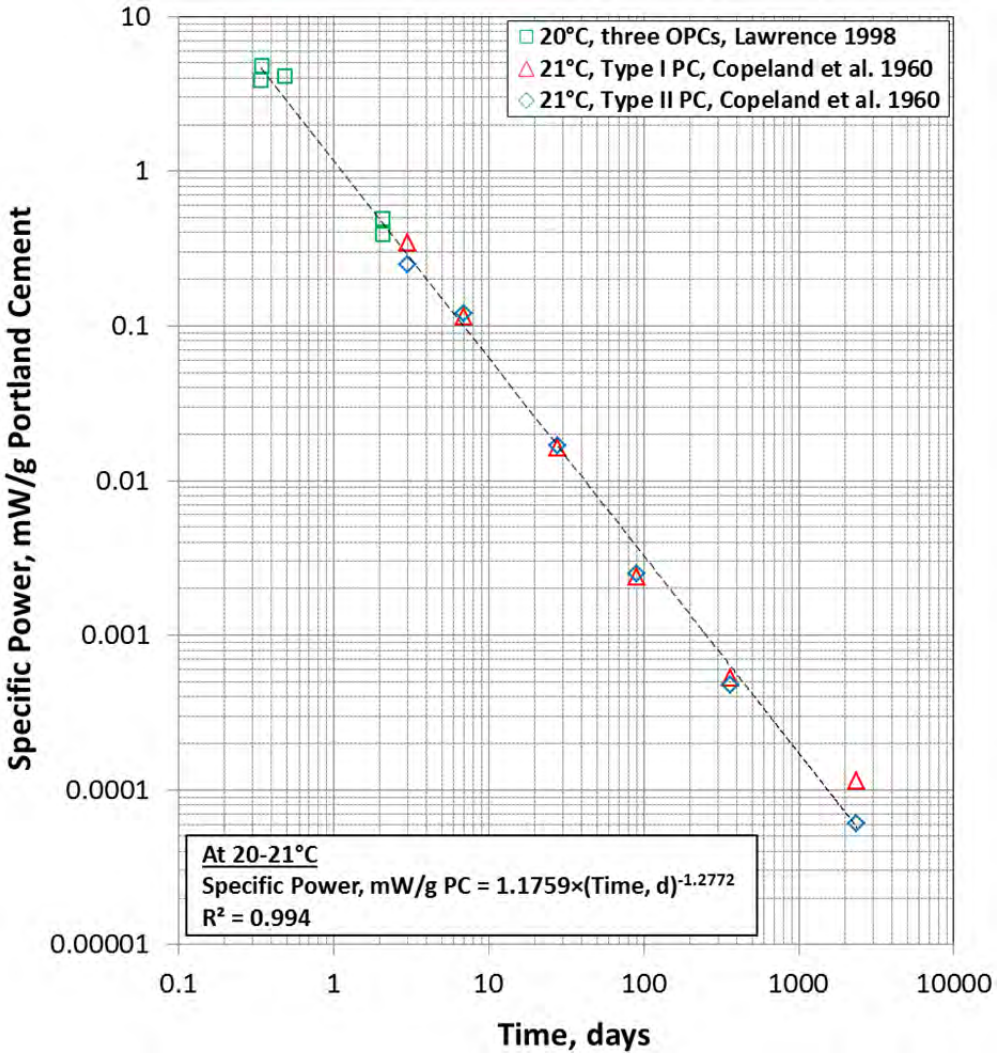

Figure 7.3. Specific Power of Curing Portland Cement at 20-21 °C as a Function of Time (at and after the initial peak power at ~10 hours)

The Portland cement curing reaction rate, and thus the rate of heat generation (power), increases with increasing temperature. The effect of temperature on the heat generation rate has been estimated for Type I and IV Portland cements taken to about 70% curing at 4.4, 21.0, 43.4, 71.0, and 110 °C and for a "standard" cement at 4.4, 23.3, and 40 °C (Table 12 and Figure 15 of Copeland et al. 1960). These data have been fit to Arrhenius equations in which the logarithms of the heat evolution rates (specific powers) are found to be inversely proportional to the inverse absolute temperature. The extents of reaction for these test items were estimated to be approximately equal based on hydration heat and non-evaporable water concentration measurements. It is noted that the specific powers were calculated over extended times, including the induction time before the hydration reactions become fully engaged, and thus are much lower than the peak powers as shown, for example, in Figure 7.1 at ~10 hours where the specific power at ~20 °C is about 4 mW/g of Portland cement.

It is seen that the heat evolution rate data for the results gathered by Copeland and colleagues (1960) follow the Arrhenius equation very closely (Figure 7.4). The activation energies, E_a, for the three

different cements also are seen to be remarkably close, with the average being 22.3 ± 0.8 kJ/mole. The activation energy is relatively small. In this case, a ~24 °C temperature increase from room temperature is needed to double the reaction rate.

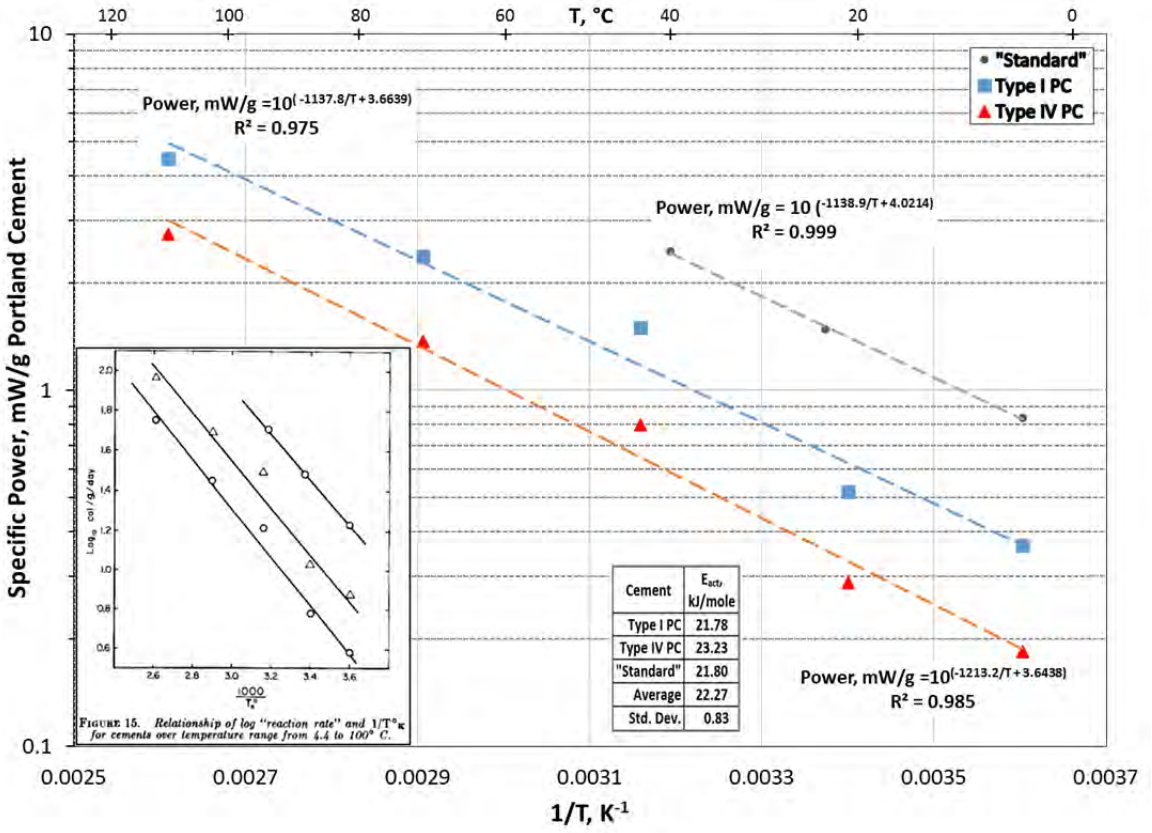

Figure 7.4. Arrhenius Plots of Specific Powers of Portland Cements (based on Table 12 and Figure 15, inset, of Copeland et al. 1960)

In other related testing, the specific power of the initial thermal spike for curing ordinary Portland cement (OPC) was found to increase from 3.45 mW/g OPC at 35 °C to 6.9 mW/g OPC at 45 °C (Kumar et al. 2012). The peak powers for these two tests occurred at ~11.5 hours and ~6.8 hours, respectively (note that these times also include the induction times). The data from the tests of Kumar and colleagues (2012) therefore show that the power doubles with only a 10 °C temperature rise.

The activation energy, E_a, based on the two measurements by Kumar and colleagues (2012) is 56.5 kJ/mole, much higher than the E_a = 22.3 kJ/mole shown for the more extensive analyses by Copeland and colleagues (1960). Although the data supporting the lower activation energy are more extensive (Copeland et al. 1960), for conservatism, the present analysis assumes the higher activation energy estimate based on the limited and more recent data (Kumar et al. 2012).

The volumetric power of the grout proposed for use in the settler tanks must be estimated so that the temperatures within the grouted settler tank waste forms containing the uranium metal particles can be projected. As noted in Section 5.0, the grout proposed for use in the settler tanks is the same as used for

the KE Discharge Chute (see Figure 6.1). Thus, the heat of Portland cement hydration is diluted by the high complement of low-heat fly ash. The weight fraction of Type I/II Portland cement (PC) in the KE Discharge Chute recipe is 0.182 (i.e., Portland cement is 26 wt% of the dry mix with water added at a weight ratio of 0.425 times the weight of the total dry mix) and the set density is 1.70 g/cm^3 (Figure 6.1). Therefore, the volumetric power of the grout is:

$$\text{Volumetric power}, \frac{\text{mW}}{\text{cm}^3\ \text{grout}} = \text{Specific power}, \frac{\text{mW}}{\text{g PC}} \times \frac{0.182\ \text{g PC}}{\text{g grout}} \times \frac{1.70\ \text{g grout}}{\text{cm}^3\ \text{grout}}$$

The volumetric power of curing the KE Discharge Chute grout as functions of time and temperature then can be projected based on:

1. Volumetric power, mW/cm^3 grout = 0.3094 g PC/cm^3 grout × specific power, mW/g PC.
2. Heat generation rates doubling with each 10 °C increase in temperature.
3. Time of the peak heat generation halving with each 10 °C increase in temperature.

As shown in Figure 7.5, the maximum volumetric heat generation rate at 20 °C is ~1.1 mW/cm^3 and occurs at about 10 hours. At 60 °C, the maximum grout heat generation rate is ~18 mW/cm^3 and occurs at about 37 minutes.

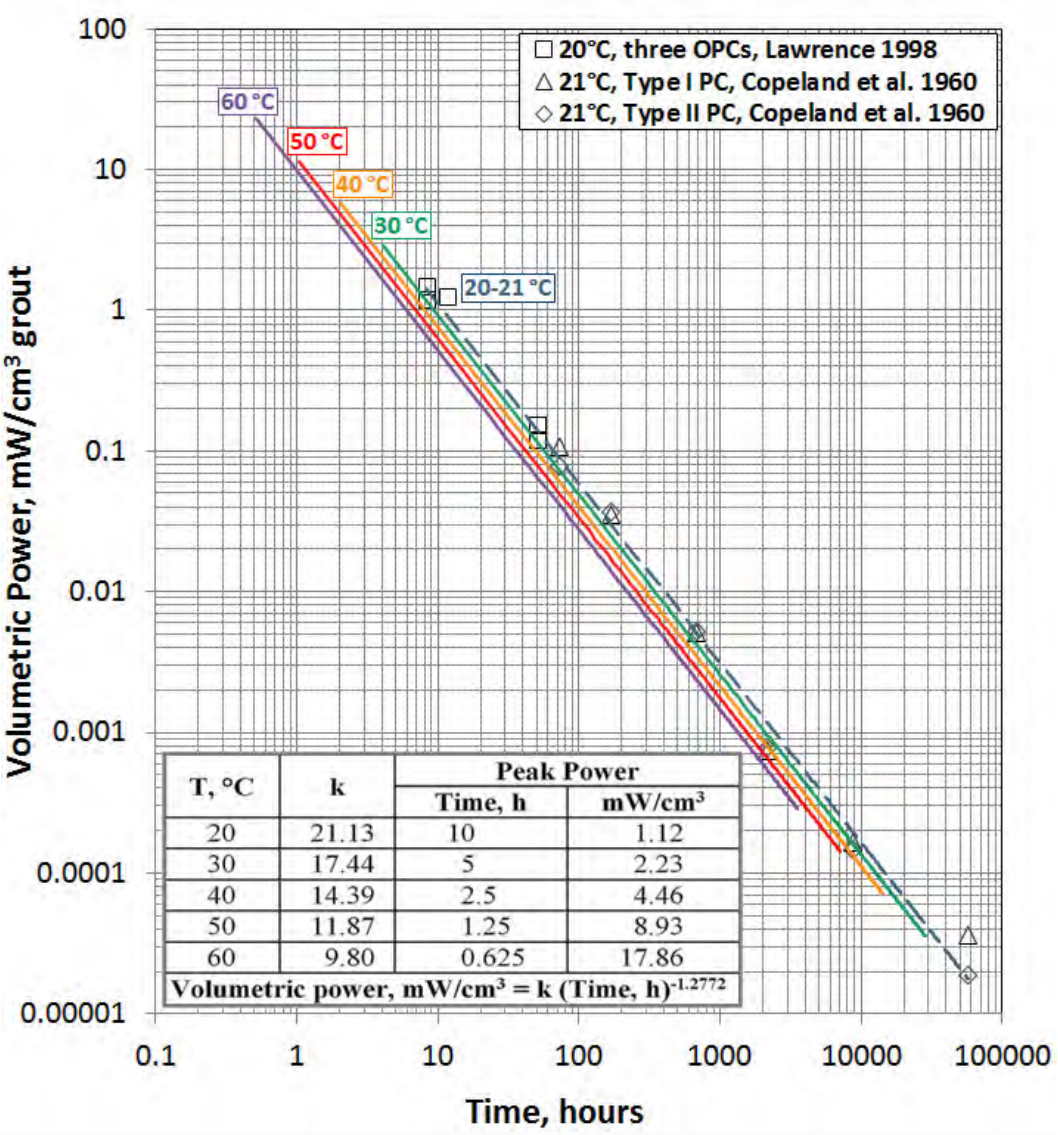

Figure 7.5. Volumetric Grout Heat Generation Rates as Functions of Time and Temperature

The total heat arising from curing the grout at 20 °C commencing at 10 hours and continuing for 20 years according to the heat evolution kinetics described in Figure 7.5, is -142 J/cm^3 of grout or -457 J/g of the contained Portland cement. Virtually identical enthalpies are projected for the integrated curing times at 30, 40, 50, and 60 °C at proportionately shorter times. The Portland cement curing enthalpy determined in this fashion is close to the average enthalpy observed in Figure 7.2 for complete curing of the Type I and Type II Portland cements [(-504 + -430)/2 =] -467 kJ/kg.

The heat arising from Portland cement hydration, if not dissipated to the surroundings, accelerates curing by increasing the grout temperature. This, in turn, further increases the heat generation rate. At the same time, external cooling dissipates the heat to moderate the power generation and grout temperature.

To scope the magnitude of the proposed settler tank stabilization operations, it is valuable to calculate the overall reaction enthalpies available in grouting the settler tanks and complete reaction of their contained uranium metal. From Table 2.1, the uranium metal inventory in the settler tanks is 123.9 kg and as stated in Section 5.0, the uranium metal corrosion reaction enthalpy is -513.2 kJ/mole. Therefore, the heat evolved in reacting all of the uranium metal to extinction is:

$$123.9 \text{ kg U} \times \text{mole}/0.238 \text{ kg} \times -513.2 \text{ kJ/mole} = -2.67\times10^{5} \text{ kJ}$$

The contained volume of the settler tanks is 9677 liters (Section 3.0) with only ~56 liters occupied by sludge (Table 2.1), to give a maximum available grout volume of 9621 liters obtained by completely filling all of the settler tanks. The estimated hydration enthalpy for Type I/II Portland cement is -467 kJ/kg cement (Figure 7.2). Therefore, the total heat evolved upon curing the grout in the settler tanks is:

$$9621 \text{ L grout} \times 1.70 \text{ kg grout/L grout} \times 0.182 \text{ kg PC/kg grout} \times -467 \text{ kJ/kg PC} = -1.39\times10^{6} \text{ kJ}$$

The combined heat arising from running the uranium metal oxidation and grout curing reactions to completion is -1.66×10^{6} kJ.

The Weasel Pit volume is 77,053 liters (Section 3.0), meaning the water volume in the Weasel Pit is (77,053 liters [total volume] – 9621 liters [settler tank volume not occupied by sludge]) = 67,432 liters, ignoring the volume displaced by the structural steel and estimated 40 ± 30-liters of sludge on the Weasel Pit floor (Table 1 in Slotemaker 2013). The heat capacity of the water in the Weasel Pit is:

$$4.184 \text{ kJ/liter·K} \times 67{,}432 \text{ liters} = 2.82\times10^{5} \text{ kJ/K}$$

while the heat capacity of the grout is:

$$9621 \text{ liters} \times 1.70 \text{ kg/liter} \times 1.16 \text{ kJ/kg·K} = 1.90\times10^{4} \text{ kJ/K}$$

The heat capacity of the Weasel Pit contents, water, and grout, but ignoring the concrete walls and structural steel, thus is the sum of the water and grout heat capacities, or 3.01×10^{5} kJ/K.

Based on complete reaction of the uranium metal, complete curing of the Portland cement in the grout, and the heat capacity of the Weasel Pit contents, the hypothetical adiabatic temperature increase is only 5.5 °C:

$$1.66\times10^{6} \text{ kJ} \times \text{K}/3.01\times10^{5} \text{ kJ} = 5.5 \text{ K}$$

This calculation shows that the potential supplemental heat sink afforded by the balance of the KW Basin waters is unnecessary and thus that guarantee of water circulation between the Weasel Pit and the rest of the KW Basin is not required.

However, the evolution of localized heating within the uranium metal-bearing grouted settler tanks and particularly the temperature profiles experienced by the uranium metal deposits are more complicated. Specifically, volumetric heat-balance calculations must be made to determine whether the uranium metal deposit temperatures become sufficiently high to allow thermal runaway to occur. This heat-flow modeling must determine the combined effects of the heating and heat-dissipation phenomena

given the geometric and thermal properties of the Weasel Pit and its contents during and after the grouting operations.

Subsequent D4 operations also must be considered to determine whether uranium metal thermal runaway conditions can occur in retrieval, packaging, and ERDF disposal of the grouted settler tank materials and to identify process limitations and potential mitigations. These considerations are examined in Section 8.0 of this report.

8.0 Modeling of Thermal Behavior of Settler Sludge

In the previous sections, the settler tank contents, and the distribution and overall geometry of the settler tanks and Weasel Pit, have been defined. Thermodynamic models for the exothermic behavior of uranium metal oxidation and curing of Portland cement have been developed. With these inputs, heat transport finite element analysis is used to evaluate the thermal stability of various process scenarios associated with the solidification and subsequent handling of the settler tank material. The cases evaluated, input parameters used, the modeling approach, and results are presented in this section.

8.1 Approach

8.1.1 COMSOL Model

COMSOL Multiphysics, Version 4.3b (and 4.3b with heat transport module), is a finite element analysis (FEA), solver, and simulation software package for various physics and engineering applications, especially coupled phenomena, or multiphysics. The software is available in cross-platform versions (Windows, Mac, Linux). In addition to conventional physics-based user interfaces, COMSOL Multiphysics also allows entering coupled systems of partial differential equations (PDEs). The PDEs can be entered directly or using the so-called weak form. In the latter case, heat transport equations come from the heat transfer module, which has pre-programmed boundary and transport equations.

Models were set up to represent the geometries of the settler sludge application scenarios being investigated. Boundary conditions and thermal properties (density, thermal conductivity, and heat capacity) were set by the user. Heat generation sources, exothermic reactions, and radioactivity decay heats were input into the model. The model was then used to determine the temperature of the system as a function of time and location. To compensate for uncertainties in how well thermal properties are known, bounding conditions for the properties and heat sources were evaluated during modeling. The goal was to understand conditions that lead to a temperature greater than 100 °C in the uranium sludge layer. If 100 °C is reached, the configuration is considered thermally unstable because voids in the solids and water caused by water vapor seriously degrade thermal conductivity even as uranium metal reaction continues unabated. It is noted in Section 5.0 that the reaction of uranium metal with anoxic water vapor proceeds at the same rate as in anoxic liquid water of the same temperature. Finally, the model must give reliable predictions within established bounding conditions (for example, the upper bounding uranium reaction rate is 3× the nominal rate).

8.1.2 COMSOL QA Approach

Quality assurance of the COMSOL modeling done in this study was conducted in two ways: benchmark modeling and subject matter expert technical review. COMSOL Multiphysics provides “A Model Library Manual, Heat Transfer Module, 5.0 COMSOL”. This library contains numerous solved benchmark COMSOL Cases. To verify correct functioning and installation of COMSOL, the analyst programmed and evaluated the case, “Heat Conduction in a Cylinder” on both workstations used for this project. This case was taken from a NAFEMS benchmark collection and shows an axisymmetric steady-

state thermal analysis. The benchmark testing produced a result of 332.957 K (on both workstations), which matches the results stated in the benchmark case of 332.957 K at the same location of radius = 0.04 m and length = 0.04 m.

The quality of the COMSOL analyses was also assured via the use of subject matter expert technical review of the modeling set up and results. Input parameters to the model were also subjected to independent technical review. Results of the benchmarking case are included in Appendix A. Documentation of the techical review of the modeling is provided in Appendix B. Detailed records on each case modelled have been provided to the STP and are maintained in the project records.

8.1.3 Overview of Cases

Implementation of the recommended *in-situ* grouting, size-reduction, and ERDF disposal of the settler tanks involves a series of process steps that place the settler sludge under differing boundary conditions that affect thermal stability. For each of these steps, hereafter referred to as cases, a separate model was developed and assessed. The cases are summarized in Table 8.1. Also note that results in Appendix A are labeled using this case nomenclature.

Table 8.1. Overview of Cases Modeled

Case Number	Description
Case 1	Underwater grouting of highest U metal-content tank section (2D Model, Tank S5, Location B). Grout pumped into the settler tank, and stability examined with the ensuing heat of hydration from grout-former reactions. This case also includes an adiabatic test case with no heat flow beyond the settler tank walls to evaluate thermal stability with the wall of settler tank perfectly insulated.
Case 2	Grouted settler tank array backfilled with sand. 2D model of highest U metal-content cross-section in the settler tanks (located 2 to 2.75 feet into settler), water removed from the basin, and Weasel Pit backfilled with sand.
Case 3	Grouted settler tank underwater plus 14 inches of grout added to floor of Weasel Pit. 2D model of highest U metal-content cross-section with grout pour submerging bottom 2 inches of tanks S5 and N5.
Case 4	Grouted settler tank underwater plus 6 inches of grout added to floor of Weasel Pit. Same as Case 3 except top of grout floor pour is 6 inches below bottom of S5 and N5.
Case 5	Settler tank section in IP2 Waste Box 3D model. 1.25-foot section of the worst-case settler tank section placed into the IP2 waste box (10 ft × 20 ft × 10 ft) filled with wet or dry sand. This case is not a realistic disposal option; however, it illustrates 3D thermal behavior of settler tank section surrounded by fill.
Case 6	Settler tank section in 4 ft × 6 ft × 4 ft box with carbon steel cradle surrounded by sand. Carbon steel cradle is used as a heat sink. To provide good thermal connection, a thermal conductivity grease fills the space between the settler tank and the cradle.
Case 7	Settler tank section in box with carbon steel cradle embedded in high-conductivity grout, with top filled with sand. Use of high-thermal-conductivity grout in the 4 ft × 6 ft × 4 ft box improves robustness of the heat sink concept.
Case 8	Same as Case 7, but with reasonably bounding solar heating on top of box. Maximum solar heating rate, 24-h per day, imposed until steady state is established and then uranium metal reactions are initiated in model. Sand fill in top of box helps insulate settler tank section from solar insolation.

Case Number	Description
Case 9	Case 9 is Case 1 with substitution of convective cooling for the constant-temperature boundary conditions. This case examines the condition when the basin is dewatered, or if/when sections of settler tanks are stored in air.
Case 10	Same as Case 8 but with settler tank section increased to 4.25 ft. Depth of uranium-rich sludge maintained at 2.35 cm, and length of cradle increased to 5 ft with solar heating on top of box and on one side.

8.2 Model Input Parameters

8.2.1 Heat Sources

The thermal stability modeling accounts for heat generation associated with up to four sources, depending upon the case: 1) uranium metal reaction, 2) radioactive decay heat, 3) grout curing heat of hydration, and 4) solar insolation. These sources, along with the values used in modeling, are described below.

8.2.1.1 Uranium Metal Reaction and Decay Heat

The reaction rate of uranium metal in anoxic water (and in grout) is described in Section 5.0. The reaction rate is proportional to the metal surface area and is a function of temperature according to Arrhenius kinetics. To account for uncertainties in the rate equation and knowledge of the uranium metal reactive surface area, a rate multiplier, typically a factor of three, is used for conservatism. Table 8.2 summarizes the development of the heat generation terms associated with uranium metal as used for the model.

All uranium (including uranium oxide) in the settler tanks was treated as "uranium metal" for the modeling. This treatment provides approximately 15% more reaction power per unit volume than by considering only the uranium metal inventory (i.e., a uranium metal concentration of 9.2 g/cm^3 instead of 8 g/cm^3). Furthermore, uranium metal has a higher decay power than uranium oxides, since most of the ^{137}Cs dissolves and is lost from the solid matrix during uranium metal oxidation in water. The treatment of all uranium as "uranium metal" simplifies the modeling and provides a modest level of conservatism.

Uranium metal corrodes at very slow rates at the typical temperature of the KW Basin pool water (e.g., the extinction time for a 600-µm diameter particle at 20 °C, assuming anoxic corrosion, is more than 10 years). Consequently, taking credit for the consumption of uranium metal by oxidation while it resides in the settler tanks at low temperatures is speculative. Therefore, for most of the modeling cases, the uranium surface area is conservatively assumed to remain constant. This approach is not unreasonable, since reaction rates in a bed of uranium particles remain essentially constant during the time period when the first ~70 mass% of a bed of uranium metal particles are consumed (Delegard and Schmidt 2009; Schmidt et al. 2003; and Appendix G of Schmidt and Sexton 2009). In most of the cases modeled, conditions of thermal instability or thermal runaway, if reached, occurred within a period of days.

To model cases at which thermal stability over a longer time period was of interest (e.g., section of the settler tank packaged in disposal boxes, awaiting burial at ERDF), while the box is at elevated

temperature for a prolonged period of time, a heat generation cut-off point was included in the model to appropriately simulate the extinction of uranium metal.

Table 8.2. Parameters for Development of Heat Source Term from Uranium Metal

Parameter	Unit	Value/equation	Reference
U_{metal} particle diameter	µm	= ¾ (Max diameter) = ¾ (600) = 450	Section 2.0 and Johnson 2014
U_{metal} surface area per unit mass	cm^2/gU_{metal}	7.02	450 µm spherical particles, U metal density = 19 g/cm^3
Rate U + 2 $H_2O \rightarrow UO_2 + 2\ H_2$	$\log_{10}$rate[mg(loss)/cm^2-h], where T = 297 to 623 K	9.9752 - 3565.8/T	Johnson 2014
Rate Multiplier	Safety Basis Factor × Nominal Rate	3×	Johnson 2014
Reaction Heat	J/g_{Umetal}	513.2 kJ/mol × 1000/ 238g/gmol = 2156.3	See Section 2.0 and Delegard and Schmidt 2009
[U_{metal}] in settler tank	$g_{Umetal}/cm^3_{settler}$	9.2	See Section 2.0 and Sloughter 2013
Power from U_{metal} corrosion at 60 °C in settler tank	mW $/cm^3_{settler}$	7.3	Calculation at 60 °C given for relative comparison to decay heat.*
Decay Heat (July 9, 2012)	W/MTU (watt per metric ton uranium)	97.9	Johnson 2014
Decay Heat	$mW/cm^3_{settler}$	0.90	Calculation for comparison purposes

$$* \frac{9.2\ \text{g U}}{\text{cm}^3} \times \frac{7.02\ \text{cm}^2}{\text{g U}} \times \frac{1.88\times10^{-4}\ \text{g U}}{\text{cm}^2\cdot\text{hour}} \times \frac{\text{hour}}{3600\ \text{sec}} \times \frac{2156.3\ \text{J}}{\text{g U}} = \frac{7.3\ \text{mW}}{\text{cm}^3}$$

8.2.1.2 Grout Curing Heat of Hydration

As discussed in Section 6.0, due to similarity of performance objectives, including strength adequate for subsequent sectioning and removal, low curing heat, and technical underpinning through extensive developmental testing, the recipe used for grouting the KE Basin Discharge Chute has been chosen for modeling the immobilizing of the settler tank contents and for grouting the floor of the Weasel Pit. The thermal power generated by the K East Discharge Chute grout in its curing (i.e., hydration) reactions depends largely on the grout's complement of Type I/II Portland cement, with much less dependence on the content of Class F fly ash, the other principal grout ingredient. Also, as noted in Section 7.0, the thermal power increases with temperature according to Arrhenius kinetics.

The specific power of Portland cement hydration reactions at 20 °C in the first 50 hours is shown in Figure 7.1. This thermal output curve is widely characteristic of Portland cement, showing an immediate relatively high spike upon mixing the dry Portland cement with water. This heat spike is caused by dissolution of calcium hydroxide. The heating rate then rapidly drops, reaching a minimum within one hour, before climbing again to reach a maximum at about 8 to 12 hours at 20 ° C as the numerous cement hydration reactions commence. The heating rate then declines predictably as the hydration reactions

continue for extended times (years). The specific thermal power of Portland cement hydration with time is shown in Figure 7.3.

The effect of temperature on Portland cement hydration reactions also was examined in Section 7.0. An extensive set of tests showed the hydration reactions followed Arrhenius kinetics over ~4 to 110 °C curing temperatures with ~24-degree temperature rise needed for the hydration rates to double. A much less extensive data set showed that Portland cement hydration rates doubled with only a 10 °C rise. Conservatively, we assume here that the more temperature-dependent rate increase is observed, with rates doubling with each 10 °C rise.

We also make the extremely conservative assumption that the initial grout temperature is 60 °C. The initial temperature of the grout mixture used in the KE Discharge Chute pour was 25 °C (or 77 °F; Figure 6.3). We project the hydration rate, and thus the thermal power, at 60 °C to be 16-times the rates and powers measured (as described in Section 7.0) at 20 °C and the time showing the greatest thermal power to be 10/16 hour, or ~37 minutes.

The specific (mass-based) power of the Portland cement hydration reactions are converted to volume-based powers for the Portland cement–fly ash grout by noting that:

Volumetric power, mW/cm^3 grout = 0.3094 g PC/cm^3 grout × specific power, mW/g PC.

To model the initial thermal power from grout curing, we assume that the immediate initial calcium hydroxide dissolution reaction occurs in the grout mixing tank. We then assume that the mixed grout, at 60 °C, is quickly added to the settler tanks or Weasel Pit floor and from there follows a point-by-point heat-generation profile corresponding to that shown in Figure 7.1, but compressed in time by a factor of 16 and enhanced in power by a factor of 16 as compared with the contours exhibited at 20 °C. The profile is provided for the first four hours at 60 °C. Two more values, at about two weeks and four weeks reaction time at 60 °C, constitute the final input power data. These last two values are derived for the thermal power equation for 60 °C shown in Figure 7.5. The power outputs at times after four hours and between these points are modeled as straight-lines and thus are conservative.

8.2.1.3 Solar Insolation

Solar insolation data for Latitude 46° N were taken from the Sludge Technical Databook (Table 4-34 of Johnson 2014). For modeling, only the values of the horizontal surface facing upwards were used. For conservatism, we assume 24 hours-per-day and 7 days-per-week direct solar heating of the waste box, ambient air temperatures of 50 °C, and ground temperatures reaching 50 °C. Such conditions are highly unlikely without human intervention. Because of the extra complexity of adding radiative and convective heat transport, a reasonably bounding scenario was developed. In this scenario, the sun was assumed to be directly overhead and continually heating the box at an approximate noonday heating of 990 W/m^2 [314 $BTU/(h \times ft^2)$]. The top of the box and the side walls were allowed to be cooled both radiatively and convectively with an ambient air temperature of 50 °C. The ground underneath the box was assumed to remain at constant 50 °C, with the initial box and content temperature being at 50 °C.

In simulations to evaluate solar heating from the top and one side, the heating rate on one side for the box was set at 495 W/m^2 (i.e., 50% of the solar heating rate applied to the top of the box). Other cases were also evaluated, including 50% maximum on top, and 50% maximum on one side. The approach

used for the side heating was the same as used for the top: the box was allowed to heat up over a number of days to achieve equilibrium before the uranium rate equation was activated.

8.2.2 Geometry of Settler Tanks, Weasel Pit, and Disposal Boxes

The key dimensions/geometry of the systems modeled are summarized in Table 8.3.

Table 8.3. Component Dimensions used in Modeling

Parameter	Value	Reference
Settler Tank: Dimensions: (20-in, sch 10 pipe, SST-TP-304)	ID = 49.5 cm (19.5 in)	DOE 2000. See Section 3.0 for more details on Weasel Pit dimensions.
	OD = 50.8 cm (20 in)	
	Wall = 0.635 cm (¼ in)	
	L = 5.25 m (16 ft)	
Location of Tanks N5 and S5 above Weasel Pit floor	32.1 cm (12.625 in)	
Center-to-Center Spacing of Settler Tank, 2 × 5 array	66 cm × 66 cm (26 in × 26 in)	
Weasel Pit	W = 1.47 m (58 in) average L = 9.83 m (32-ft 3-in) Depth = 4.88 m (16 ft)	
IP2 Waste Box: Constructed of 10 gauge ASTM A 1110 carbon steel	W = 3.05 m (10 ft) L = 6.10 m (20 ft) H = 3.05 m (16 ft)	IP2-1800-TL Overview, Drwg 970-156-05, Size B, 2/10/2010. Sheet 1-7, Container Technologies Industries, LLC
Custom ERDF Box: Assume it is constructed of 10 gauge ASTM A 1110 carbon steel	W = 1.22 m (4 ft) L = 1.83 m (6 ft) H = 1.22 m (4 ft)	Personal communication, AJ Schmidt, PNNL, with GM Davis, CHPRC, 1/28/2015.
Heat Sink Dimensions: Heavy-wall carbon steel pipe, cut axially.	ID = 52 cm (20.5 in) Wall thickness = 0.64 to 10 cm (0.25 to 4 in) Length = 99 cm (3.25 ft) or longer	Specialty Pipe & Tube, Inc. 1-713-676-2891 www.specialtypipe.com
Heat Sink Mass per Linear Ft	1-in thick: ~53 kg/ft (120 lb/ft) 2-in thick: ~110 kg/ft (250 lb/ft) 4-in thick: ~240 kg/ft (530 lb/ft)	Calculated
Gap between heat sink and settler tank section	0.159 to 1.27 cm ($^{1}/_{16}$ to ½ in)	Assumed

The bounding uranium metal rich sludge depth in the settler tanks was discussed in Section 2.1 (Table 2.4) and the results used in the models, a bounding cross-section of the North and South tank banks, are presented in Table 8.4.

Table 8.4. Depth of Uranium Metal Sludge in Settler Tanks

Parameter	Location	Value	
Bounding Depth in a Segment	Tank S5, location B, 1.25-ft. segment	Depth = 2.23 cm	
Bounding Cross-section for 10 tanks	2.0 to 2.75 feet in from tank entrance	South Bank cm	North Bank cm
Tank 1		0.686	0.986
Tank 2		1.004	0.716
Tank 3		1.149	0.533
Tank 4		1.433	0.602
Tank 5		2.235	0.459

8.2.3 Values for Physical Properties Used for Modeling

Physical property values for thermal conductivity, density, and specific heat were taken from the Sludge Databook (Johnson 2014), the technical literature, or otherwise derived as described in this report (Table 8.5). Where a range of values was found, a reasonably conservative value was selected.

Table 8.5 Thermal Conductivity, Density, and Specific Heat Values for Modeling

Parameter Name	Description	Unit*	Nominal Value Used	Range Explored	Reference*
ksludge	Uranium metal-rich layer inside settler tanks	W/(m·K)	3.9	0.3 to 3.9	Table 4-18, Johnson 2014
Rhosludge		kg/m^3	9600	constant	U_{metal} (60v%) + Water (40v%). Table 4-19, Johnson 2014
Cpsludge		J/(kg·K)	290	constant	
kwall	Settler tube construction material, 304 stainless steel	W/(m·K)	16.2	constant	CRC 1980; CRC 1978; McGannon 1971; MatWeb, material property database; The Engineering ToolBox (ETB)
rhowall		kg/m^3	8030	constant	
Cpwall		J/(kg·K)	500	constant	
kgrout	Grout, based on formula used for grouting the KE Discharge Chute	W/(m·K)	0.5	0.1 – 1.7	ETB; References, Section 7
rhogrout		kg/m^3	1720	constant	Calculation based on composition
Cpgrout		J/(kg·K)	1165	constant	
kdrysand	Dry sand, proposed as a Weasel Pit backfill material	W/(m·K)	0.13	0.12 -0.3	Table 3.2, Poloski et al. 2002; ETB
rhodrysand		kg/m^3	1900	constant	Table 3.1, Poloski et al. 2002
Cpdrysand		J/(kg·K)	700	constant	silica, Table 4-19, Johnson 2014
kwetsand	Wet sand, proposed as a Weasel Pit backfill material	W/(m·K)	0.5	0.5 – 1.3	Table 3.2, Poloski et al. 2002, ETB
rhowetsand		kg/m^3	1900	constant	60% sand, 40% water (vol)
Cpwetsand		J/(kg·K)	1430	constant	60% sand, 40% water (vol)
ksink	Carbon steel heat block/half-pipe used for heat sink in disposal box	W/(m·K)	30	constant	Assume 1% carbon steel; k up to 43 W/m·K); ETB; Cp ~stainless steel
rhosink		kg/m^3	8000	constant	
Cpsink		J/(kg·K)	500	constant	
kpaste	Paste for good thermal connectivity between heat sink and set tube section	W/(m·K)	0.67	0.5 to 4.0	Vendor literature (e.g., Dow Corning® 340 Heat Sink compound)*
rhopaste		kg/m^3	2100	constant	
Cpaste		J/(kg·K)	1000	constant	
kHTCgrout	High-thermal-conductivity grout for heat sink in disposal box	W/(m·K)	1.0	constant	(0.7 to 1.7 W/mK) CETCO Geothermal Grout™ Enhanced Thermally Conductive Grout Technical Data. CETCO 2013
rhoHTCgrout		kg/m^3	2620	constant	
Cpgrout		J/(kg·K)	1165	constant	
kair	Air that may fill the gap between the setter tank outside wall and the heat sink	W/(m·K)	0.0299 (0.022-0.028)	23–47 °C	CRC 1980
rhoair		kg/m^3	1 (1.4-1.1)	23–47 °C	
Cpair		J/(kg·K)	1009 (1005-1007)	23–47 °C	

* W = watt; m = meter; K = kelvin; kg = kilogram; J = joule
MatWeb = online resource for material property data, http://www.matweb.com/index.aspx.
ETB = The Engineering ToolBox, http://www.engineeringtoolbox.com.
Dow Corning thermal interface silicone grease, https://www.dowcorning.com/content/publishedlit/11-1712-01.pdf

Discussion on Selection of Thermal Property Values

Sludge: Sludge, for the purposes of the present report, is the settled solid contents of the settler tanks. For the uranium metal-rich portion of the sludge of most concern, property values were taken from the Sludge Databook (Johnson 2014) or were calculated from the Databook using a 60/40 volume ratio of uranium metal and water.

It was noted in Section 2.1 that the settler tanks also hold approximately 40.1 liters of non-uranium sludge. Based on Poloski et al. (2002), this sludge likely has a thermal conductivity of approximately 0.7 W/(m·K), i.e., similar to grout, and thus is not independently assessed in the modeling.

Grout: The grout used to seal the KE Discharge Chute as described in Section 6.0 was used as the grout formulation in the modeling based on its favorable low heat-generation, placing, and strength characteristics. Section 6.0 describes the density and Section 7.0 the specific heat of this grout. The thermal conductivity varies with extent of curing and is greatest immediately upon mixing. As curing proceeds, hydration reactions occur which serve to fix the water into solid phases, remove the water from the interstitial liquid phase, and lower the thermal conductivity. The thermal conductivity of air-dry hardened Portland cement pastes is about 0.5 W/(m·K) (derived from Figure 2.1 of ACI 2002b). The thermal conductivity of cured and oven-dried Portland cement is about 0.52 W/(m·K) while the thermal conductivity of oven-dried fly ash is about 0.58 W/(m·K) (both derived from Table 2.1 of ACI 2002b) at the 106 pound/foot^3 (1.72 g/cm^3) density of the KE Discharge Chute grout. However, the grout constituents are not dry. At 80% relative humidity, the cured grout would have a thermal conductivity of 0.73 W/(m·K) for the Portland cement, fly ash, and water constituents based on sum-of-fractions calculation and the influence of moisture on the Portland cement and fly ash as taken from Table 2.2 of ACI (2002b). The thermal conductivity of the waterlogged grout would be somewhat higher than this and is estimated by the present authors to range from 0.8 to 1.0 W/(m·K). The modeling calculations showed that the stability of the grouted waste form to thermal runaway was not influenced greatly by the grout thermal conductivity.

The specific heat of the KE Discharge Chute grout is also influenced by the extent of curing and the disposition of the water within the grout (i.e., whether “free” or chemically “bound”). The specific heat of 50:50, by weight (dry), fresh Portland cement and fly ash mixtures with 0.4 weight fraction water with respect to Portland cement is 1700 J/(kg·K) but decreases to about 700 J/(kg·K) after 28 days of curing at 28 °C (Figure 3c of Choktaweekarn et al. 2009). Based on a sum-of-fractions approach described by Bentz and colleagues (2011) and illustrated in Table 8.6 below, the specific heat of fresh grout is estimated to be 1755 J/(kg·K) but decreases to 1165 J/(kg·K) upon curing. This latter value was selected as the nominal specific heat of the grout.

Table 8.6. Calculation of KE Discharge Chute Grout Specific Heat by the Sum-of-Fractions Method

Component	Quantity, wt%	Density, g/cm^3	Specific Heat, J/(kg·K) fresh / cured
Water	29.82%	1.0	4179 / 2200*
Portland Cement Type I/II	18.25%	3.25	740
Class F Fly Ash	51.93%	2.3	720
Mixture	100%	1.72	1755 / 1165

* Heat capacity of bound water in cement. Specific heat of mixture calculated by rule of mixtures, Bentz et al. (2011).

High-Conductivity Grout: High-thermal-conductivity grout is recommended to enhance the heat transfer of the heat sink concept proposed for the waste disposal box. High-thermal-conductivity grout mixtures are commercially available (e.g., CETCO© enhanced thermally conductive grout; CETCO 2013), with recommended recipes that provide a final grout with thermal conductivities ranging from 0.7 to 1.7 W/(m·K).

Sand: Wet/damp sand and dry sand were investigated as backfill material for the Weasel Pit and for use as backfill material in waste boxes. Depending upon its degree of saturation, sand can behave as an insulator (dry sand) or a reasonable thermal conductor (water-saturated sand). During a campaign to measure the thermal conductivities of K Basin sludge types, a number of simulants, including wet and dry sand, were assessed (Poloski et al. 2002). Measured thermal conductivity values from this campaign fall within the range of literature values, and have been used for the modeling input. Additionally, a model for estimating physical properties of soil types (including sandy soils) as a function of saturation has been published (Campbell et al. 1994) and the predictive values (http://decagon.com/py-bin/tcc/chart) were found to be consistent with values used as input for the COMSOL modeling.

Carbon Steel Heat Sink: For a heat sink in the waste disposal box, a half-pipe, cut from a heavy-walled carbon steel pipe, has been proposed. Reported values for the thermal conductivity of carbon steel ranged from 27 to as high as 65 W/(m·K) (Handbook of Chemistry and Physics, 80th ed). To maintain some flexibility and conservatism in final material selection by STP, for COMSOL modeling, a thermal conductivity value of 30 W/(m·K) was selected. The values for density and heat capacity were kept the same for stainless steel and carbon steel.

Thermally Conductive Paste: To provide good thermal connection between the outer wall of the settler tank and the half-pipe heat sink, a paste was included in the model. Numerous thermally conductive pastes/greases (non-curing) are commercially available with compositions tailored to achieve desired thermal conductivities and viscosities. Prices for these paste material vary by more than an order of magnitude. Thermally conductive gel pads may be another option. However, a commercial source for pads with a thickness of up to ¼ inch was not found. A range of thermal conductivities for the paste was explored in the COMSOL model to allow selection of a cost-effective material. Table 8.7 provides a listing of commercial products to illustrate the range of option available.

Table 8.7. Options and Properties of Thermally Conductive Pastes

Product ID	Thermal Conductivity, W/(m·K)	Density, kg/L	Specific Heat, J/(kg·K)	Vendor
TC-5022, TC5026, TC 5121, SE4490CV, SC 102, 340 Heat Sink compound	0.54 to 4.0	2.14 to 4.06	Not Listed	Dow Corning
Thermally Conductive Grease 2031, 2035, 2036	2.7 to 4.1	Not Listed	Not Listed	3M
Cool Grease and Cool-GapFill Greases and Gel Pads	2 to >8	Not Listed	Not Listed	AI Technology, Inc.

8.3 Modeling Results

An overview description of the modeling cases evaluated is provided as Table 8.1. This section provides a description and discussion of each case, and summaries key findings and conclusion from each case. Addition details on the individual runs for each case are included in Appendix A.

8.3.1 Underwater Grouting of Highest U-Content Tank Section (Case 1)

Case 1 evaluates the heating of the uranium sludge layer in the settler tank as KE Discharge Chute formula grout is added to fill the settler tank and immobilize the sludge. While the grout cures, heat is generated by the various grout former hydration reactions. Figure 8.1 depicts a two-dimensional (2D) cross-section of the settler tank at an increment of time. In this figure, the temperature color key shows that the warmest location is at the center of the tank. The sludge layer, depicted as the horizontal line at the bottom of the tank, is essentially at the same temperature as the wall of the settler tank (a thermally stable condition).

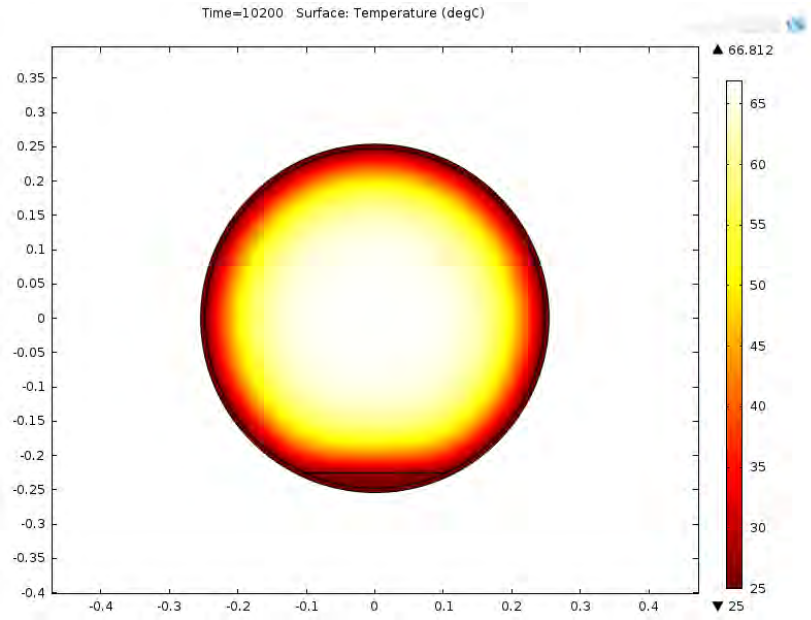

Figure 8.1. Two-Dimensional (2D) Cross-Section of a Tank Modeled in COMSOL Multiphysics

8.3.1.1 Key Parameters & Assumptions

- Two-dimensional modeling was limited to the settler tank segment with the deepest layer of uranium-rich sludge. All other sections, with less uranium metal depth, would exhibit greater thermal stability.
- Case 1 examined a single settler tank being grouted (vs. multiple tanks being grouted simultaneously).
- It was assumed that conduction and convection of Weasel Pit water outside the tank wall will keep the tank surface close to that of the Weasel Pit water temperatures. Use of this assumption is underpinned by the adiabatic calculation conducted around the Weasel Pit when all 10 settler tanks were grouted simultaneously and 100% of the uranium reacted (Section 7.0).

Sensitivity testing of the model showed that thermal conductivity of the sludge layer, the temperature of the surrounding heat sink (Weasel Pit water), and the uranium reaction rate multiplier factor were the parameters that most affected thermal stability. Therefore, thermal conductivity of the sludge layer was varied from 3.9 W/mK (fuel piece sludge) to 0.3 W/mK [i.e., equivalent to a dry mixture of K Basin simulant and tungsten cobalt metal particles (Poloski et. al. 2002)]. Exploration of the lower end of this thermal conductivity range was examined to investigate cases in which evolved gas (H_2) would displace interstitial water in the sludge bed.

8.3.1.2 Results

Two physical situations were studied with the 2D COMSOL simulation. This includes an adiabatic case (no heat losses) and a case with the surface walls and initial material temperatures set to various temperatures. The adiabatic case, not surprisingly, led to thermal runway in the model after seven-and-a-half hours. Figure 8.2 shows the temperature profile just before the uranium sludge layer temperature rises above 100 °C, solved with baseline parameters.

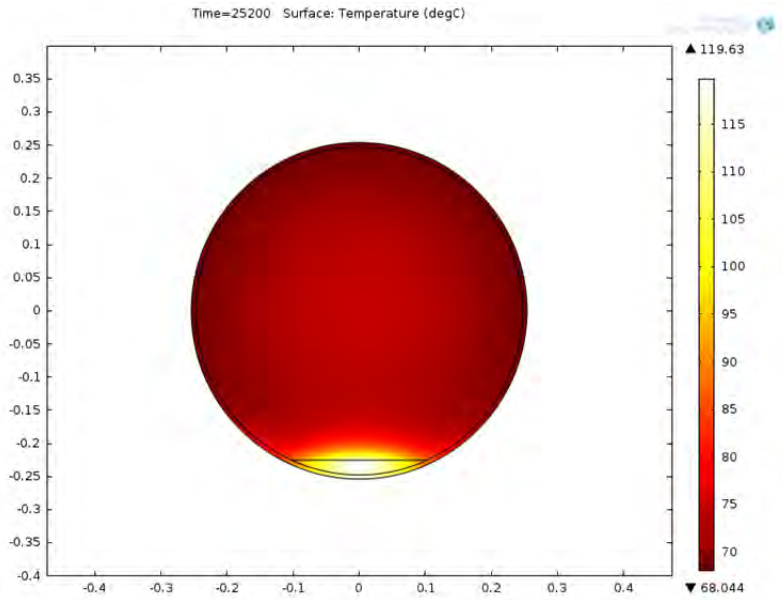

Figure 8.2. 2D Cross-Section of Grouted Tank Seven Hours After Initial Grouting with Adiabatic Tank Wall Boundaries (i.e., no heat flow)

The maximum temperature of the uranium sludge with time is shown below in Figure 8.3.

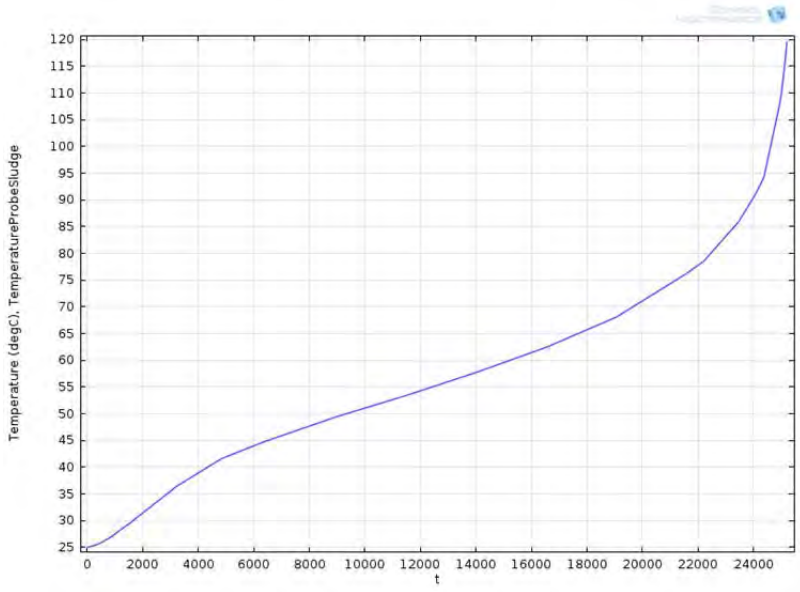

Figure 8.3. Maximum Uranium Sludge Temperature in Centigrade Plotted versus Time (seconds) for Adiabatic Boundary Conditions

In contrast, if heat dissipation is allowed by setting the wall temperatures to a constant temperature of 25 °C, the baseline parameters give a very stable result. Figure 8.4 and Figure 8.5 below show the temperature profiles in a 2D cross-section and the maximum uranium sludge temperature with time.

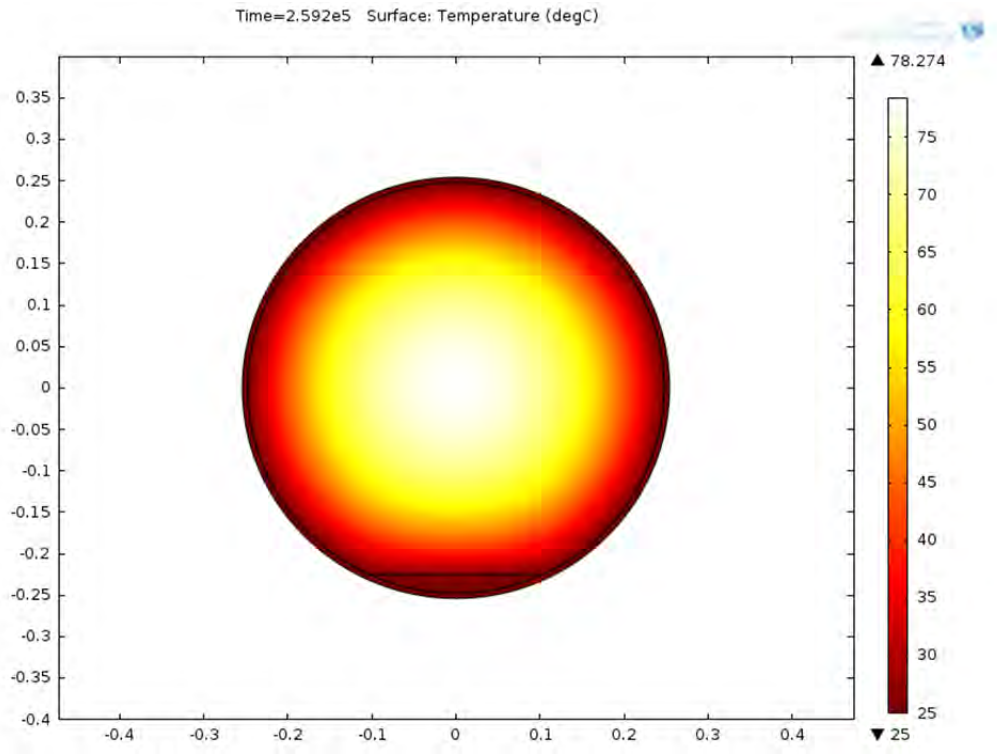

Figure 8.4. 2D Cross-Section of Grouted Tank 72 Hours After Initial Grouting with Tank Wall Boundary Set to 25 °C

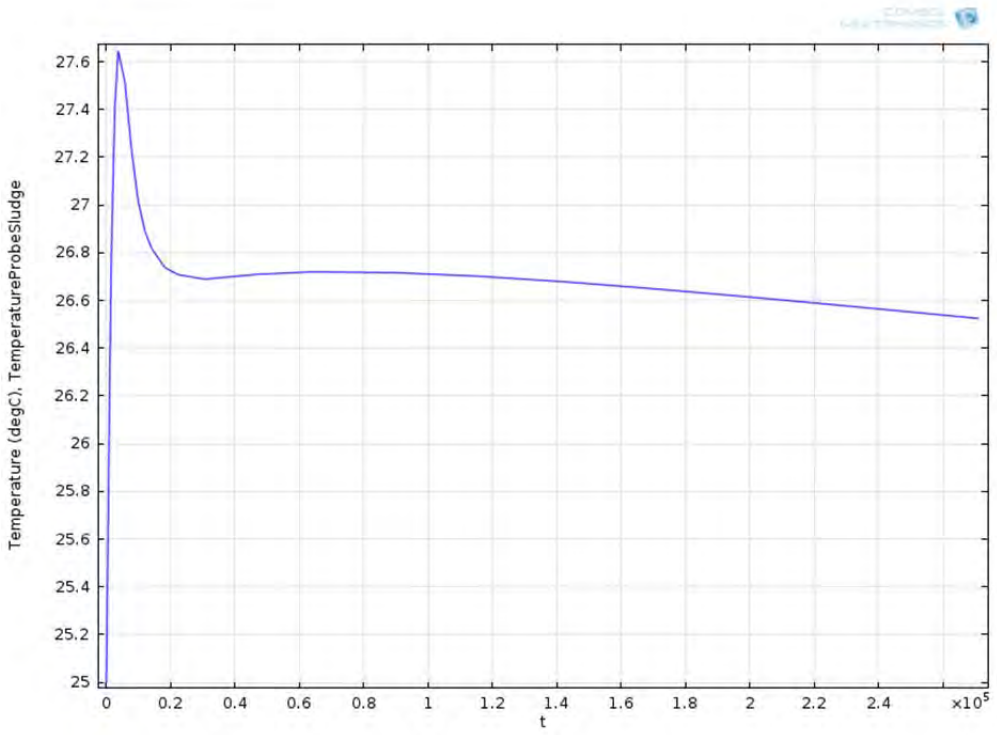

Figure 8.5. Maximum Uranium Sludge Temperature in Celsius Plotted versus Time (seconds) with Tank Wall Boundary Set to 25 °C

To test the importance of the assumption of the tank wall temperature being close to basin pool water temperature, the wall temperatures and the initial material temperatures were varied. In addition, varying uranium sludge depths (maximum depth or two times the maximum depth) were evaluated along with increased uranium sludge reaction rates (1× versus 3×). The minimum wall and starting temperatures before the uranium sludge temperature would ultimately climb to or above 100 °C are shown below in Figure 8.6. At the baseline fuel piece sludge thermal conductivity [3.9 W/(m·K)], thermal stability is maintained for all cases examined if the basin pool is ≤ 60 °C (140 °F). As show in Figure 8.6, conditions of thermal instability only occur when two or three parameters are simultaneously taken to bounding conditions.

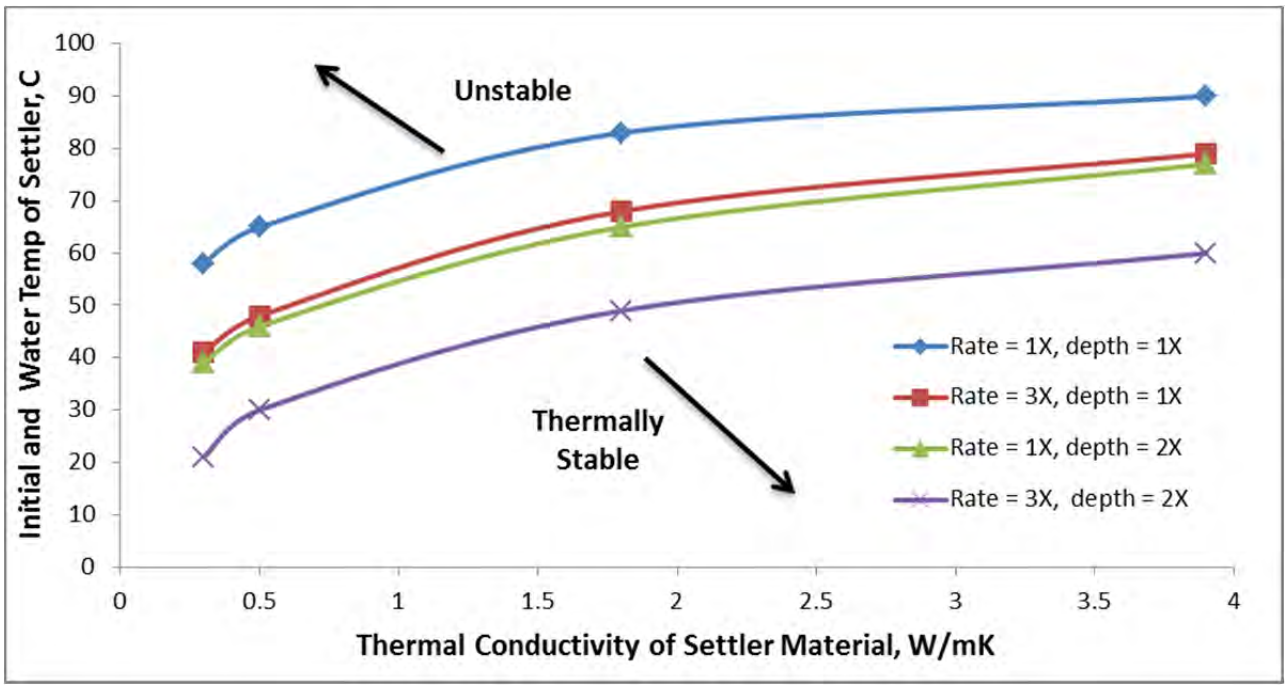

Figure 8.6. Sensitivity of Thermal Stability of Grouted Tank as a Function of Sludge Thermal Conductivity, Rate Multiplier, and Sludge Depth

8.3.1.3 Conclusions

In conclusion, for Case 1, the maximum amount of possible heat generated by the grout and the uranium sludge will only raise the temperature of the Weasel Pit 5.5 °C. While local water temperatures around the tanks will rise, the total temperature increase before instability results, at a rate multiplier of 3×, is greater than 75 °C. This is highly unlikely given natural convection and conduction that will occur in water. If more defense-in-depth is desired, circulation of water around the tanks during grouting could be pursued to maintain forced convection at the wall temperatures at or very near to the bulk pool temperature.

8.3.2 Grouted Settler Tanks Backfilled with Sand (Case 2)

This case examined the stability of the uranium sludge in a 2D cross-section of the Weasel Pit with the Weasel Pit backfilled with either wet or dry sand. Based on input from STP, the time frame needed to

maintain thermal stability for this work evolution (draining the KW Basin, filling the Weasel Pit with backfill, shearing the settler tanks, and placing the settler tank sections in a waste disposal boxes) is four days.

8.3.2.1 Key Parameters & Assumptions

- The time frame needed to maintain thermal stability for this work evolution is four days. In this section, thermal stability was evaluated for five days.
- Grout in the settler tank will be mostly cured before the KW pool is drained and most of the hydration reactions will have occurred (i.e., cure time of 28 days or longer).
- Adiabatic boundary conditions at the Weasel Pit walls were assumed (i.e., no credit assumed for the heat capacity of the cement structure of the Weasel Pit).
- Uranium metal sludge depth is the highest cross-section level for each tank (Table 8.4).
- Physical properties for the backfill material are as defined in Table 8.8, based on Poloski et al. 2002.

Table 8.8. Thermal Properties of Sand Used for Backfill

Case	Void Fraction	Wt Fract. Water	Density, kg/m^3	Cp, J/(kg·K)	K, [W/(m·K)]
Dry Sand	0.4	0	1600	700	0.13
Moist/Damp Sand	0.4	0.11	1800	1050	0.78
Wet Sand	0.4	0.2	2000	1400	1.3

Cp, pure components: water = 4180 J/kg·K; sand/silica = 700 J/kg·K
Solids thermal conductivity of silica = ~1.6 W/m·K

8.3.2.2 Results

Simulation of dry and wet sand hinged on changing the sand thermal conductivity. The wet sand conductivity was set to 1.3 W/(m·K) with the dry sand conductivity being set to 0.13 W/(m·K). Assuming an initial system temperature of 25 °C, the maximum temperature rise in the sludge was 2.6 °C for wet sand and 3.6 °C for dry sand. Figure 8.7 below shows the temperature profile of the dry sand solution. The temperature rise of the dry sand versus time is shown in Figure 8.8.

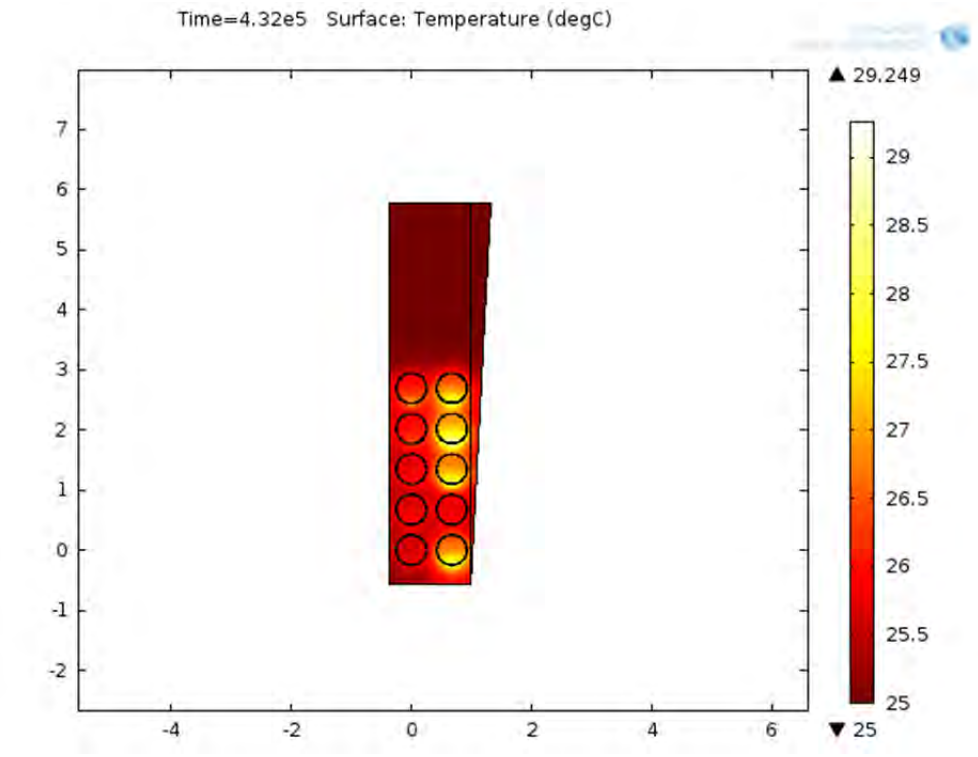

Figure 8.7. Weasel Pit Temperature Prediction After Five Days from Backfilling with Dry Sand

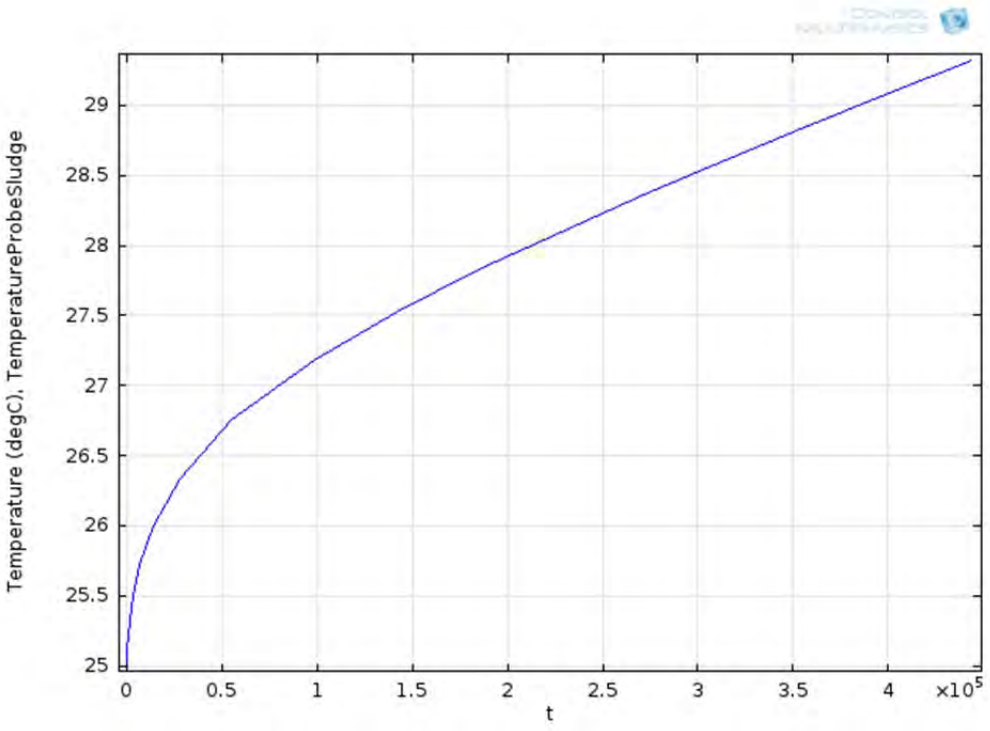

Figure 8.8 Maximum Temperature in Celsius of the Uranium Sludge for the Dry Sand versus Time in Seconds

The smaller change in temperature over time when the Weasel Pit is backfilled with wet sand is displayed in Figure 8.9.

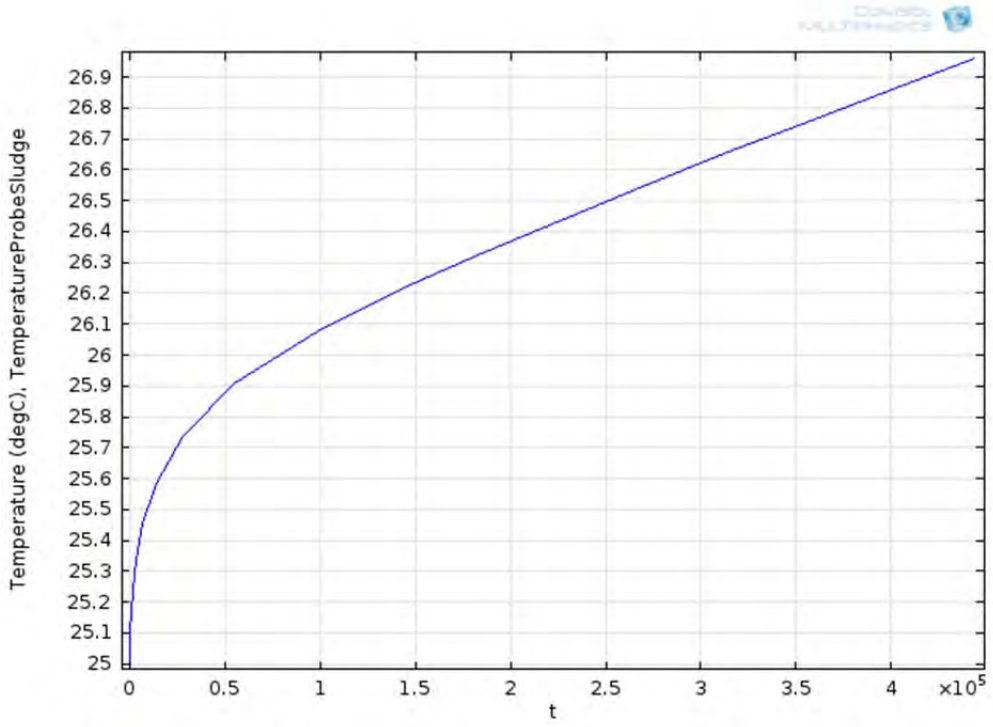

Figure 8.9. Maximum Temperature in Celsius of the Uranium Sludge for the Wet Sand versus Time in Seconds

8.3.2.3 Conclusions

In conclusion, the temperature change simulated of the uranium sludge was minimal for both wet and dry sand. This leads to the conclusion that addition of room-temperature sand will not lead to adverse heating of the uranium sludge over a five-day period of time. At 1× uranium reaction rates, the uranium sludge is stable with an initial system temperature up to 44 °C for five days, and at 3× it is stable up to 26 °C. Increasing the conductivity and heat capacity by addition of water (wet sand) leads to stability of 56 °C at 1× and 39 °C at 3× uranium rates, respectively, for a five-day period.

8.3.3 Grouted Settler Tank Underwater + 14 Inches of Grout Added to Floor of Weasel Pit (Case 3)

Case 3 explores grouting of the floor of the Weasel Pit before draining the water from the basin. Based on the drawings, it was estimated that the bottom of the N5 and S5 tanks is 12 inches from the bottom of the Pit (KW Fuel Storage Basin IWTS Settler System Assembly & Details, As-Built, Drwg No. H-1-83330, Rev 7, Sheet 1/3, 6/7/2000). From these dimensions, the addition of 14 inches of grout on the bottom of the Weasel Pit with water above the grout was investigated. Figure 8.10 below shows the temperature profile of the 14-inch-grouted Weasel Pit after 16.7 hours at 1× uranium reaction rate with wall boundary conditions set at 25 °C.

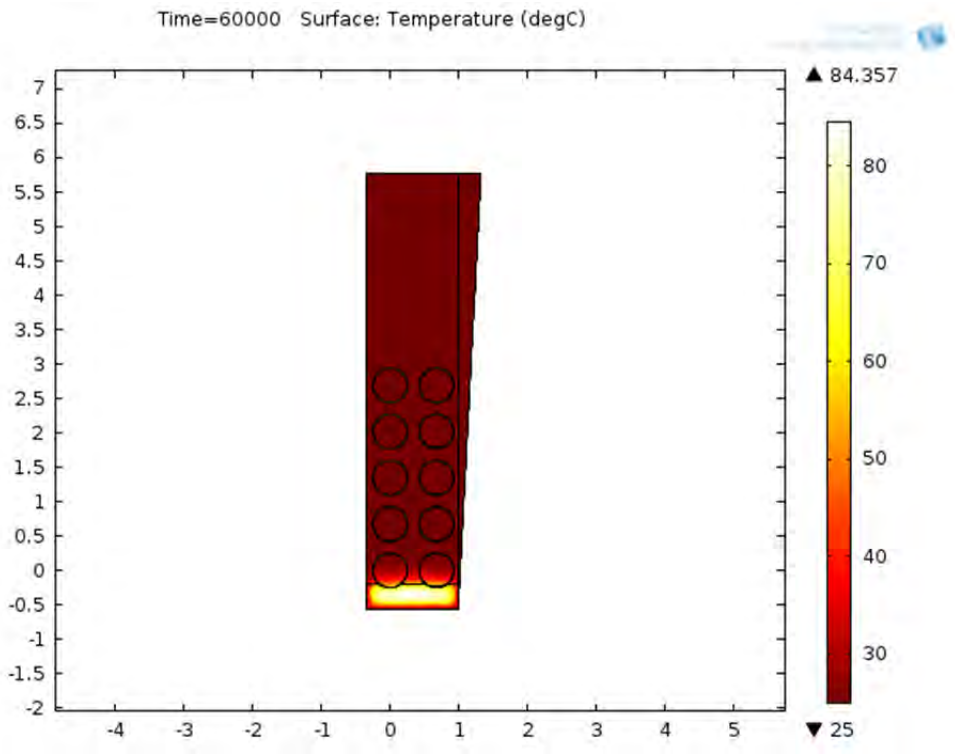

Figure 8.10. 2D Cross-Section of the Weasel Pit That Shows the 10 Tanks Plus the 14 Inches of Grout

8.3.3.1 Key Parameters & Assumptions

- Grout in the settler tank will be mostly cured before grout is poured on the Weasel Pit floor; most of the hydration reactions will have occurred inside the settler tanks (i.e., cure time of 28 days or longer).
- Grout heating rates of the added 14 inches of grout on the floor are identical to the 60 °C rates used for the grout inside the settler tanks.
- With 14-inch depth, the bottom 2 inches of tanks N-5 and S-5 are submerged in the grout pour.
- Uranium metal sludge depth is the highest cross-section level for each tank (Table 8.4).
- Water is at the basin temperature and starts at 25 °C.

8.3.3.2 Results

For Case 3, the boundary conditions at the Weasel Pit walls were varied from adiabatic to constant wall temperatures. In addition, the uranium reaction rates were varied from normal reaction rate to the rate multiplier of 3×. It was found that in all cases the uranium heated above 100 °C in the N5 and S5 tanks within about a day's time. Below in Figure 8.11 a 2D cross-section of the tanks and Weasel Pit is shown with constant-temperature boundary conditions. The maximum temperature of the uranium sludge plotted versus time is shown in Figure 8.12.

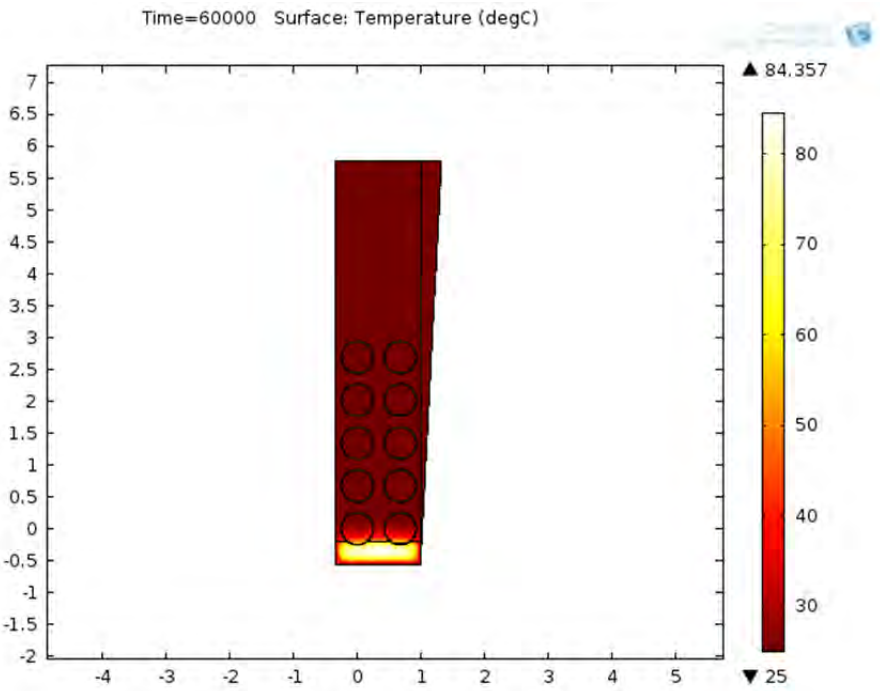

Figure 8.11. Weasel Pit with 14 Inches of Grout and Constant-Temperature Wall Boundary Conditions at a 1× Uranium Sludge Heating Rate

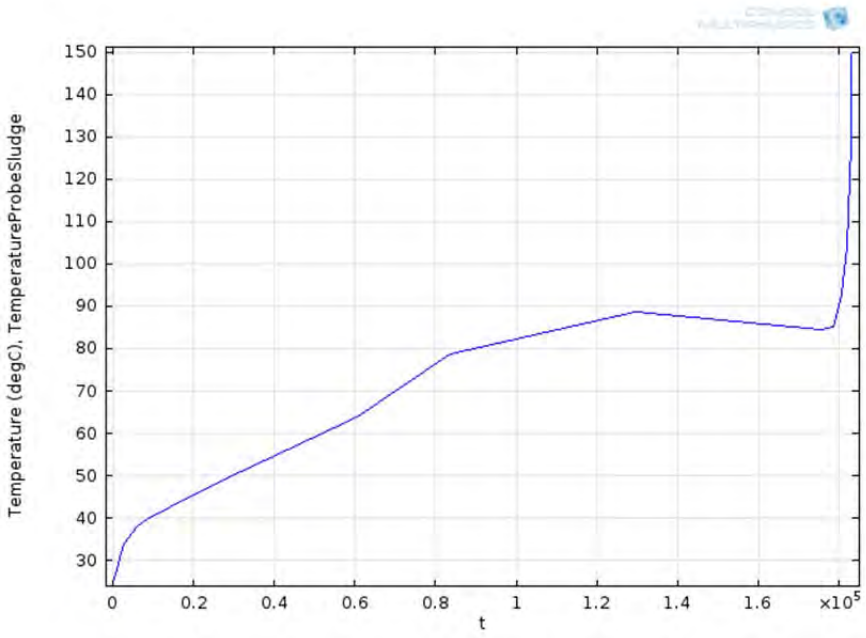

Figure 8.12. Weasel Pit Maxium Uranium Sludge Temperature (seconds) versus Time for the Constant-Temperature Boundary Conditions with 1× Uranium Sludge Heating Rate

Note: The discontinuity in the temperature profile with time in Figure 8.12 is a numerical artifact of running the model with a varying time step interval. Absolute results are affected slightly, but the artifact has no impact on conclustions.

8.3.3.3 Conclusions

Based on these modeling results, grouting the floor of the Weasel Pit to a depth that is in contact with the bottoms of the N5 and S5 tanks will result in the uranium sludge being heated to a point of instability. Unlike Case 1, where cooling of the uranium sludge is due to heat conduction through the settler wall to the water, in Case 3, the uranium sludge is cooled primarily through the grout above it. Case 3 has poor thermal connection with the basin water, leading to quick heating by the grout on the floor, which promotes the uranium sludge's reactions, leading to potential instability.

8.3.4 Grouted Settler Tank Underwater + 6 Inches of Grout Added to Floor of Weasel Pit (Case 4)

Case 4 focuses on grouting the floor of the Weasel Pit with a six-inch pour of grout. This gives the N5 and S5 tanks some thermal insulation, via the water between the grout pour and the bottoms of the tanks, from the heat produced by the grout. In Figure 8.13, a 2D cross-section of the tanks and Weasel Pit is shown with constant-temperature boundary conditions and a 1× uranium heating rate.

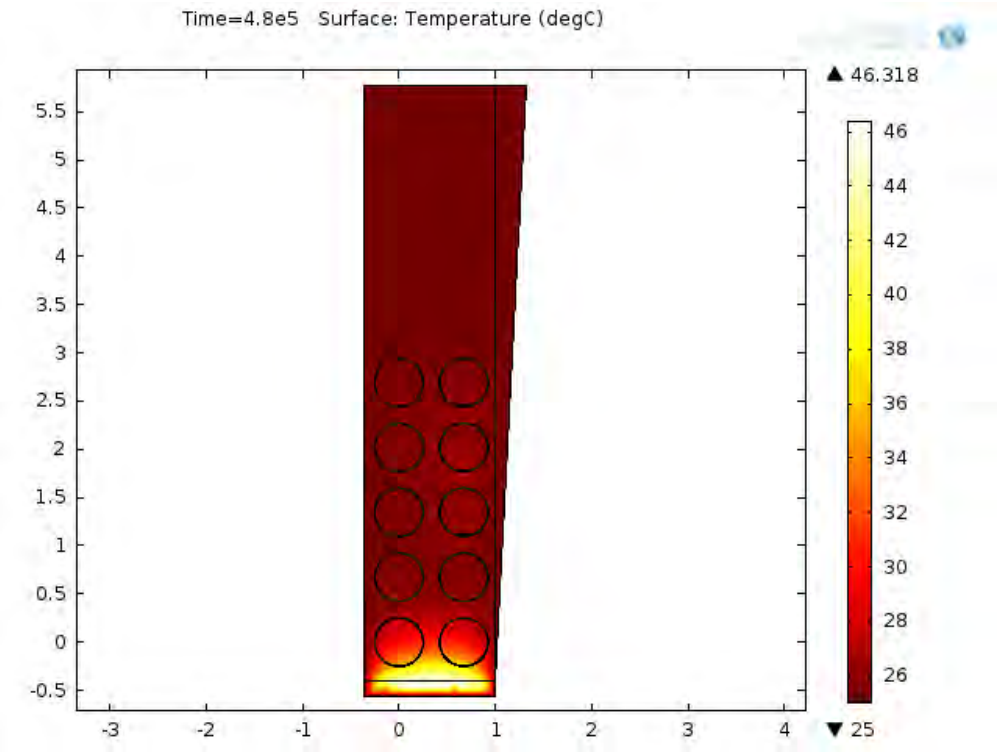

Figure 8.13. 2D Cross-Section of the Weasel Pit That Shows the 10 Tanks Plus the 6 Inches of Grout

8.3.4.1 Key Parameters & Assumptions

- Grout in the settler tank will be mostly cured before grout is poured on the Weasel Pit floor; most of the hydration reactions will have occurred inside the settler tanks (i.e., cure time of 28 days or longer).

- Grout heating rates of the added 6 inches of grout on the floor are identical to the 60 °C rates used for the grout inside the settler tanks.
- With 6 inches of grout depth, the bottoms of tanks N-5 and S-5 are about 6 inches from the top of the grout pour.
- Uranium metal sludge depth is the highest cross-section level for each tank (Table 8.4).
- Water is at the basin temperature and starts at 25 °C. No credit is taken for convective heat transfer in the water (conduction only).

8.3.4.2 Results

For Case 4, the boundary conditions were varied from adiabatic to constant wall temperatures. In addition, the uranium reaction rates were varied from 1× to three times the normal rate (3×). It was found that in two cases the uranium heated above 100 °C in the N5 and S5 tanks. The cases that were stable had constant-temperature boundary conditions. Below in Figure 8.14, a 2D cross-section of the tanks and Weasel Pit is shown with constant-temperature boundary conditions and a 1× uranium heating rate. Results at 3× were effectively the same. The maximum temperature of the uranium sludge plotted versus time is shown in Figure 8.15.

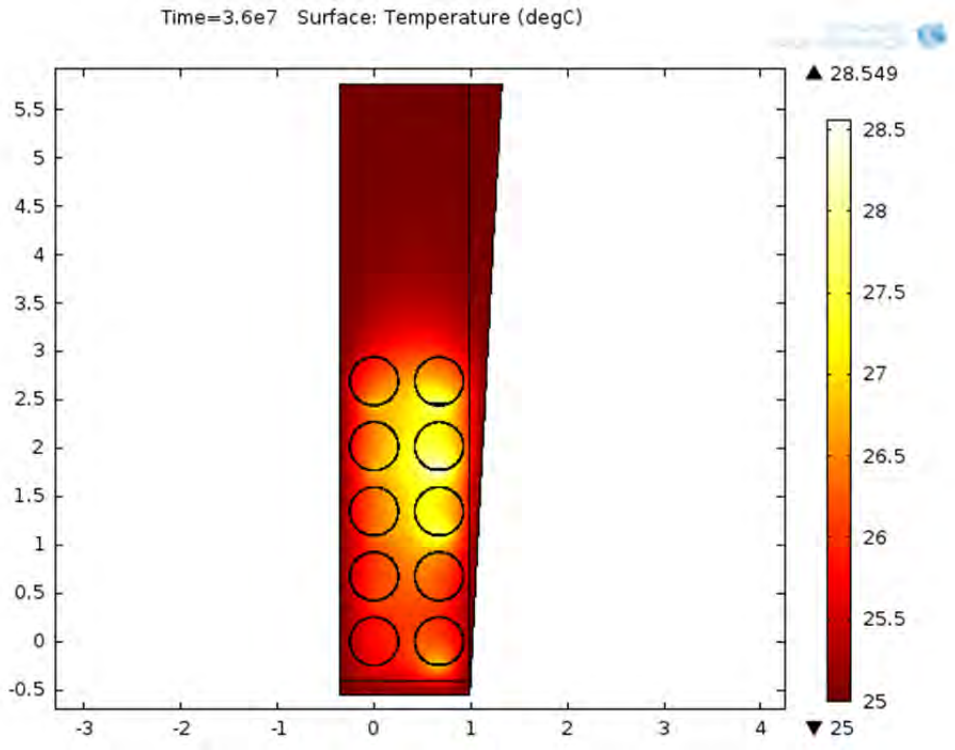

Figure 8.14. Weasel Pit with 6 Inches of Grout and Constant-Temperature Wall Boundary Conditions at a 1× Uranium Sludge Heating Rate After 416 Days

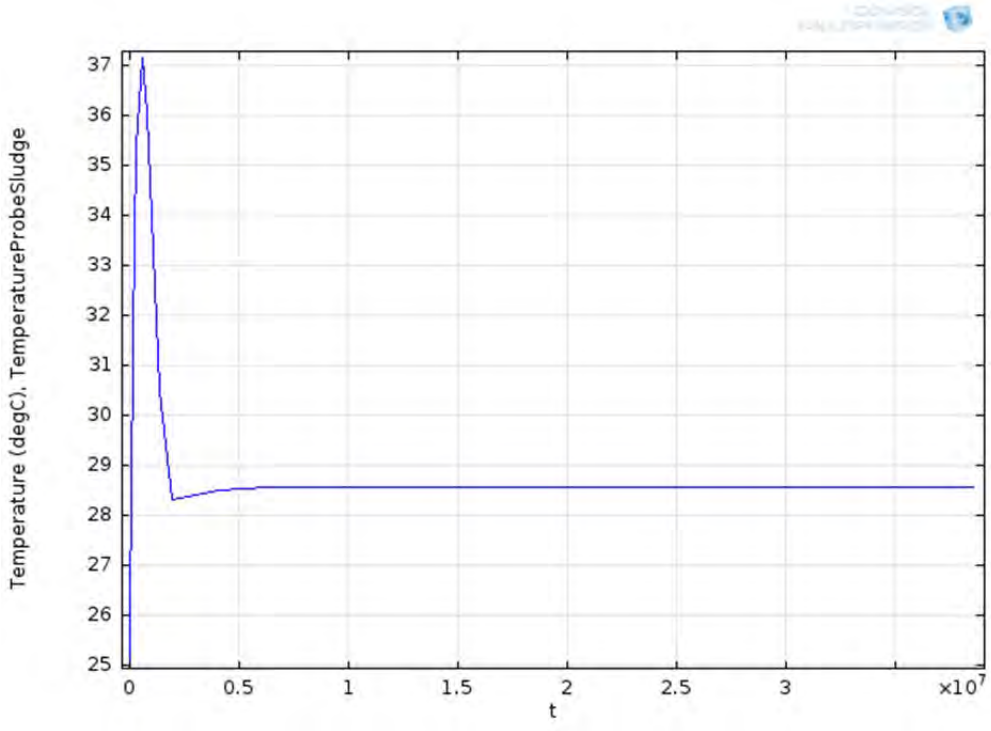

Figure 8.15. Weasel Pit Maxium Uranium Sludge Temperature versus Time (seconds) for the Constant-Temperature Boundary Conditions with 1× Uranium Sludge Reaction Rate

When the boundary conditions were changed to adiabatic, it is not surprising that eventuallly the system heated up. This is because all the grout was given a long-term heating rate of 2.51 W/m^3 and the uranium sludge did not have a cutoff on heat genration for these calculations, nor was conventive heat tranfer in water included in the model. Figure 8.16 shows the temperature continuing to increase for the adiabatic case at the 1× uranium reaction rate.

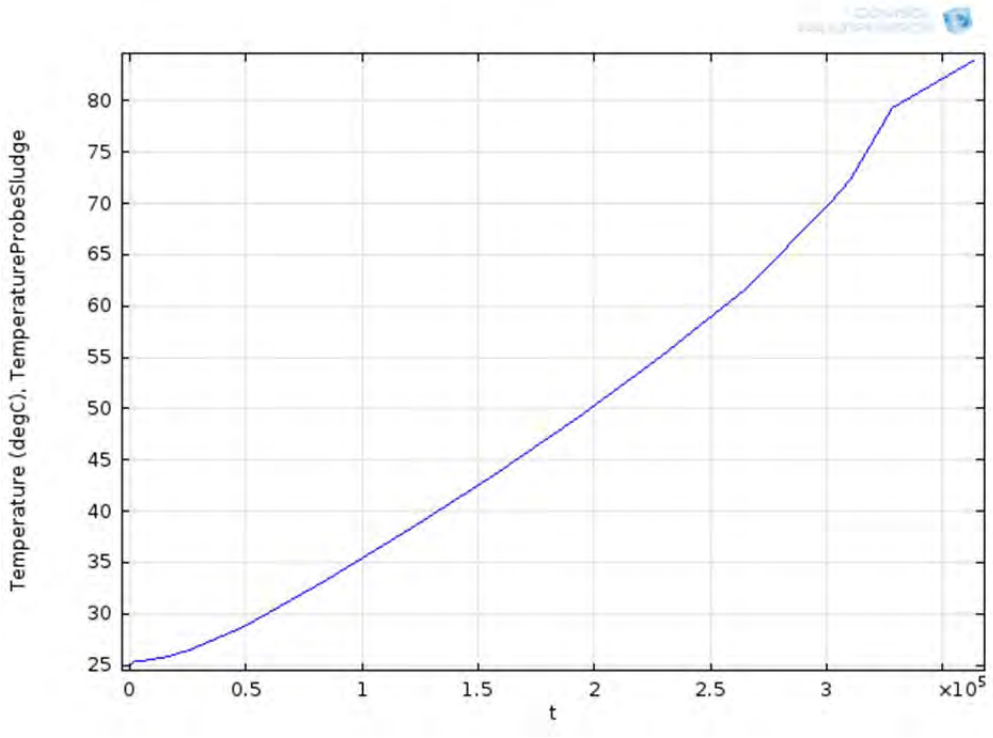

Figure 8.16. Weasel Pit Maxium Uranium Sludge Temperature versus Time (seconds) for the Adiabatic Boundary Conditions with 1× Uranium Sludge Heating Rate

Note: The discontinuity in the temperature profile with time in Figure 8.16 is a numerical artifact of running the model with a varying time step interval. Absolute results are affected slightly, but the artifact has no impact on conclustions.

8.3.4.3 Conclusions

These simulations show that grouting the Weasel Pit with 6 inches of grout is likely very safe. While the actual system will not have perfectly maintained wall temperatures, the natural convection of water will likely provide additional cooling. In this model we have ignored fluid flow in water and its effects on heat transport and have only included conduction.

8.3.5 Settler Tank Section in IP2 Waste Box (Case 5)

Case 5 examines a 1.25-foot section of the S5 tank put into the IP2 waste box (10 ft × 20 ft × 10 ft) that is filled with wet, moist, or dry sand. The section of tank is filled with the highest depth of uranium sludge (2.23 cm). Below in Figure 8.17 is depiction of the IP2 box with the 1.25-foot section placed in the middle with moist stand. This simulation was performed in three dimensions (3D) with constant-temperature boundary conditions. Case 5 was examined for exploratory and illustration purposes only. The IP2 box would not support the mass of the sand considered in this case.

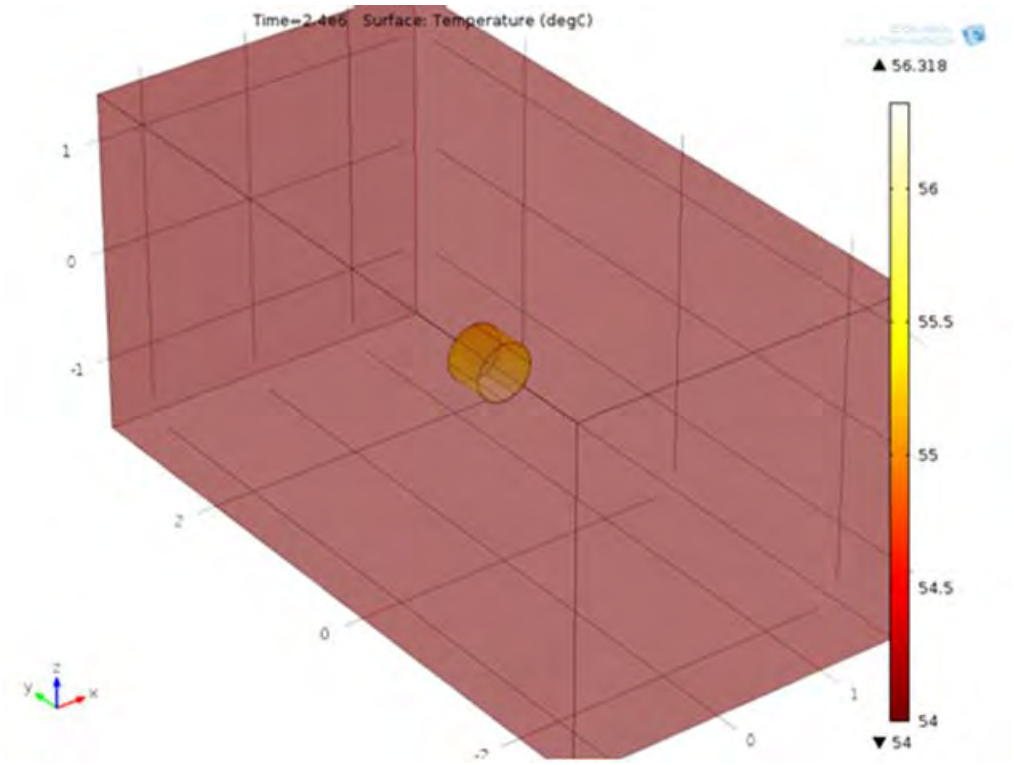

Figure 8.17. Moist Sand-Filled IP2 Box with Uranium Sludge Reacting at 1× Rate and Constant-Temperature Boundary Conditions

8.3.5.1 Key Parameters & Assumptions

- Grout in the settler tank will be mostly cured before the KW pool is drained and most of the hydration reactions will have occurred (i.e., cure time of 28 days or longer).
- U metal loading in the section: worst-case 1.25-ft section (Tank 5S, Location B).
- No solar heating.
- Constant-temperature boundary conditions.
- Outside steel components of the box were ignored.
- Physical properties for the backfill material are as defined in Table 8.8, based on Poloski et al. (2002).

8.3.5.2 Results

Multiple simulations were run to find the initial and wall temperatures that resulted in either a stable solution or unstable result (i.e., uranium sludge temperatures above 100 °C). In addition, 1× and 3× uranium reaction rates were used in these simulations. For dry sand properties [K = 0.13 W/(m·K)] it was found that stable solutions only existed up to 34 °C for 1× uranium reaction rates and 15 °C for a reaction rate multiplier of 3×. Figure 8.18 below shows the solution for 1× uranium reaction rate with dry sand,

with starting and wall temperatures of 34 °C. Figure 8.19 shows the maximum temperature profile of the uranium sludge over time for the dry sand 1× uranium rate case.

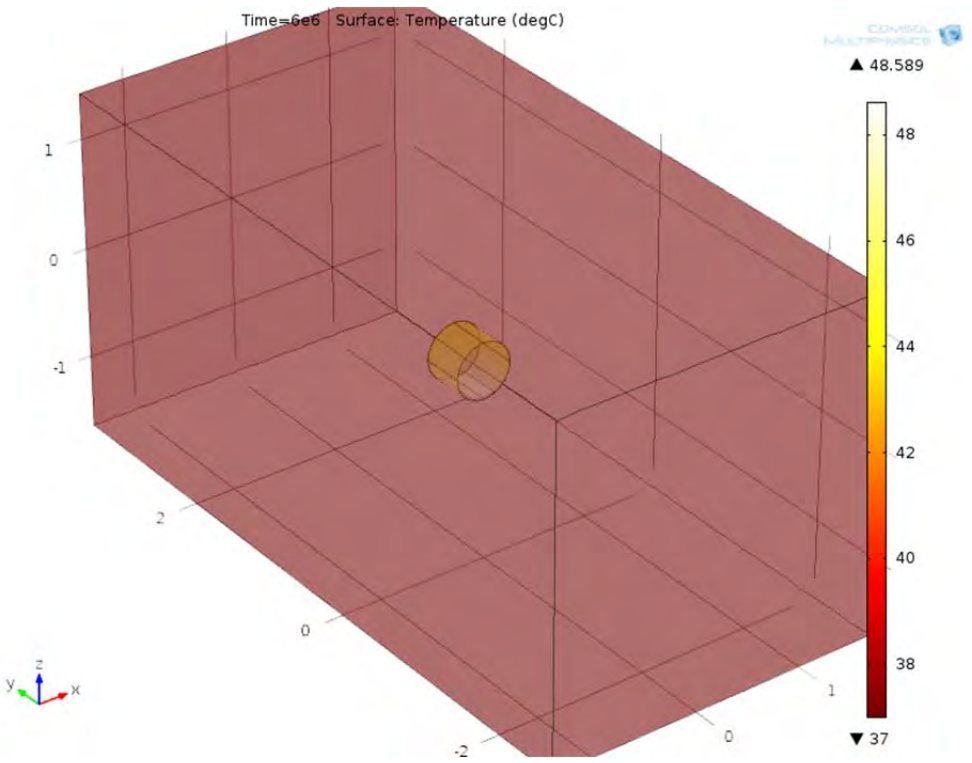

Figure 8.18. IP2 Waste Box with 1× Uranium Sludge Reaction Rate with Dry Sand Surrounding the Tank Section

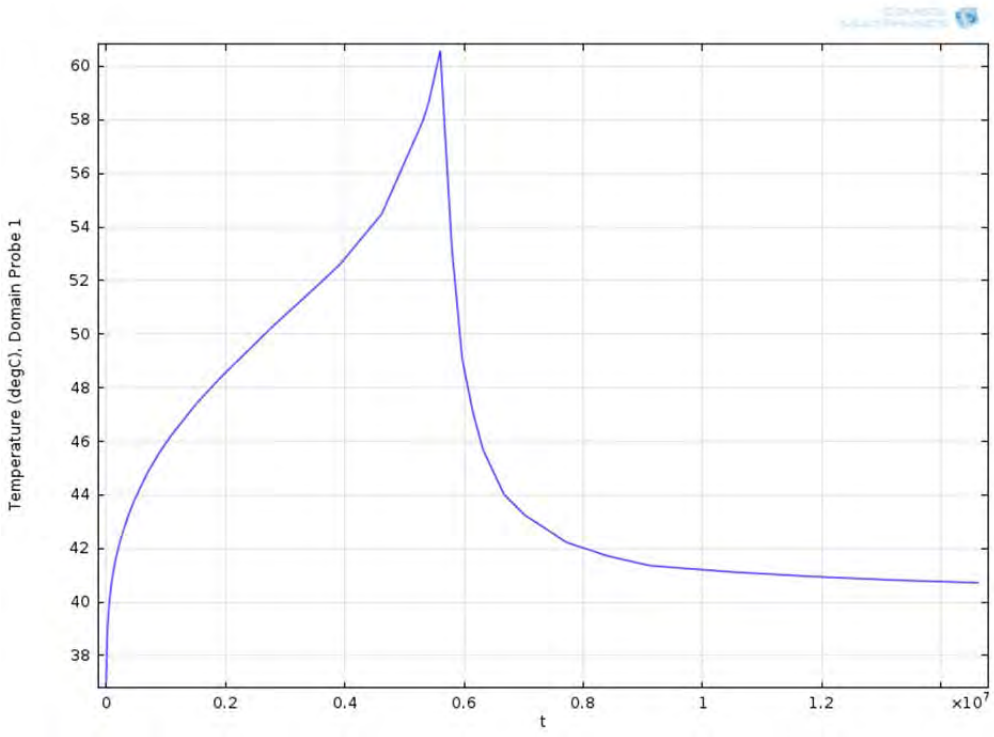

Figure 8.19. Maximum Temperature Profile of the Uranium Sludge Over Time (seconds) for the Dry Sand 1× Uranium Rate Case

Changing the properties of the sand to simulate moist sand [K = 0.78 W/(m·K)] improved the maximum temperature for the 1× uranium rate multiplier to 51 °C, and to 34 °C for the 3× rate multiplier.

8.3.5.3 Conclusions

Case 5 highlights the importance of the physical properties of materials surrounding the settler tube section. If surrounded by a low-thermal-conductivity material, the settler tank thermal behavior will be essentially adiabatic and thermally unstable. The initial temperature of the fill material is also an important consideration for maintaining thermal stability. The dry sand simulations of an IP2 box show lower than 50 °C stability of the uranium sludge. Moist sand also shows lower than 50 °C stability for 3× uranium reaction rates but not for 1× uranium rates. Given that active cooling may not be desired, an alternative dry storage system is developed in Case 6.

8.3.6 Settler Tank Section in 4-ft × 6-ft × 4-ft Box with Carbon Steel Cradle Surrounded by Sand (Case 6)

Case 6 explores modifying the storage of the 1.25-foot tank section by placing it in a carbon steel cradle (i.e., a heavy-walled pipe, bisected axially) that is then surrounded by sand in a smaller box (Figure 8.20). To provide good thermal contact between the carbon steel cradle and the 1.25-foot tank section, a layer of thermally conductive paste is proposed. Different gaps of thermally conducive paste are explored with different cradle wall thicknesses and uranium heating rates.

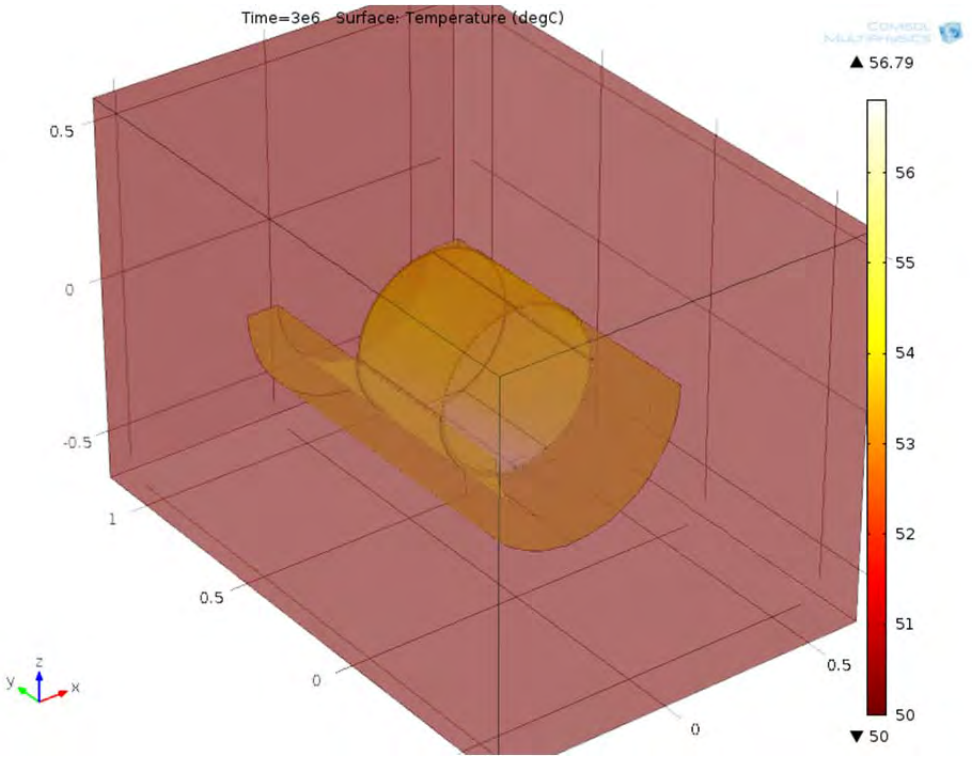

Figure 8.20. Settler Tank Section Fitted into a Steel Cradle with Thermally Conductive Paste in Between, with the Waste Box Filled by Dry Sand

8.3.6.1 Key Parameters & Assumptions

- Grout in the settler tank will be mostly cured before the KW pool is drained and most of the hydration reactions will have occurred (i.e., cure time of 28 days or longer).
- U metal loading in the section: worst-case 1.25-ft. section (Tank 5S, Location B).
- The uranium metal reaction cuts off upon expending 100% of the maximum heat of reaction, based on uranium metal content in the sludge of 9.2 g/cm^3. Decay heat, based on the uranium metal content, continues indefinitely.
- No solar heating.
- Constant-temperature boundary conditions.
- Outside steel components of the box were ignored.
- Thermal conductivity of the paste was set at 0.67 W/(m·K).
- Physical properties for the backfill material (dry sand) are as defined in Table 8.8, based on Poloski et al. (2002).

8.3.6.2 Results

Case 6 simulations primarily varied the cradle thickness from 4 inches down to ½ inch. Initial material and wall temperatures were set at 50 °C in all the simulations. We found that the uranium sludge

was stable at 1× uranium reaction rates down to a cradle thickness of 1 inch with ¼-in and $^{1}/_{8}$-in gaps filled with thermal paste (0.67 W/(m·K). Half-inch cradle thicknesses showed uranium sludge temperatures increasing to above 100 °C for both the ¼-in and $^{1}/_{8}$-in paste thicknesses. With the 3× uranium reaction rate multiplier, the sludge was not stable for the cradle thicknesses and paste gaps studied here.

Figure 8.21 shows the solution for a 1-inch-thick cradle with $^{1}/_{8}$-inch of paste thickness at a 1× reaction rate; Figure 8.22 shows the maximum uranium sludge temperature with time.

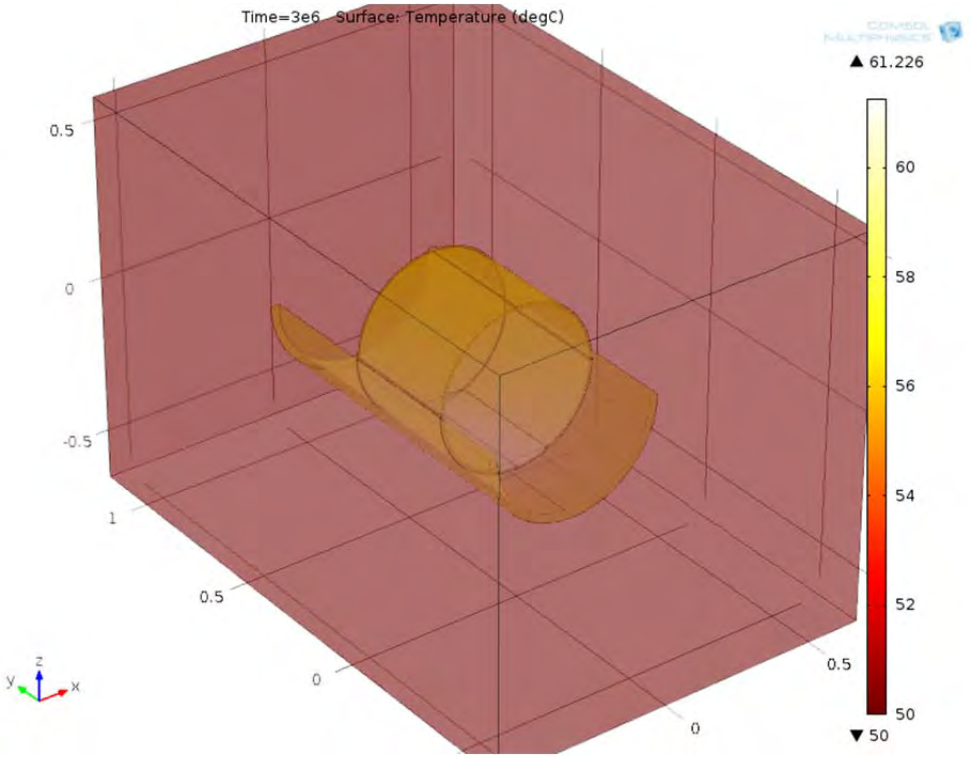

Figure 8.21. 1-Inch Cradle Thickness with $^{1}/_{8}$-Inch Paste Thickness at 1× Uranium Reaction Rate

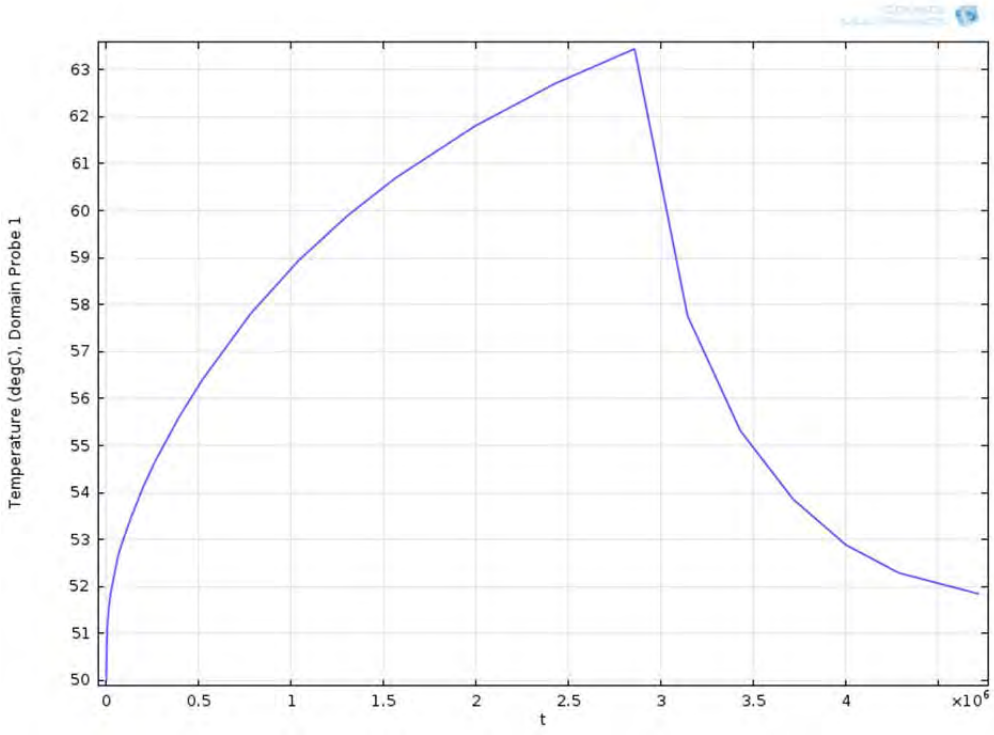

Figure 8.22. Maximum Uranium Sludge Temperature with Time (seconds) for 1-Inch Cradle Thickness with $^{1}/_{8}$-Inch Paste Thickness at 1× Uranium Reaction Rate

8.3.6.3 Conclusions

In simulations, the uranium sludge is stable when the worst-case 1.25-foot-long section of setter tank is placed in a steel cradle of 1-inch or greater thickness, with a thermally conductive medium in-between, at 1× uranium heating rates. At a uranium rate multiplier of 3×, simulations showed the maximum temperatures rising to above 100 °C in the uranium sludge at even the maximum 4-inch cradle thickness simulated.

8.3.7 Settler Tank Section in 4-ft × 6-ft × 4-ft box with Carbon Steel Cradle Embedded in High-Conductivity Grout, with Top Filled with Sand (Case 7)

Case 7 explores augmentation of the cradle heat sink by the addition of high-conductivity grout around the steel tank cradle in the lower 2 feet of the box. The high-conductivity grout exhibits a thermal conductivity of about 1 W/m·K in comparison to the dry sand (0.13 W/m·K). Figure 8.23 shows the arrangement of the steel cradle placed in the high-conductivity grout with sand placed in the top half of the box.

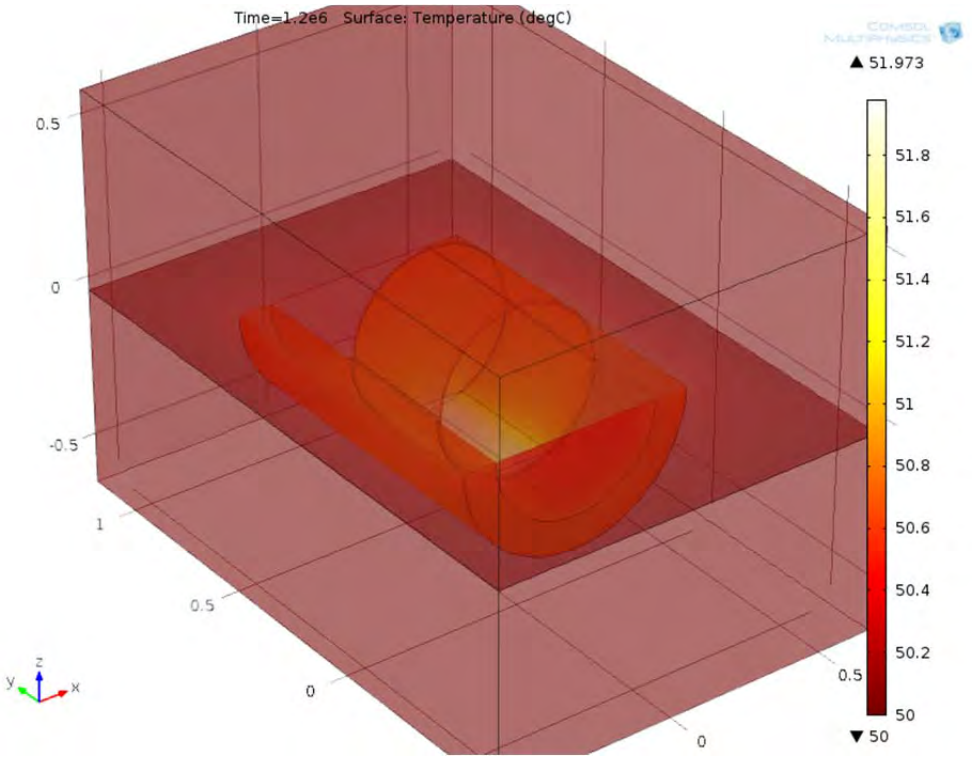

Figure 8.23. Tank Section Fitted Into a Steel Cradle with Thermally Conductive Paste In-Between, with Bottom Half of Box Filled with Grout and Top Half Filled with Dry Sand

8.3.7.1 Key Parameters & Assumptions

- Grout in the settler tank will be mostly cured before the KW pool is drained and most of the hydration reactions will have occurred (i.e., cure time of 28 days or longer).
- U metal loading in the section: worst-case 1.25-ft. section (Tank 5S, Location B).
- The uranium metal reaction cuts off upon expending 100% of the maximum heat of reaction, based on uranium metal content in the sludge of 9.2 g/cm^3. Decay heat, based on the uranium metal content, continues indefinitely.
- No solar heating.
- Constant-temperature boundary conditions.
- Outside steel components of the box were ignored.
- Physical properties for the backfill material and high-conductivity grout are as defined in Table 8.5, and for the dry sand are as defined in Table 8.8.

8.3.7.2 Results

Case 7 was evaluated with an approach that followed the approach used in Case 6: varying the cradle thickness from 4 inches to ¼-inch, paste thicknesses between ¼-in and $^1/_8$-in, with 1× and 3× uranium reaction rates. However, with the high-conductivity grout providing an additional heat sink, the uranium

sludge was kept below 100 °C with steel cradle thickness down to ¼-inch with both ¼-in and $^{1}/_{8}$-in conductive paste thicknesses for the 1× uranium reaction rate cases. In addition, the 3× uranium rate was stable with ¼-inch of thermally conductive paste with a cradle thickness of 2 inches or more. With the conductive paste gap reduced to $^{1}/_{8}$-inch, the 3× uranium rate was stable at 1-inch or more cradle thickness. Figure 8.24 below shows the $^{1}/_{8}$-inch thermally conductive paste gap with 1-inch of cradle thickness. The maximum temperature of the uranium sludge with time for the 3× uranium sludge rate and $^{1}/_{8}$-inch thermally conductive paste is shown in Figure 8.25.

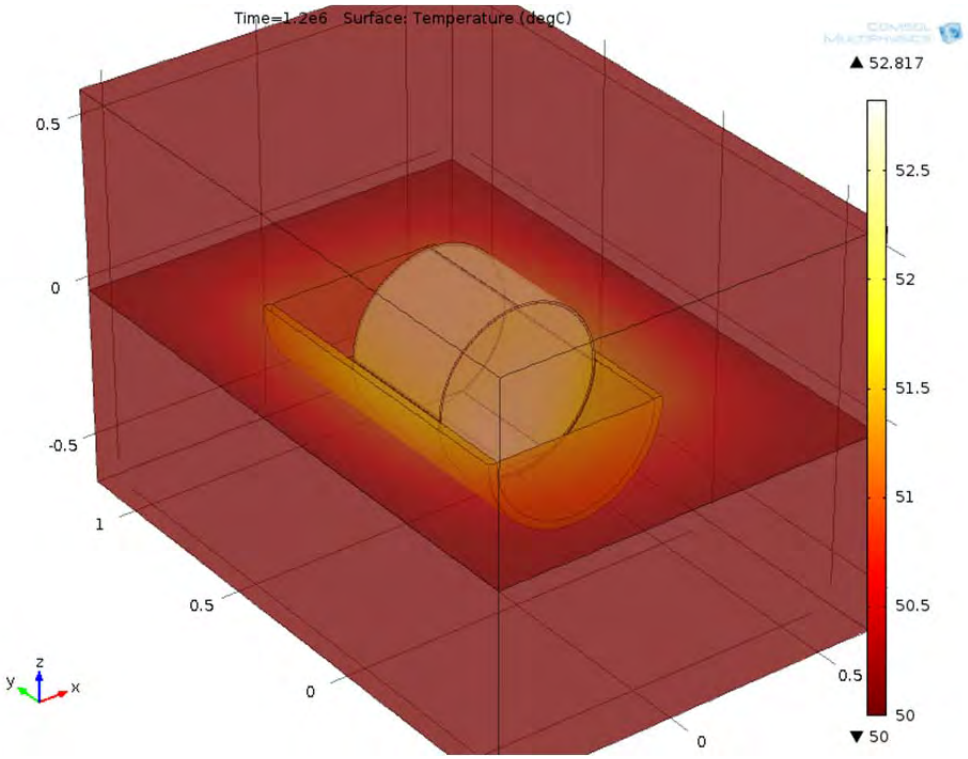

Figure 8.24. 3× Uranium Sludge Reaction Rate with $^{1}/_{8}$-Inch Thermally Conductivity Paste with 1-Inch of Cradle Thickness

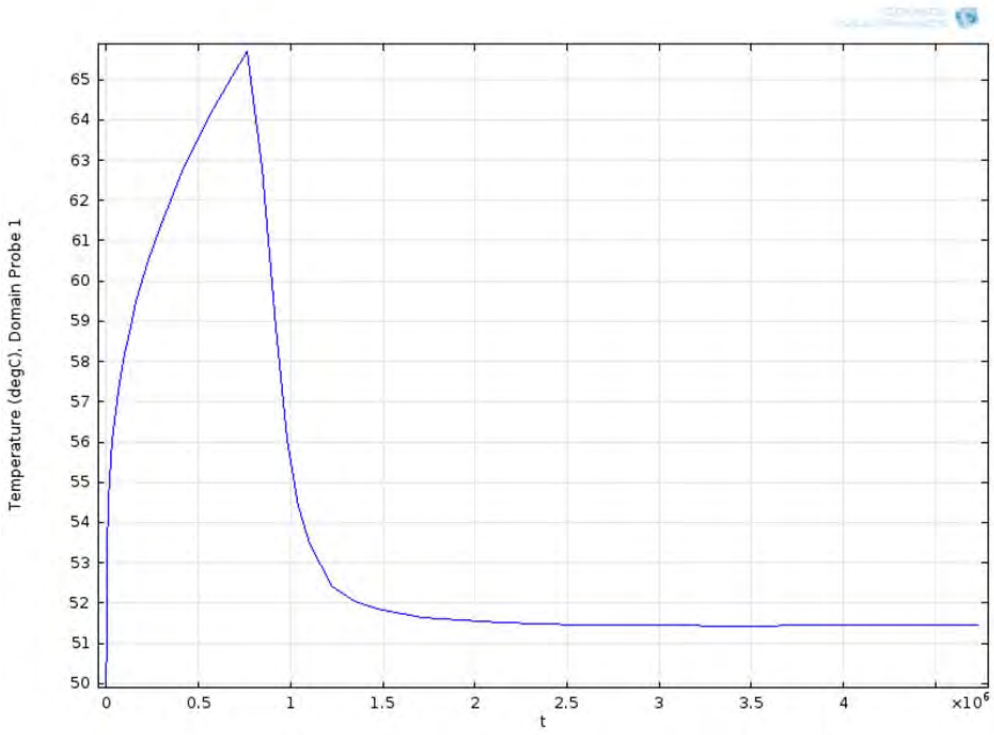

Figure 8.25. Maximum Sludge Temperature with Time (seconds) for 3× Uranium Sludge Rate with $^{1}/_{8}$-Inch Thermally Conductivity Paste with 1-Inch of Cradle Thickness

With a 1× uranium reaction rate, filling the gap with air between the steel cradle and settler tank section appears also to provide a stable solution if the gap is small enough. Figure 8.26 below shows ¼-inch cradle thickness with $^{1}/_{8}$-inch gap filled with air at 1× uranium sludge reaction rate. The progression of uranium sludge temperature with time can be seen in Figure 8.27.

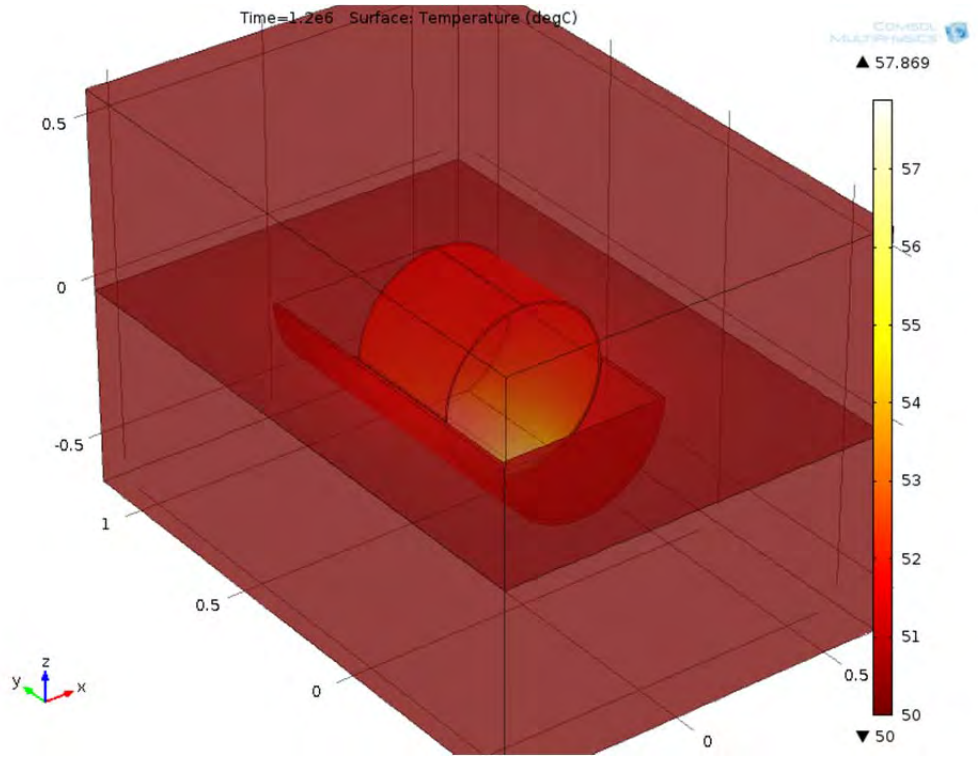

Figure 8.26. Temperature Profile for ½-Inch Cradle Thickness with $^{1}/_{8}$-Inch Gap Filled with Air at 1× Uranium Sludge Reaction Rate

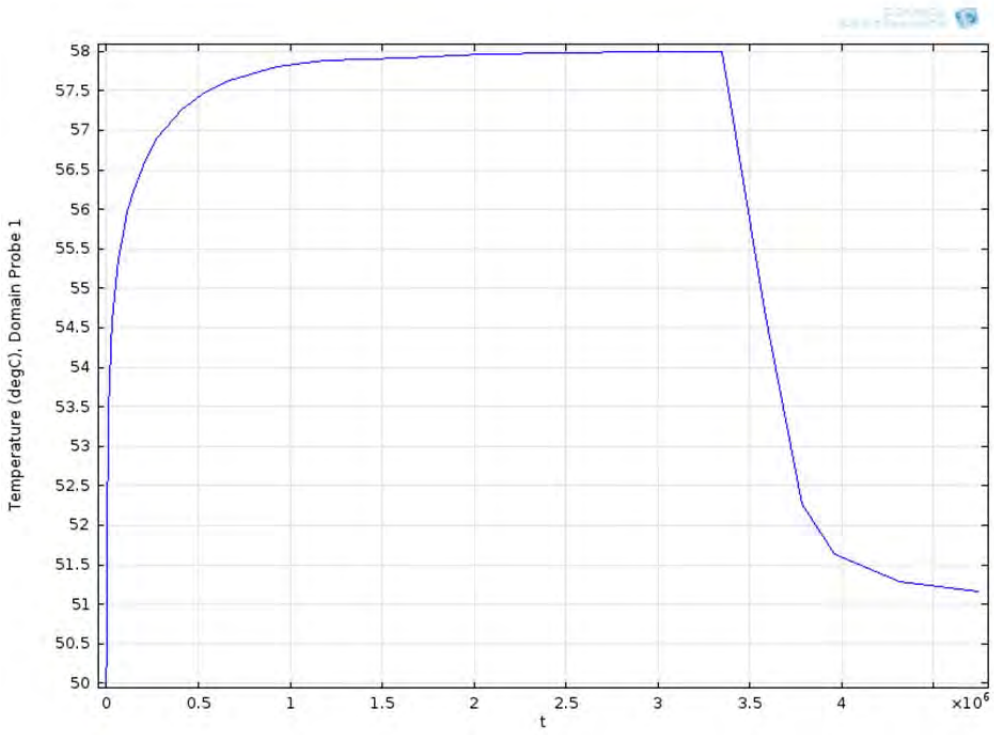

Figure 8.27. Uranium Sludge Temperature with Time (seconds) for ½-Inch Cradle Thickness with $^{1}/_{8}$-Inch Gap Filled with Air at 1× Uranium Sludge Reaction Rate

8.3.7.3 Conclusions

Addition of high-conductivity grout to the bottom half of the box greatly enhances the robustness of the heat sink around the settler tank section. Simulations show stable solutions at 50 °C initial and wall temperatures with a proper amount of cradle thickness and sufficient thermal connect between the settler section and the heat sink. Simulations specifically show stability for the 1× uranium reaction rate at or above ¼-inch cradle thicknesses, with gaps no larger than ¼-inch filled with a conductive thermal paste, or $^1/_8$-inch maximum gap thickness if the gap contains just air. A 3× uranium rate multiplier requires a gap no larger than ¼-inch filled with thermally conductive paste, with at least 2 inches of cradle thickness and the cradle embedded into high-conductivity grout. Decreasing the cradle thickness to 1-inch is possible for the 3× uranium heating rates if the conductive-paste gap is no larger than $^1/_8$-inch.

8.3.8 Settler Tank Section in Box with Cradle Embedded in High-Conductivity Grout, Top Filled with Sand, with Solar Heating and Convective and Radiative Cooling (Case 8)

Case 8 explores the addition of solar heating and convective and radiative cooling to Case 7. Because of the added complexity of adding radiation and convection heat transport, a reasonably bounding scenario was developed. In this scenario, the sun is assumed to be directly overhead and heating the box 24 hours per day, seven days per week (24/7), at an approximate noonday heating rate of 990 W/m^2 [314 BTU/(h·ft^2)]. The top of the box and the side walls are allowed to be cooled both radiatively and convectively with an ambient temperature of 50 °C. The ground underneath the box is assumed to remain at a constant 50 °C temperature with the initial starting temperature of the box and its contents being at 50 °C, the same as Case 7. Figure 8.28 shows the box and its contents after a steady-state profile temperature develops from the sun's radiation, but before the uranium metal reaction is allowed to start.

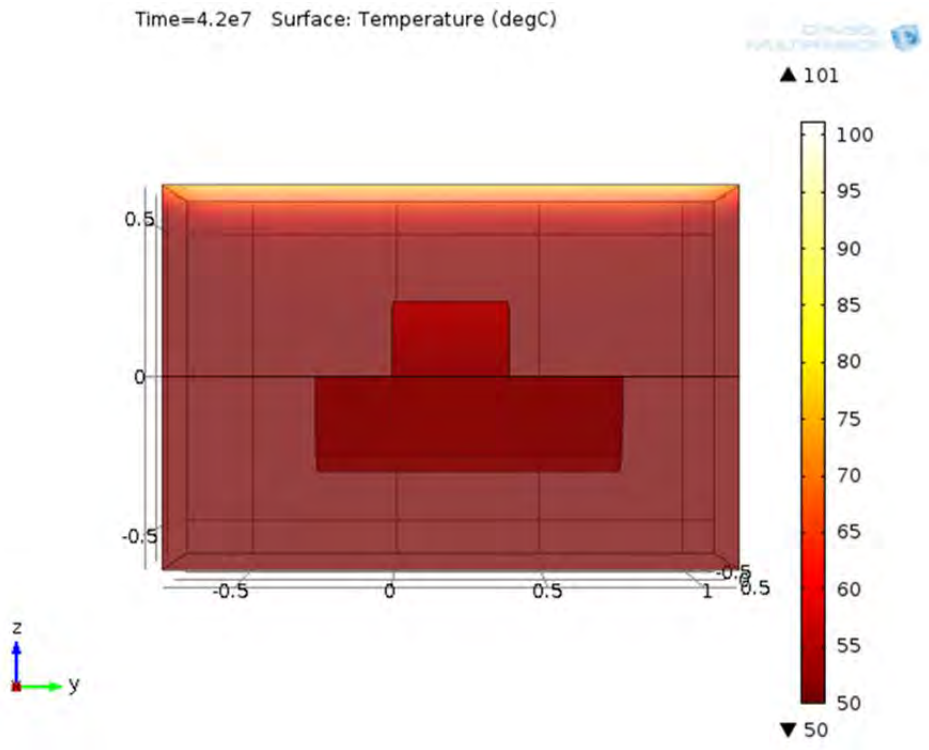

Figure 8.28. Settler Tank Section with 2-Inch Cradle Thickness with Solar Radiation and Convective and Radiative Cooling at Steady-State without Uranium Reactions

8.3.8.1 Input Parameters & Assumptions

- Grout in the settler tank will be mostly cured before the KW pool is drained and most of the hydration reactions will have occurred (i.e., cure time of 28 days or longer).
- U metal loading in the section: worst-case 1.25-ft. section (Tank 5S, Location B).
- The uranium metal reaction cuts off upon expending 100% of the maximum heat of reaction, based on uranium metal content in the sludge of 9.2 g/cm^3. Decay heat, based on the uranium metal content, continues indefinitely.
- Constant solar heating directly above the box at 990 W/m^2.
- Convective and radiative cooling of all the sides except the bottom of the waste box.
- Bottom of waste box at a constant 50 °C temperature.
- Outside steel components of the box were ignored.
- Physical properties for the backfill material and high-conductivity grout are as defined in Table 8.5, and for the dry sand are as defined in Table 8.8.
- Cradle thickness set at 1-inch.

8.3.8.2 COMSOL results

Case 8 explored Case 7 scenarios that had been shown to be stable. A steady-state temperature profile was allowed to develop before the uranium sludge temperature-dependent heating was allowed to begin at 4×10^7 seconds (463 days). The normal Case 7 cutoff was used for the temperature-dependent heat being generated. With conservative parameters, the waste box top reached a temperature of around 100 °C, as shown in Figure 8.29 below.

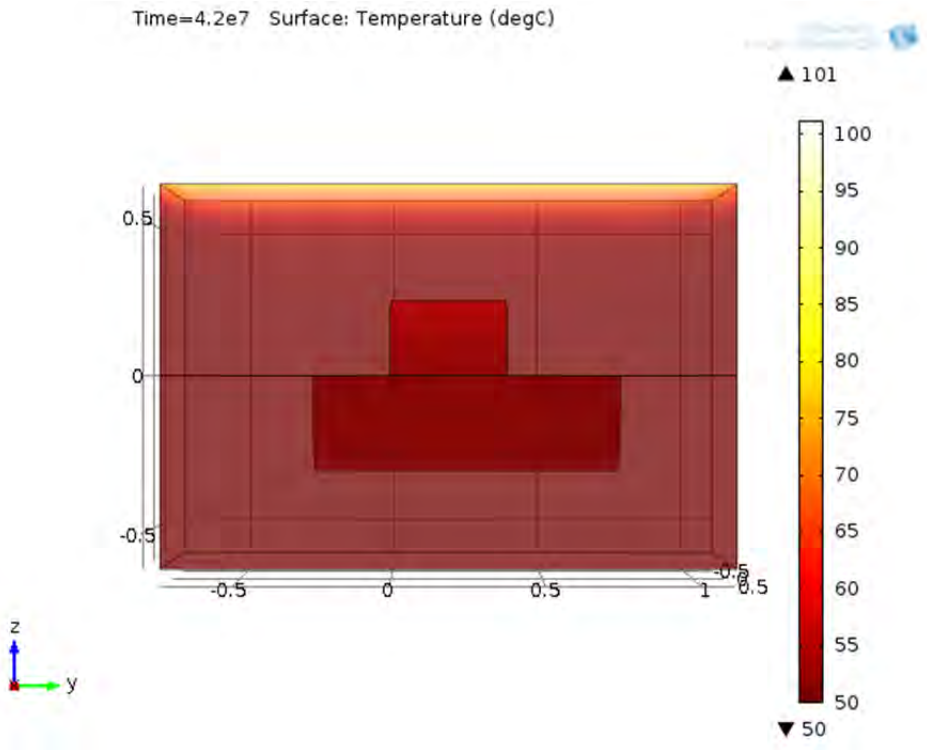

Figure 8.29. Temperature Profile of Waste Box with Solar Heating: 1× Uranium Sludge Reaction Rate, ¼-Inch Thermally Conductivity Paste, 1-Inch Cradle Thickness

Figure 8.30 shows the maximum temperature of the uranium sludge with time in blue and the overall waste box's maximum box temperature in green. An isosurface plot of the waste box after temperature-dependent heating is enabled is shown in Figure 8.31.

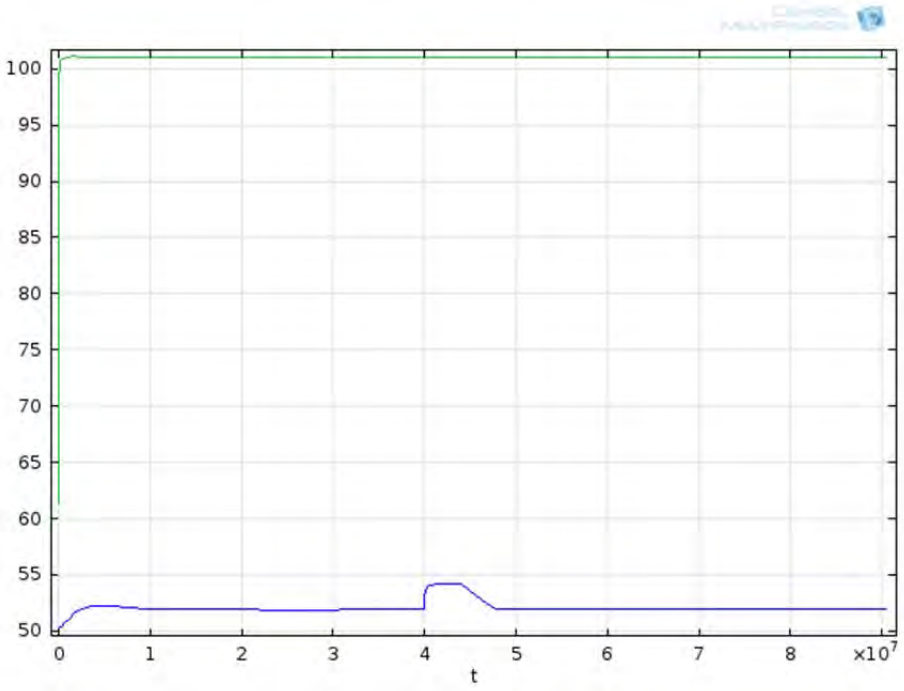

Figure 8.30. Maximum Sludge Temperature (blue line) and Maximum Waste Box Temperature (green line) with Time (seconds): 1× Uranium Sludge Reaction Rate, ¼-Inch Thermally Conductivity Paste, 1-Inch Cradle Thickness

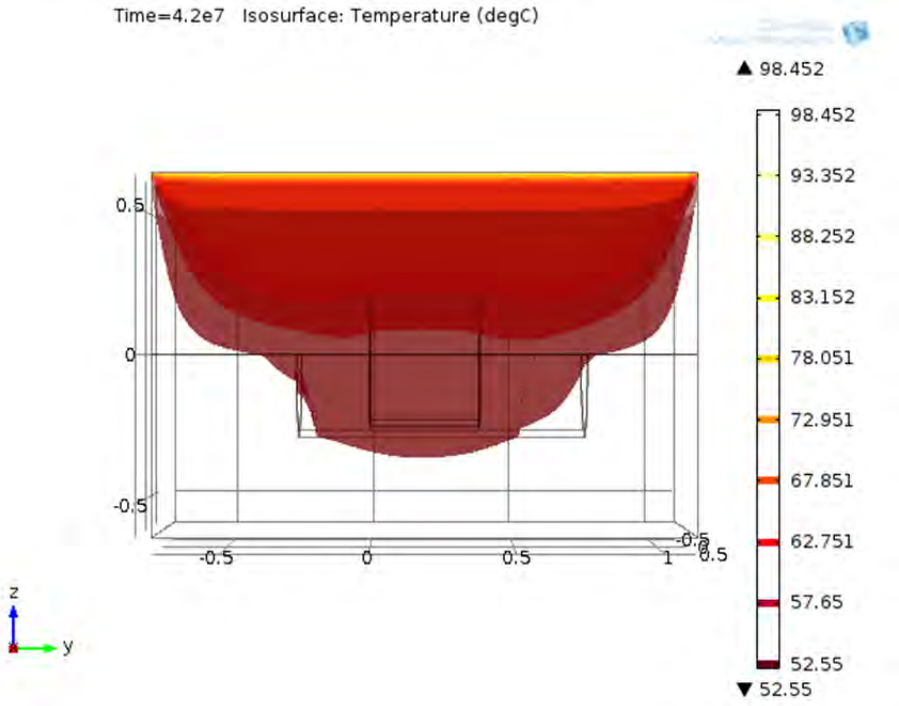

Figure 8.31. Isosurface Plot of Waste Box After Temperature-Dependent Heating Is Enabled: 1× Uranium Sludge Reaction Rate, ¼-Inch Thermally Conductivity Paste, 1-Inch Cradle Thickness

Generally Case 7 studies that were stable without solar radiation were also stable after the addition of solar radiation. One reason for this is that the dry sand in the upper half of the box insulates the uranium sludge from the sun's radiation.

The one scenario that was not stable when simulated included a 1-inch cradle thickness with 3× uranium heating rates and $^{1}/_{8}$-inch gap filled with thermally conductive paste. Increasing the paste's conductivity from 0.67 W/(m·K) to 1 W/(m·K) led to thermal stability, as shown in Figure 8.32, Figure 8.33, and Figure 8.34.

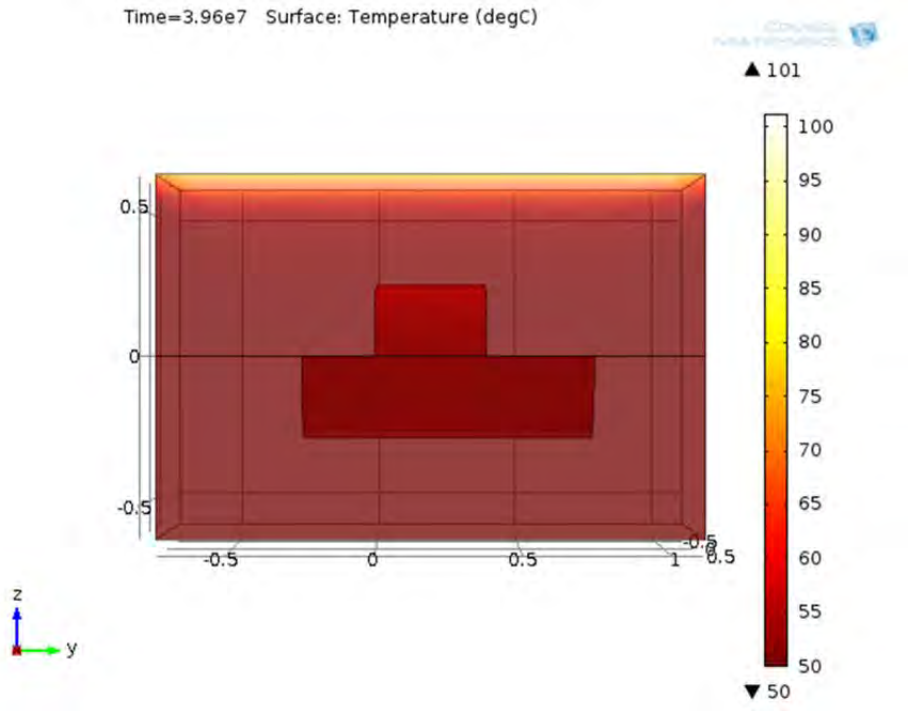

Figure 8.32. Temperature Profile of Waste Box with Solar Heating Before Uranium Sludge Heating: 3× Uranium Sludge Reaction Rate, $^{1}/_{8}$-Inch Thermally Conductivity Paste, 1-Inch Cradle Thickness, Thermal Paste Conductivity of 1 W/(m·K)

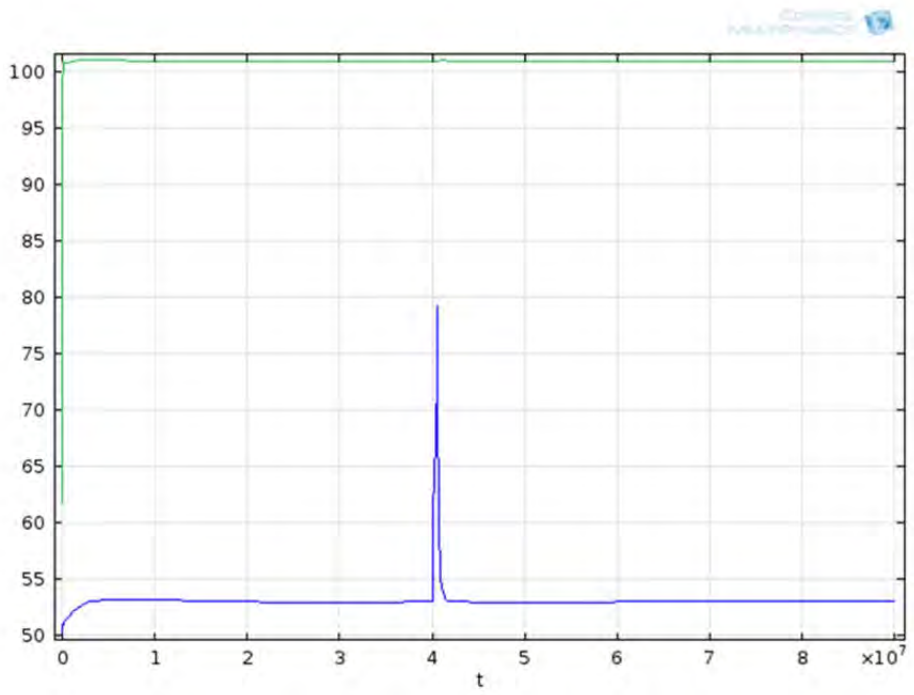

Figure 8.33. Maximum Sludge Temperature (blue line) and Maximum Waste Box Temperature (green line) with Time (seconds): 3× Uranium Sludge Rate, $^{1}/_{8}$-Inch Thermally Conductivity Paste, 1-Inch Cradle Thickness, Thermal Paste Conductivity of 1 W/(m·K).

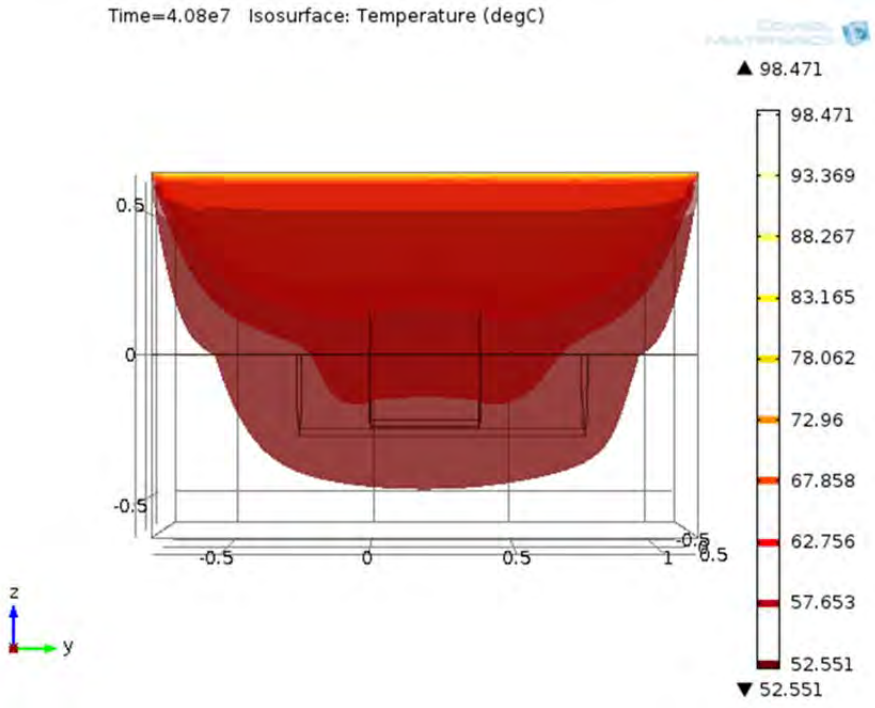

Figure 8.34. Isosurface Plot of Waste Box with Solar Heating After Uranium Sludge Heating: 3× Uranium Sludge Reaction Rate, $^{1}/_{8}$-Inch Thermally Conductivity Paste, 1-Inch Cradle Thickness, Thermal Paste Conductivity of 1 W/(m·K)

8.3.8.3 Conclusions

Adding solar heating in a bounding way to the top surface of the box did not significantly alter the stability of waste box as described in Case 7. Given that 24/7 direct solar heating of the waste box and ambient air temperatures of 50 °C with ground temperatures reaching 50 °C are not likely ever possible without human intervention, the waste box should always prove more stable than the bounding cases simulated in Case 8.

8.3.9 Case 9 is Case 1 with Substitution of Convective Cooling for the Constant-Temperature Boundary Conditions with Long-Term Grout Heat Generation Being Used

This case examines the condition when the grout inside the settler tanks has mostly cured and the KW basin is dewatered, or if/when sections of settler tanks are stored in air as they wait to be loaded into a waste box. For Case 9, convective cooling boundary conditions are used instead of the constant-temperature boundary condition used in Case 1.

8.3.9.1 Input Parameters & Assumptions

- Modeling was limited to the settler tube section with the deepest layer of uranium-rich sludge. All other sections, with less uranium metal depth, would exhibit greater thermal stability.
- Case 9 examined a single settler tube after being grouted, with convective heat transport.
- Convective heat transport was simulated with a heat transport coefficient of 7.9 W/(m^2·K) and 3 W/(m^2·K). This is in the typical range of heat transport coefficients for steel to air with low air flow [10 W/(m^2·K)] to free convection [5 W/(m^2·K)].

8.3.9.2 COMSOL Results

Adding the convective boundaries (instead of constant-temperature boundaries) decreased the stability temperature of the tubes in comparison to Case 1. However, the temperatures are still below room temperature of 24 °C (75 °F) even at conditions of 3× uranium sludge reaction rates with 2× the baseline uranium depth. Figure 8.35 shows the stability temperature for the grouted tubes under different uranium sludge depths and reaction rates with a heat transport coefficient for steel to air at 7.9 W/(m^2·K). Figure 8.36 is a similar plot, but with a heat transport coefficient reduced to 3.0 W/(m^2·K).

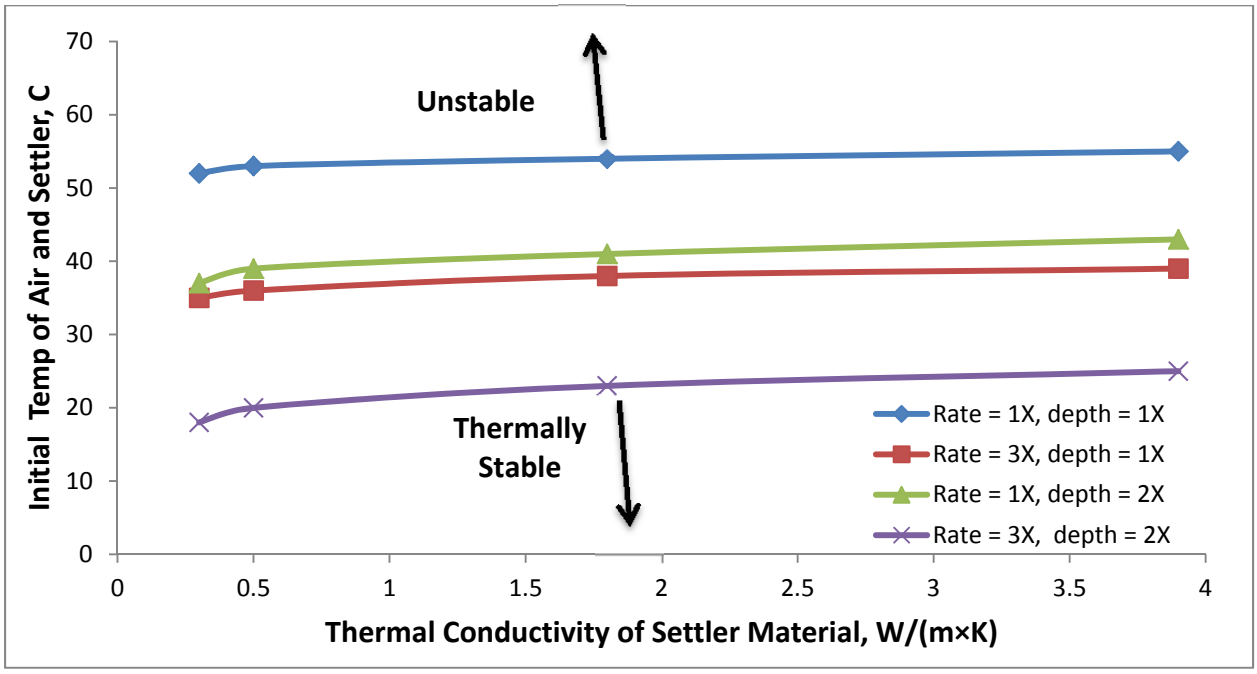

Figure 8.35. Sensitivity of Thermal Stability of Grouted Tube as a Function of Sludge Thermal Conductivity, Uranium Reaction Rate Multiplier, and Sludge Depth for Case 9, with Heat Transfer Coefficient of 7.9 W/(m^2·K)

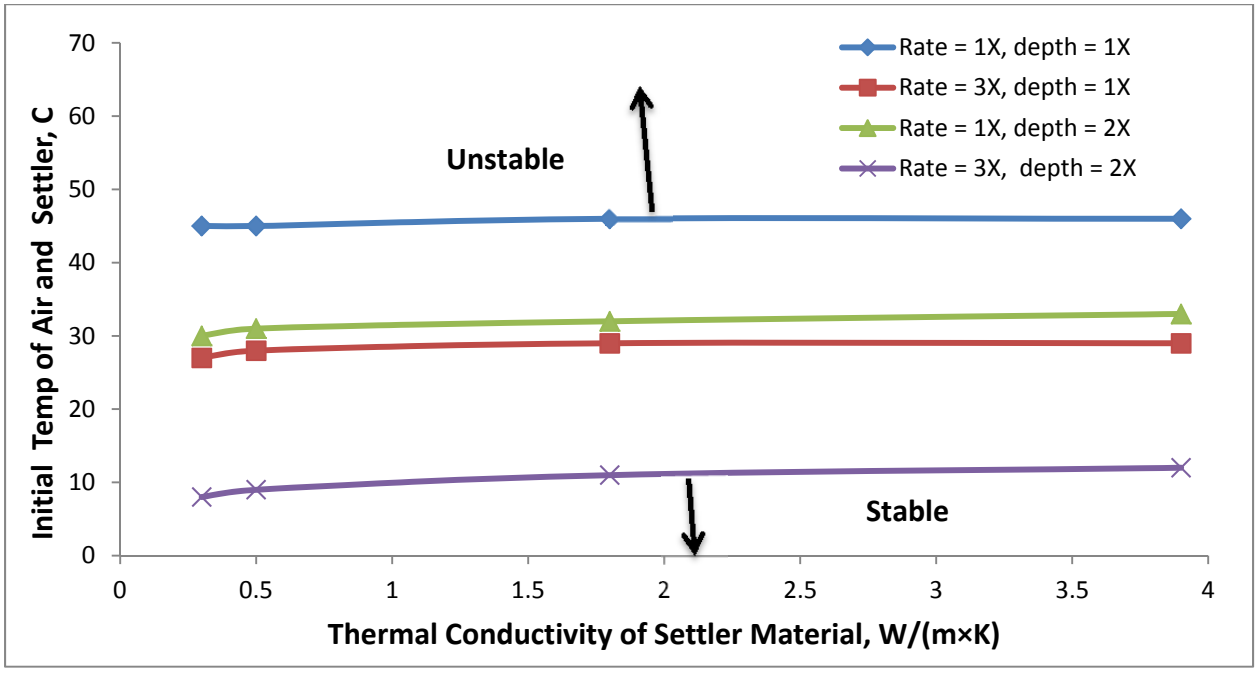

Figure 8.36. Sensitivity of Thermal Stability of Grouted Tube as a Function of Sludge Thermal Conductivity, Uranium Reaction Rate Multiplier, and Sludge Depth for Case 9, with Heat Transfer Coefficient of 3 W/(m^2·K)

Figure 8.37 shows the 2D cross-section of a grouted tube 30 days after removal from the Weasel Pit water and Figure 8.38 shows the maximum temperature of the uranium sludge with time.

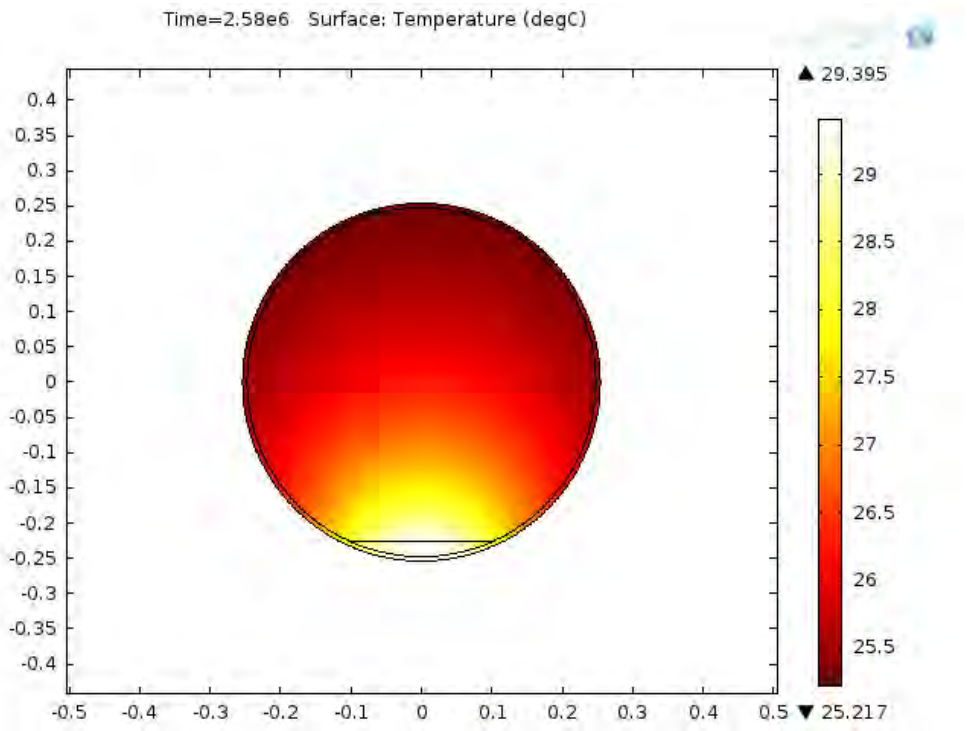

Figure 8.37. 2D Cross-Section of Grouted Tube 30 Days After Removal From Weasel Pit with Convective Tube Boundaries: 1× Uranium Reaction Rate, Heat Transfer Coefficient at 7.9 W/(m^2·K), Ambient Temperature at 25 °C

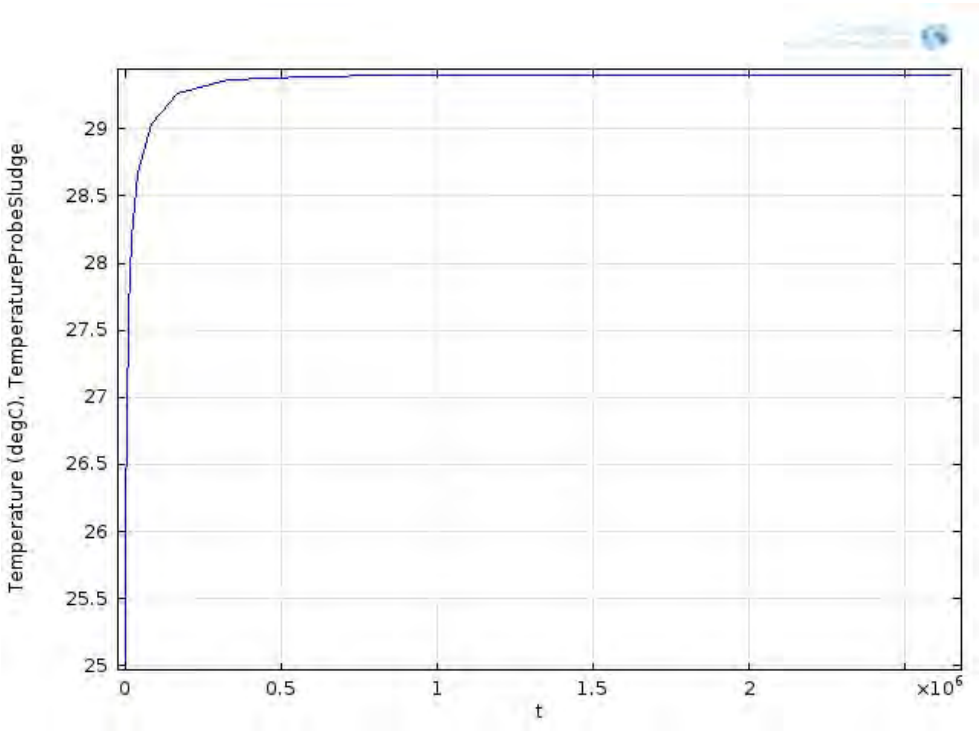

Figure 8.38. Maximum Uranium Sludge Temperature in Celsius versus Time (seconds) for Convective Boundary Conditions after Removal rrom Weasel Pit

8.3.9.3 Conclusions

Uranium sludge stability should be maintained during the time between removal from the Weasel Pit and storage in the waste box as long as ambient air temperatures are at or below room temperature. When storing the grouted tubes, care should be taken to ensure air contact around the tube walls (i.e., not burying the uranium sludge end in the ground). Also, avoiding placement of the uranium sludge in a position closest to the sun will help keep the temperature of the sludge in line with the simulation. Keeping the sludge positioned closest to the ground with air in contact should avoid any heat buildup occurring. The addition of active cooling with sprinklers would also increase the temperature stability. Performing the removal and storage of the grouted tubes during the winter months will provide lower-than-room-temperature ambient air conditions.

8.3.10 Longer Settler Tank Section (4.25 ft) in Box (Case 10)

Case 10 is equivalent to Case 8, but considers a longer settler tube section (4.25-ft length vs. the 1.25-ft section) at the maximum sludge depth of 2.35 cm. The box includes a 5-ft. cradle embedded in high-conductivity grout, top filled with sand, with solar heating and convective and radiative cooling. The goal of this case study is to explore the stability of a longer length of the settler tube being loaded into the waste box. The configuration with longer settler tank and cradle are shown in Figure 8.39.

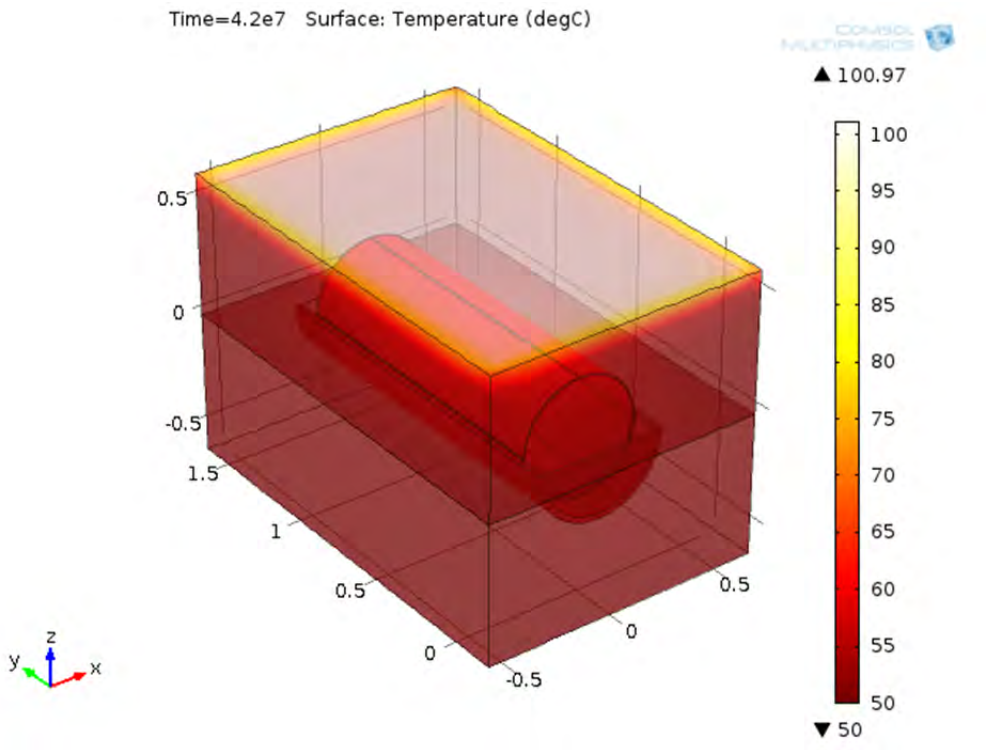

Figure 8.39. Temperature Profile for 4.25-ft Section with 1-Inch Cradle Thickness and ¼-Inch Gap Filled with High-Conductivity Paste (0.67 W/m·K) at 1× Uranium Sludge Reaction Rate

8.3.10.1 Input Parameters & Assumptions

- Grout in the settler tube will be mostly cured before the KW pool is drained and most of the hydration reactions will have occurred (i.e., cure time of 28 days or longer).
- U metal loading in the section: worst-case depth (2.35 cm) but 4.25-ft section (Tube 5S, Locations A + B + C)
- The uranium metal reaction cuts off upon expending 100% of the maximum heat of reaction, based on uranium metal content in the sludge of 9.2 g/cm^3. Decay heat is based on the uranium metal content, continues indefinitely.
- Constant solar heating directly above the box at 990 W/m^2 or from the side.
- Convective and radiative cooling of all the sides except the bottom of the waste box.
- Bottom of waste box at a constant 50 °C temperature.
- A case that considered side heating (from solar) was examined.
- As in Case 8, a steady-state temperature profile was allowed to develop before the uranium sludge temperature-dependent heating was allowed to begin at 4×10^7 seconds (463 days).
- Outside steel components of the box were ignored.
- Initial temperature of 50 °C was used for system components.

- Physical properties for the backfill material and high-conductivity grout are as defined in Table 8.5, and for the dry sand are as defined in Table 8.8.
- Cradle thicknesses of 1 to 4 inches were examined.
- A range of paste thermal conductivities was explored.

8.3.10.2 COMSOL Results

At a 1× reaction rate, a gap width of ¼-in, and paste at a thermal conductivity of 0.67 W/m·K, the configuration, as shown in Figure 8.39, was thermally stable with a cradle thickness of 1-in. An isosurface plot of the waste box after temperature-dependent heating was enabled is shown in Figure 8.40 and a profile of the temperature as a function of time is given in Figure 8.41.

At a uranium metal reaction rate multiplier of 3×, thermal stability was not achieved, even when increasing the cradle thickness to 4 inches, increasing the paste thermal conductivity to 1.5 W/m·K, and decreasing the gap to $^{1}/_{8}$-inch.

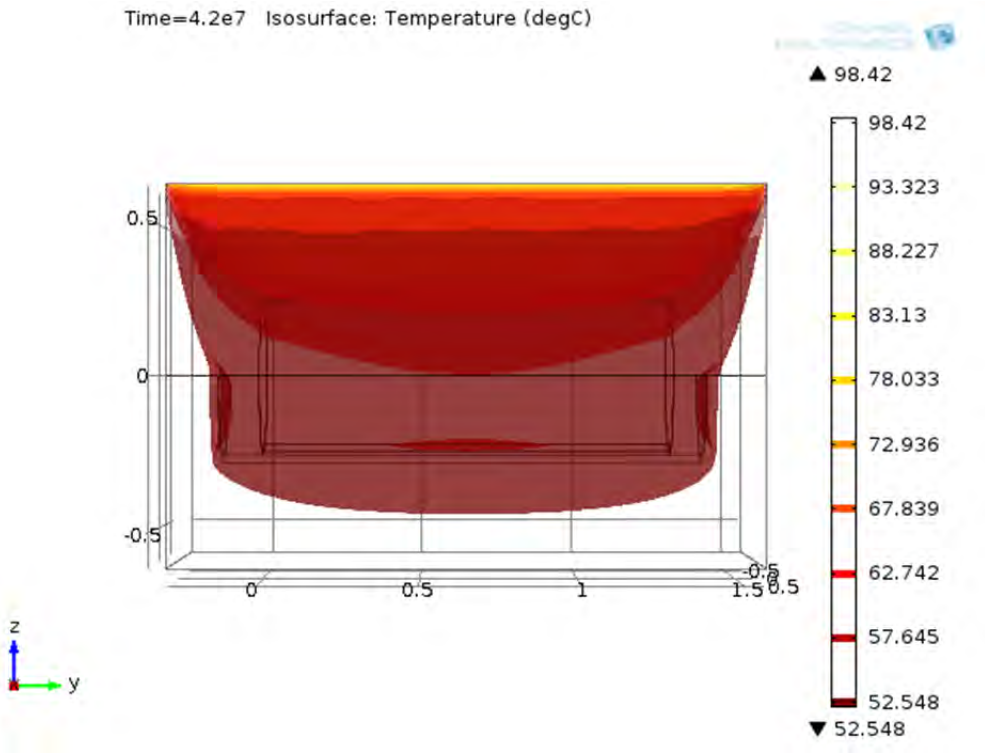

Figure 8.40. Isosurface Plot of Waste Box with Solar Heating After Uranium Sludge Heating: for 4.25-ft Section with 1-Inch Cradle Thickness and ¼-Inch Gap Filled with Paste (0.67 W/m·K) at 1× Uranium Sludge Reaction Rate

As was done in Case 8, Case 10 also delays the temperature-dependent heating component of the uranium sludge until 4×10^{7} seconds (463 days) have passed. This can be seen in Figure 8.41 below, which graphs the maximum temperatures of the waste box and uranium sludge.

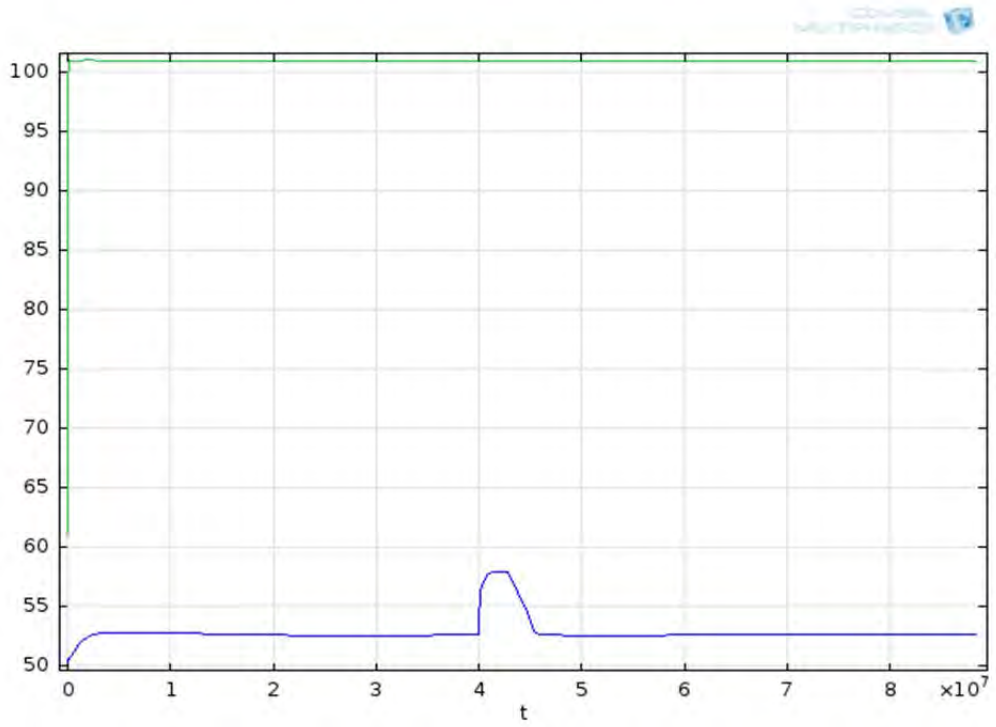

Figure 8.41. Maximum Sludge Temperature in Celsius (blue line) and Maximum Waste Box Temperature (green line) with Time (seconds) for 4.25-ft Section: 1× Uranium Sludge Reaction Rate, ¼-Inch Thermally Conductive Paste, 1-Inch Cradle Thickness, Thermal Paste Conductivity of 0.67 W/(m·K)

However, it was found that once the uranium sludge reaction rates were increased to 3×, the longer tube/cradle geometry yielded unstable results. Cradle thickness was varied up to 4 inches, with $^{1}/_{8}$-inch paste gaps and paste conductivities of 1.5 W/(m·K), all with the same results. Figure 8.42 shows an unstable simulation at 3× uranium reaction rate.

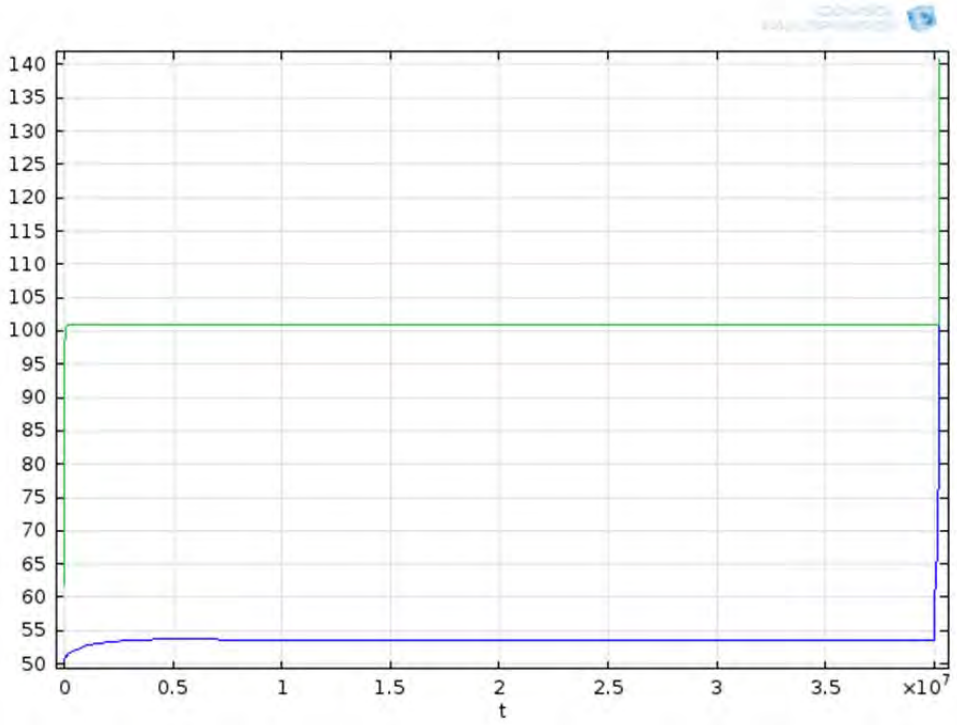

Figure 8.42. Maximum Sludge Temperature (blue line) and Maximum Waste Box Temperature (green line) with Time (seconds): 3× Uranium Sludge Reaction Rate, $^{1}/_{8}$-inch Thermally Conductive Paste, 2-Inch Cradle Thickness, Thermal Paste Conductivity of 1.5 W/(m·K)

Solar radiation hitting the side of the container was also explored in Case 10. Unsurprisingly. the high-conductivity grout is a better conductor of heat than the dry sand, and when it is in direct contact with the heated box it can conduct more heat to the tube section. In addition, the longer tube and cradle length decreases the distance heat would have to conduct through the grout.

Two different radiation scenarios were explored that involve side heating. Scenario 1 set the sun's radiation hitting the top of the box at 50% of the 990 W/m^2 maximum, with the other 50% hitting the side of the box. Scenario 2 – which is physically impossible but provides a bounding case – set 100% (990 W/m^2) of the sun's radiation hitting the top of the box and an additional 50% hitting the side of the box. Both scenarios are discussed below.

Figure 8.43 shows the temperature profile at 1× uranium reaction rate for Scenario 1.

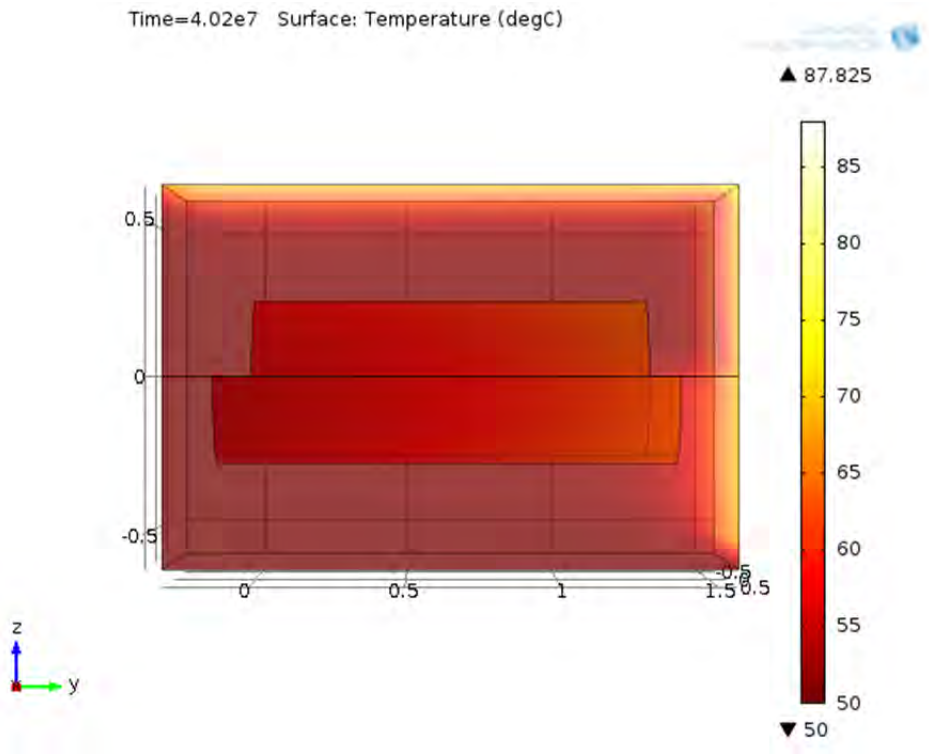

Figure 8.43. Temperature Profile of Waste Box With Solar Heating from Top and the Right Side: 1× Uranium Sludge Reaction Rate, ¼-inch Thermally Conductive Paste, 1-Inch Cradle Thickness, Thermal Paste Conductivity of 0.67 W/(m·K)

It can be seen that the high-thermal-conductivity grout conducts the heat received by the box into the bed better than the sand does. This is more readily evident in the isosurface plot in Figure 8.44.

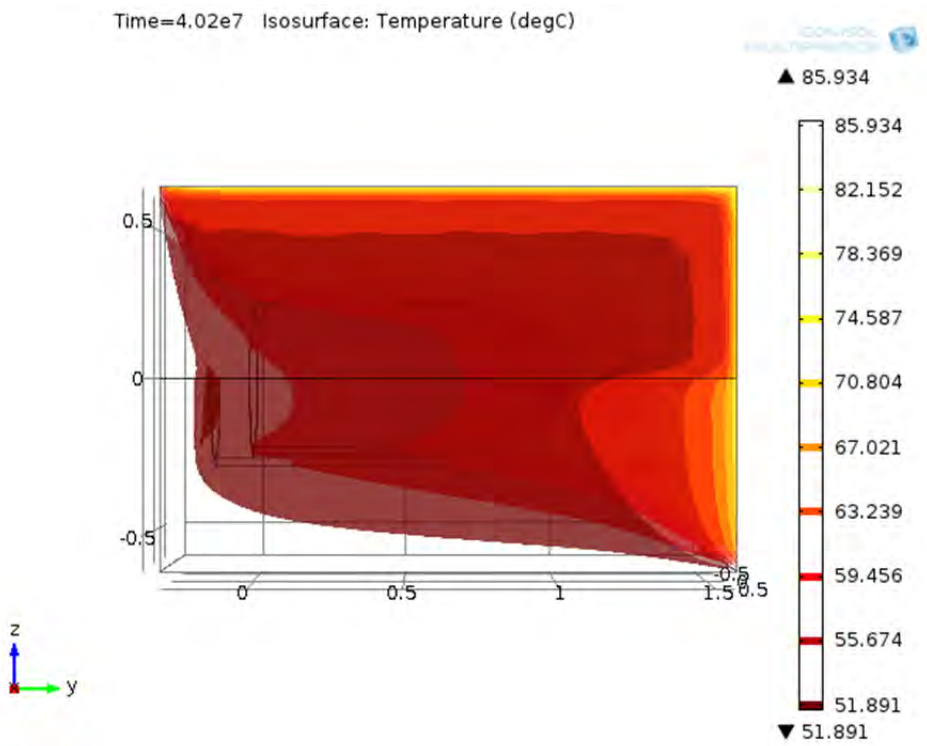

Figure 8.44. Isosurface Temperature Profile of Box with Solar Heating (50% from Top and 50% from Side): 1× Uranium Sludge Reaction Rate, ¼-inch Thermally Conductive Paste, 1-Inch Cradle Thickness, Thermal Paste Conductivity of 0.67 W/(m·K)

The added heat from the side increases the maximum temperature the uranium sludge experiences. This can be seen in Figure 8.45, which graphs the maximum box and maximum uranium sludge temperatures.

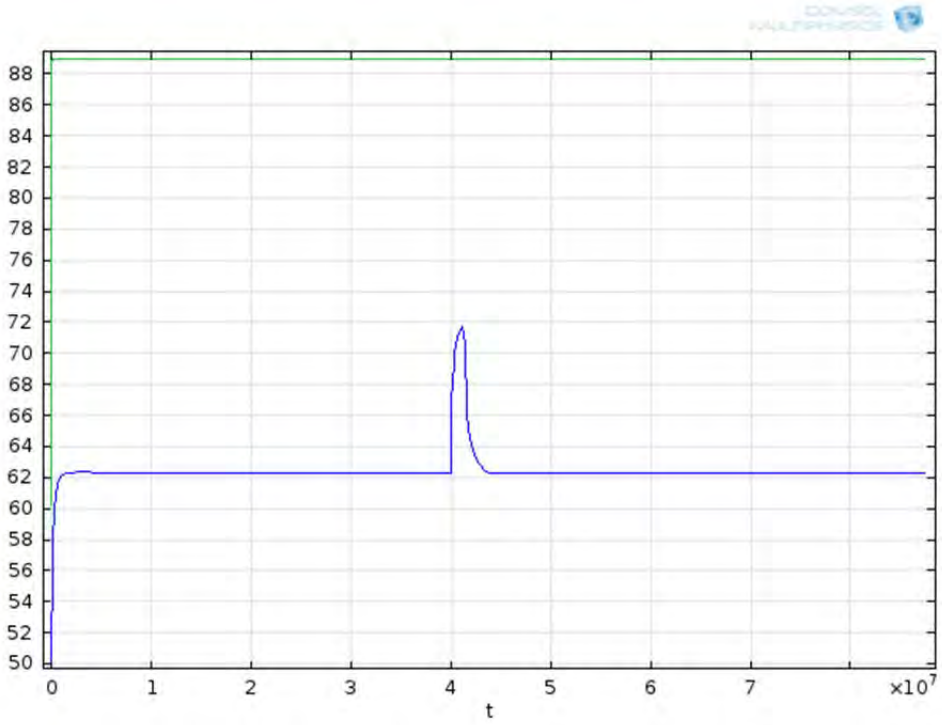

Figure 8.45. Maximum Sludge Temperature (blue line) and Maximum Waste Box Temperature (green line) with Time (seconds) for Waste Box with 50% Top and 50% Side Heating: 1× Uranium Sludge Reaction Rate, ¼-Inch Thermally Conductive Paste, 1-Iinch Cradle Thickness, Thermal Paste Conductivity of 0.67 W/(m·K)

Instead of a temperature of around 57 °C, a temperature close to 72 °C is reached.

Scenario 2, the simulation performed with 100% solar radiation hitting the top of the box and 50% solar radiation hitting the side, is physically impossible but provides a bounding case. The isosurface plot of this scenario is shown in Figure 8.46.

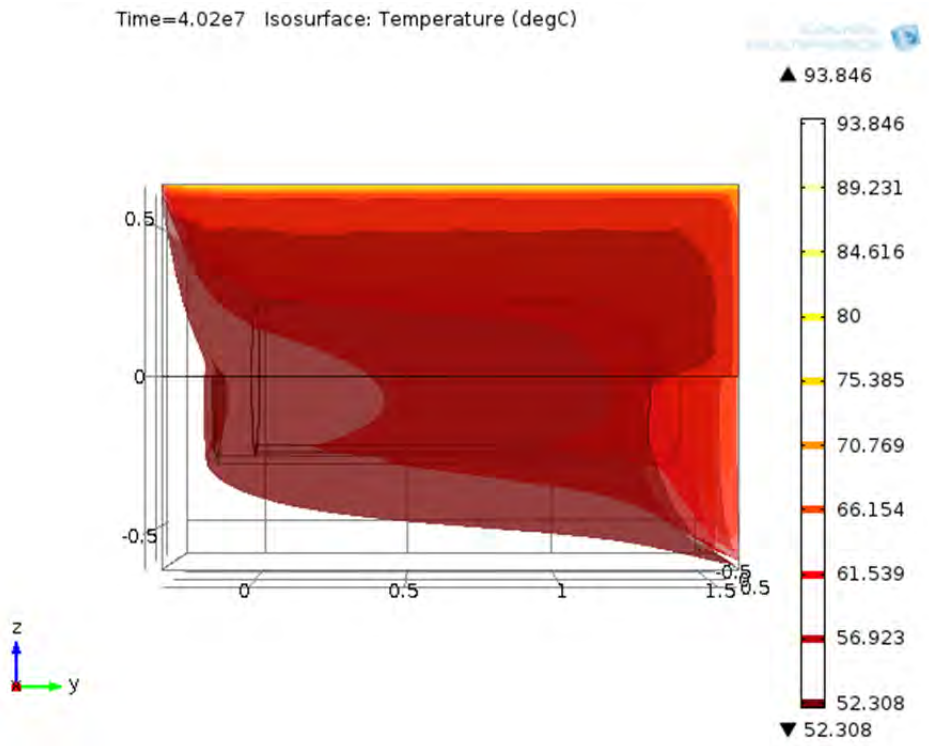

Figure 8.46. Isosurface Temperature Profile of Waste Box with Solar Heating (100% from Top and 50% from Side): 1× Uranium Sludge Reaction Rate, ¼-Inch Thermally Conductive Paste, 1-Inch Cradle Thickness, Thermal Paste Conductivity of 0.67 W/(m·K)

Once again, the simulation at 1× uranium sludge reaction rate was stable. This shows that the dry sand effectively insulates the uranium sludge from solar radiation.

8.3.10.3 Conclusions

Uranium sludge stability can be maintained with longer tube and cradle lengths if a maximum of 1× uranium sludge reaction rate is expected. At higher (3×) rates, a different setup is needed (e.g., shorter tube lengths and a longer cradle as shown in Case 8). In addition, solar radiation from the side may affect the stability of the waste box. The ends of the longer settler tank sections and cradle are closer to the side wall, which increases the impacts from the side radiation. However, these simulations can be considered a worst-case scenario because when solar radiation hits from an angle, ambient temperatures drop, which will result in higher convective cooling. Simulations done here are at constant radiative heating and ambient temperature condition, which would not be experienced in reality. In reality, during the night temperatures will drop, cooling the waste box, the sun will only hit a particular side for a short time, and the solar radiation hitting the top of the box will not be at maximum intensity all the time (as was assumed in the simulations).

9.0 Conclusions and Recommendations

Based on process knowledge, the ten settler tanks present in the Weasel Pit of the KW Basin are estimated to contain about 124 kilograms of finely divided (i.e., less than 600-µm) uranium metal, 22 kg of uranium dioxide, and another 55 kg of other radioactive sludge. The presence of finely divided uranium metal in the sludge is of concern because of the potential for thermal runaway reactions of the uranium metal with water and the formation of flammable hydrogen gas as a product of the uranium-water reaction. The Sludge Treatment Project (STP), managed by CH2MHill Plateau Remediation Company (CHPRC), is charged with managing the settler tanks and arranging for their ultimate disposal by burial in Hanford's Environmental Restoration Disposal Facility (ERDF) as part of deactivation, decontamination, decommissioning, and demolition (D4) of the KW Basin. In an untreated/unstabilized form, the settler tank sludge could be considered pyrophoric and treatment/packaging to stabilize the sludge is required for disposal at ERDF.

This report evaluates the thermal stability of the contents of the settler tanks during planned grouting and subsequent handling and packaging for disposition to ERDF. Technical bases for the thermal properties and boundary conditions for the operations were developed and documented. Modeling of the various scenarios was conducted with a commercial finite element analysis solver, and simulation software package (COMSOL Multiphysics, Version 4.3). Observations, Conclusions, and Recommendations from this evaluation are summarized here.

Underwater grouting of Settler Tanks. The first step in the D4 sequence is to fill the settler tanks with grout, as they currently sit in the Weasel Pit, submerged in water. Heat is released from grout hydration reactions, with most of the curing heat released in about 28 days.

- The formulation used for grouting the K East Discharge Chute was selected as the leading candidate for use in the settler tanks based on its previous use in the K Basins and the commonality of process objectives established for its implementation (i.e., good flow properties, low heat generation rate, sufficient set strength to allow its size-reduction without undue crumbing).
- The Weasel Pit water provides a heat sink sufficient to allow simultaneous grouting of all settler tanks. An adiabatic calculation showed that the simultaneous grouting and instantaneous curing of all 10 settler tanks and 100% reaction of the contained uranium metal would raise the temperature of the water within the Weasel Pit by only 5.5 °C.
- With the temperature of the settler tank wall equal to the water temperature, the grouting operation is thermally stable at all reasonable water/basin pool temperatures [i.e., pool temperature 79 °C (174 °F) or less] and at a uranium metal reaction rate multiplier of 3×.
- The baseline thermal conductivity of uranium metal particles in water (fuel piece sludge) is set at 3.9 W/(m·K) in the Sludge Databook. However, if the thermal conductivity of the sludge layer is degraded by an order of magnitude (postulated reduction from worst-case gas bubble retention with particle bed dry-out), thermal instability could be encountered at basin pool temperatures of >40 °C (104 °F) at a reaction rate enhancement factor of 3× or if the sludge depth inside the worst-case settler tank is doubled.

Behavior of post-grouted settler tank array during Weasel Pit D4 activities. After grouting the settler tanks (and after the nominal 28-day cure time), debris on the Weasel Pit floor *may* be encapsulated by pouring a 6- to 14-inch-thick layer of grout, while the Weasel Pit is filled with water.

- If the grout is poured to a depth of 14 inches (to encapsulate debris on the pit floor), the bottom 2 inches of settler tanks N-5 and S-5 will be bathed in grout. The resulting grout-curing heat will cause thermal instability in N-5 and S-5.

- If grout is poured to a depth of 6 inches, allowing ~6 inches of water between top of the grout pour and bottom of tanks N-5 and S-5, thermal instability is highly unlikely when including the heat convention term for the pool water.

To summarize, if grout is used to encapsulate the Weasel Pit floor, controls should be implemented to keep the top of the pour well below the bottom two settler tanks.

Draining of the KW pool and backfilling Weasel Pit with dry/wet sand (5 days). The KW Basin will be emptied of water, the tanks will be briefly exposed to air, and the settler tanks will be covered with a backfill material. While covered, the settler tanks will be sectioned by a mechanical shear, and the sections will be lifted out and loaded into waste disposal boxes. The STP project estimates that draining, backfill, shearing, and removal of the sections will be completed in 4-days' time. Backfill materials considered included a controlled-density fill (CDF; a self-compacting low-strength grout), dry sand, and wet sand. For modeling, PNNL examined a 5-day window of thermal stability for this work evolution.

- A series of simulations of the settler tanks exposed to boundary condition of convective cooling with air at a constant temperature was performed to examine stability behavior after pool water drainage, or while awaiting load-in into a waste box. Under the conditions modeled, with a uranium reaction rate multiplier of 1×, the baseline sludge thermal stability is maintained if the air temperature is <46 °C. At a reaction rate multiplier of 3×, thermal instability can be incurred at air temperatures >29 °C.

- Because of the heat of hydration associated with Portland cement constituents and the inability to reject sufficient heat from the grouted settler tanks, use of CDF in not recommended.

- The thermal conductivity of dry sand may be as low as 0.13 W/(m·K); consequently, dry sand can serve as a thermal insulator. In this case, the settler tank array will be thermally unstable within 5 days if the initial dry sand temperature exceeds 44 °C (111 °F).

- The thermal conductivity of water-saturated sand (~1.3 W/m·K) is an order of magnitude higher than that of dry sand. Therefore, saturated or even damp sand (~0.78 W/m·K) is a reasonable choice for use as backfill.

In summary, it is recommended that the dewatering, backfilling, shearing, and waste box loading operations be scheduled for the cooler months of the year because of the limited ability to reject heat from grouted settler tanks after the KW basin is drained of water. Exposure to warm air or warm dry sand must be avoided. Wet or damp sand is recommended for the backfill material. If exposure to warm air cannot be avoided, active cooling with sprinklers should be considered.

Waste Disposal Box. After sectioning, segments of the settler tank will be loaded into waste disposal boxes for transport to and disposal at ERDF. In consultation with ERDF staff, STP estimated that the time between box loading at KW and box burial at ERDF will be on the order of 30 days. For most modeling of the waste box thermal stability, the worst-case 1.25-ft-long section (deepest layer of sludge) from Tube S5 was considered. However, a final case was developed to model a 4.25-ft-long section at the worst-case uranium loading.

Based on consultation with STP staff and after evaluation of a number of alternatives, the following configuration is suggested to provide long-term and robust thermal stability:

- Box: Size: 4(L) × 6(W) × 4 (H) ft steel box, painted white to maximize solar reflectance.

- Internals: Lower half of box should be fitted with ~20- to 21-inch inside-diameter heavy-wall carbon steel half-pipe that is 1 to 2 inches in wall thickness and 3.25 to 5 ft long to act as a cradle, heat conductor, and particularly as a heat sink. The 1-in wall thickness is sufficient to maintain thermal stability of the worst-case sludge depth at a 1× uranium reaction rate. A 2-inch cradle thickness will provide additional margin for a 3× uranium reaction rate multiplier.

- The half-pipe and its support structure should be embedded in high-thermal-conductivity grout [thermal conductivity ≥ 1.0 W/(m·K)] to extended the heat sink and to provide shielding from radioactivity. The high-thermal-conductivity grout will be added to depth of 2 feet. The waste box, with half-pipe and high-thermal-conductivity grout, should be made up well in advance of use to allow the grout a cure time of 28 days or more.

- To provide good thermal connectivity between settler tank section and half-pipe, a non-curing thermal conductivity paste/grease should be placed on the half-pipe before the settler tank section is lowered into place. As the section is lowered, the paste will fill gaps between the half-pipe and tank section. The thermal conductivity of the paste/grease must be ≥0.67 W/(m·K). Thermal stability was examined with a paste thickness of up to ¼ inch. High-thermal-conductivity paste/grease is available and will provide additional robustness to the configuration stability.

- After the settler tank section is in place, the upper half of the disposal box should be filled with cool dry sand. The sand will provide shielding and insulate the settler section from solar heating while the box is awaiting burial at ERDF.

- For this configuration to be effective, the settler tanks must be marked such that they are oriented in the box with the uranium sludge layer on the bottom of the tank and in contact with the heat sink. Such alignment should be readily observed because of the presence of strengthening ribs on the bottom length of the settler tanks.

- Tolerance in thermal stability for a gap size wider than ¼ inch with a higher-thermal-conductivity paste (e.g., greater than 1 W/m·K) may be possible. However, additional modeling would be required to determine the sensitivity among the other critical parameters (including thickness of cradle, reaction rates, etc.).

- At the baseline uranium metal reaction rate (1×), simulations with initial outside ambient and interior temperatures of 50 °C show that with the recommended waste disposal box configuration,

thermal stability will be maintained for a 4.25-ft worst-case section with a 1-in-thick cradle, during severe top and side solar heating. In addition, a 1.25-ft section configuration remains stable even with an air gap of $^{1}/_{16}$ in between the tank and half-pipe.

- At a rate multiplier of 3× and a 2-in-thick cradle, thermal stability is maintained for the worst-case 1.25-ft section with initial outside ambient and interior temperatures of 50 °C. However, with a 4.25-ft section and solar heating from the top, thermal stability was not demonstrated, even with a 4-in-thick cradle and $^{1}/_{8}$-inch gap.

The suggested waste box configuration is sufficiently robust to handle to a 4.25-ft settler tank section loaded with uranium metal at the maximum depth estimated for a single location with a conservative treatment of solar heating. However, when additional conservatism was stacked on (e.g., reaction rate multiplier of 3×) thermal stability was not shown when the length of tube section was increased from 1.25 to 4.25 ft.

Further Considerations. STP D4 staff and designers must weigh-in on potential refinements to the implementability of the recommended waste box configuration, including the use of nominal vs. safety basis sludge parameters. There are many areas for potential refinement and optimization, but waste box designers must guide the focus for future optimizations. Also, with refinements, some of the conservatism could be reduced.

Key areas of input for designers and D4 staff consideration include:

- What is a readily achievable gap between the settler tank section (whose shapes may be distorted by shearing) and the cradle?
- What are the implications/restrictions on the overall weight of the package? Should refinements be focused on reducing the heat sink mass or even the mass of the high-conductivity grout heat sink?
- What are the benefits of the use of an even higher-thermal-conductivity grout?
- Are there benefits to adjusting the grout fill level in the box?
- Instead of a half-pipe heat sink cradle, should a ⅓- or ¼-pipe section be considered?
- Should end pieces of the cradle be designed with a closure or be left open?

10.0 References

ACI. 2002a. *Effect of Restraint, Volume Change, and Reinforcement on Cracking of Mass Concrete*. ACI 207.2R-95, American Concrete Institute, Farmington Hills, MI.

ACI. 2002b. *Guide to Thermal Properties of Concrete and Masonry Systems*. ACI 122R-02, American Concrete Institute, Farmington Hills, MI.

ASTM C939-10, Standard Test Method for Flow of Grout for Preplaced-Aggregate Concrete (Flow Cone Method), ASTM International, West Conshohocken, PA, 2010, www.astm.org

Bentz DP, MA Peltz, A Durán-Herrera, P Valdez, and CA Juárez. 2011. "Thermal Properties of High-Volume Fly Ash Mortars and Concretes". *Journal of Building Physics* 34(3):263-275.

Bentz DP, CF Ferraris, and KA Snyder. 2013. "Best Practices Guide for High-Volume Fly Ash Concretes: Assuring Properties and Performance". NIST Technical Note 1812, National Institute of Standards and Technology, Gaithersburg, MD. Available at: http://concrete.nist.gov/~bentz/NIST.TN.1812.pdf.

Campbell GS, JD Jungbauer, Jr, WR Bidlake, and RD Hungerford. 1994. "Predicting the Effect of Temperature on Soil Thermal Conductivity". Soil Science 158:307-313.

Casbon MA 2014. Environmental Restoration Disposal Facility Waste Acceptance Criteria. WCH-191, Rev. 3, Washington Closure Hanford, Richland WA.

CETCO. 2013. "Geothermal Grout™". CETCO, Hoffman Estates, IL. http://www.cetco.com/DesktopModules/Bring2mind/DMX/Download.aspx?Command=Core_Download&PortalId=0&EntryId=4344

Choktaweekarn P, W Saengsoy, and S Tangtermsirikul. 2009. "A Model for Predicting the Specific Heat Capacity of Fly-Ash Concrete". Science Asia 35:178-182. http://scienceasia.org/2009.35.n2/scias35_178.pdf

Copeland LE, DL Kantro, and G Verbeck. 1960. *Chemistry of Hydration of Portland Cement*. Research Department Bulletin 153 of the Research and Development Laboratories of the Portland Cement Association, Skokie, IL. Reprinted from Chemistry of Cement, Monograph 43, Volume I, Session N, Paper IV-3, pp. 429-465, in Proceedings of the Fourth International Symposium on the Chemistry of Cement, National Bureau of Standards, U.S. Department of Commerce, Washington, DC. Available at: http://www.asocem.org.pe/bivi/sa/dit/icem/rx153.pdf.

CRC. 1980. CRC Handbook of Tables for Applied Engineering Science, 2nd edition. CRC Press, Inc., Cleveland, OH.

CRC. 2000. CRC Handbook of Chemistry and Physics, 80th edition. CRC Press, Inc., Cleveland, OH.

CRC. 1978. CRC Handbook of Chemistry and Physics, 59th edition. CRC Press, Inc., Cleveland, OH.

Delegard CH and AJ Schmidt. 2009. *Uranium Metal Reaction Behavior in Water, Sludge, and Grout Matrices.* PNNL-17815, Rev. 1, Pacific Northwest National Laboratory, Richland, Washington. Available at: http://www.pnl.gov/main/publications/external/technical_reports/PNNL-17815rev1.pdf.

DOE. 2000. *KW Fuel Storage Basin IWTS Settler System Assembly & Details*. Drawing H-1-83330, Rev. 7, Sheets 1 through 3. U.S. Department of Energy, Richland, WA.

Fuels Production Department. 1979. "Unusual Occurrence Report". UO 79-27, dated August 2, 1979.

Gydesen CH. 1982. *Preliminary Engineering Study Report Uranium Oxide Facility Project H-596*. UNI-2102, UNC Nuclear Industries, Richland, WA.

Honeyman JO. 2013. *Sludge Treatment Project Decision Support Board Second Settler Tank Retrieval Evaluation*. PRC-STP-00805, Rev. 0, CH2M Hill Plateau Remediation Company, Richland, WA.

Johnson ME. 2014. *Spent Nuclear Fuel Project Technical Databook, Volume 2, Sludge*. HNF-SD-SNF-TI-015, Rev 25, CH2M Hill Plateau Remediation Company, Richland, WA.

Kim SG. 2010. "Effect of Heat Generation from Cement Hydration on Mass Concrete Placement". Thesis, Iowa State University, Ames, IA. http://lib.dr.iastate.edu/cgi/viewcontent.cgi?article=2674&context=etd.

Kumar M, SK Singh, and NP Singh. 2012. "Heat Evolution During the Hydration of Portland Cement in the Presence of Fly Ash, Calcium Hydroxide, and Super Plasticizer". *Thermochimica Acta* 548:27-32.

Landsman SD. 2014. *Distribution of Less Than 600 Micron Sludge Added to the 105-KW Basin IWTS Settler Tanks during Pretreatment and Processing of Knock-Out Pot (KOP) Material*. PRC-STP-CN-O-00912, Rev. 0, CH2M Hill Plateau Remediation Company, Richland, WA.

Langan BW, K Weng, and MA Ward. 2002. "Effect of Silica Fume and Fly Ash on Heat of Hydration of Portland Cement". Cement and Concrete Research 32:1045-1051.

Lawrence CD. 1998. "Physicochemical and Mechanical Properties of Portland Cements". Chapter 8 in Lea's Chemistry of Cement and Concrete, 4th edition, PC Hewlett, editor. Butterworth-Heinemann, Oxford, UK.

Leshikar GA. 2010. *Residual Sludge Volume Estimates for K-West Basin IWTS Settler Tanks following Fiscal Year 2010 Sludge Retrieval and Borescopic Inspection.* PRC-STP-00275, Rev. 0, CH2M Hill Plateau Remediation Company, Richland, WA.

Massazza F. 1998. "Pozzolana and Pozzolanic Cements". Chapter 10 in Lea's Chemistry of Cement and Concrete, 4th edition, PC Hewlett, editor. Butterworth-Heinemann, Oxford, UK.

McGannon HE. 1971. The Making, Shaping and Treating of Steel. 9th edition, Herbick and Held, Pittsburgh, PA.

Muller FE. 2015. Personal communication, e-mail "RE: Grout Composition Used in 105-KE Discharge Chute" to CH Delegard, 5 January 2015.

Poloski AP, PR Bredt, A Schmidt, RG Swoboda, JW Chenault, and SR Gano. 2002. Thermal Conductivity and Shear Strength of K Basin Sludge. PNNL-13911, Pacific Northwest National Laboratory, Richland, WA. http://www.pnl.gov/main/publications/external/technical_reports/PNNL-13911.pdf

Schmidt AJ. 2013. "Hanford Experience in Grouting/Cementation of Uranium Metal and Implications for Grouting Uranium Metal in Settler Tanks". Letter report 53451-L83 to JP Sloughter, Pacific Northwest National Laboratory, Richland, WA.

Schmidt AJ and RA Sexton. 2009. *Supporting Basis for SNF Project Technical Databook.* SNF-7765, Rev. 3D, CH2M Hill Plateau Remediation Company, Richland, WA.

Schmidt AJ, CH Delegard, SA Bryan, MR Elmore, RL Sell, KL Silvers, SR Gano, and BM Thornton. 2003. *Gas Generation from K East Basin Sludges and Irradiated Metallic Uranium Fuel Particles – Series III Testing*. PNNL-14346, Pacific Northwest National Laboratory, Richland, WA. Available at: http://www.pnl.gov/main/publications/external/technical_reports/PNNL-14346.pdf.

Sexton RA. 2011. *K Basin Closure Project Technical Databook KOP Material (OCRWM)*. HNF-SD-SNF-TI-015, Volume 3, Rev. 2, CH2M Hill Plateau Remediation Company, Richland, WA.

Shimskey RW, JM Billing, SJ Bos, CA Burns, CD Carlson, DS Coffey, RC Daniel, CH Delegard, MK Edwards, SK Fiskum, LR Greenwood, SA Jones, M Luna, D Neiner, BM Oliver, KN Pool, AJ Schmidt, SI Sinkov, LA Snow, CZ Soderquist, ML Thomas, CJ Thompson, T Trang-Le, and MW Urie. 2013. *Characterization Data Package for Containerized Sludge Samples Collected from Engineered Container SCS-CON-230*. PNNL-20470, Rev. 1, Pacific Northwest National Laboratory, Richland, WA.

Slotemaker CJ. 2013. *Calculation of Sludge Volume and Radioactivity on the 105KW Basin and Pit Floors Based on Sludge Depth Measurements in February and March 2013.* ECF-100KR2-13-0011, Rev. 0, CH2M Hill Plateau Remediation Company, Richland, WA.

Sloughter JP. 2011. *STP KOP Disposition Sub Project Pretreatment Uranium Balance.* PRC-STP-CN-CH-00570, Rev. 0, CH2M Hill Plateau Remediation Company, Richland, WA.

Sloughter JP and JA Pottmeyer. 2013. *Project Transition/Closeout Report for the Sludge Treatment Project Knockout Pot Disposition Subproject*. PRC-STP-00750, Rev. 0, CH2M Hill Plateau Remediation Company, Richland, WA.

Sloughter JP. 2013. *STP KOP Disposition Subproject KOP Processing Systems Uranium Balance*. PRC-STP-CN-CH-00742, Rev. 0, CH2M Hill Plateau Remediation Company, Richland, WA.

Stephens P. 2015. Personal communication. Telecon Cal Delegard with Pat Stephens, Pacific International Grout Company, pat@pigcoinc.com, 360-733-5270, 29 January 2015.

Thomas M. 2007. *Optimizing the Use of Fly Ash in Concrete*. IS548, Portland Cement Association, Skokie, IL. Available at: http://www.cement.org/docs/default-source/fc_concrete_technology/is548-optimizing-the-use-of-fly-ash-concrete.pdf?sfvrsn=4

Weakley EA. 1973. "Method for Processing Scrap Fissile Material into a Form Suitable for Shipping". US Patent 3,779,938, US Government Patent and Trademark Office, Washington, DC. Available at: http://pdfpiw.uspto.gov/.piw?PageNum=0&docid=03779938&IDKey=630F7CEAFB6B%0D%0A&HomeUrl=http%3A%2F%2Fpatft.uspto.gov%2Fnetahtml%2FPTO%2Fpatimg.htm.

Weakley EA. 1976. *History and Status of Environmental Improvements for Fuels Production Division*, UNI-652, United Nuclear Industries, Inc., Richland, WA.

Weakley EA. 1980. *Interim Report on Concreted Uranium Fines and Chips Billet Curing Tests: A Basis for Resuming Shipment of Concreted Uranium Scrap Billets*. UNI-1454, United Nuclear, Richland, WA.

Weakley EA. 1982. *Technical Criteria Uranium Chips and Fines Burning Facility*. UNI-1864 Rev 1, United Nuclear Industries, Inc., Richland, WA.

Yanochko RM, RM Suyama, SP Burke, HP Fox, DL John, TK Orgill, RL Maurer, JE Sailer, and AM Umek. 2005. *Project Experience Report – Encapsulation of the 105-KE Basin Discharge Chute*. D&D-27352, Rev. 0, Fluor Hanford, Richland, WA.

Appendix A

Condensed Output for COMSOL Models

Appendix A

Condensed Output for COMSOL Models

Nomenclature and Overview of Cases Modeled

Case Number	Description
Case 0	Benchmark To verify correct functioning and installation of COMSOL, the analyst programmed and evaluated the case, "Heat Conduction in a Cylinder" (which was taken from a NAFEMS benchmark collection and shows an axisymmetric steady-state thermal analysis).
Case 1	Underwater grouting of highest U metal-content tank section (2D Model, Tank S5, Location B). Grout pumped into the settler tank, and stability examined with the ensuing heat of hydration from grout-former reactions. This case also includes an adiabatic test case with no heat flow beyond the settler tank walls to evaluate thermal stability with the wall of settler tank perfectly insulated.
Case 2	Grouted settler tank array backfilled with sand. 2D model of highest U metal-content cross-section in the settler tanks (located 2 to 2.75 feet into settler), water removed from the basin, and Weasel Pit backfilled with sand.
Case 3	Grouted settler tank underwater plus 14 inches of grout added to floor of Weasel Pit. 2D model of highest U metal-content cross-section with grout pour submerging bottom 2 inches of tanks S5 and N5.
Case 4	Grouted settler tank underwater plus 6 inches of grout added to floor of Weasel Pit. Same as Case 3 except top of grout floor pour is 6 inches below bottom of S5 and N5.
Case 5	Settler tank section in IP2 Waste Box 3D model. 1.25-foot section of the worst-case settler tank section placed into the IP2 waste box (10 ft × 20 ft × 10 ft) filled with wet or dry sand. This case is not a realistic disposal option; however, it illustrates 3D thermal behavior of settler tank section surrounded by fill.
Case 6	Settler tank section in 4 ft × 6 ft × 4 ft box with carbon steel cradle surrounded by sand. Carbon steel cradle is used as a heat sink. To provide good thermal connection, a thermal conductivity grease fills the space between the settler tank and the cradle.
Case 7	Settler tank section in box with carbon steel cradle embedded in high-conductivity grout, with top filled with sand. Use of high-thermal-conductivity grout in the 4 ft × 6 ft × 4 ft box improves robustness of the heat sink concept.
Case 8	Same as Case 7, but with reasonably bounding solar heating on top of box. Maximum solar heating rate, 24-h per day, imposed until steady state is established and then uranium metal reactions are initiated in model. Sand fill in top of box helps insulate settler tank section from solar insolation.
Case 9	Case 9 is Case 1 with substitution of convective cooling for the constant-temperature boundary conditions. This case examines the condition when the basin is dewatered, or if/when sections of settler tanks are stored in air.
Case 10	Same as Case 8 but with settler tank section increased to 4.25 ft. Depth of uranium-rich sludge maintained at 2.35 cm, and length of cradle increased to 5 ft with solar heating on top of box and on one side.

*Note: PNNL has provided electronic versions of extended output for each case modeled to CHPRC.

QA case study same results obtained for both 4.3b license and computers tested us
file: heat conduction in cylinder V&V
Evaluation of results
For the point r = 0.04 and z = 0.04 I obtained 332.957 K 557 elements
Finer mesh
Benchmark result was 332.97 K at the same location (Summary), NAFEMS, 1986
Reference: A. D. Cameron, J. A. Casey, and G. B. Simpson,
NAFEMS Benchmark Tests for Thermal Analysis

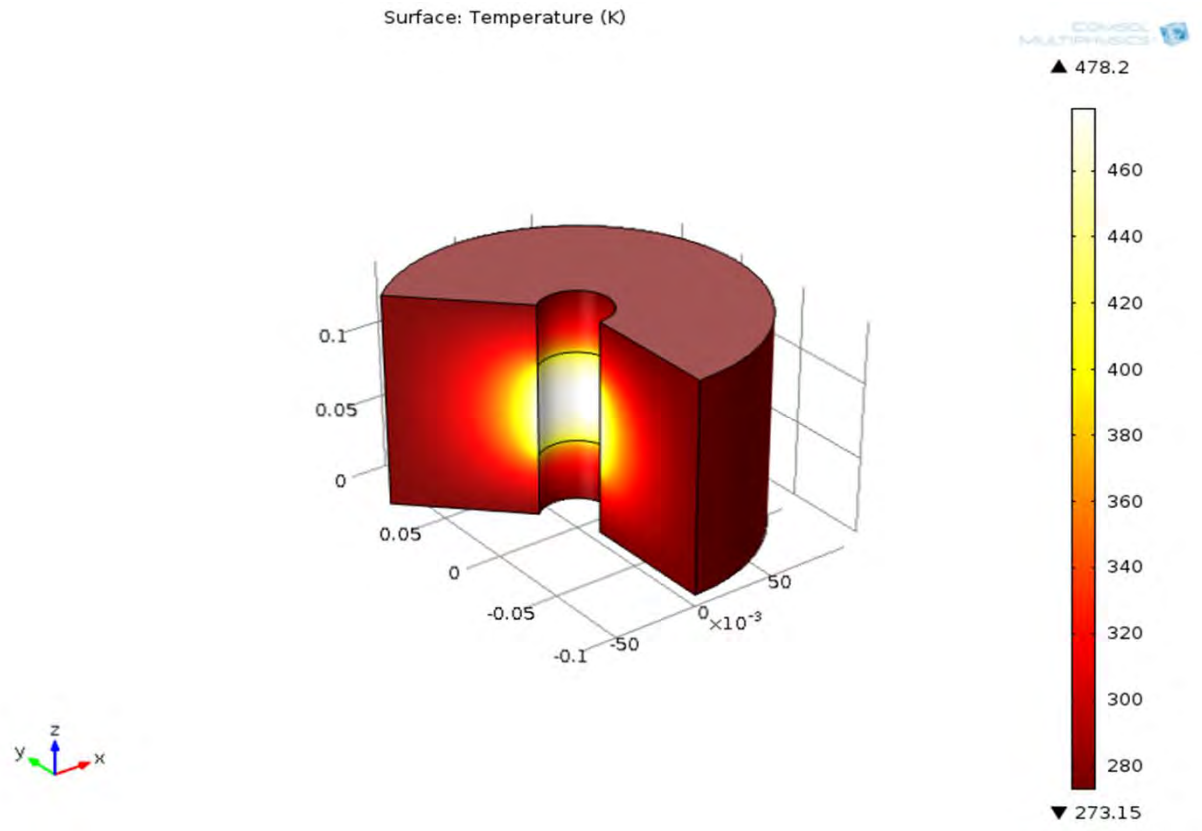

ing this V&V model test

Comsol 4.3b	Same as the expected result of 332.957K from the Comsol literature

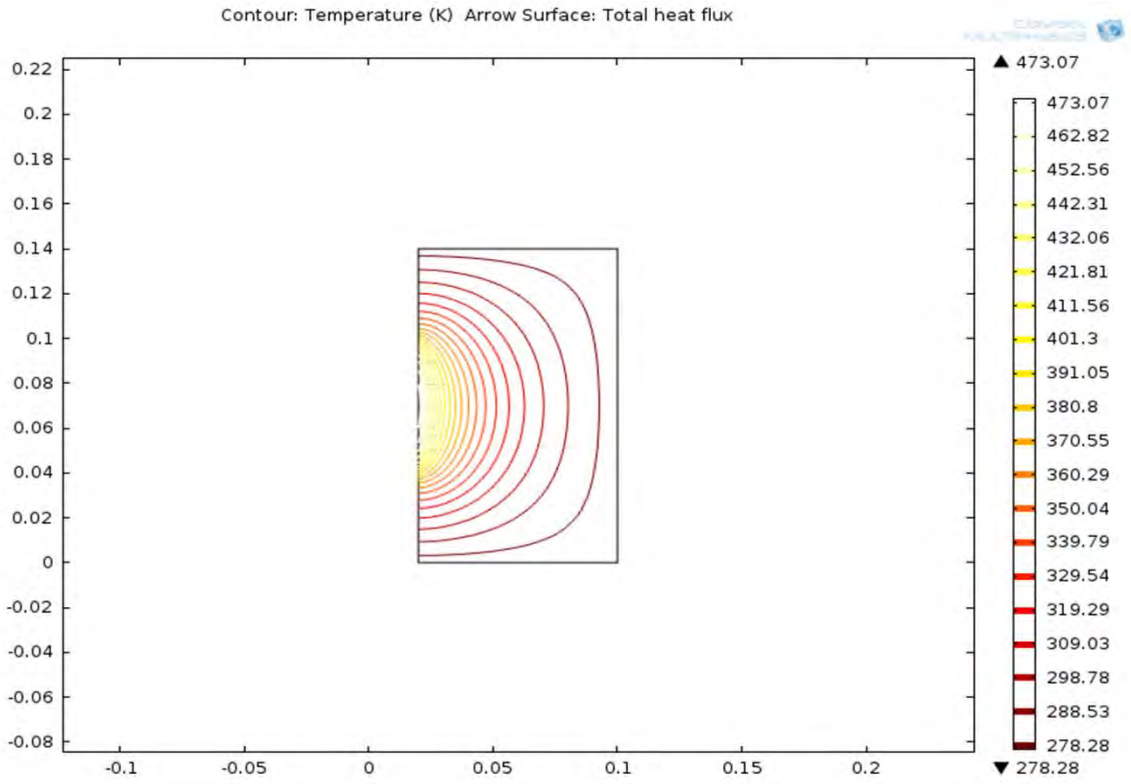

Case 1
file: K basin time dependent4.mph
file: K basin time dependent4.docx

U Thermal Conductivity	Stability Limit Temperature r=f(Temp) Baseline U depth	r=f(Temp) 2X Baseline U depth	r=3*f(Temp) 2X Baseline U depth	r=3*f(Temp) Baseline U depth
3.9	90	77	60	79
1.8	83	65	49	68
0.5	65	46	30	48
0.3	58	39	21	41

Basline U depth is 2.23 cm

insulating boundary condition case
Goes unstable in 7 hours

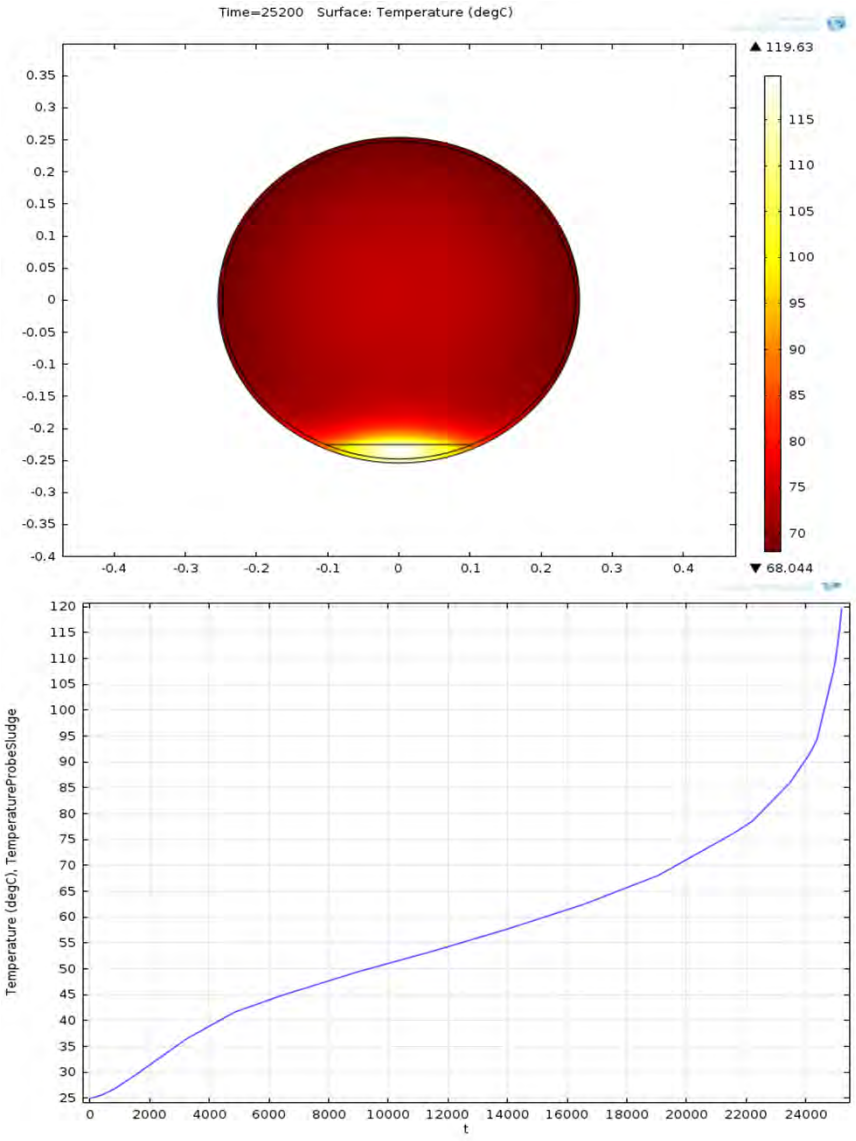

Baseline

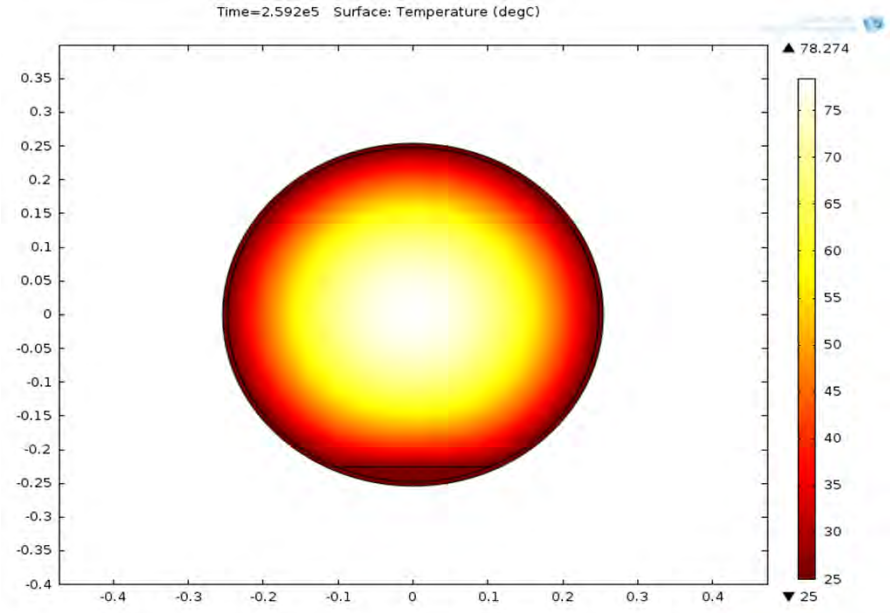
Time=2.592e5 Surface: Temperature (degC)
▲ 78.274
75
70
65
60
55
50
45
40
35
30
25
▼ 25
0.35
0.3
0.25
0.2
0.15
0.1
0.05
0
-0.05
-0.1
-0.15
-0.2
-0.25
-0.3
-0.35
-0.4
-0.4
-0.3
-0.2
-0.1
0
0.1
0.2
0.3
0.4

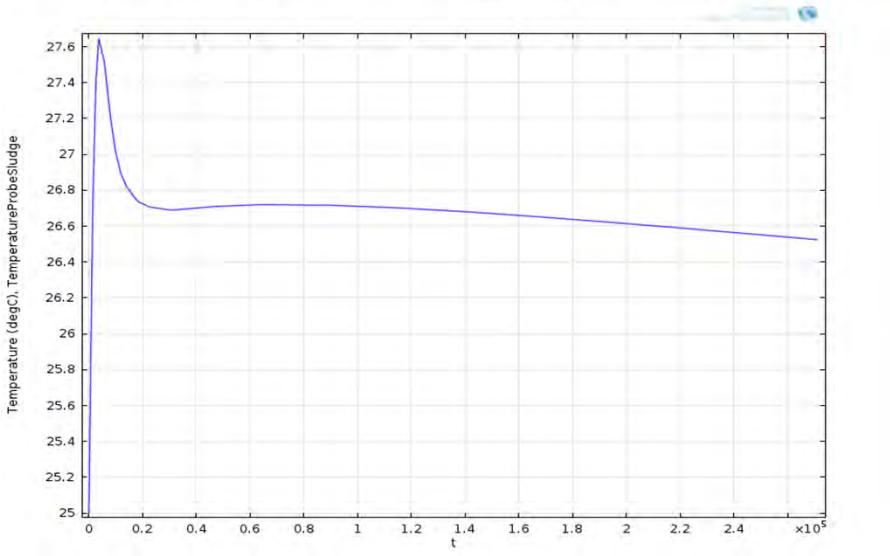
Temperature (degC), TemperatureProbeSludge
27.6
27.4
27.2
27
26.8
26.6
26.4
26.2
26
25.8
25.6
25.4
25.2
25
0
0.2
0.4
0.6
0.8
1
1.2
1.4
1.6
1.8
2
2.2
2.4
×10^5
t

Parameters

Name	Expression	Description
radius	0.254	m
wall	6.35E-03	m
depth	0.0223	m
Twall	273.15 + 25	K
ksludge	3.9	[W/(m*K)]
rhosludge	9.60E+03	[kg/m^3]
Cpsludge	290	[J/(kg*K)]
kwall	16.2	[W/(m*K)]
rhowall	8.03E+03	[kg/m^3]
Cpwall	5.00E+02	[J/(kg*K)]
kgrout	0.5	[W/(m*K)]
rhogrout	1.72E+03	[kg/m^3]
Cpgrout	1165	[J/(kg*K)]
tstop	14400	at tstop grout heating becomes Qgrout2
Tinital	Twall	
Tsludge	Twall	
Qgrout2	2.51[W/m^3]	

Case 2
file: K basin all tubes.mph
file: K basin all tubes.docx
Wet sand conductivity (ksand=1.3 W/mK)
Uranium rate 1X

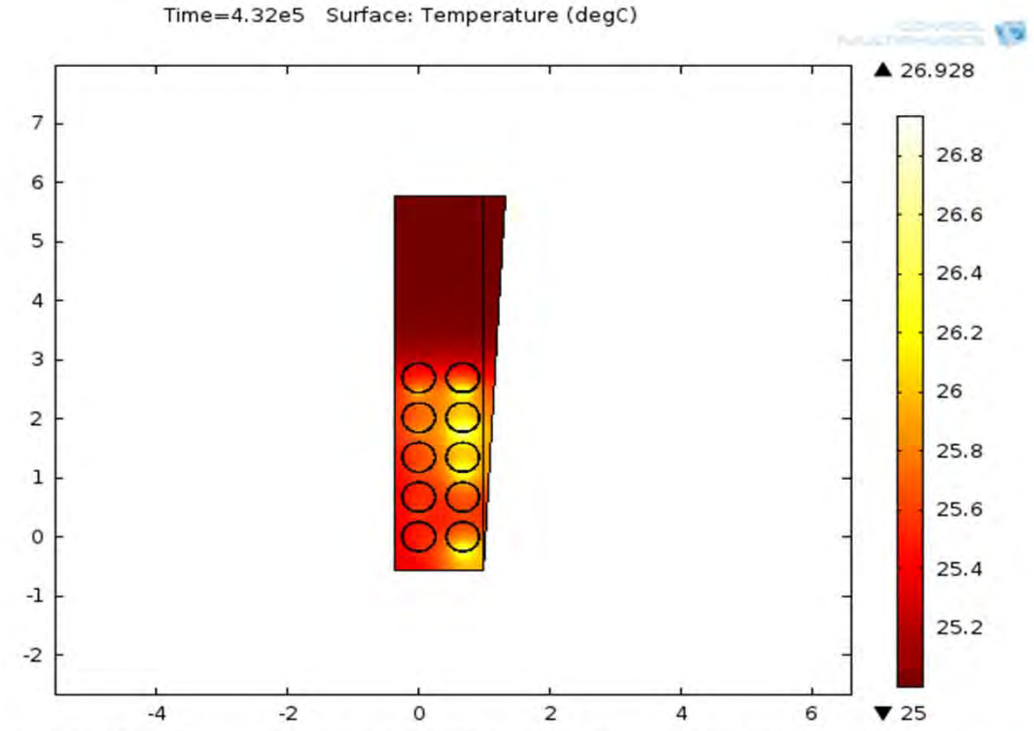

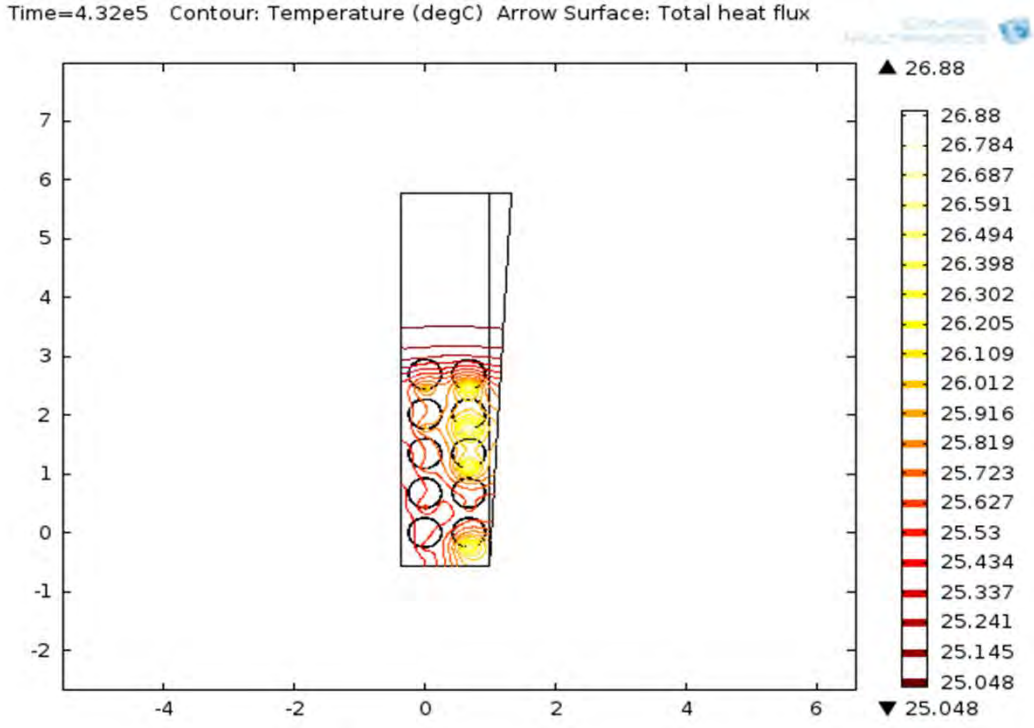

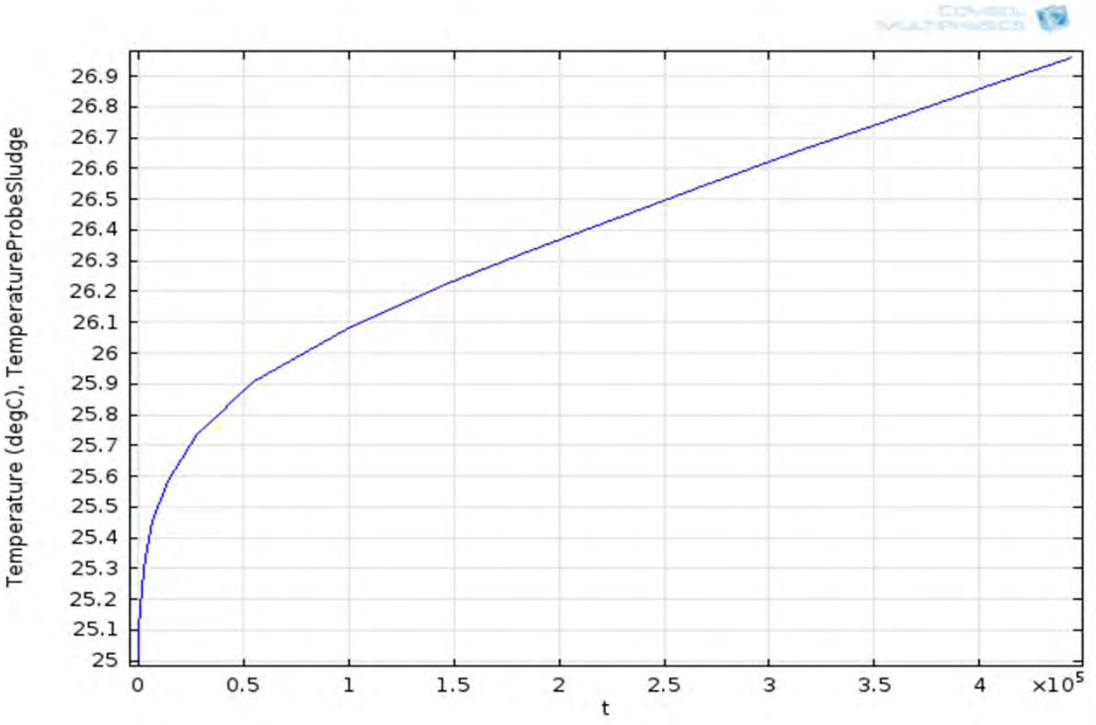

1.95916 degree increase in maximum uranium sludge temperature

Dry sand conductivity (ksand=0.13 W/mK)
Uranium rate 1X

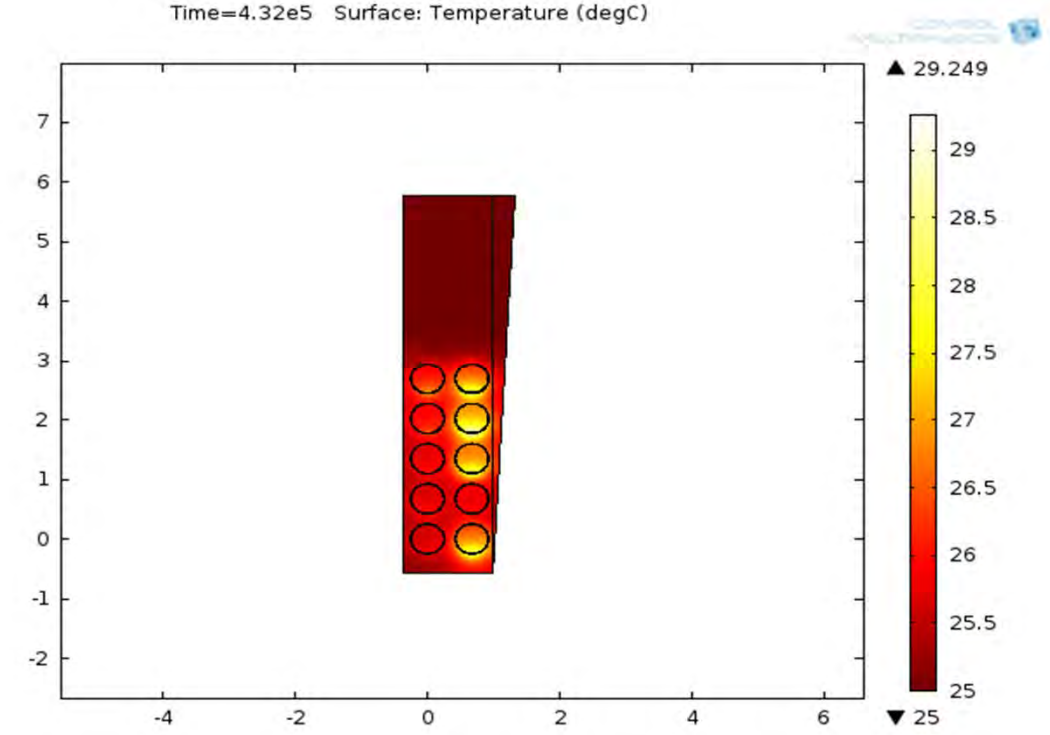

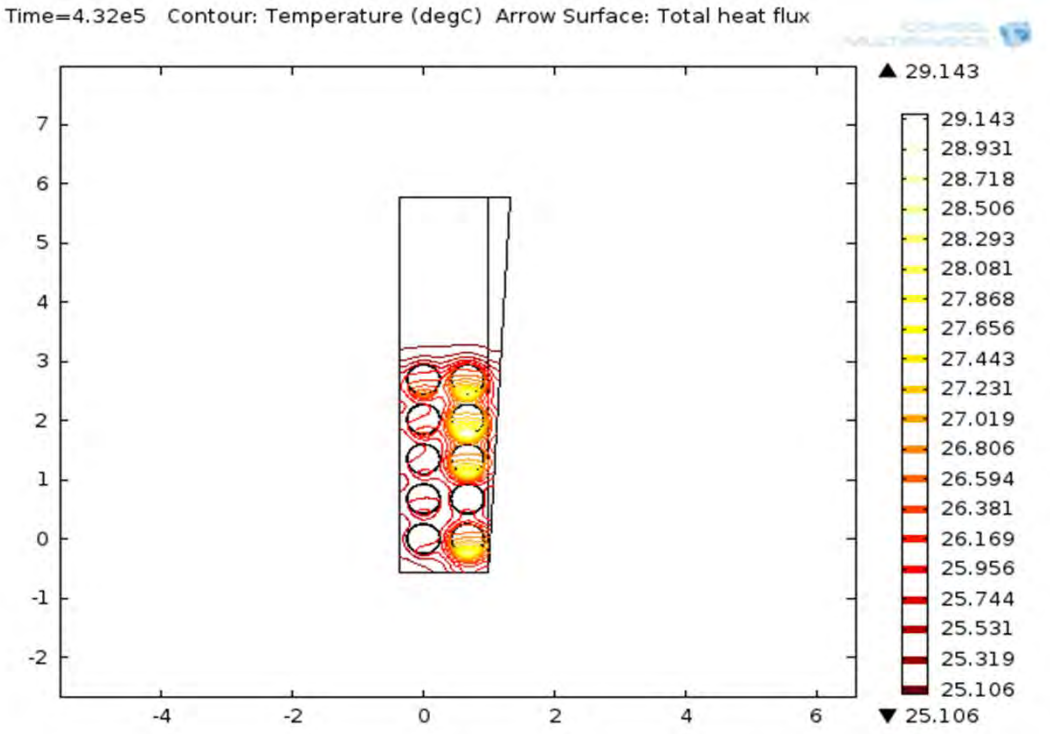

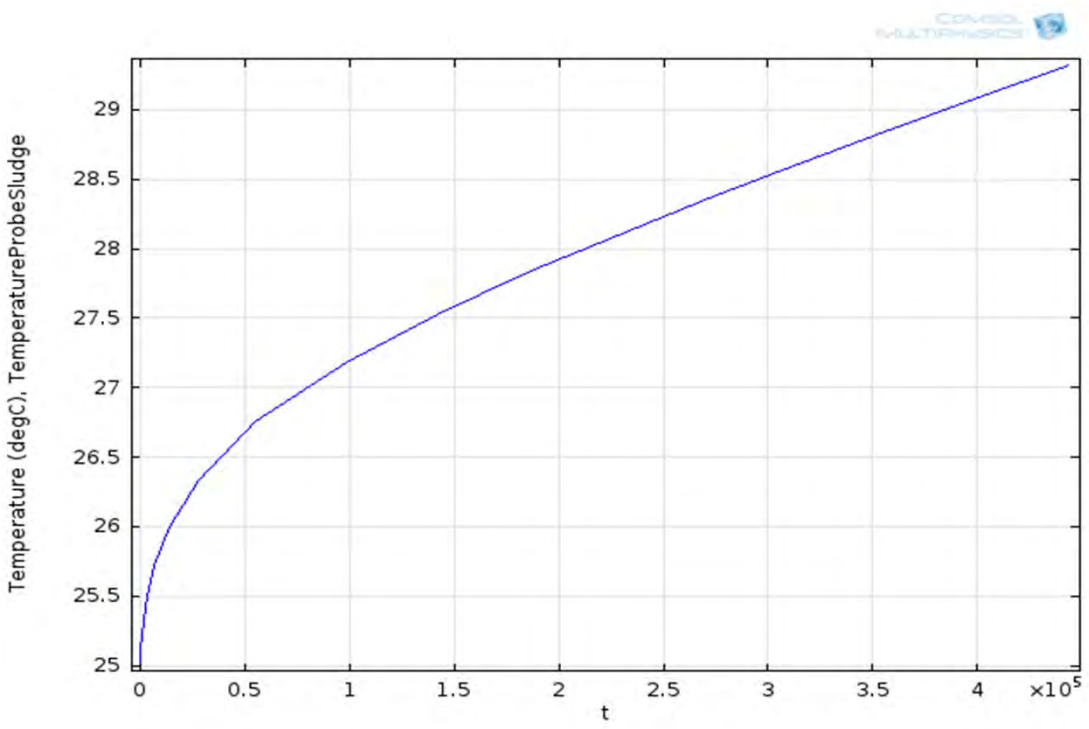

4.31721 degree increase in maximum uranium sludge temperature

Increasing starting temperature until stability limit is reached
Stable up to 44C
Dry sand conductivity (ksand=0.13 W/mK)
Uranium rate 1X

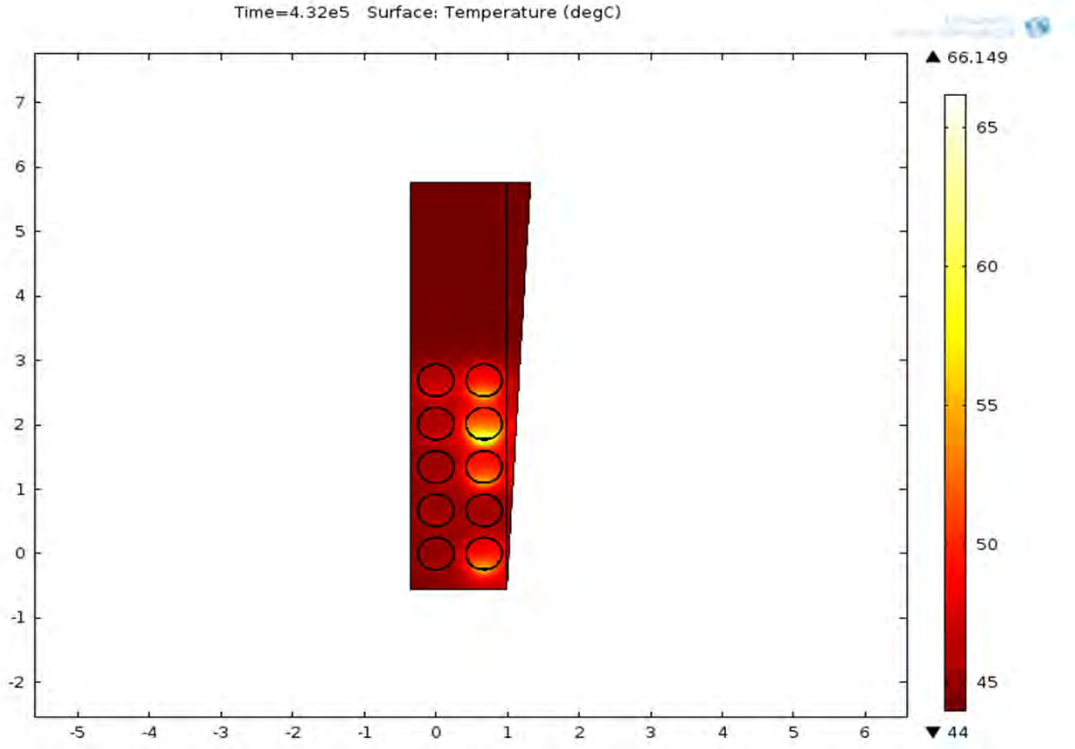

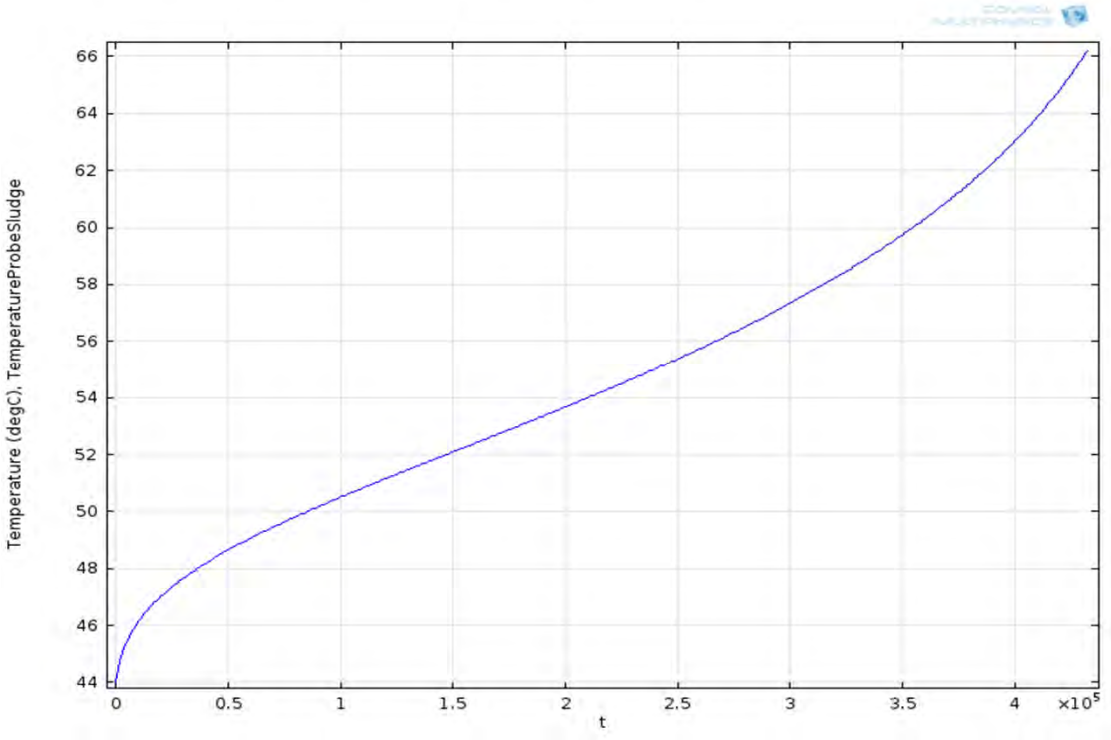

Increasing starting temperature until stability limit is reached
Stable up to 26C
Dry sand conductivity (ksand=0.13 W/mK)
Uranium rate 3X

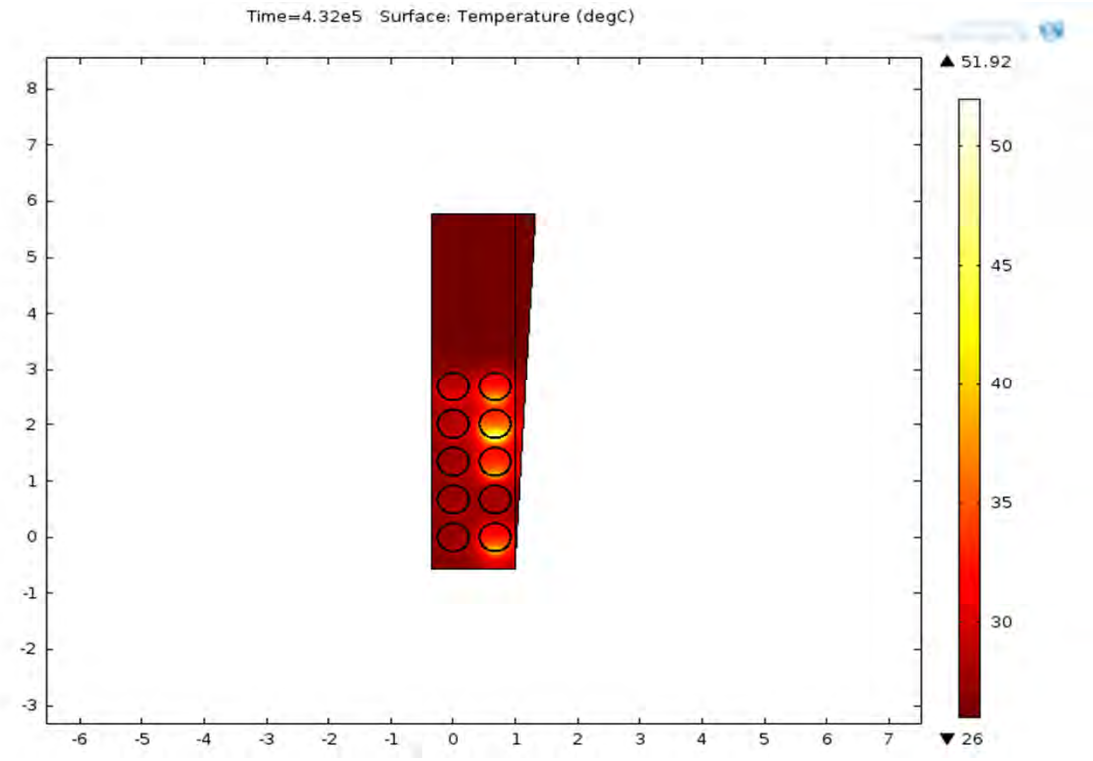

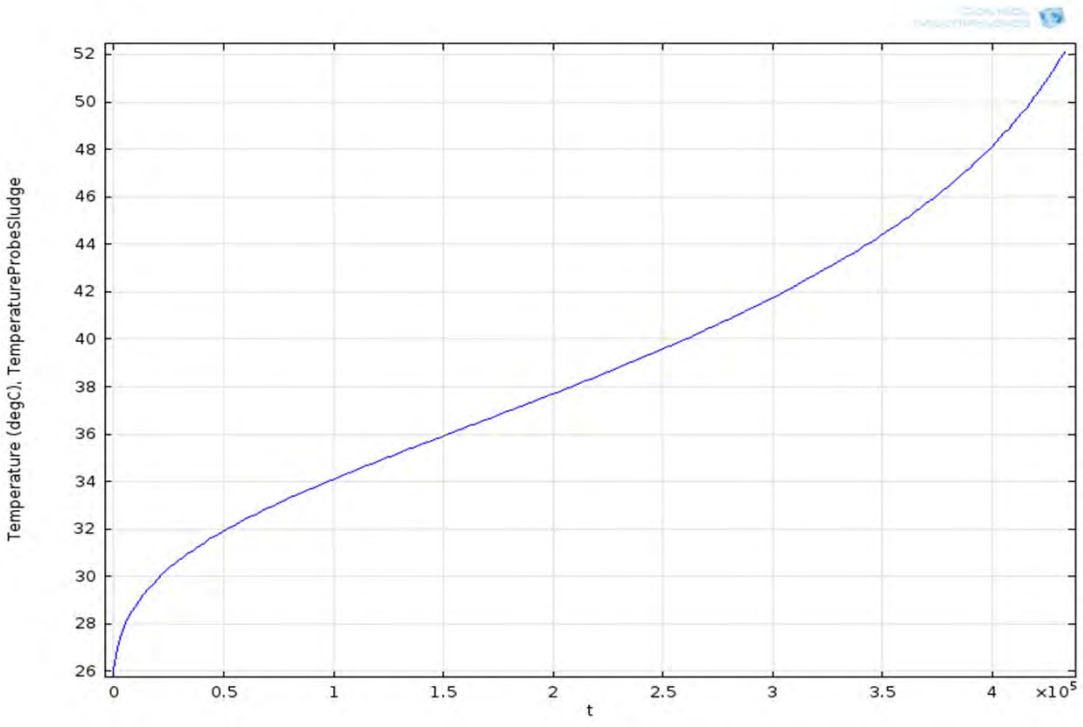

Increasing starting temperature until stability limit is reached
Stable up to 39C
Wet sand conductivity (ksand=1.3 W/mK)
Uranium rate 3X

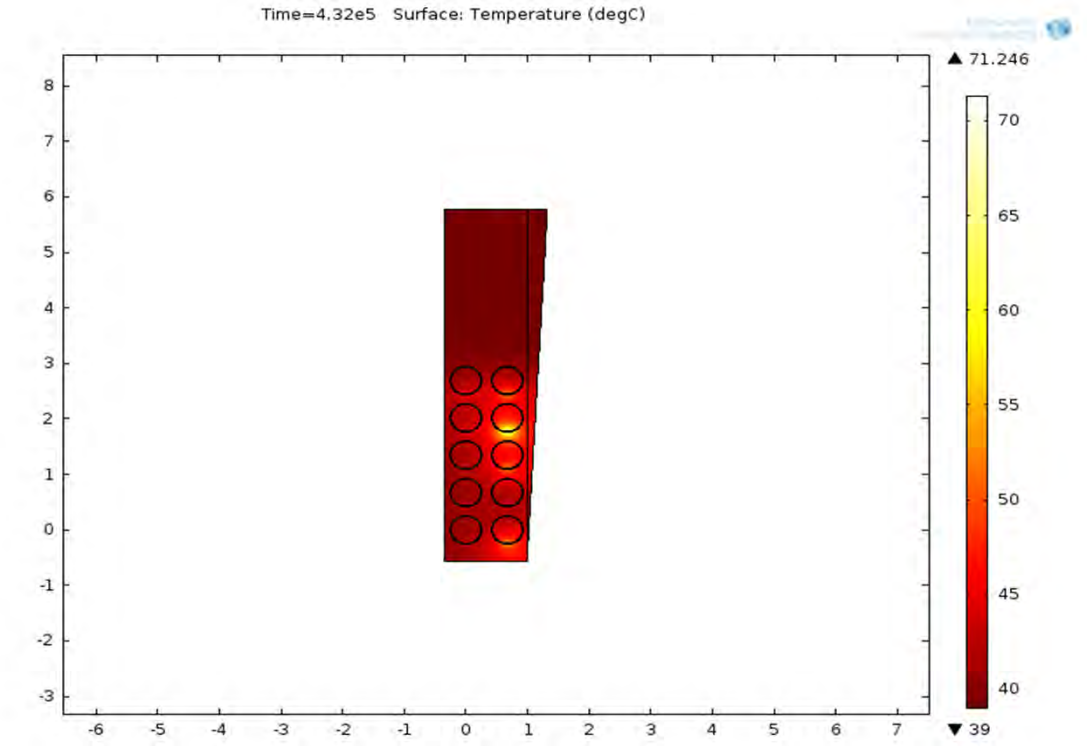

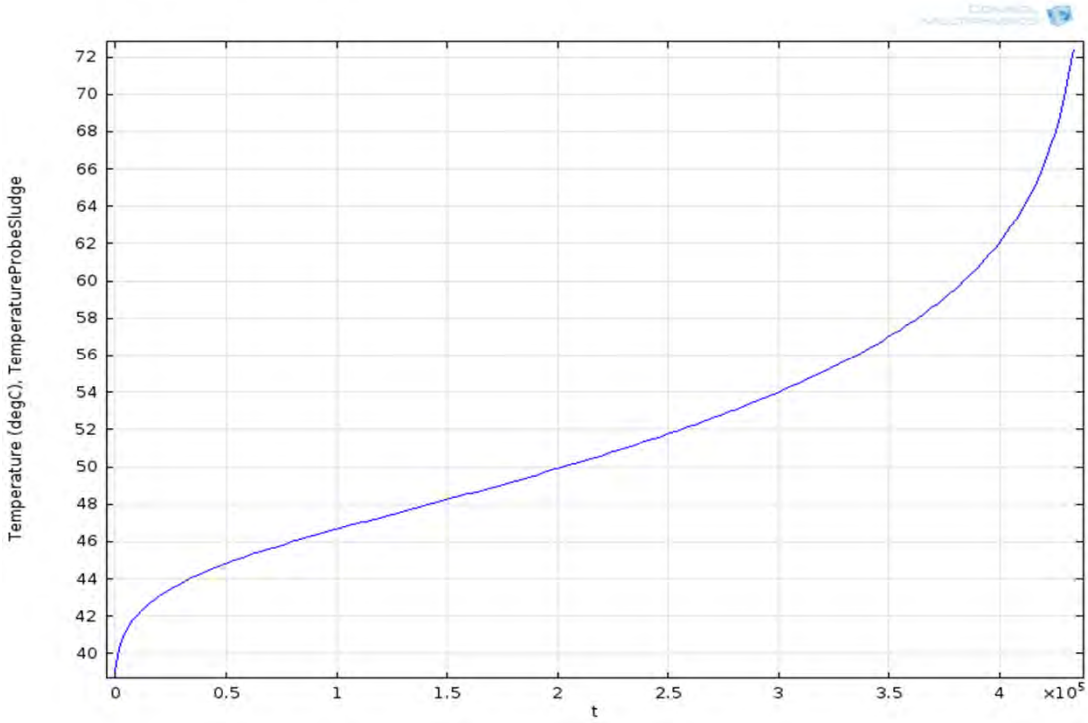

Increasing starting temperature until stability limit is reached
Stable up to 56C
Wet sand conductivity (ksand=1.3 W/mK)
Uranium rate 1X

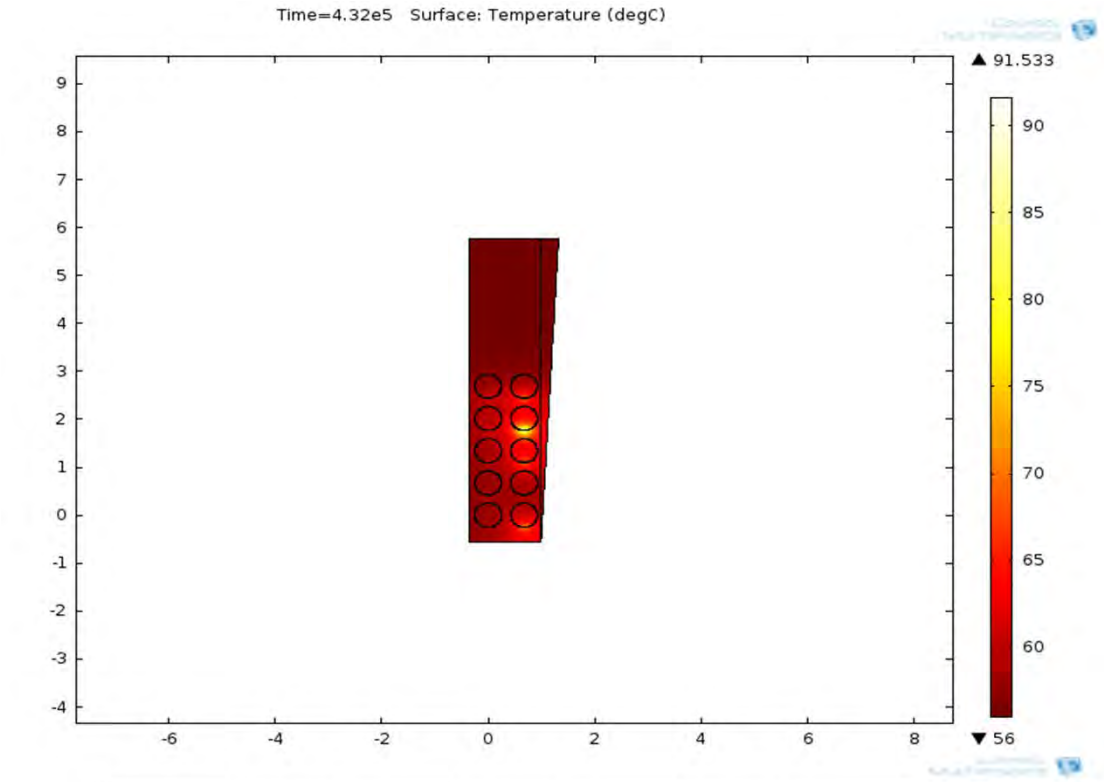

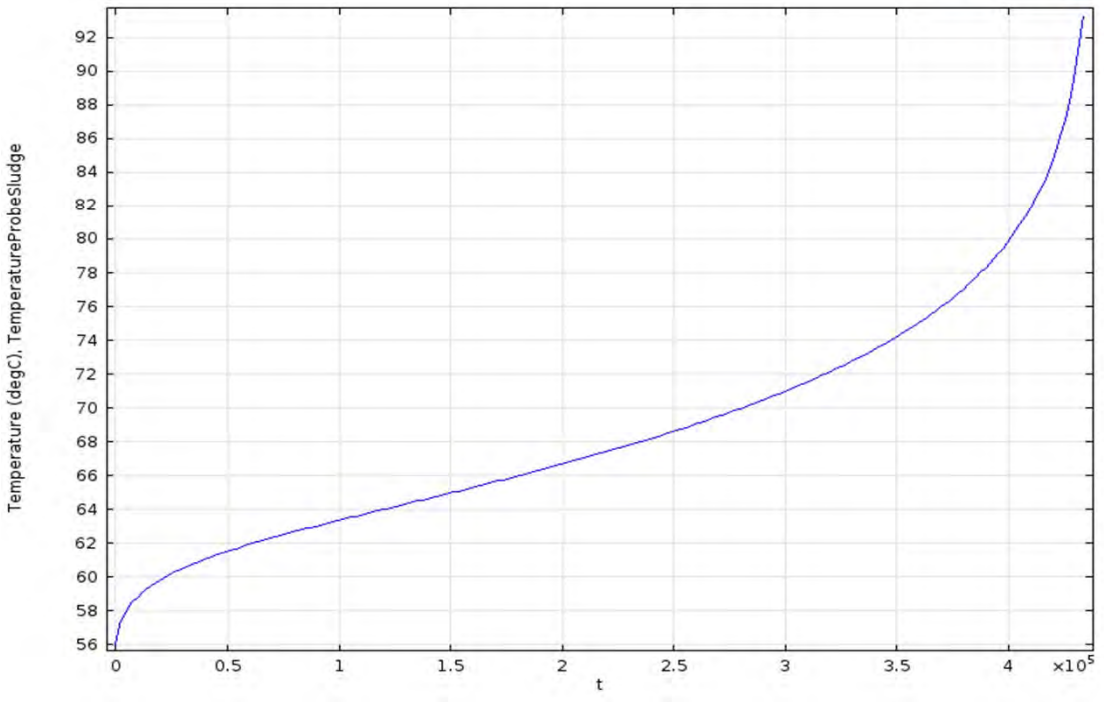

Case 3
file: K basin all tubes with 14in grout.mph
file: K basin all tubes with 14in grout.docx
Uranium heating normal (1X)
Walls at 25C

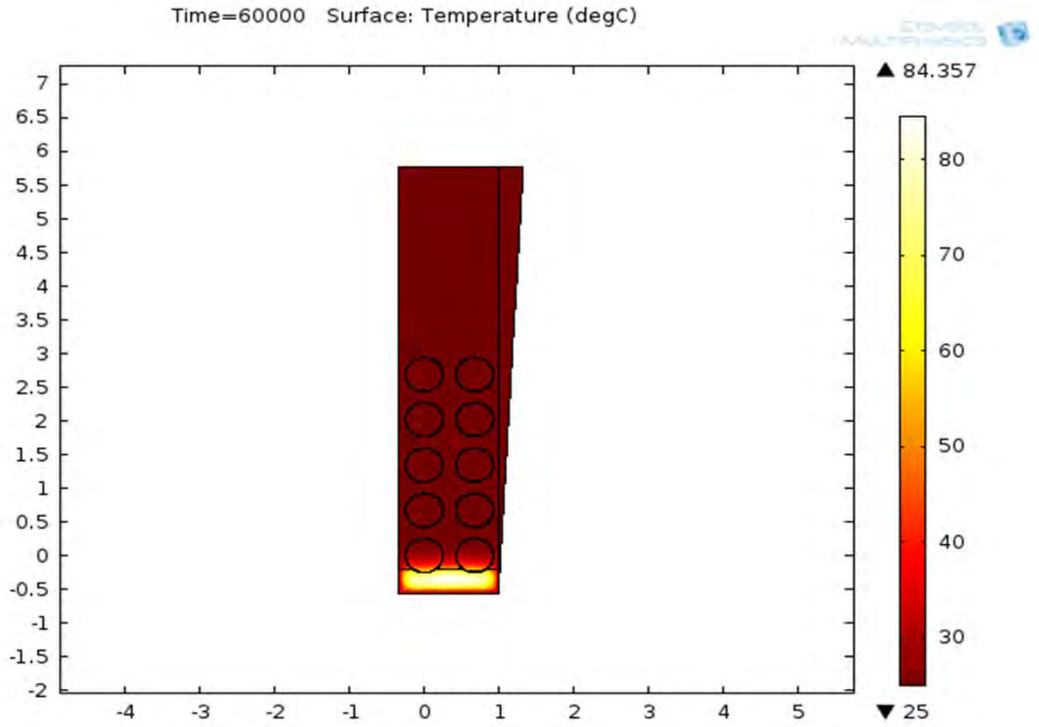

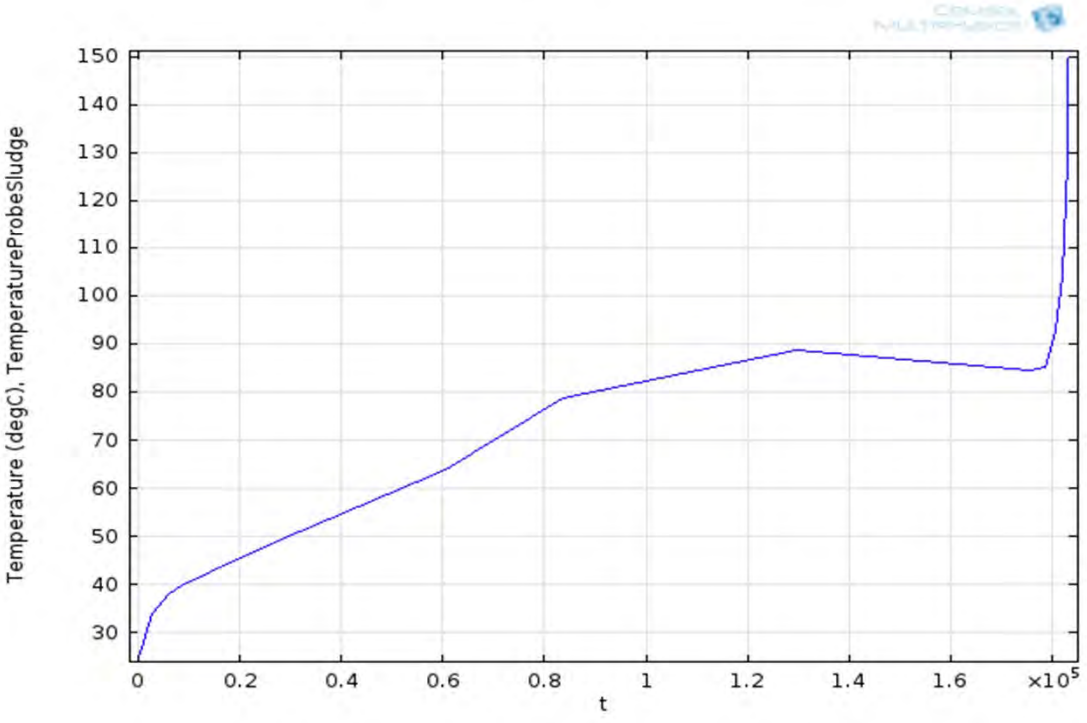

Changing slope with time is due to Comsol automatically verying its time step size.
Time to instability 50.6 hours

Uranium heating at thee times normal (3X)
Walls at 25C

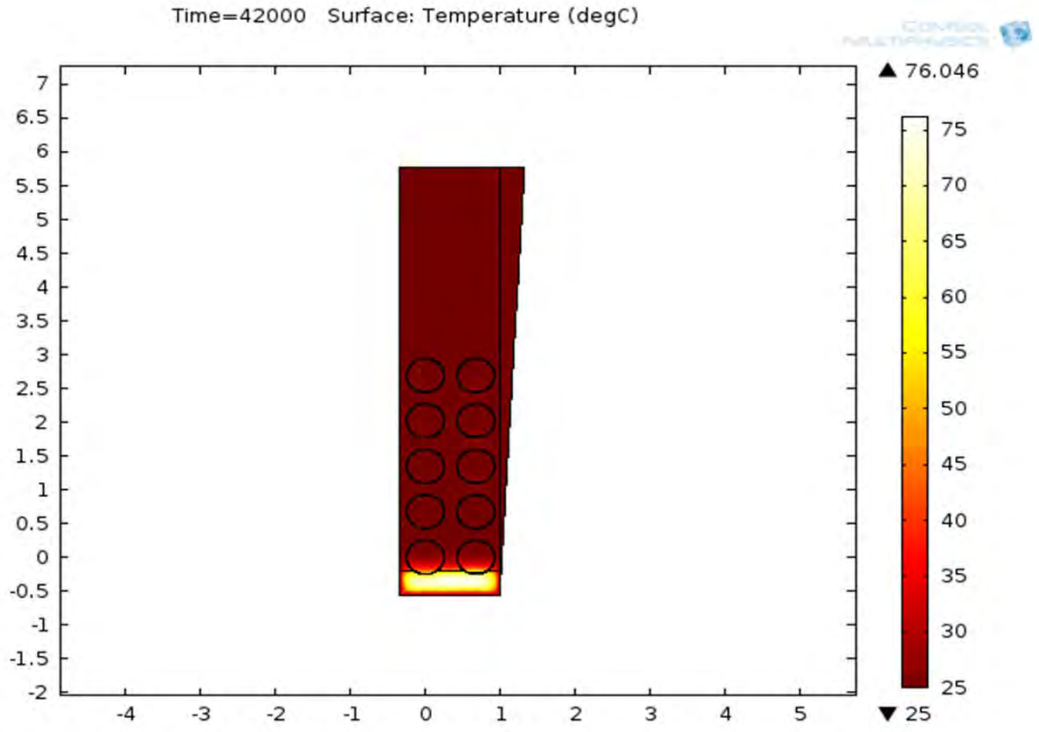

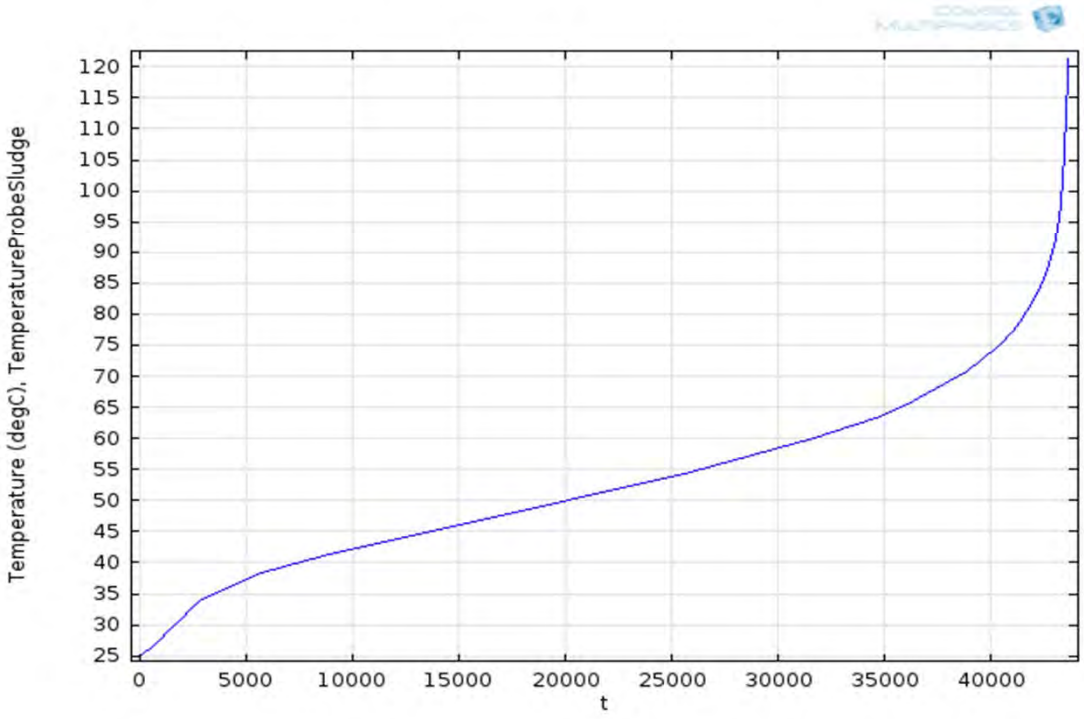

Time to instability 12.20194 hours

Uranium heating normal (1X)
Adiabatic wall boundary conditions

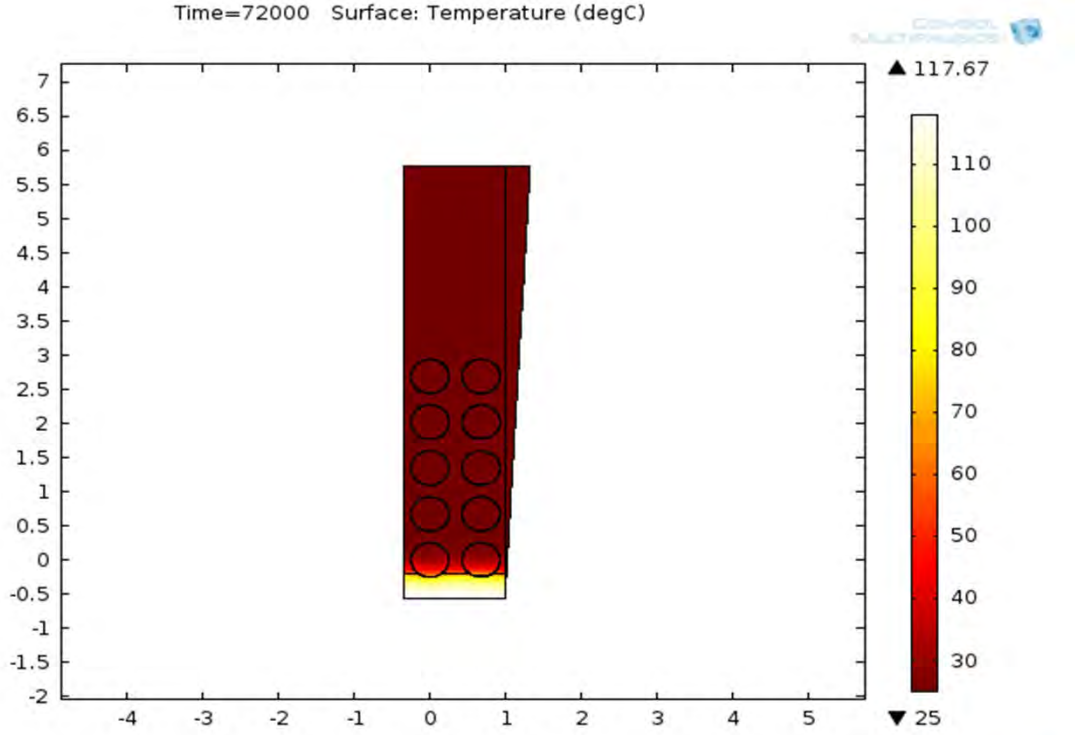

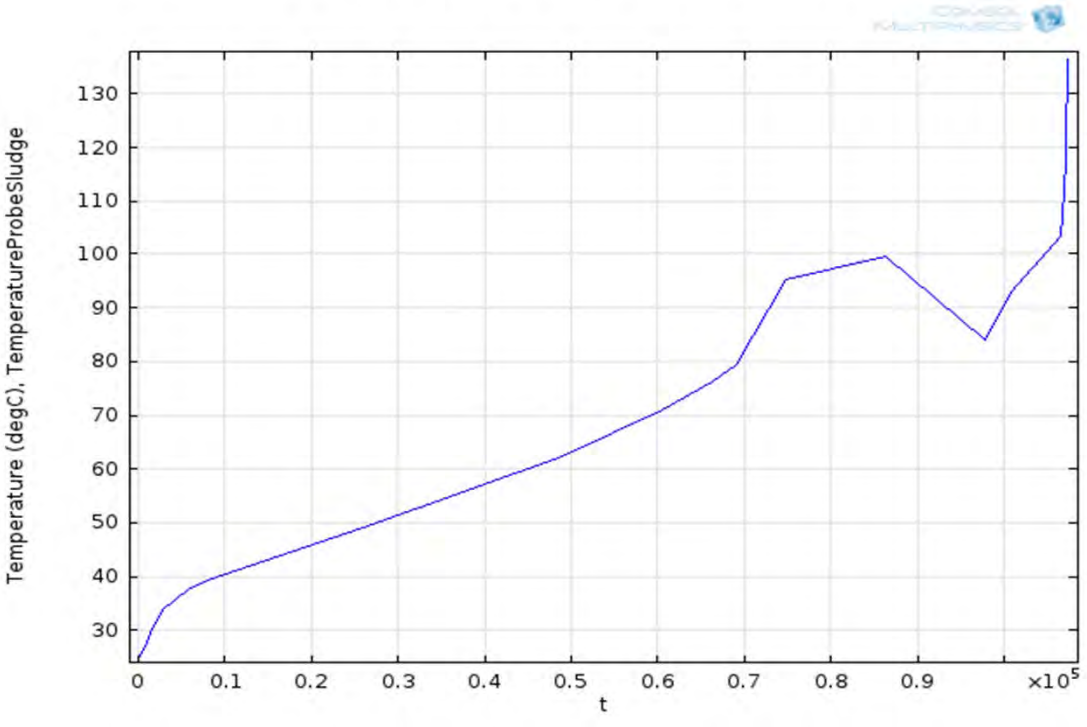

Changing slope with time is due to Comsol automatically verying its time step size.
Time to instability 29.825 hours

Uranium heating at thee times normal (3X)
Adiabatic wall boundary conditions

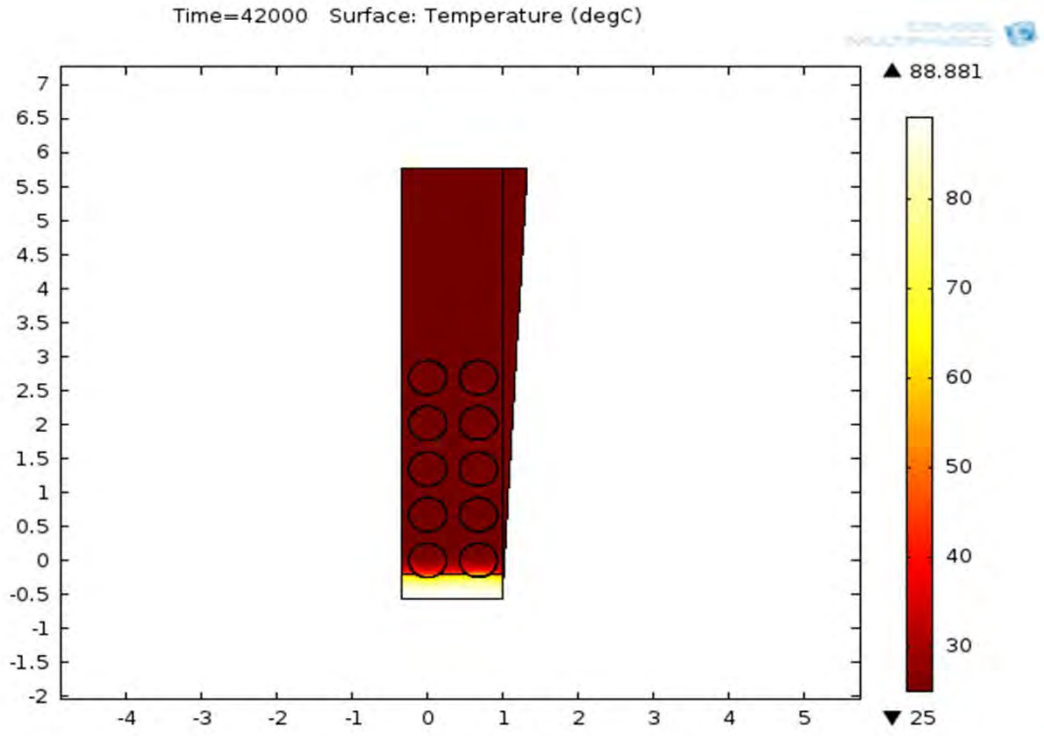

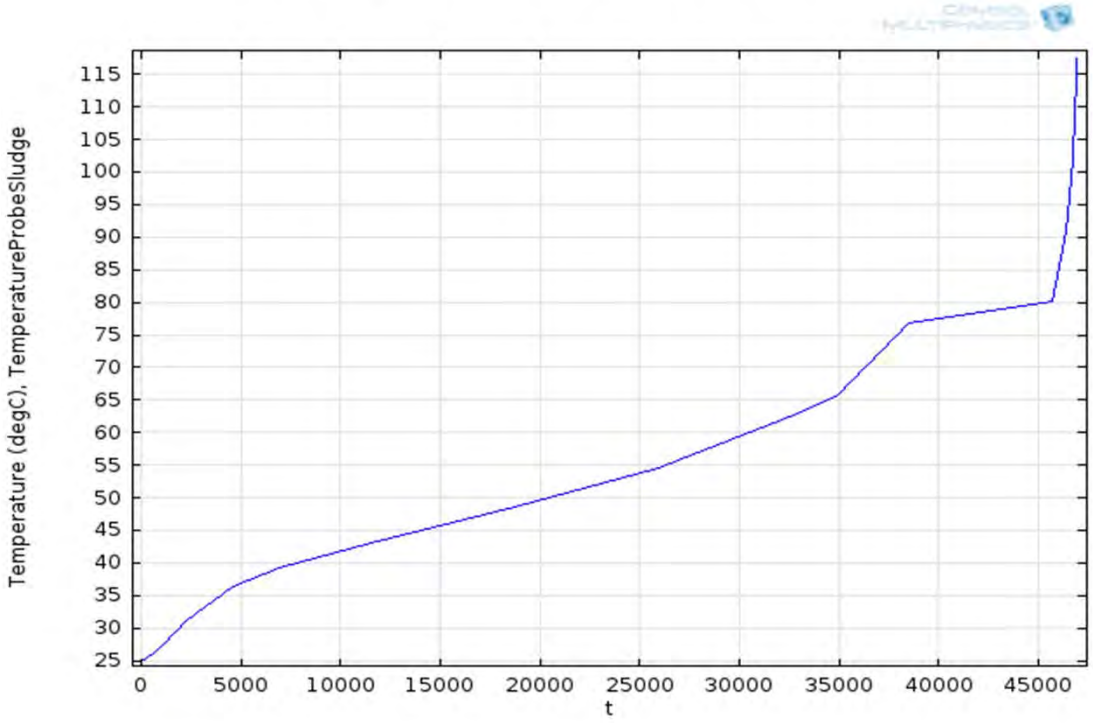

Changing slope with time is due to Comsol automatically verying its time step size.
Time to instability 13.03583 hours

Case 4
file: K basin all tubes with 6in grout.mph
file: K basin all tubes with 6in grout.docx
Uranium heating normal (1X)
Walls at 25C

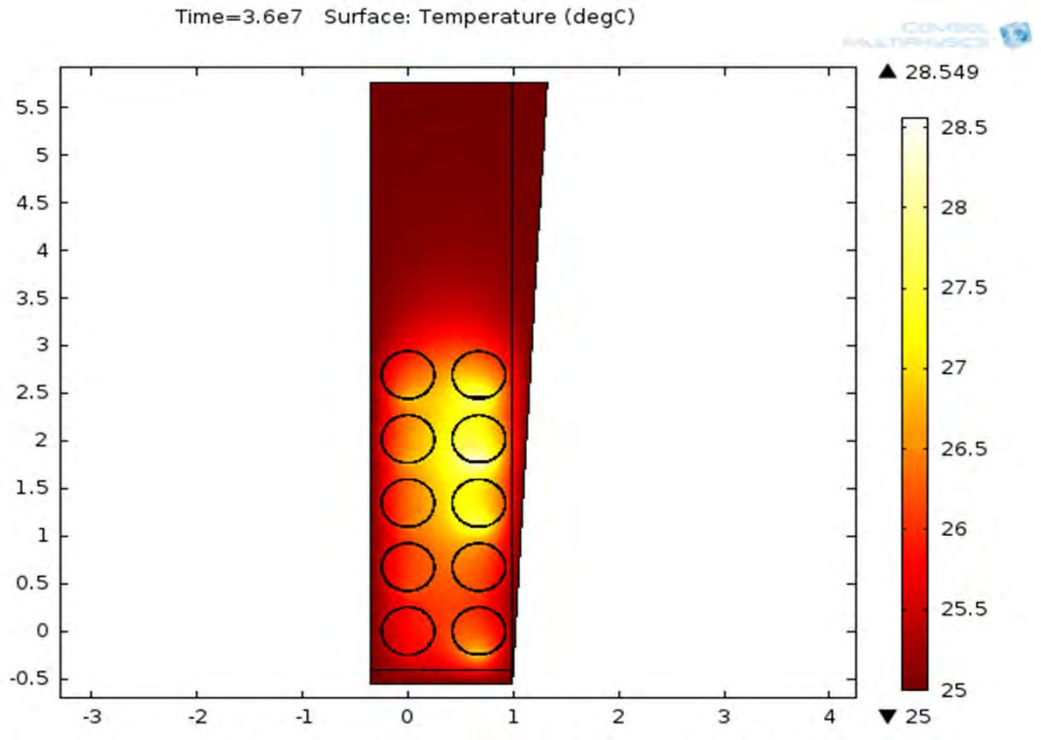

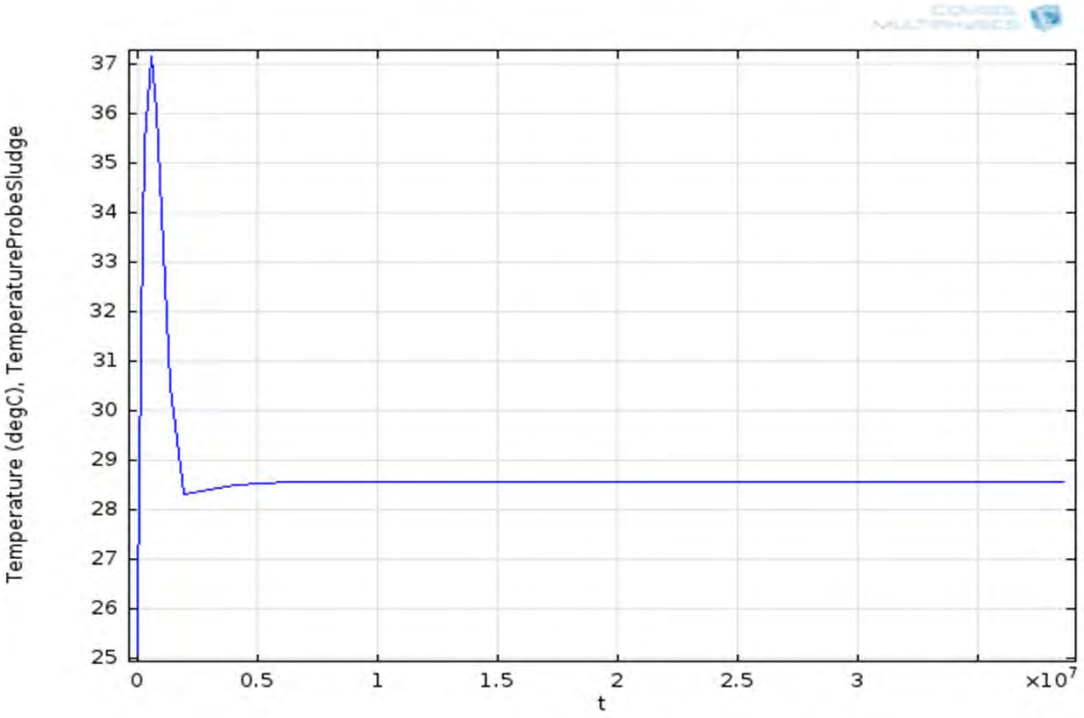

Time to instability Never

Uranium heating at thee times normal (3X)
Walls at 25C

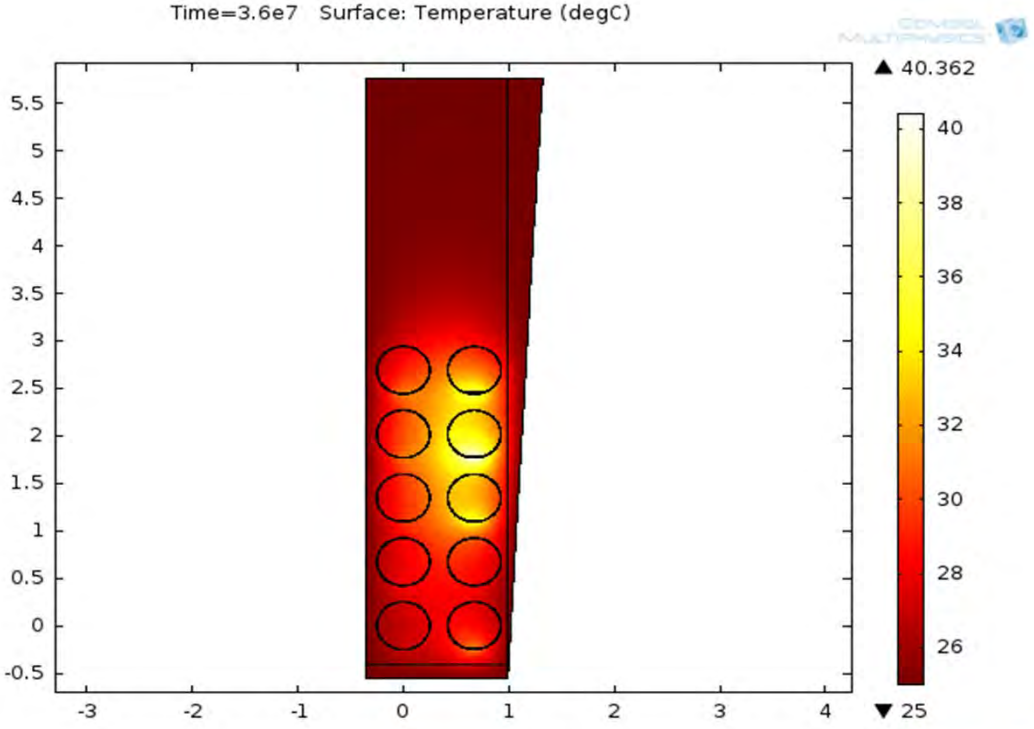

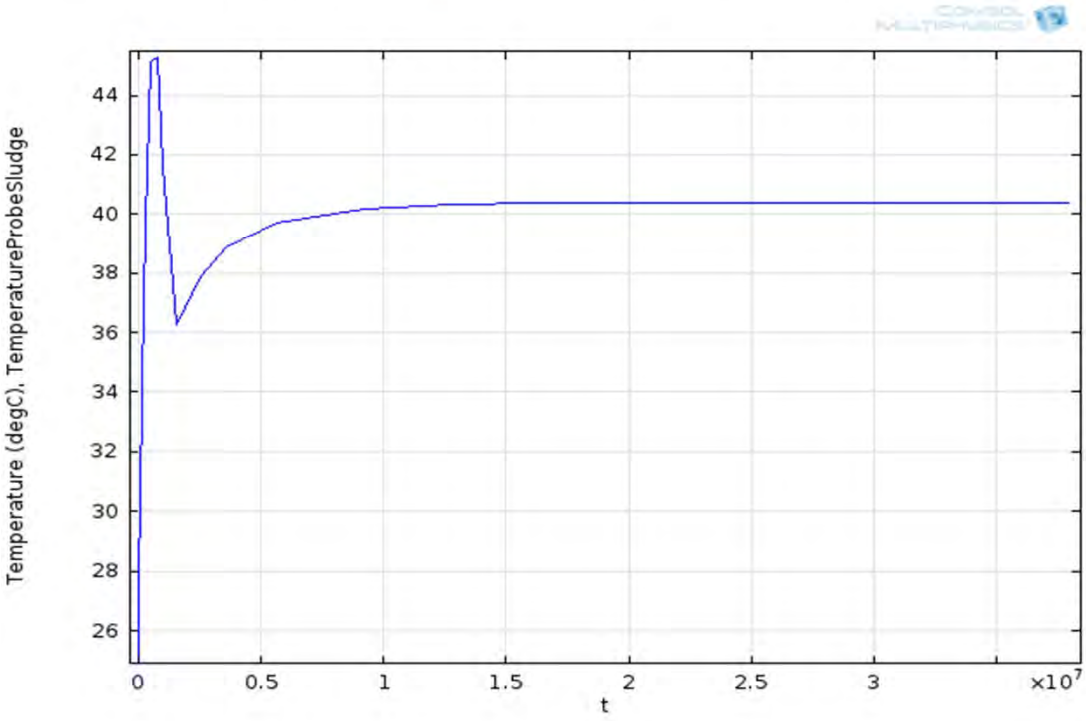

Time to instability Never

Uranium heating normal (1X)
Adiabatic wall boundary conditions

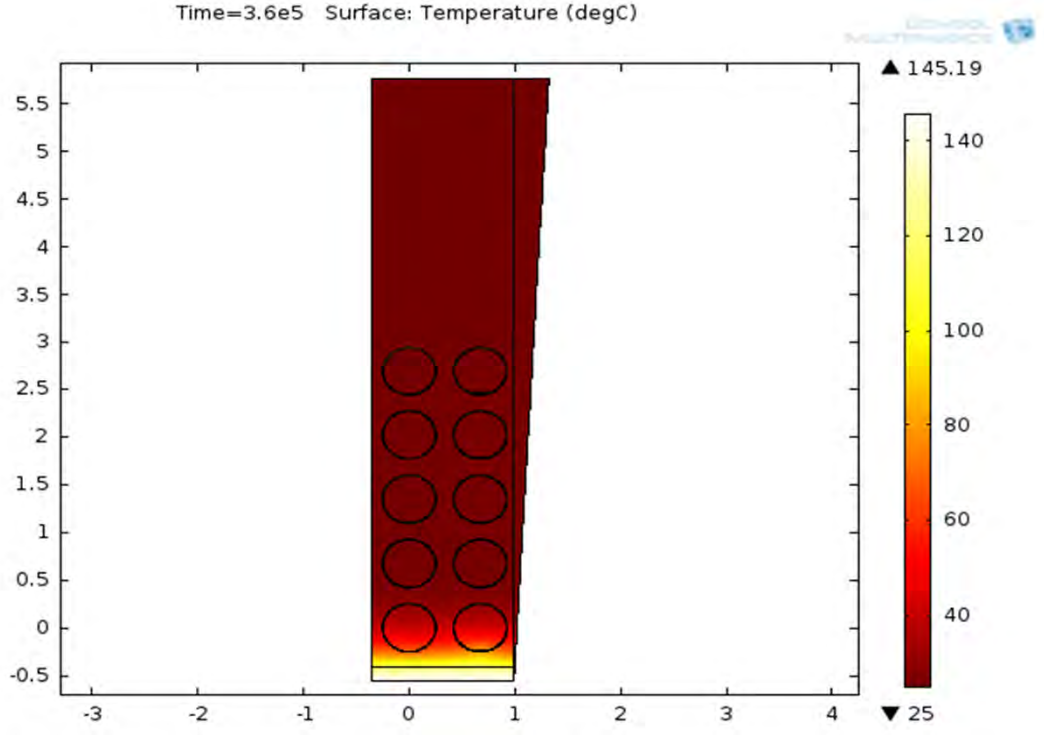

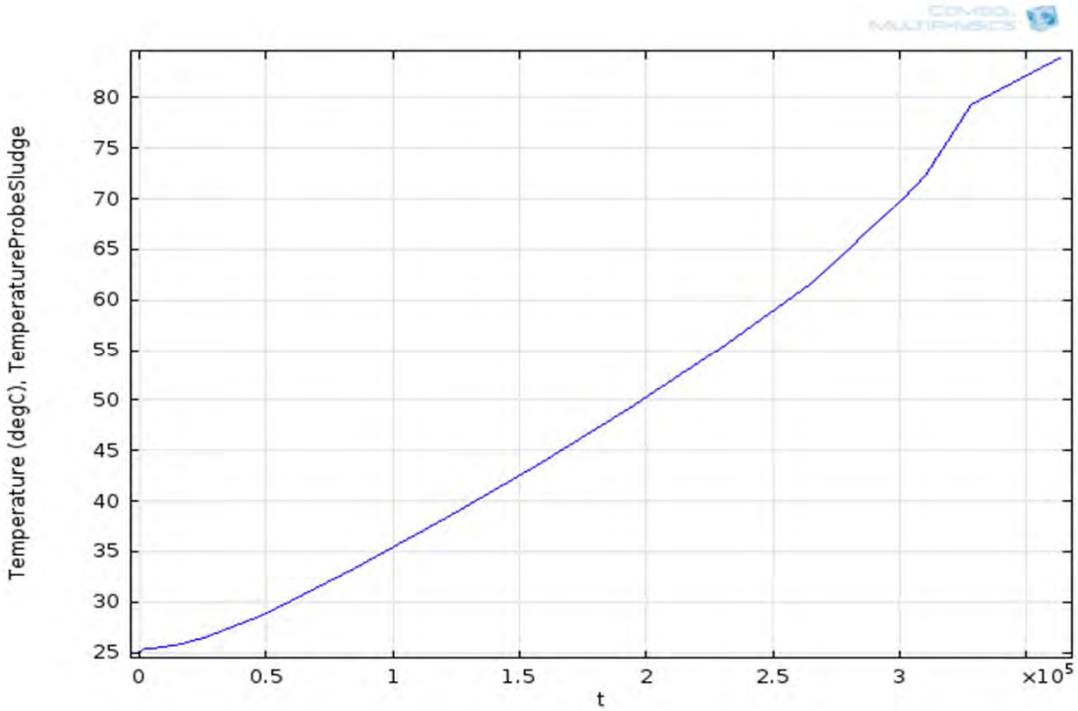

Changing slope with time is due to Comsol automatically verying its time step size.
Time to instability 4.201389 days

Uranium heating at thee times normal (3X)
Adiabatic wall boundary conditions

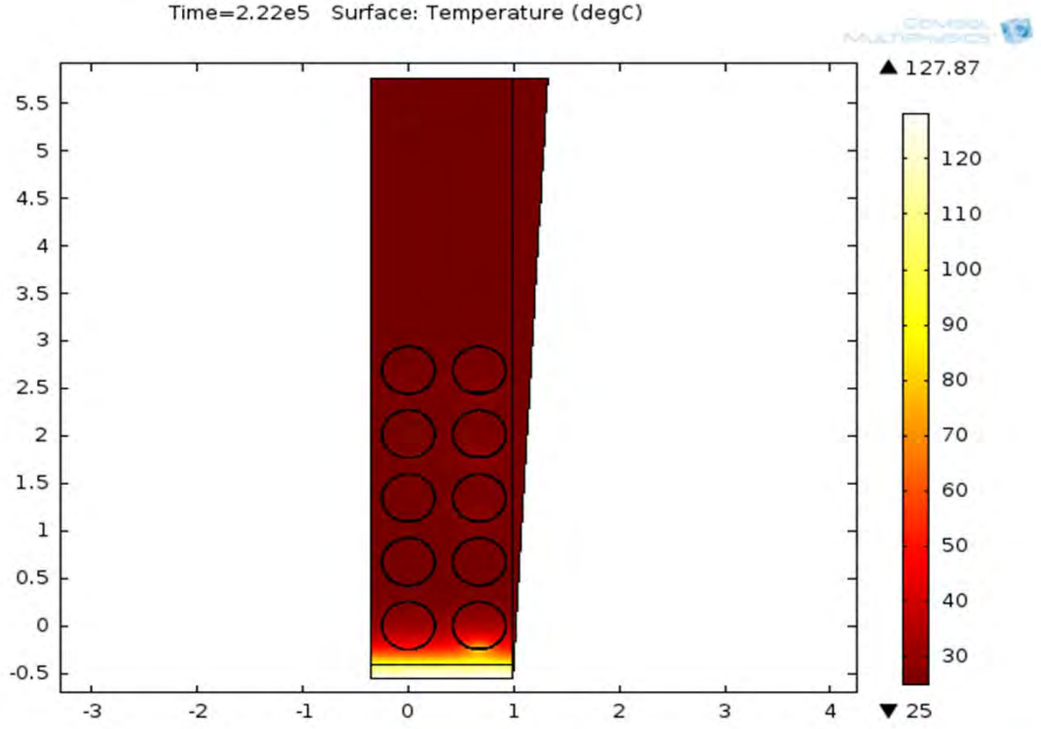

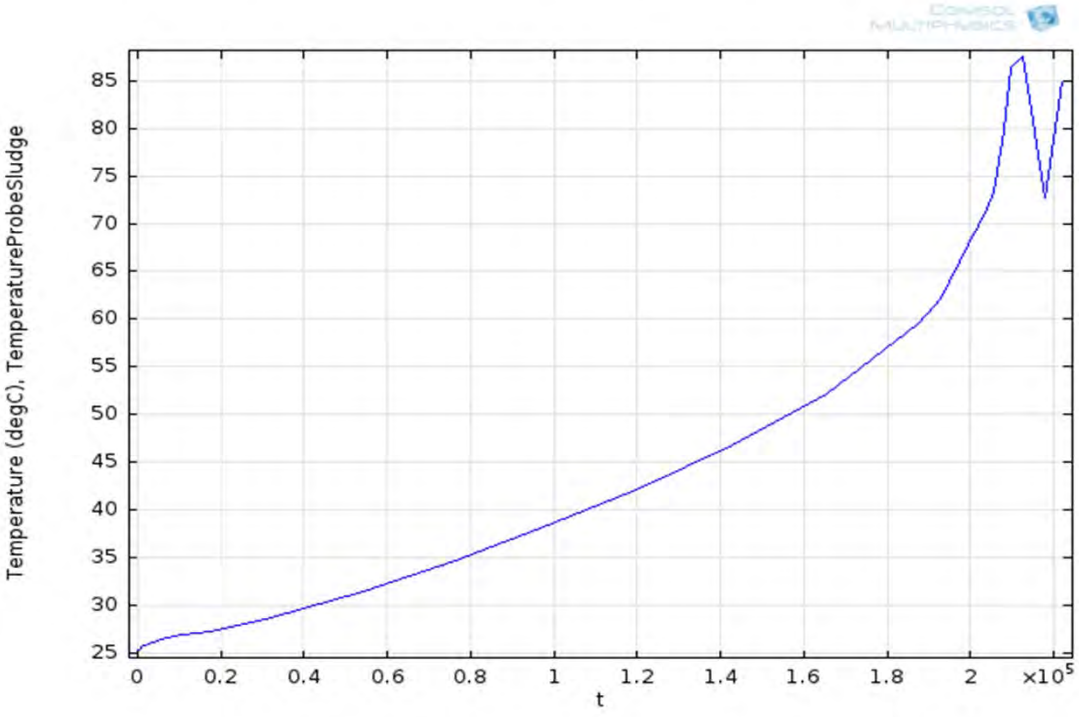

Changing slope with time is due to Comsol automatically verying its time step size.
Time to instability 2.511574 days

Case 5
file: K basin Box.mph
file: K basin Box.docx
Moist sand k =0.78 W/mK
cut off at 2.145E6 J/kg
Normal Uranium heating
starting at 50C and is not stable
stable at 54C unstable at 55C

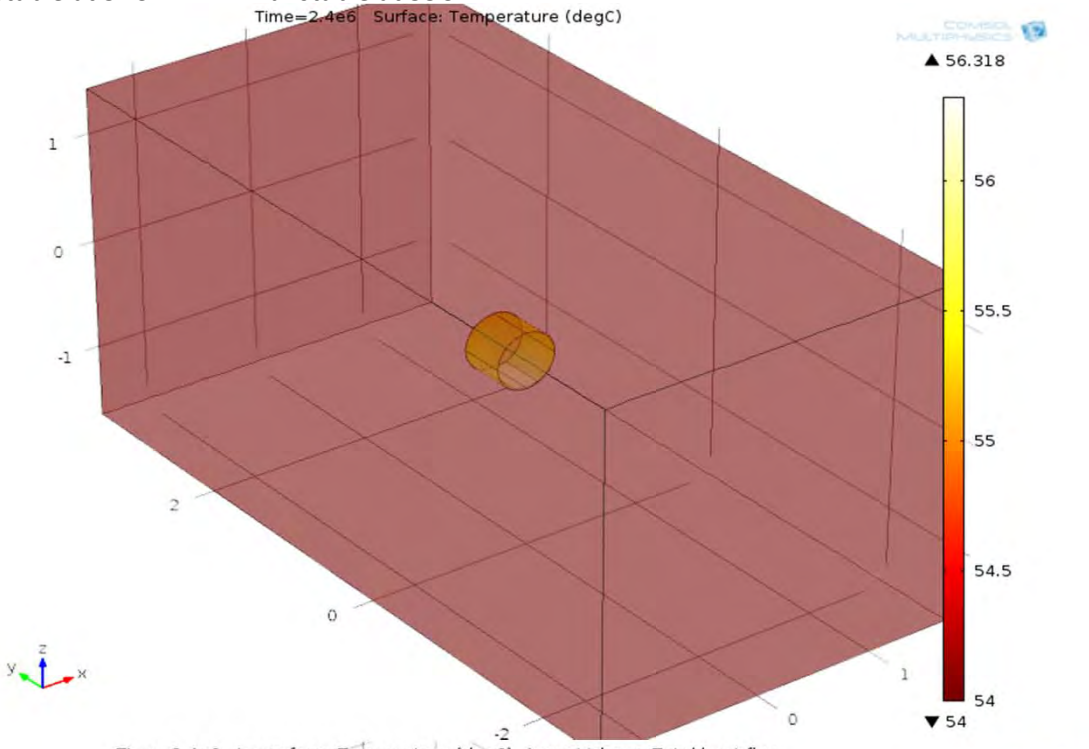

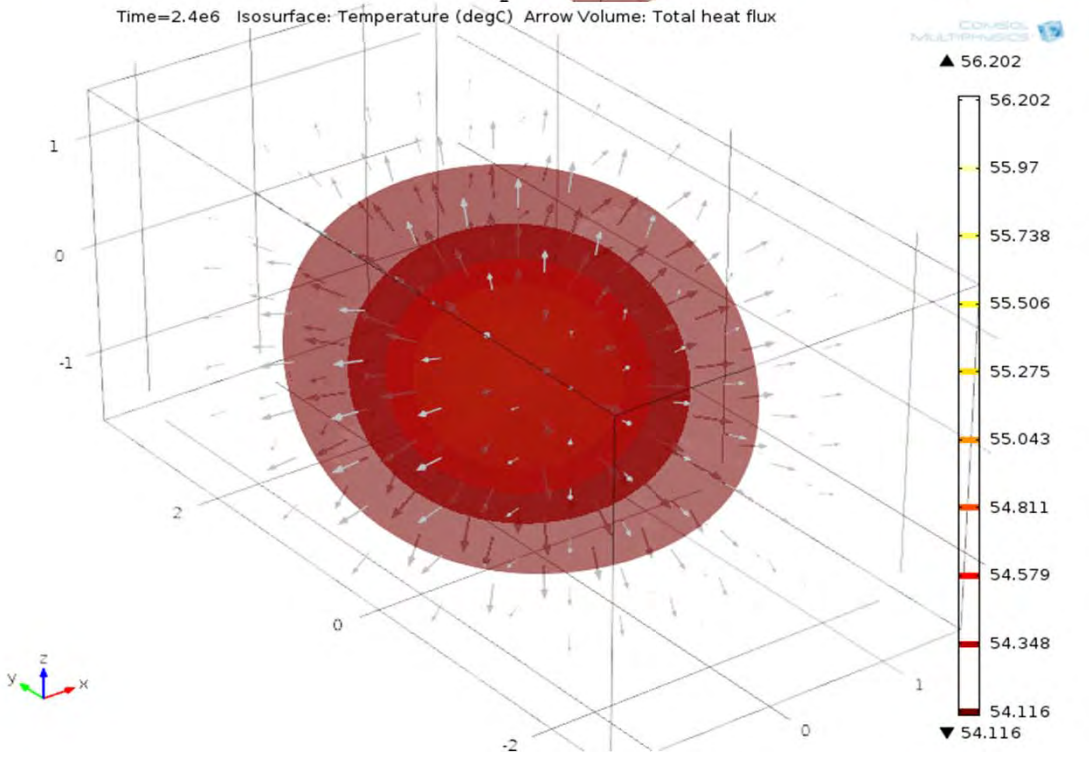

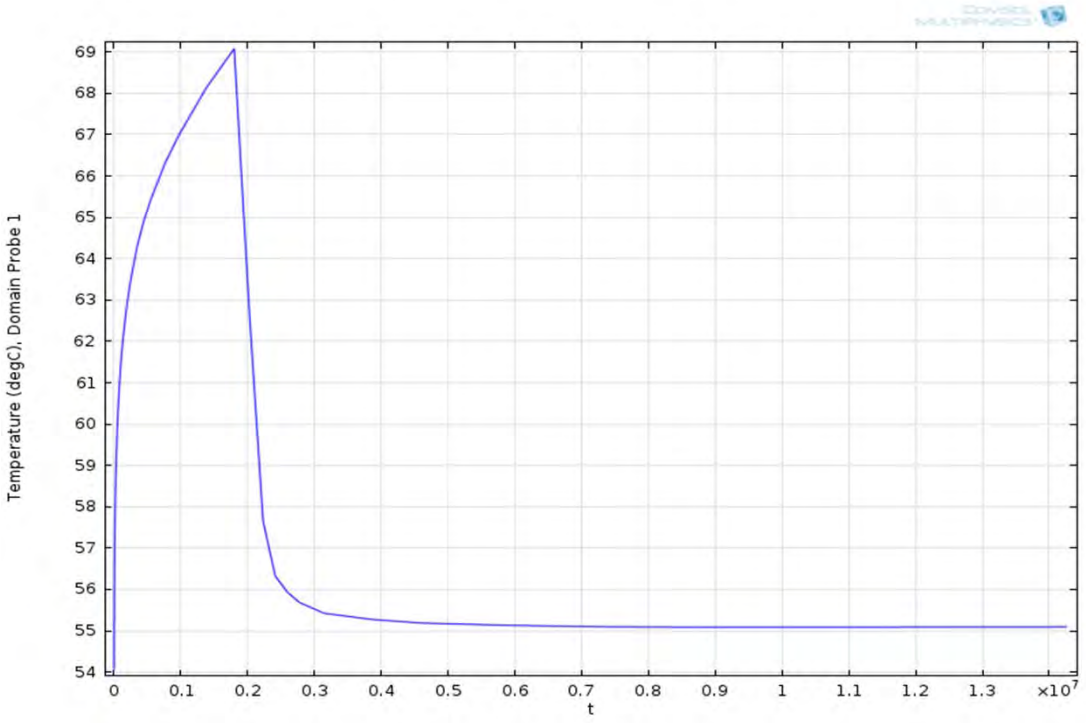
Temperature (degC), Domain Probe 1
69
68
67
66
65
64
63
62
61
60
59
58
57
56
55
54
0
0.1
0.2
0.3
0.4
0.5
0.6
0.7
0.8
0.9
1
1.1
1.2
1.3
×10^7
t

Moist sand k =0.78 W/mK
3X Uranium heating
starting at 50C and is not stable
stable at 37C unstable at 38C
results below are at 31 initial and wall temperature

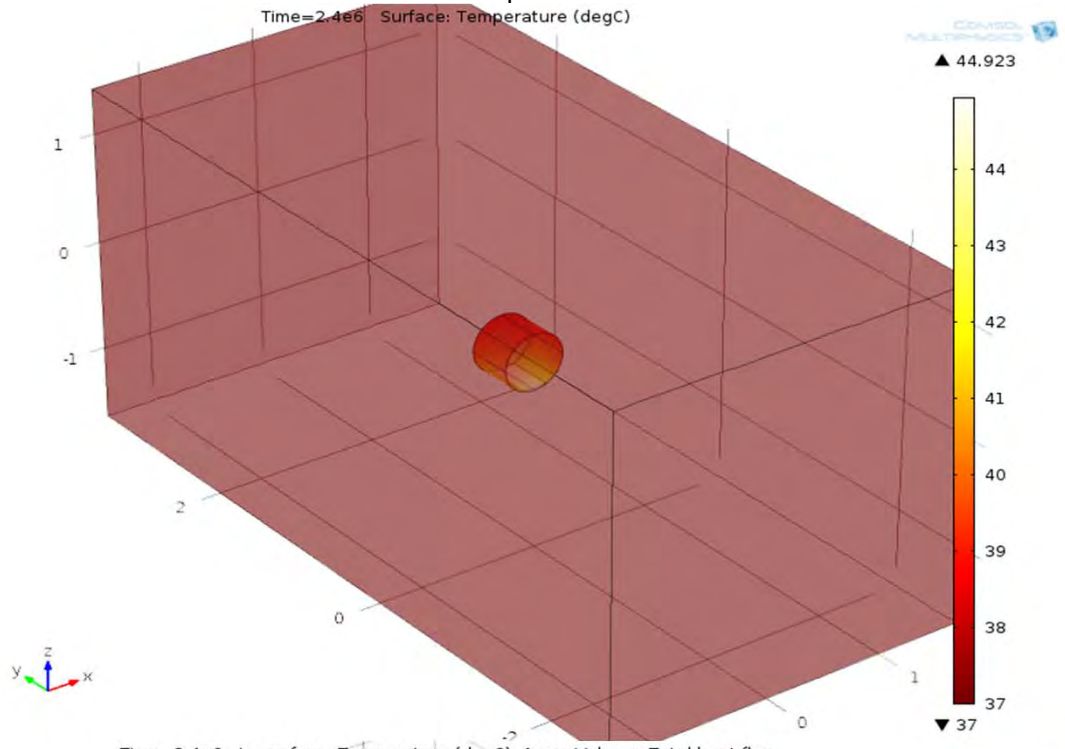

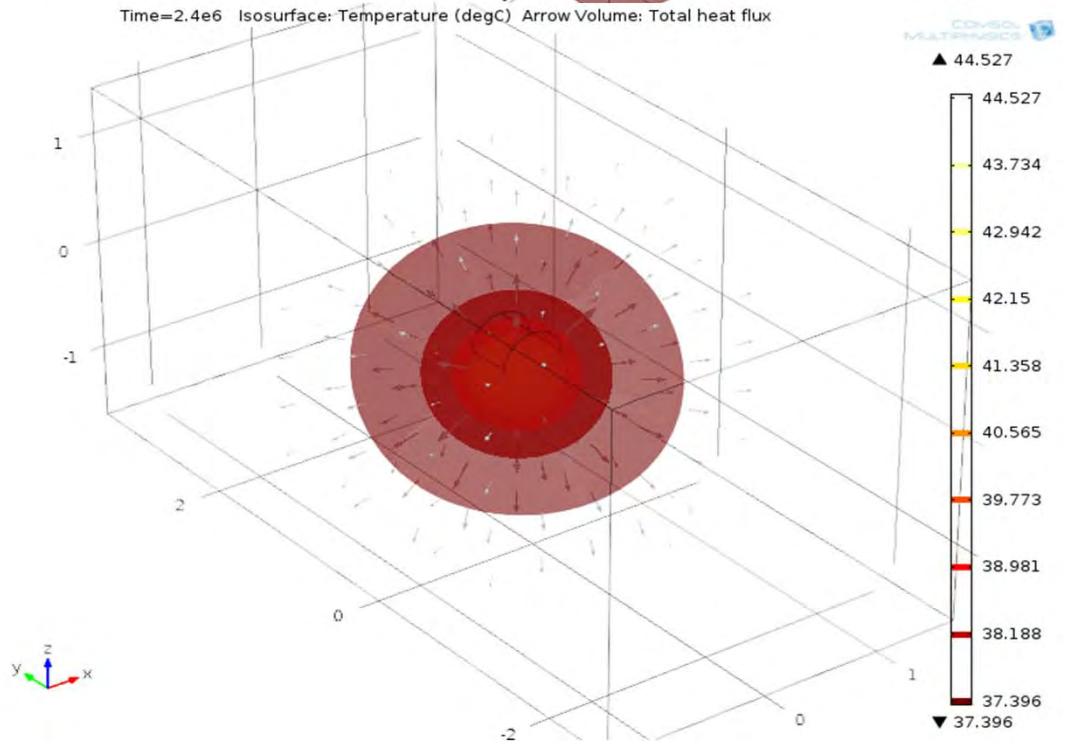

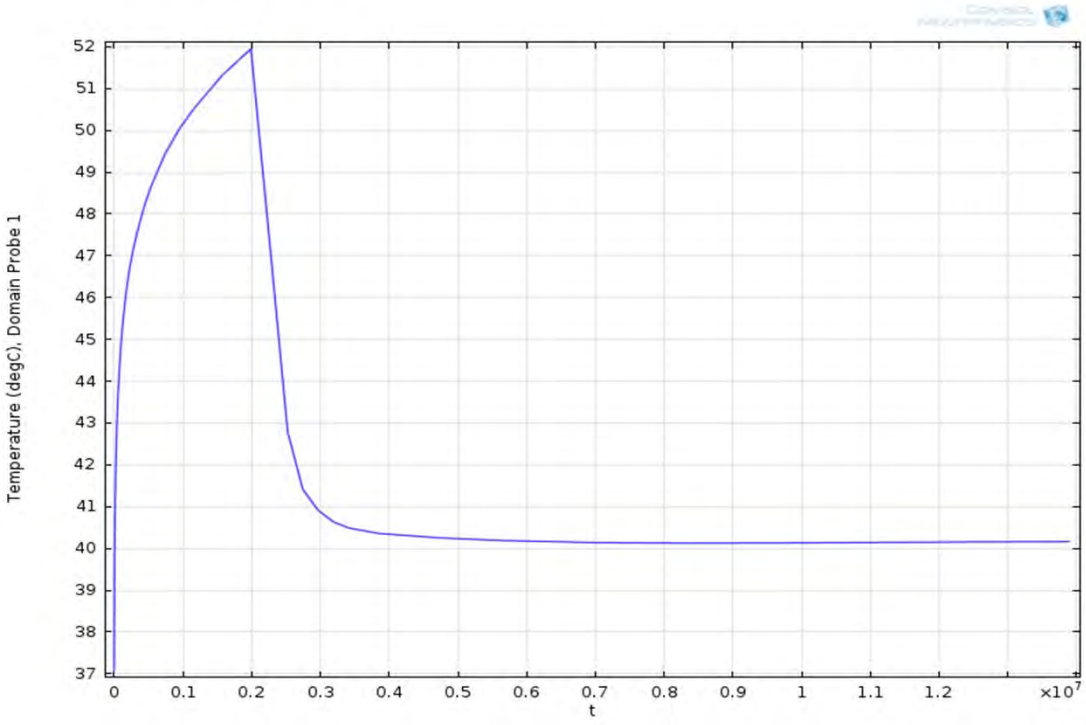
Temperature (degC), Domain Probe 1
52
51
50
49
48
47
46
45
44
43
42
41
40
39
38
37
0
0.1
0.2
0.3
0.4
0.5
0.6
0.7
0.8
0.9
1
1.1
1.2
×10^7
t

dry sand k =0.13 W/mK
cut off at 2.145E6 J/kg
Normal Uranium heating
stable at 376C unstable at 38C

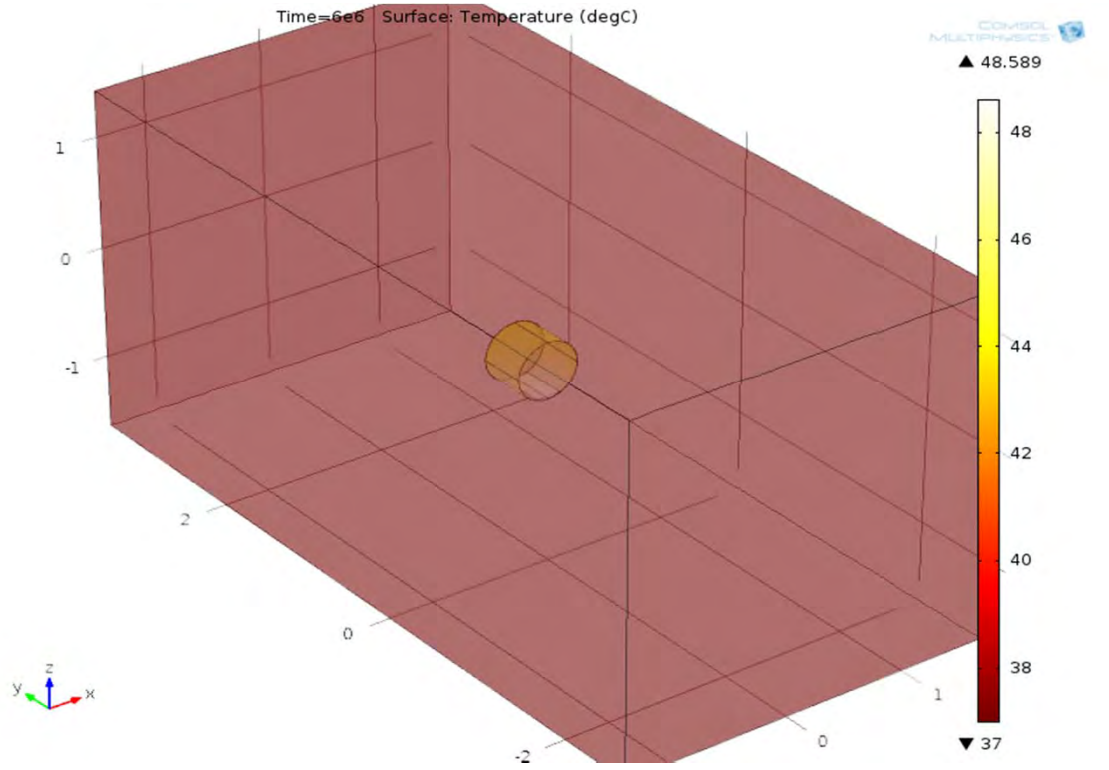

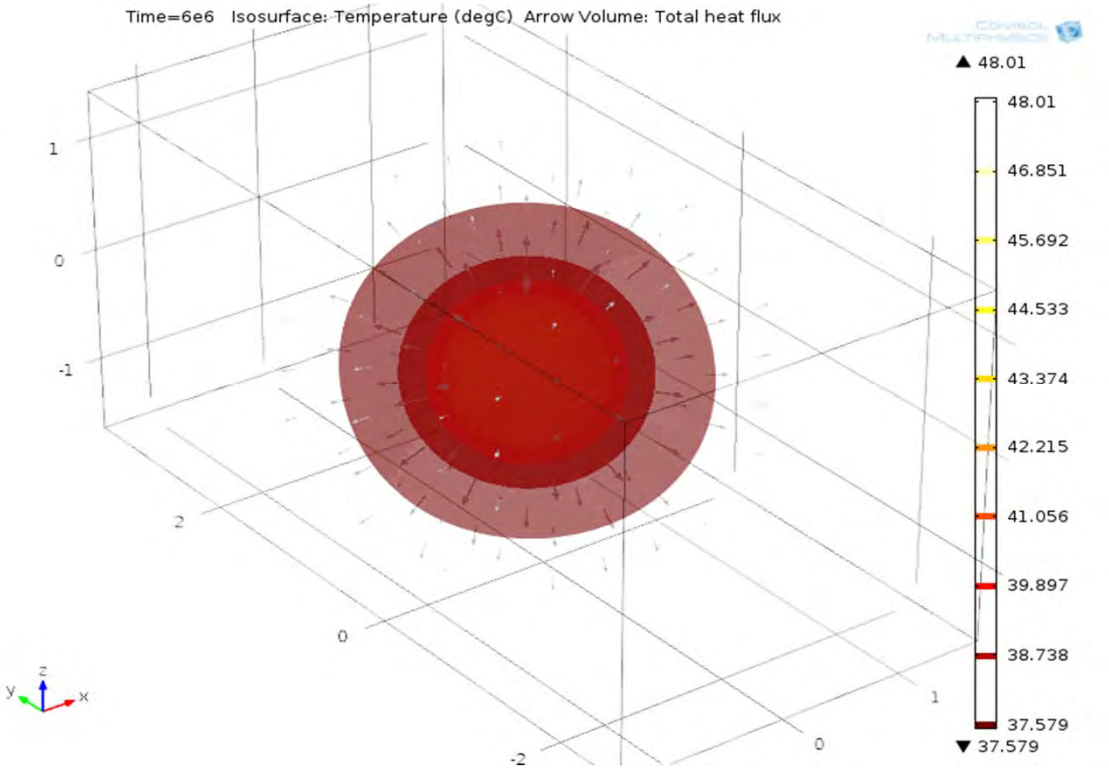

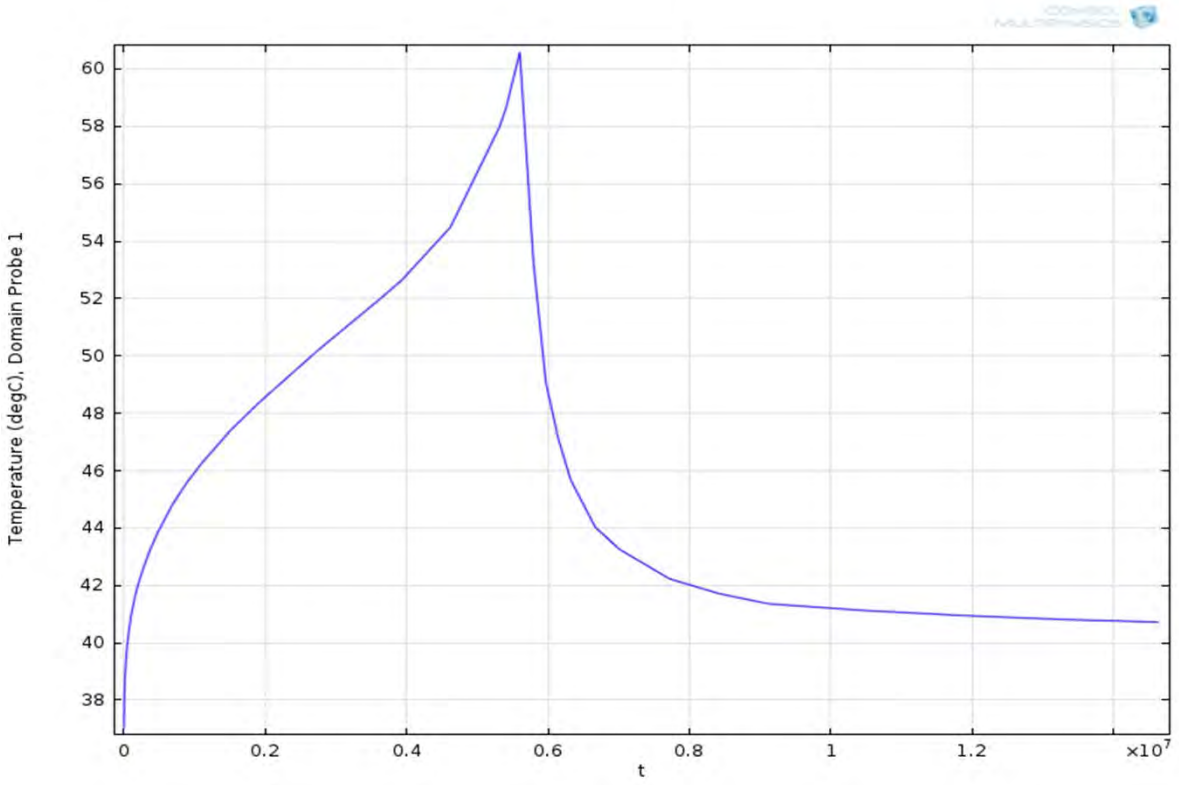
Temperature (degC), Domain Probe 1
60
58
56
54
52
50
48
46
44
42
40
38
0
0.2
0.4
0.6
0.8
1
1.2
×10^7
t

dry sand k =0.13 W/mK
3X Uranium heating
starting at 50C and is not stable
stable at 17C unstable at 18C

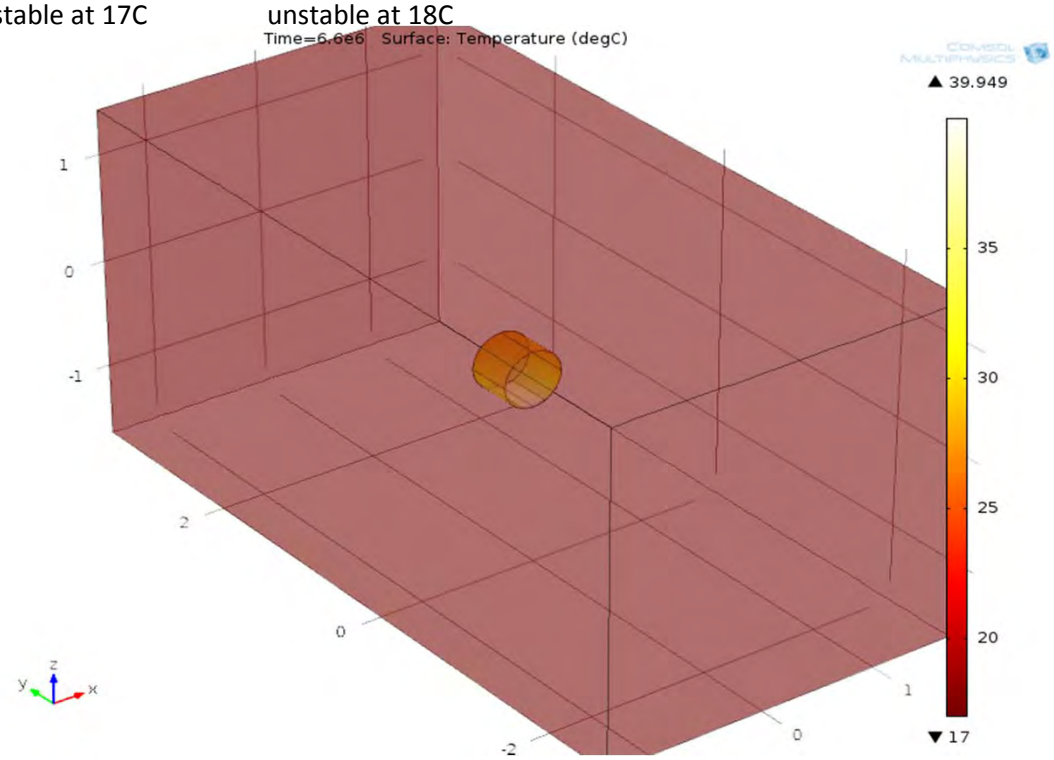

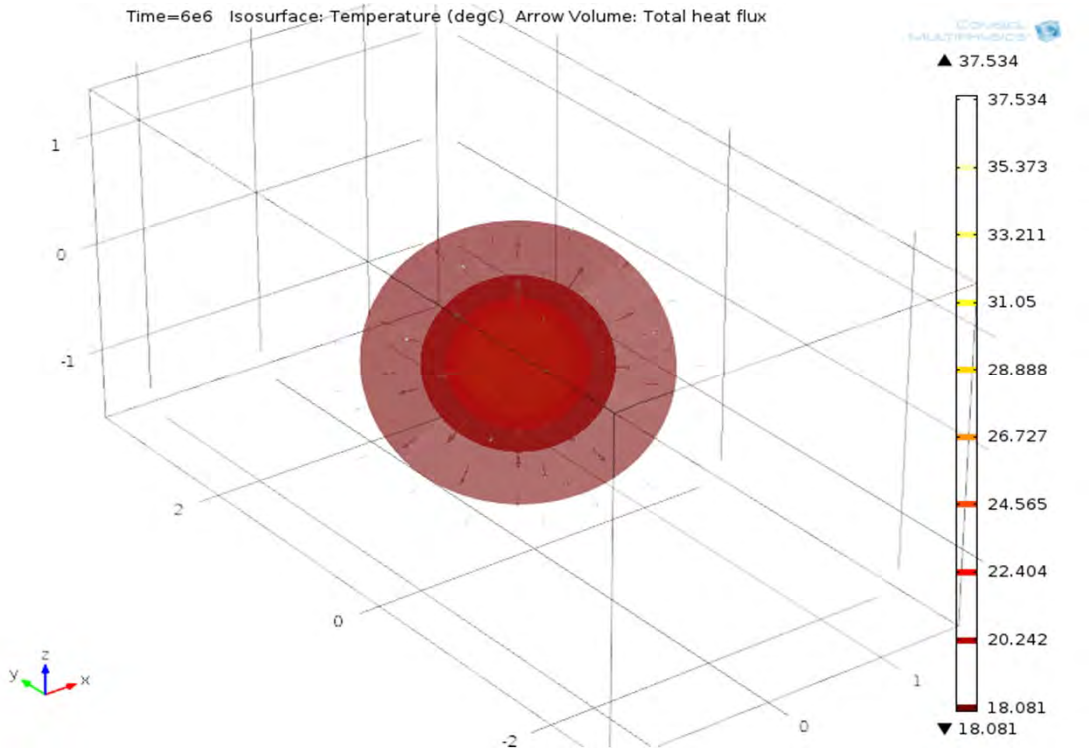

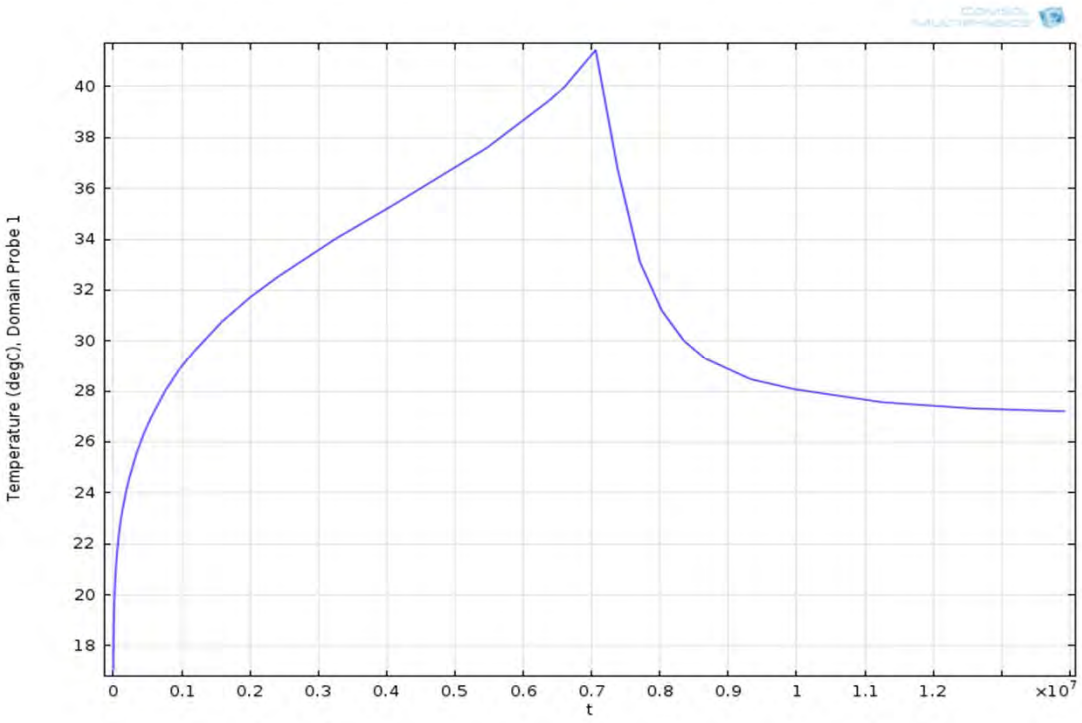
Temperature (degC), Domain Probe 1
40
38
36
34
32
30
28
26
24
22
20
18
0
0.1
0.2
0.3
0.4
0.5
0.6
0.7
0.8
0.9
1
1.1
1.2
×10^7
t

Case 6
file: K basin Box HeatSinkTube.mph
file: K basin Box HeatSinkTube.docx
dry sand k =0.13 W/mK
paste k = 0.67 W/mK
cut off at 2.145E6 J/kg
1/4 inch paste thickness
4 inch cradle thickness
1X Uranium rate: is stable At 3X Uranium is not stable

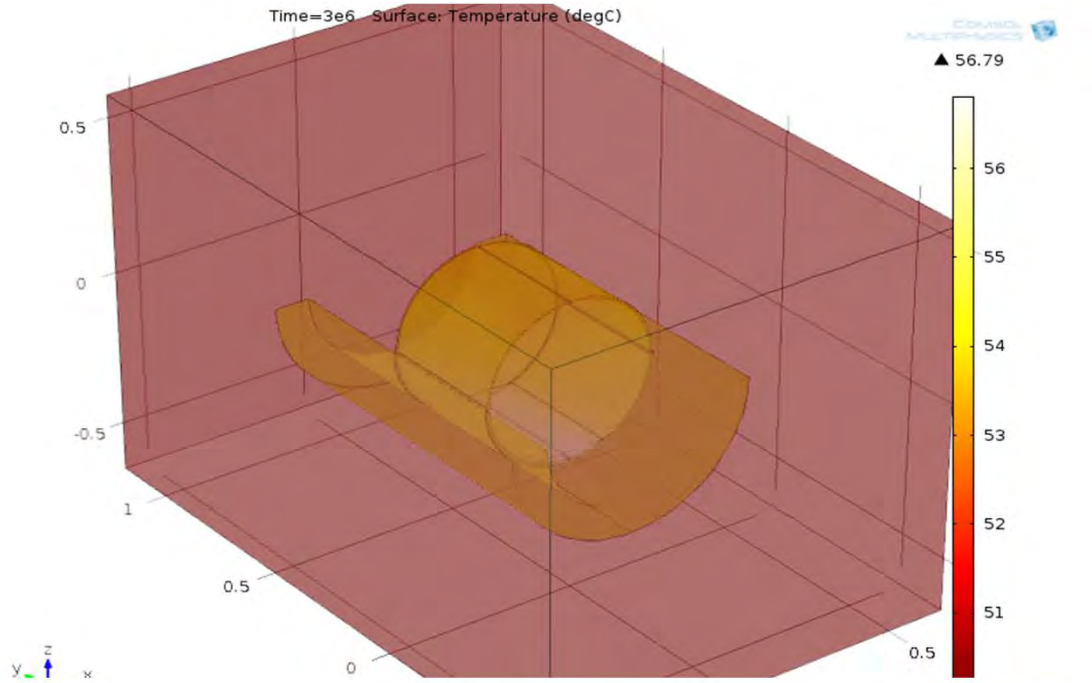

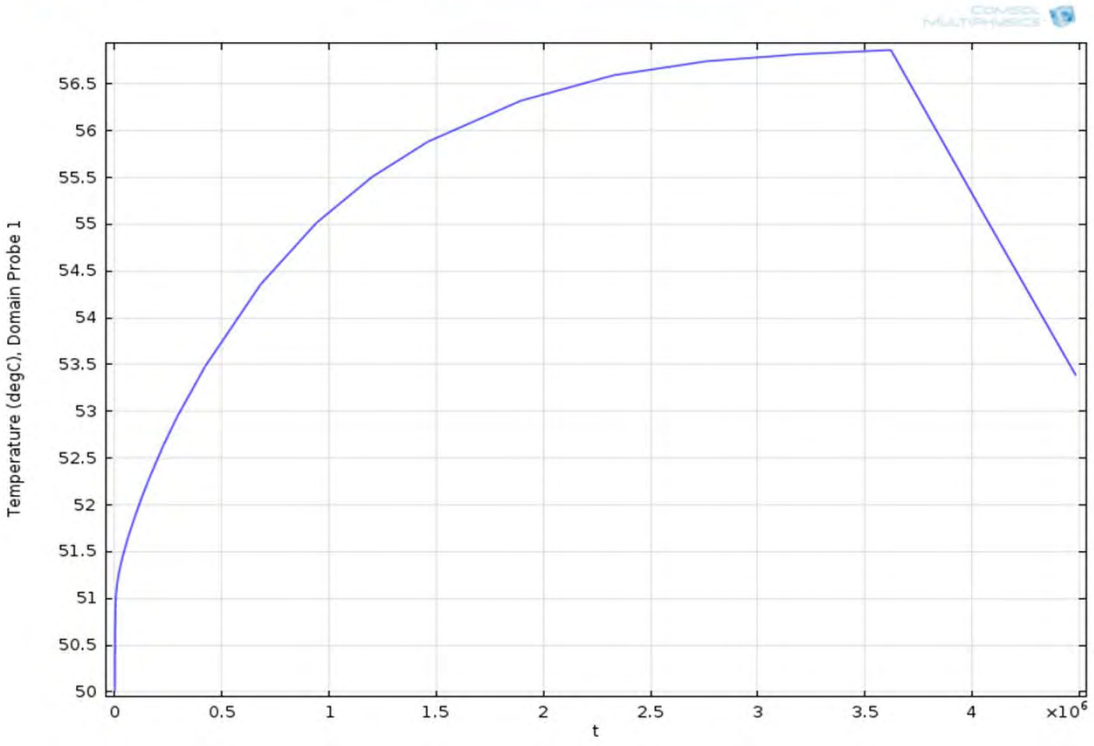

1/4 inch paste thickness
2 inch cradle thickness
1X Uranium rate: is stable

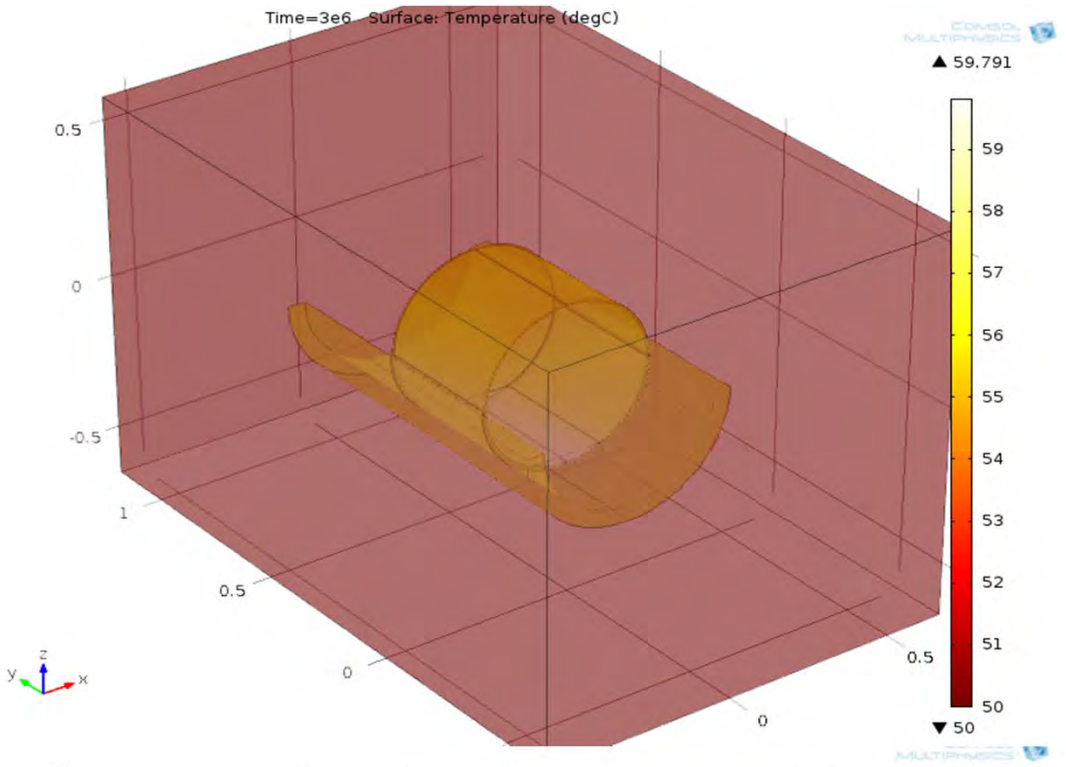

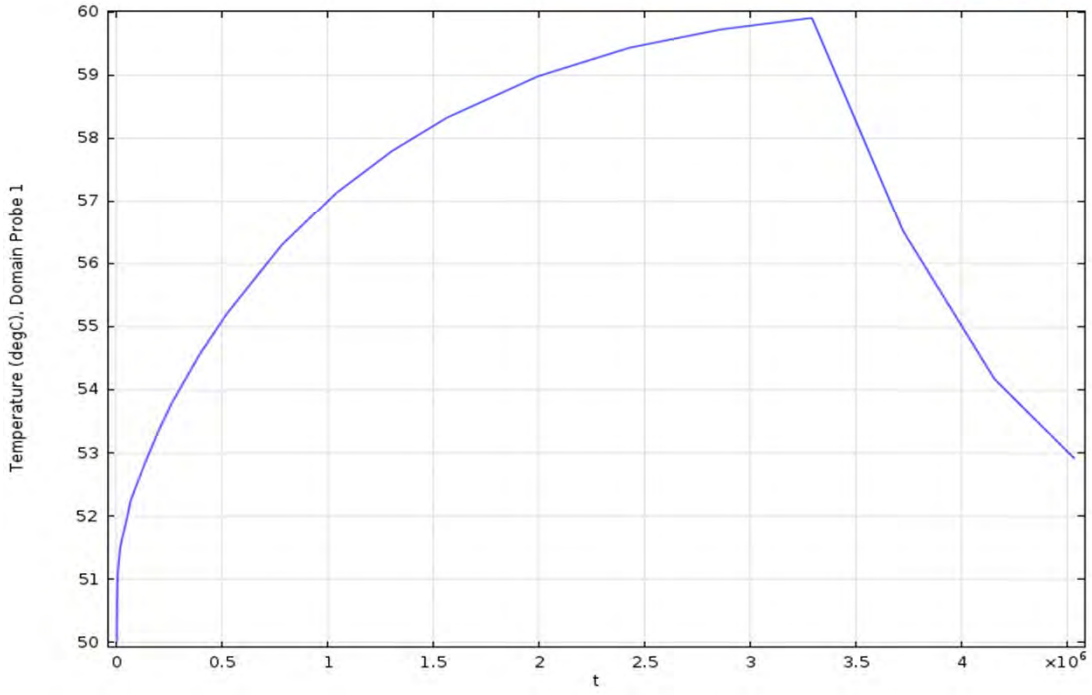

1/4 inch paste thickness
1 inch cradle thickness
1X Uranium rate: is stable

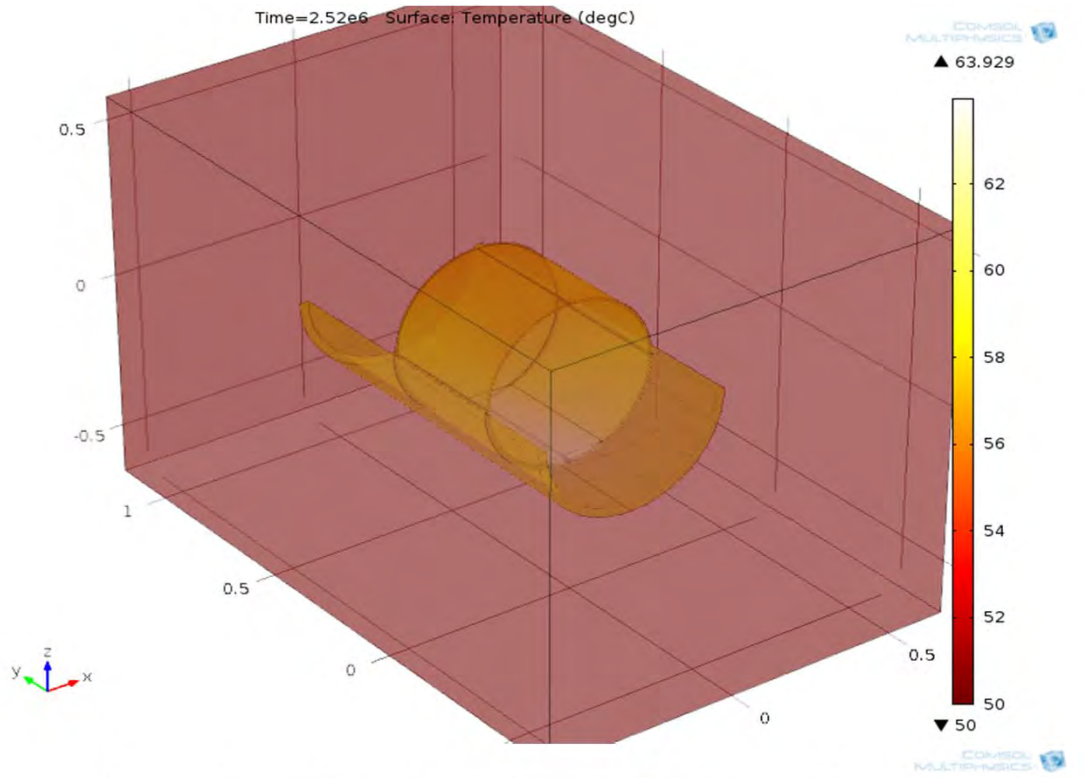

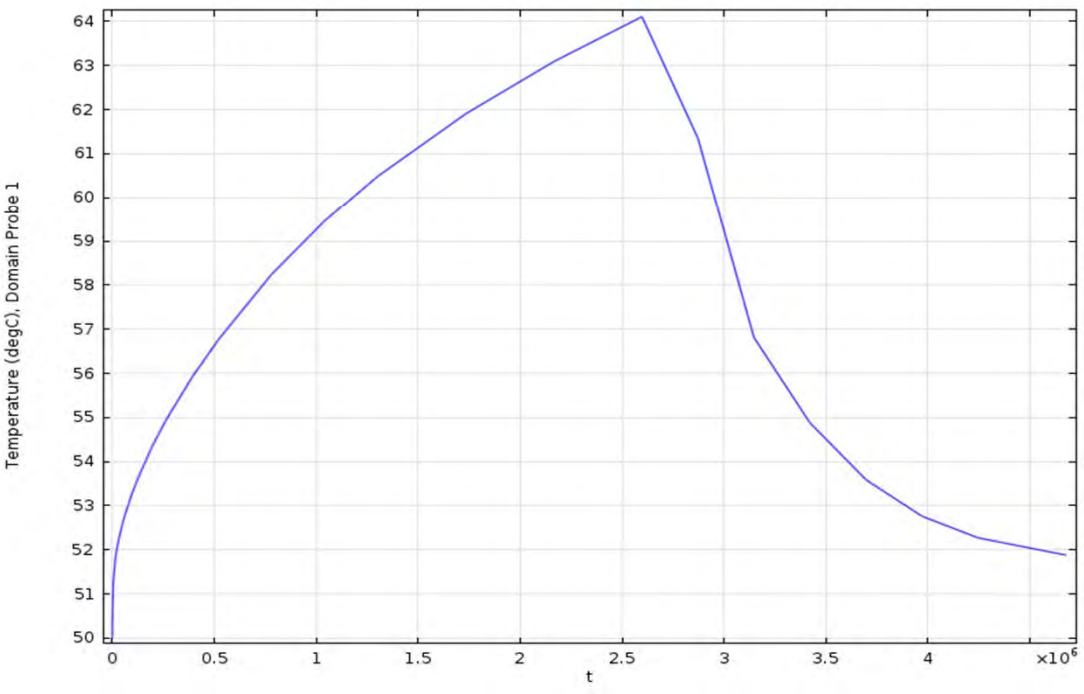

1/4 inch paste thickness
1/2 inch cradle thickness
1X Uranium rate: is stable

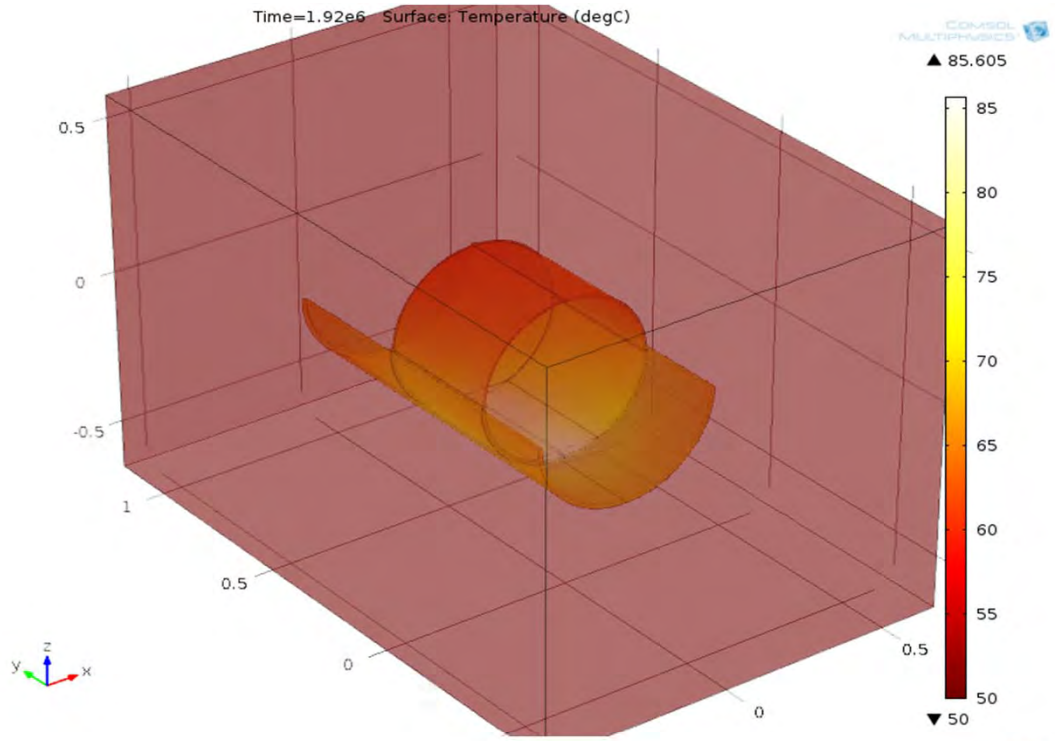

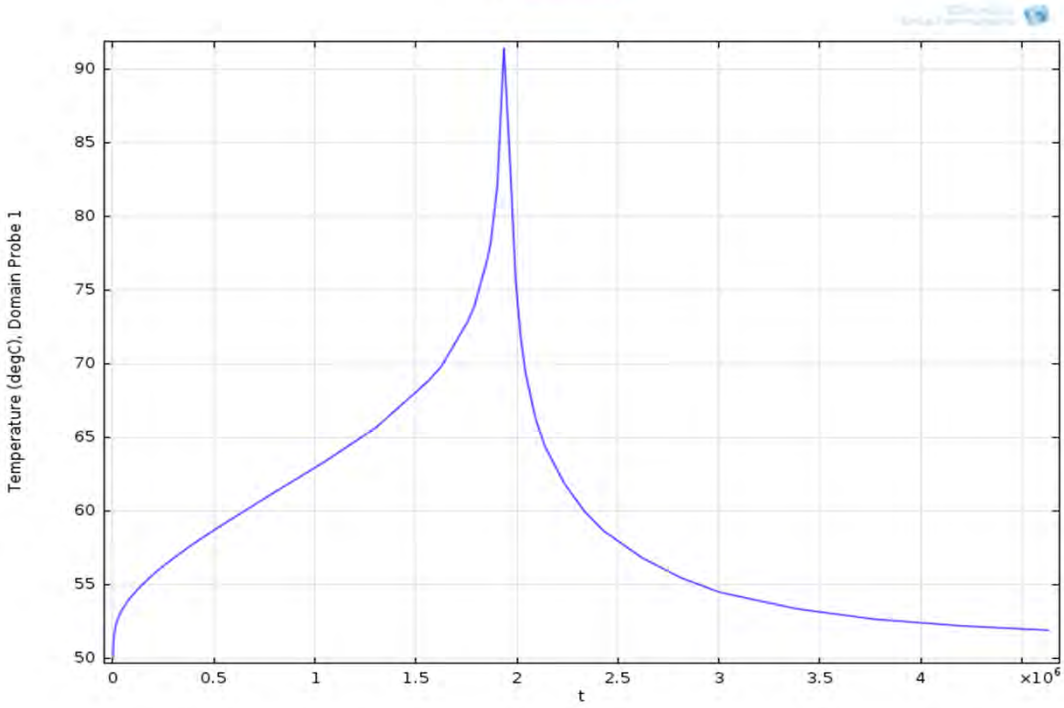

1/8 inch paste thickness
4 inch cradle thickness
1X Uranium rate: is stable At 3X Uranium is not stable

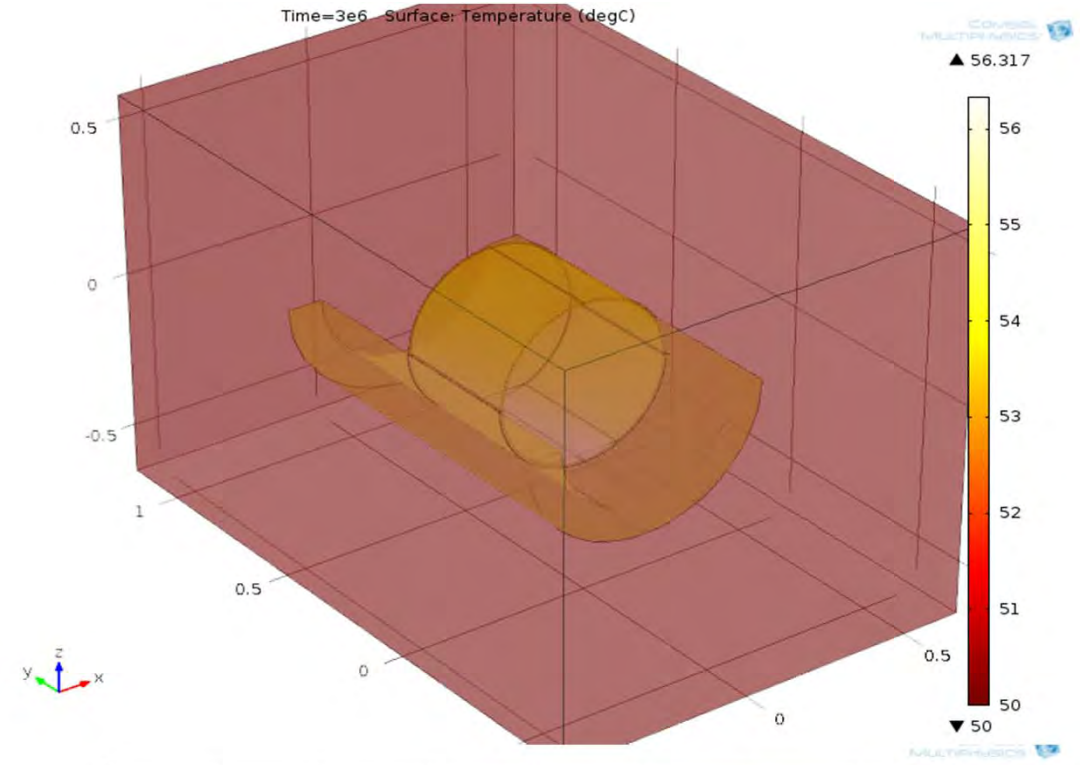

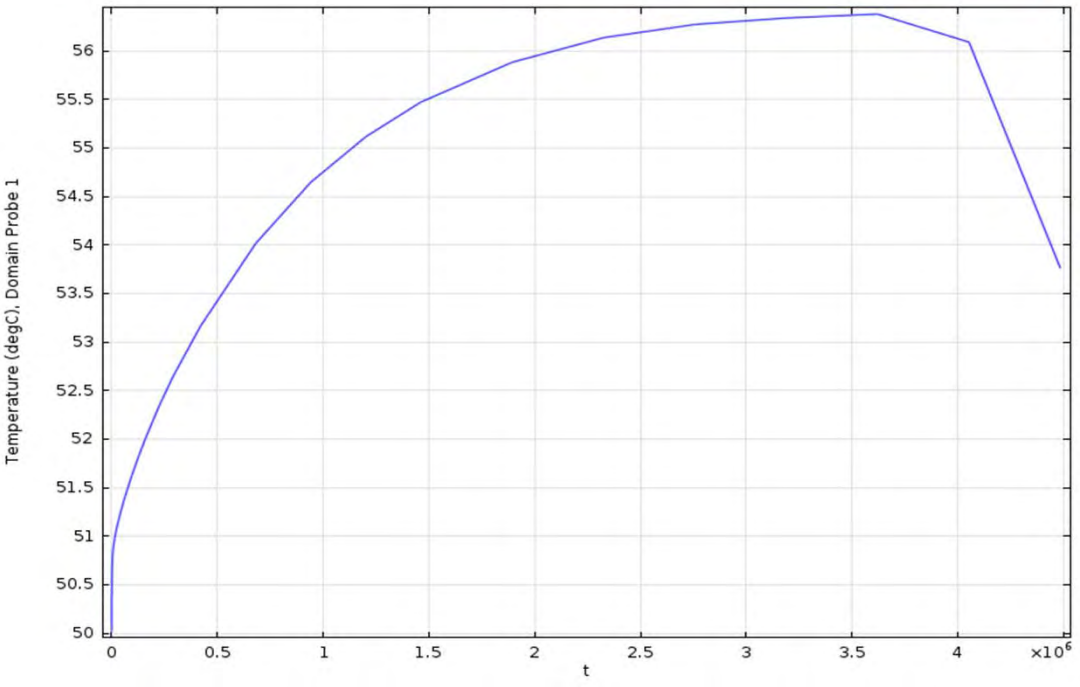

1/8 inch paste thickness
2 inch cradle thickness
1X Uranium rate: is stable

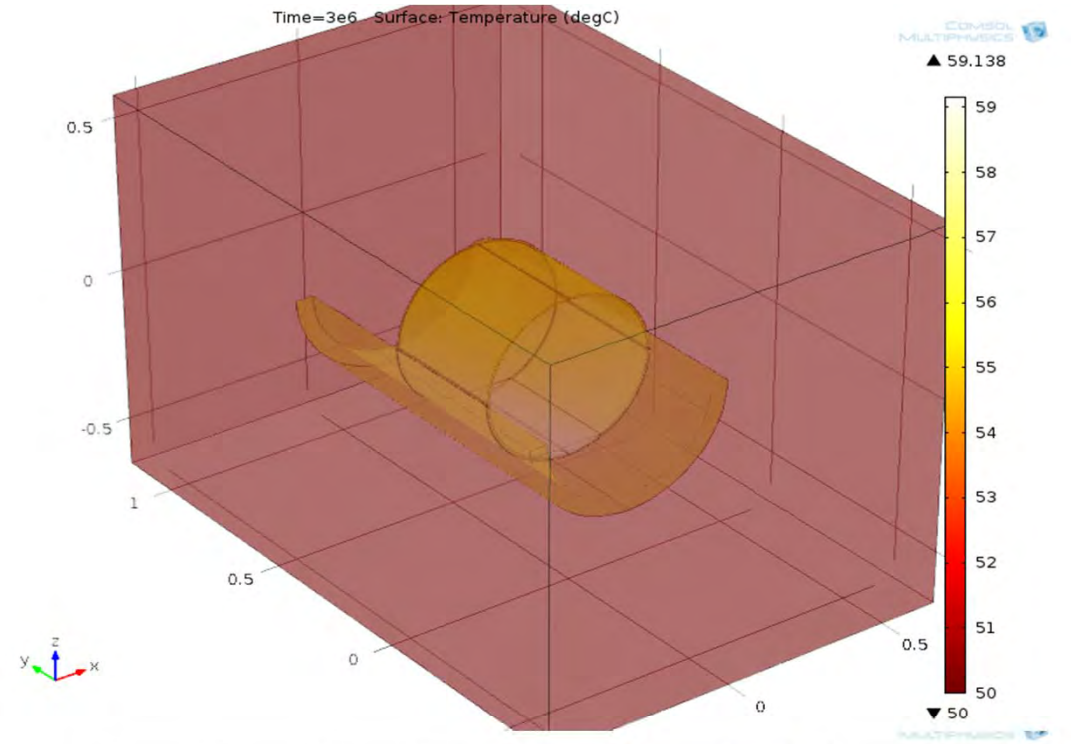

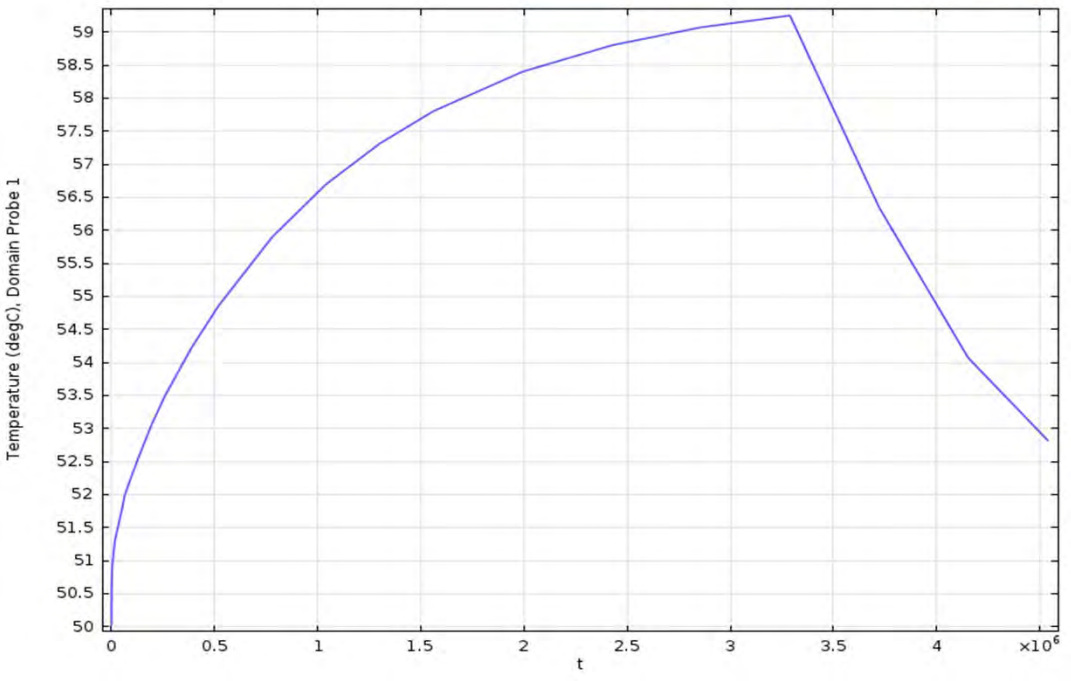

1/8 inch paste thickness
1 inch cradle thickness
1X Uranium rate: is stable

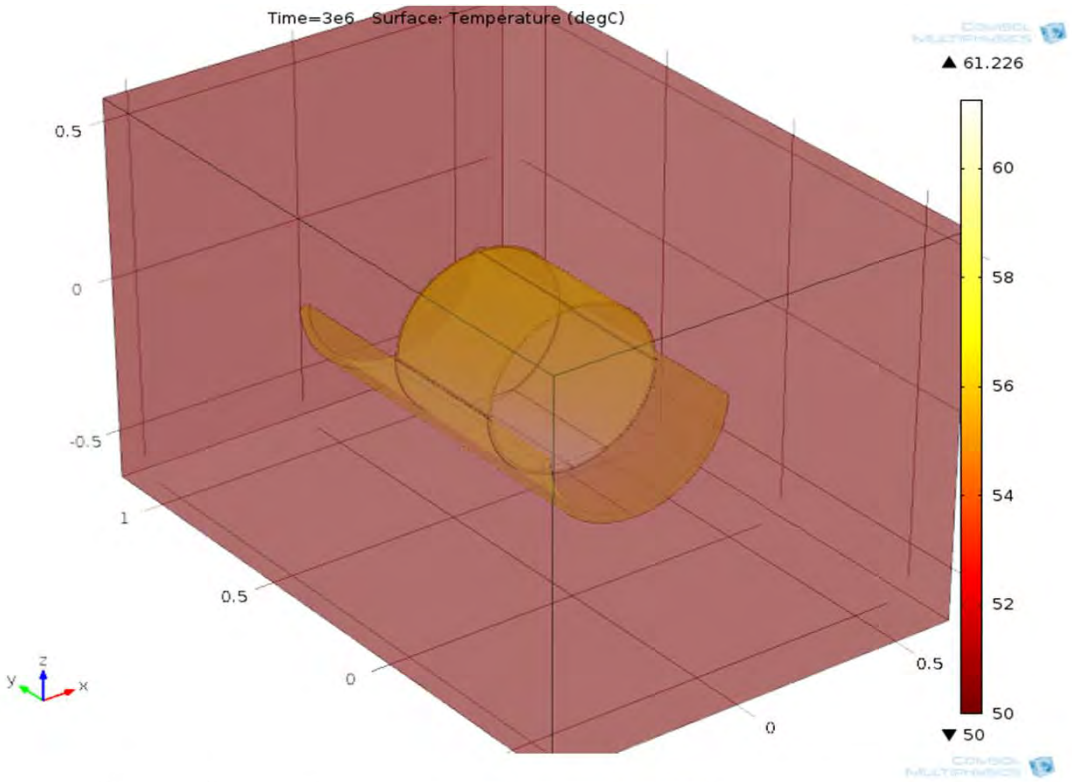

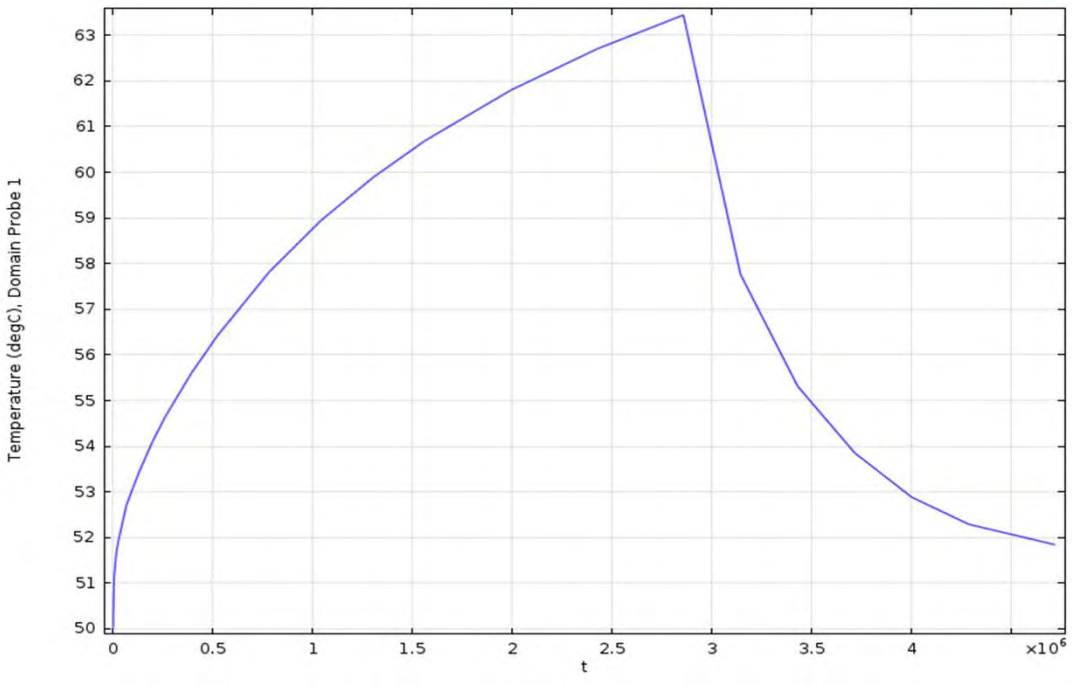

1/8 inch paste thickness
1/2 inch cradle thickness
1X Uranium rate: is not stable

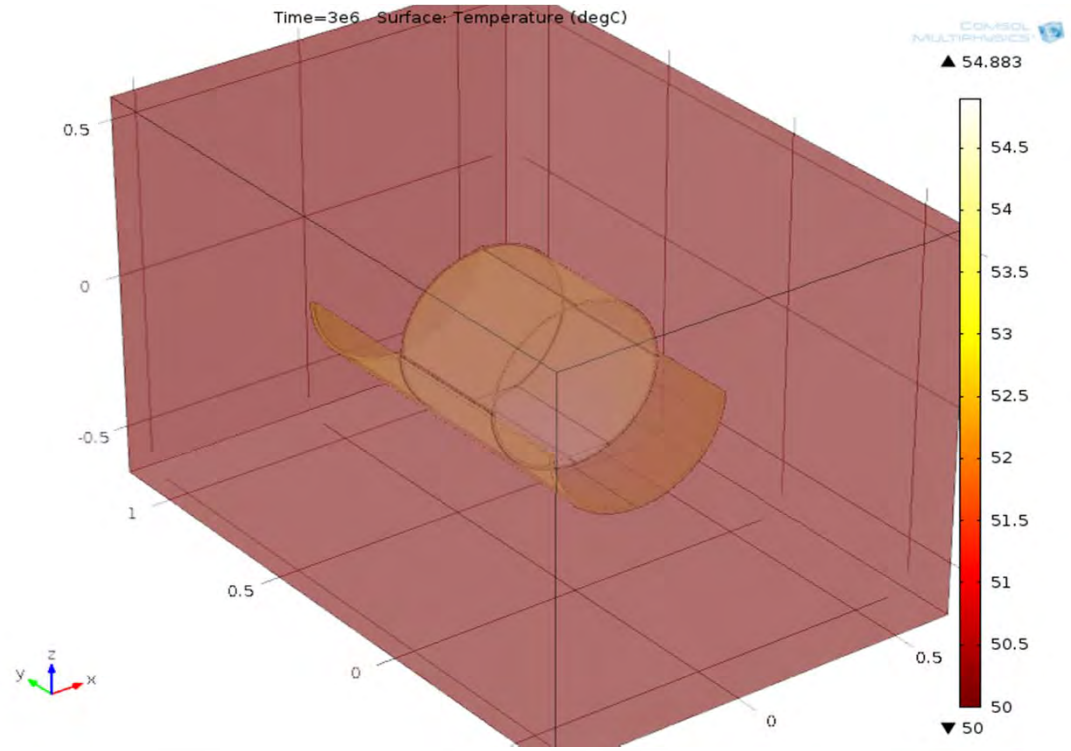

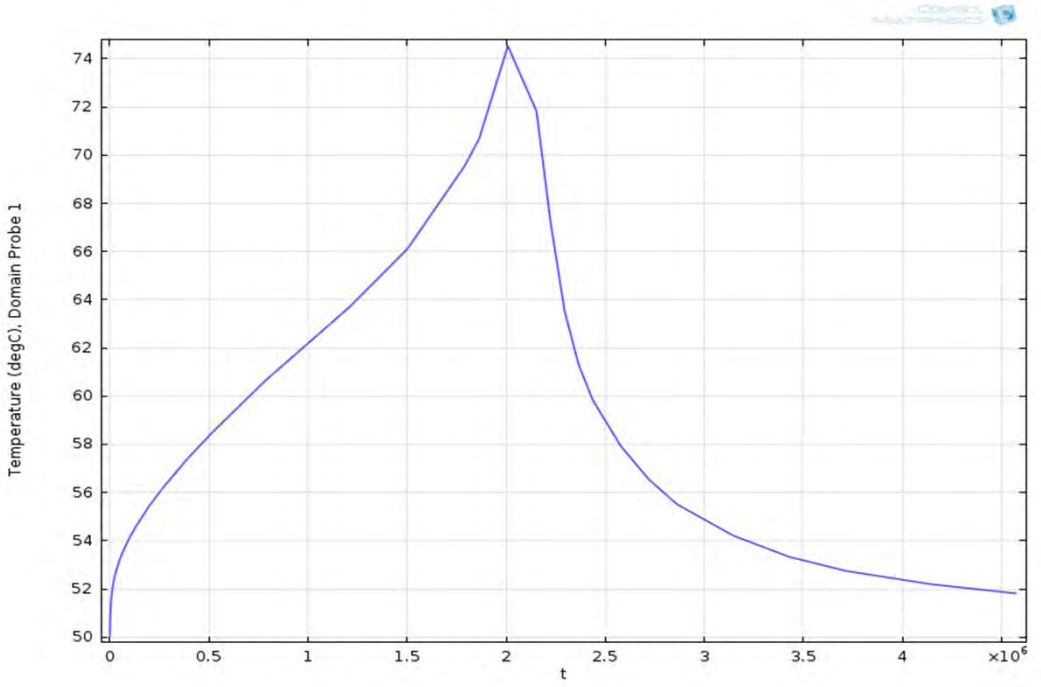

Case 7
file: K basin Box HeatSinkTube Grout in box.mph
file: K basin Box HeatSinkTube Grout in box.docx
dry sand k =0.13 W/mK
paste k = 0.67 W/mK
cut off at 2.145E6 J/kg
1/4 inch paste thickness
4 inch cradle thickness
1X Uranium rate: is stable

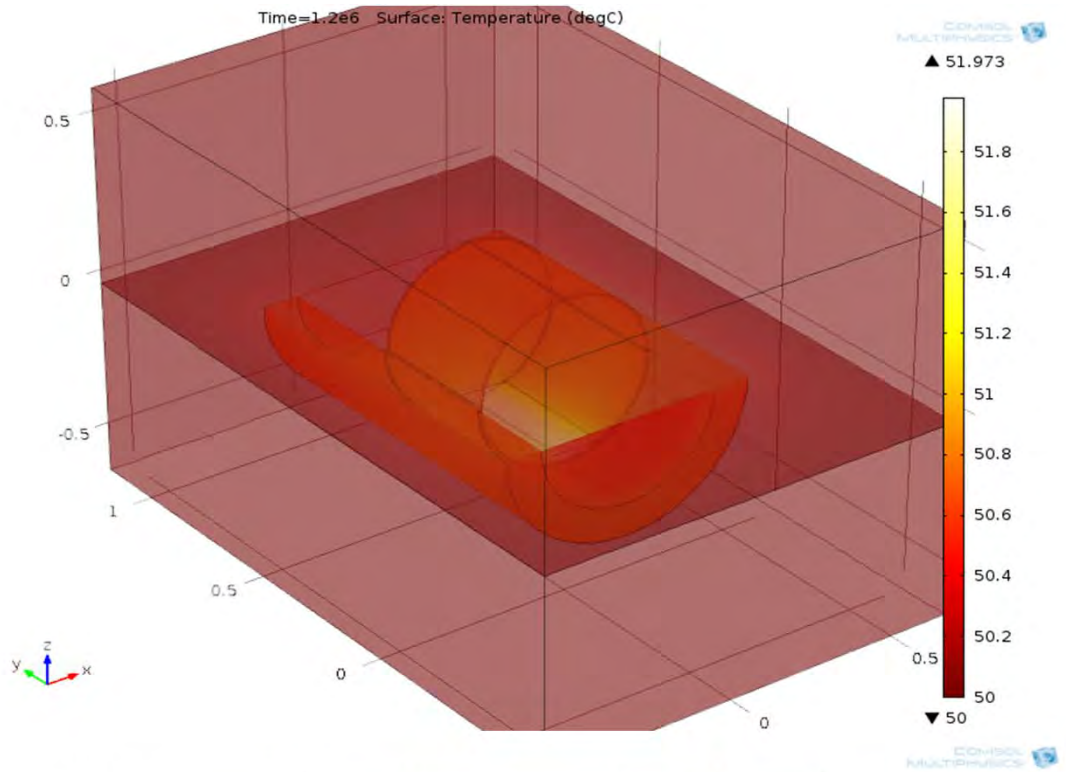

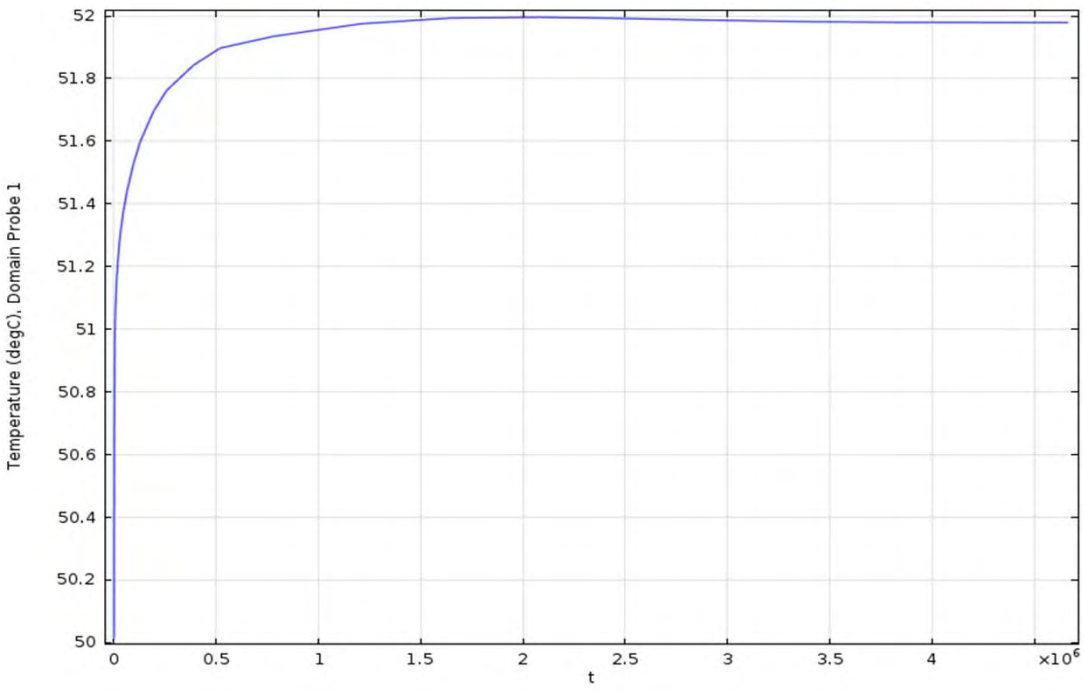

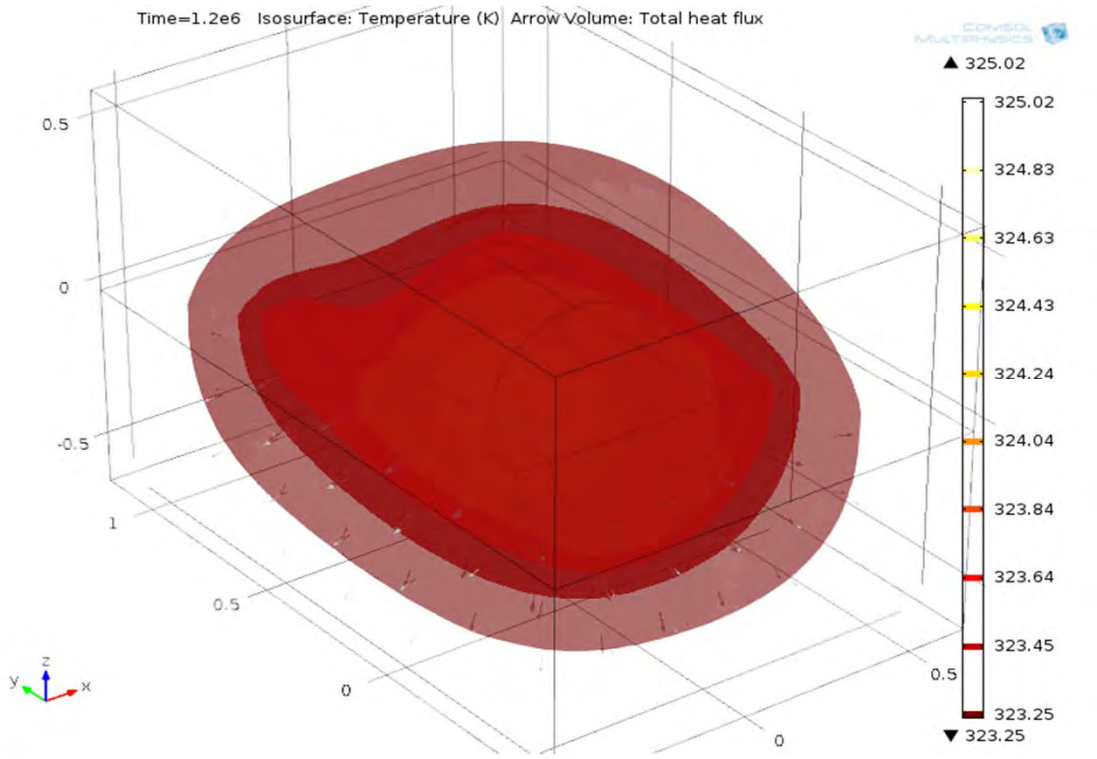
Time=1.2e6 Isosurface: Temperature (K) Arrow Volume: Total heat flux
▲ 325.02
325.02
324.83
324.63
324.43
324.24
324.04
323.84
323.64
323.45
323.25
▼ 323.25
0.5
0
-0.5
1
0.5
0
0.5
0
z
y
x

At 3X Uranium is stable

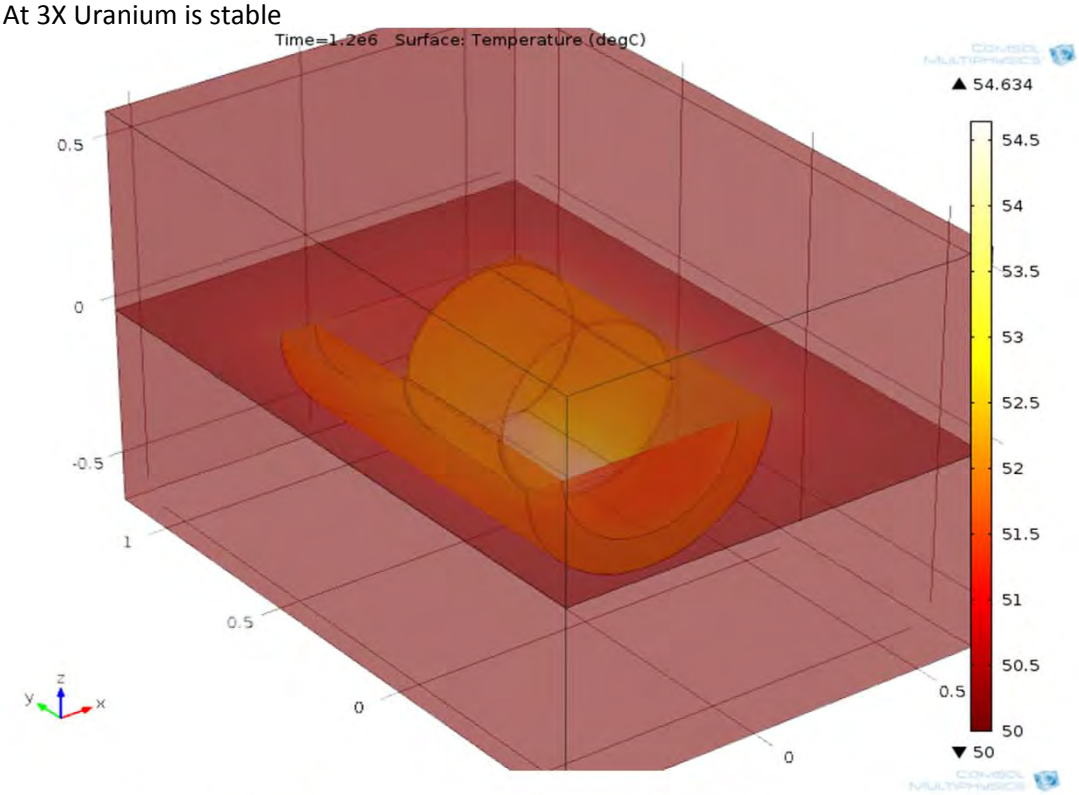

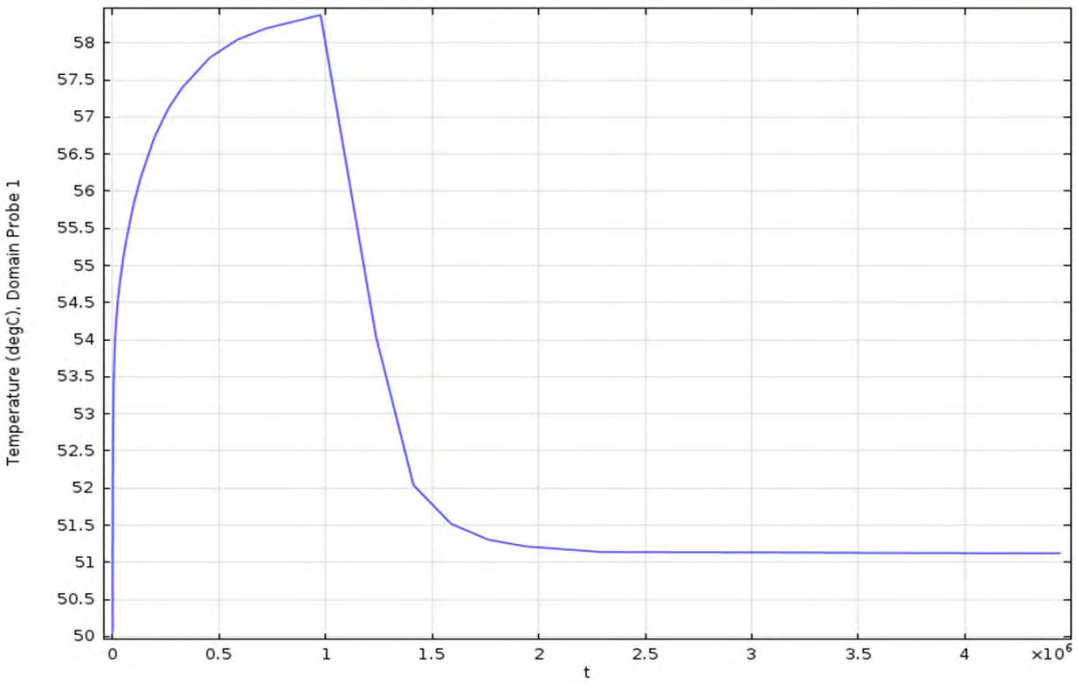

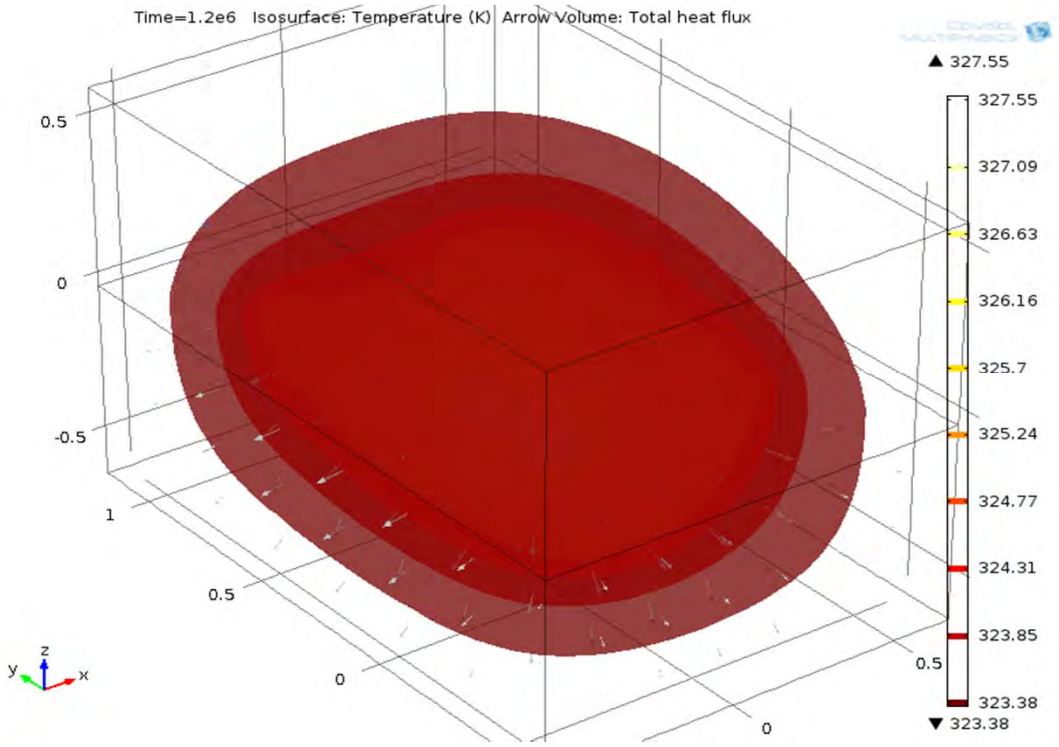
Time=1.2e6 Isosurface: Temperature (K) Arrow Volume: Total heat flux
▲ 327.55
327.55
327.09
326.63
326.16
325.7
325.24
324.77
324.31
323.85
323.38
▼ 323.38
0.5
0
-0.5
1
0.5
0
0.5
0
z
y
x

1/4 inch paste thickness
2 inch cradle thickness
1X Uranium rate: is stable

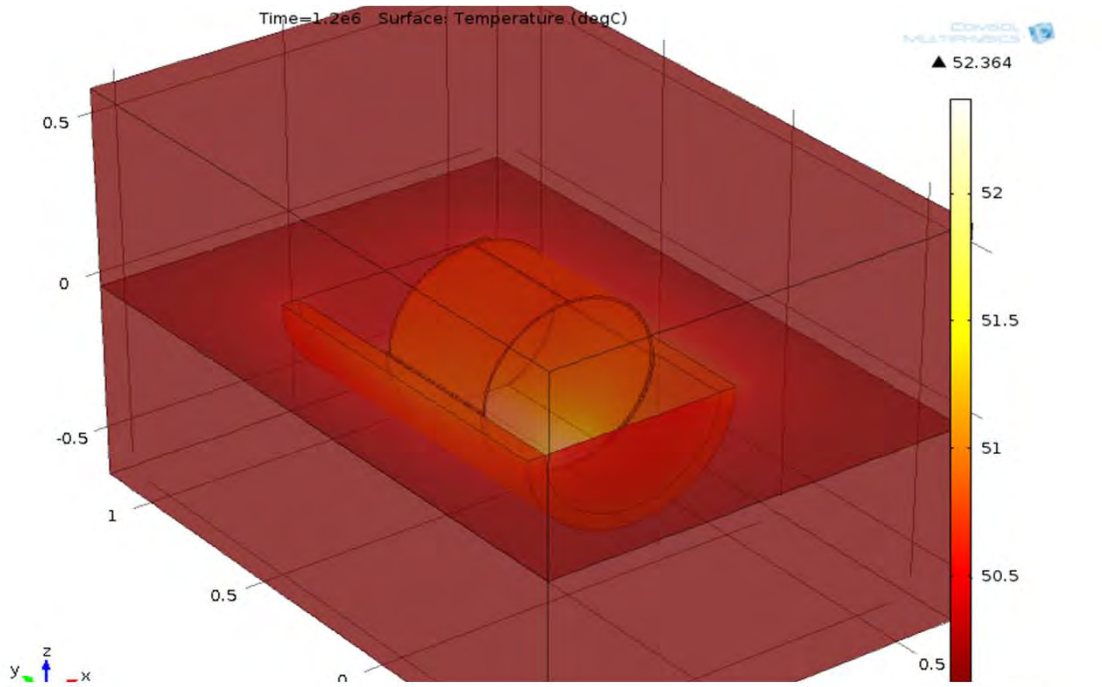

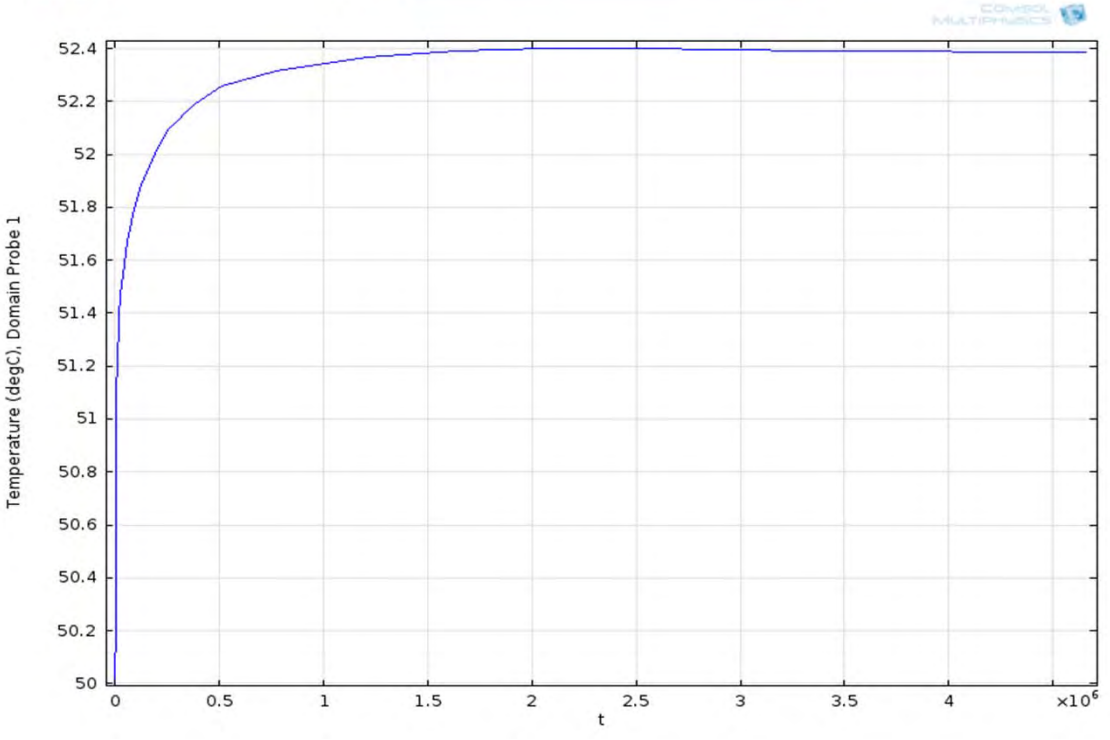

1/4 inch paste thickness
2 inch cradle thickness
3X uranium stable

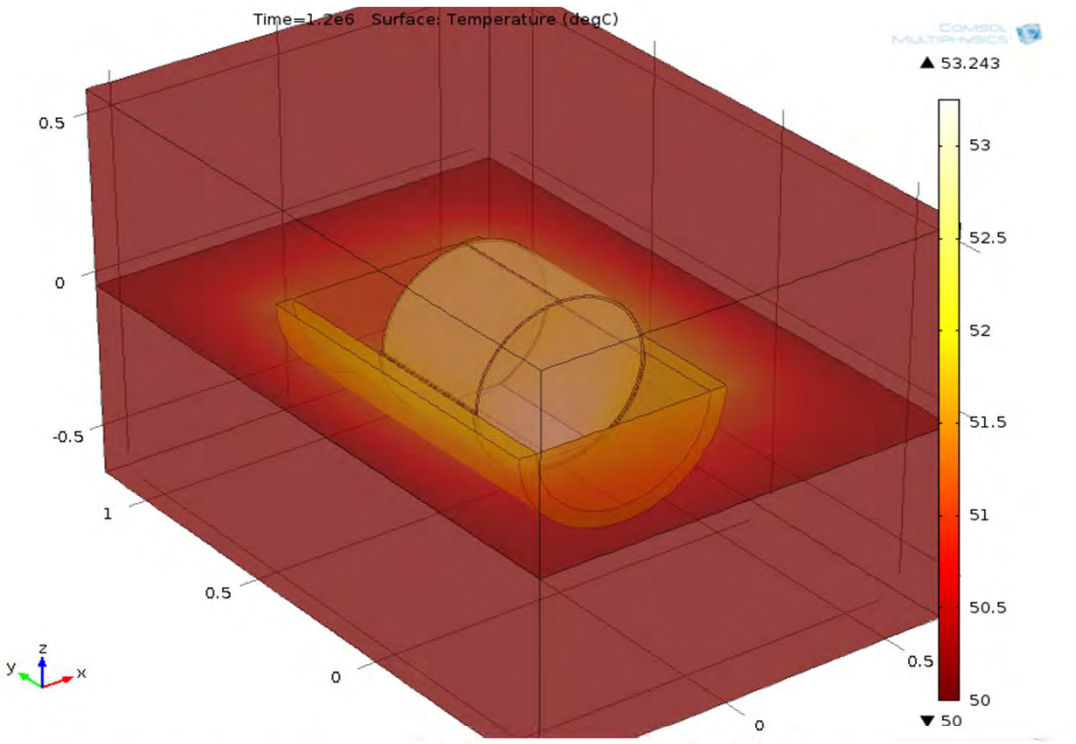

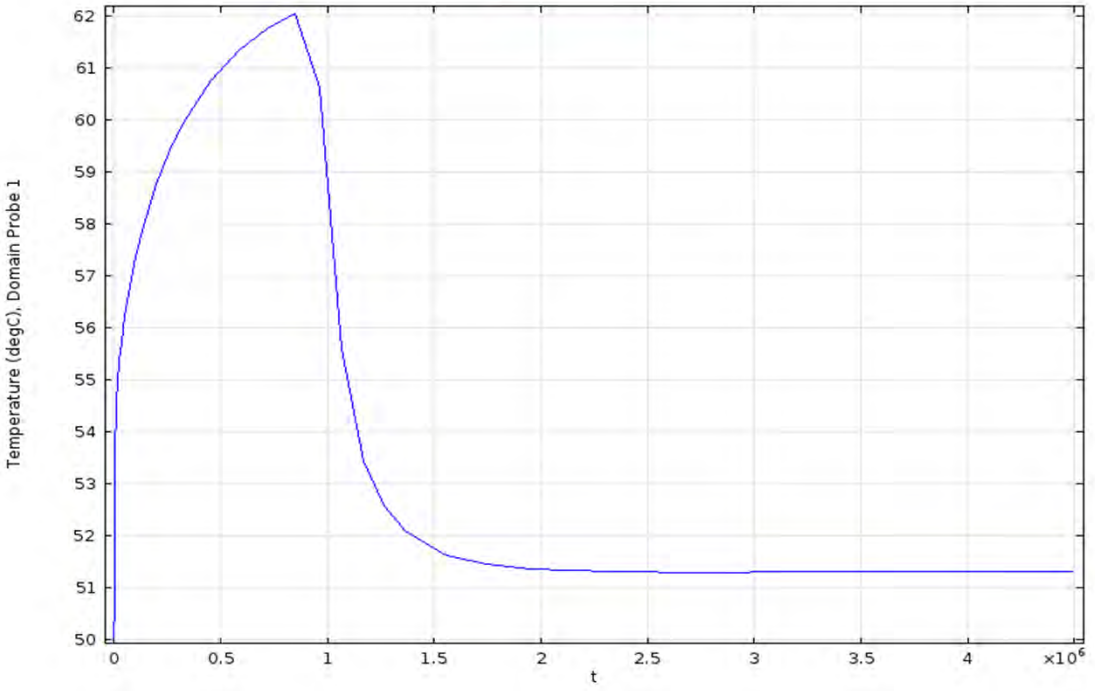

1/4 inch paste thickness
1 inch cradle thickness
1X Uranium rate: is stable

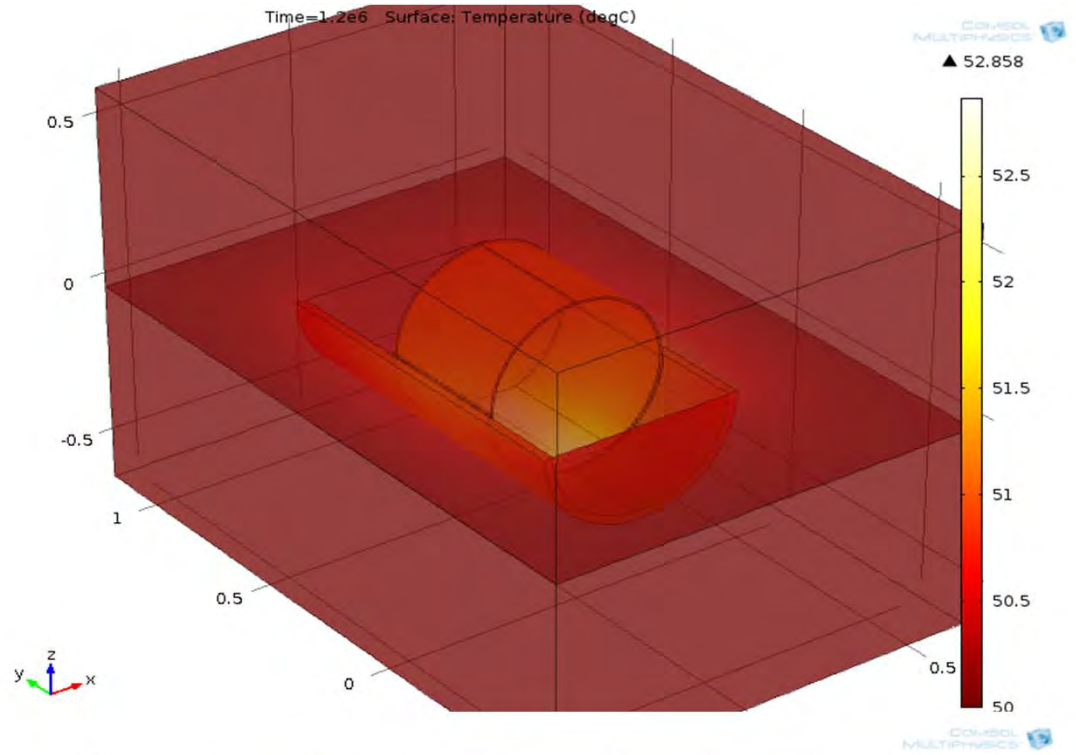

3X uranium is not stable

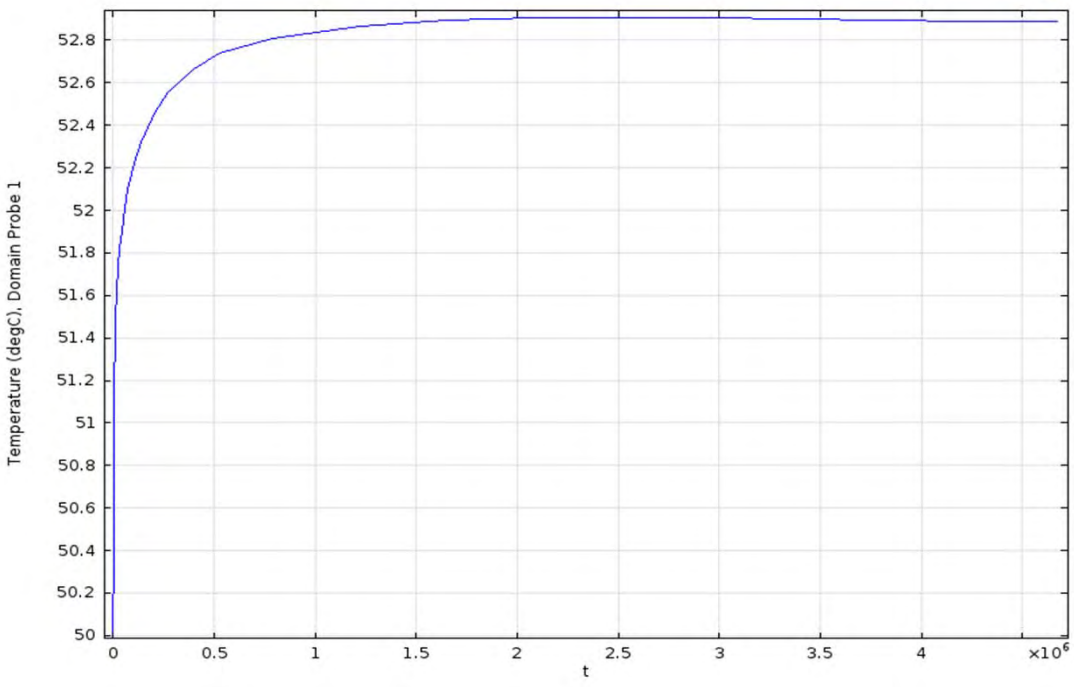

1/4 inch paste thickness
1/2 inch cradle thickness
1X Uranium rate: is stable

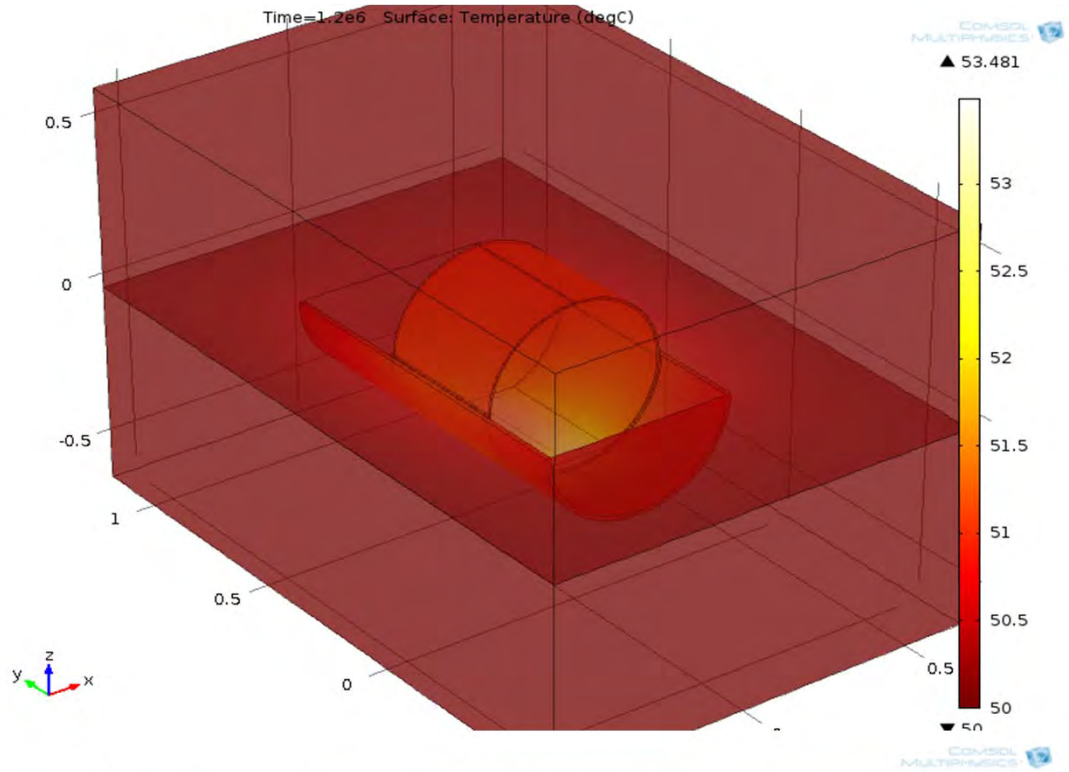

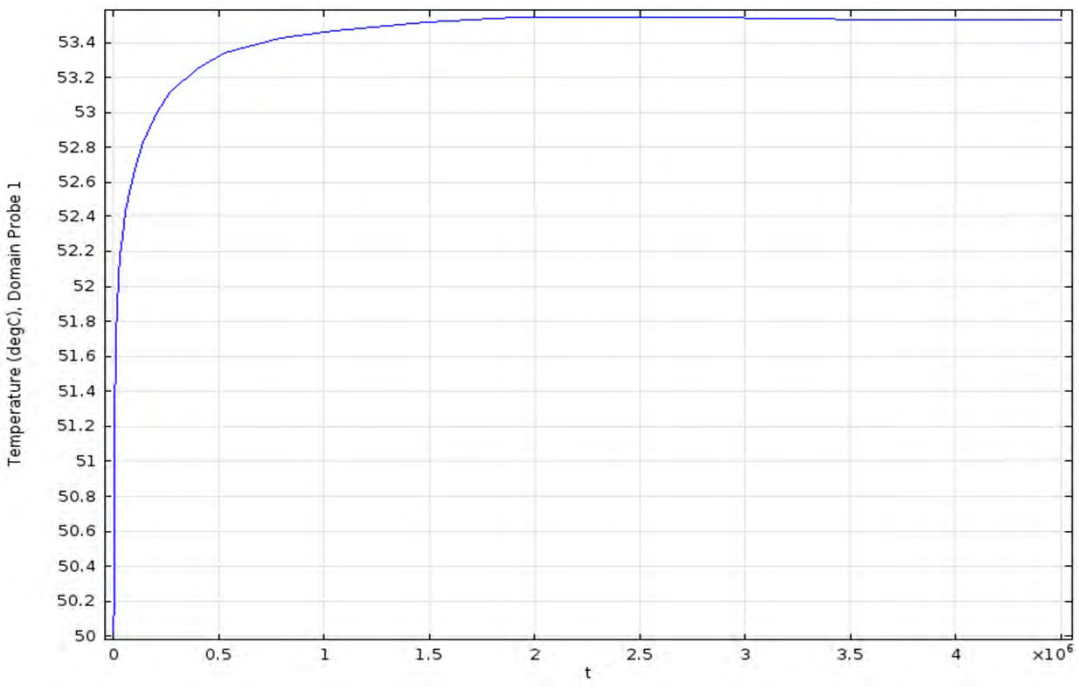

1/4 inch paste thickness
1/4 inch cradle thickness
1X Uranium rate: is stable

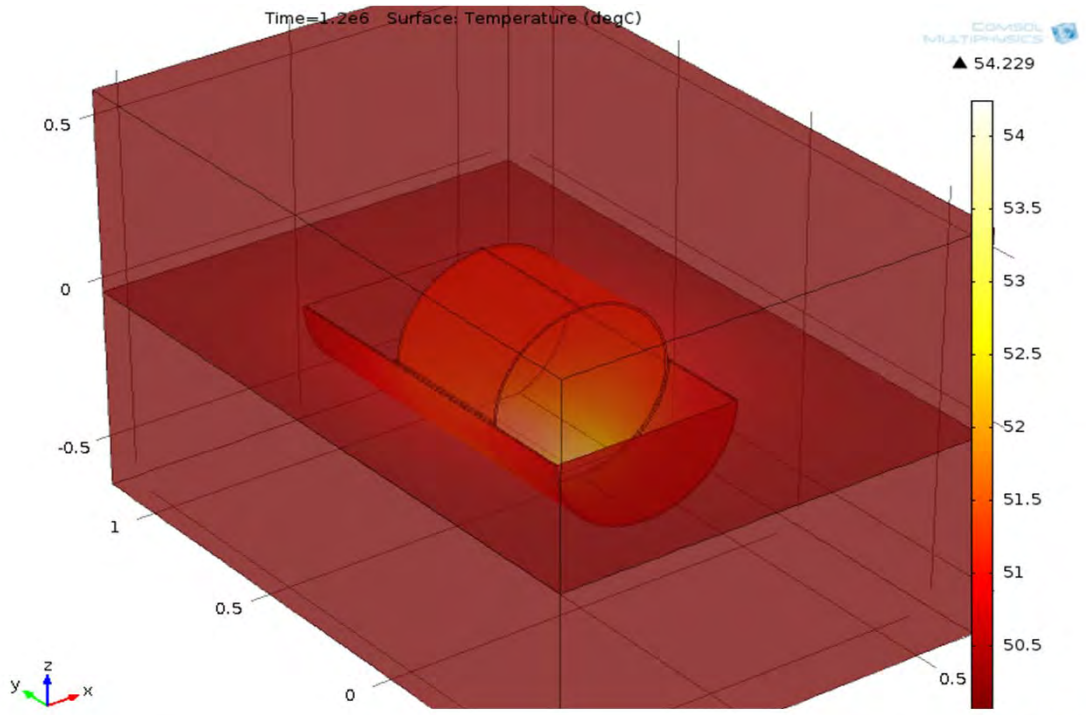

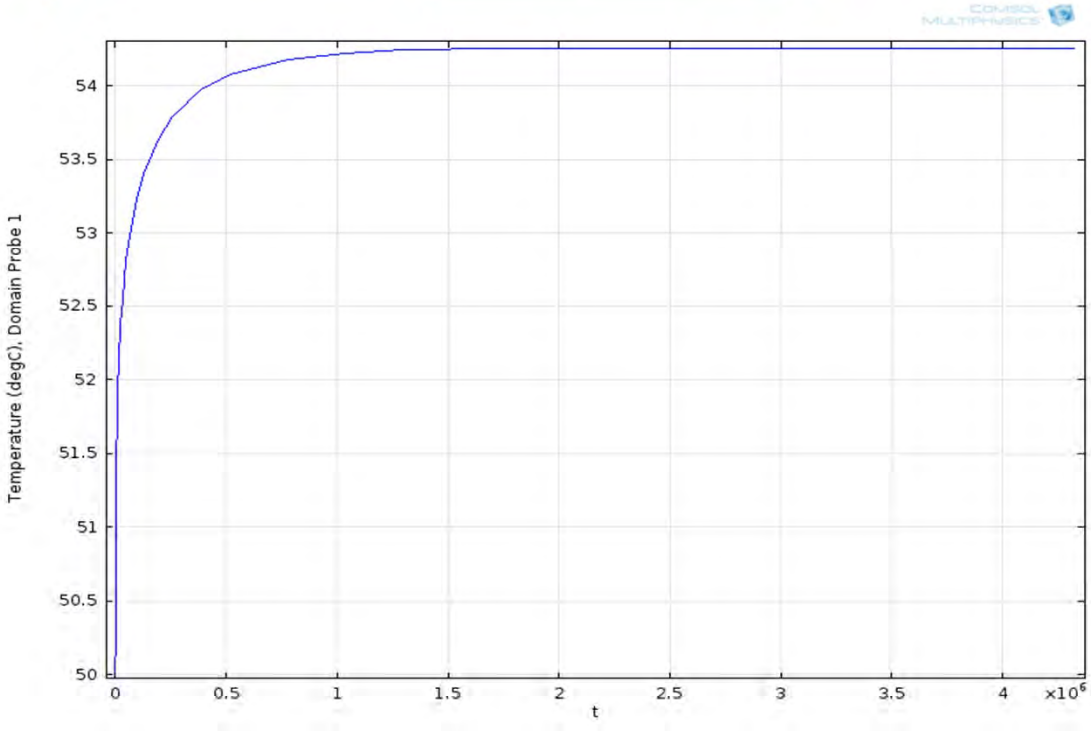

1/8 inch paste thickness
4 inch cradle thickness
1X Uranium rate: is stable

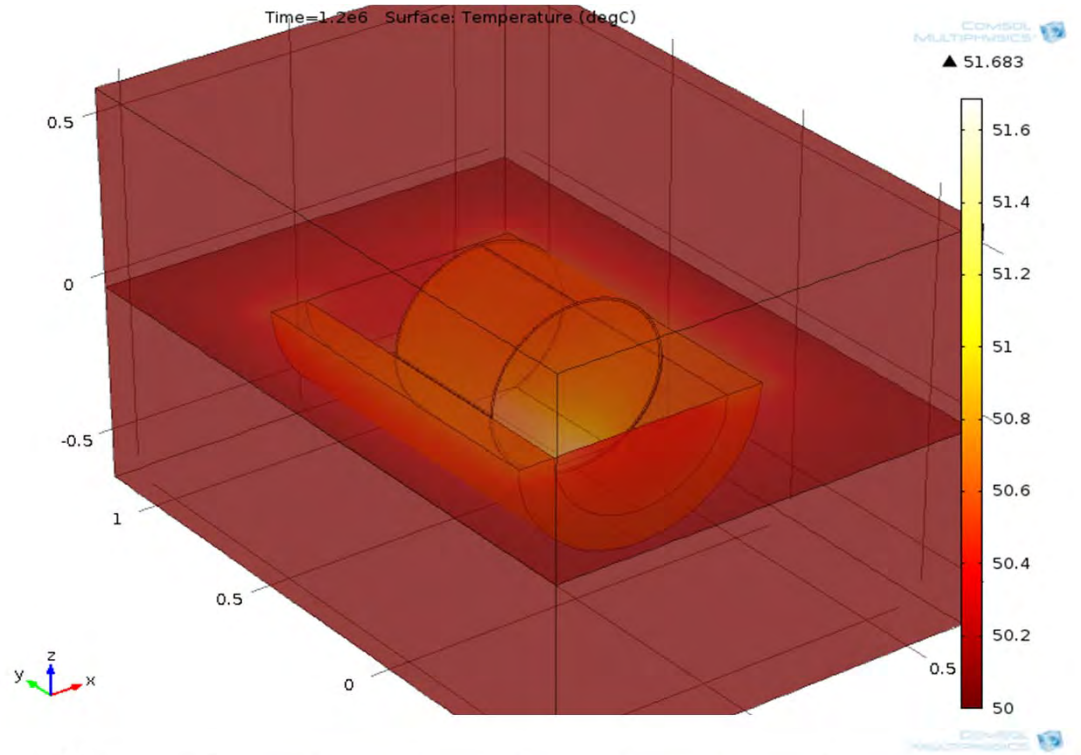

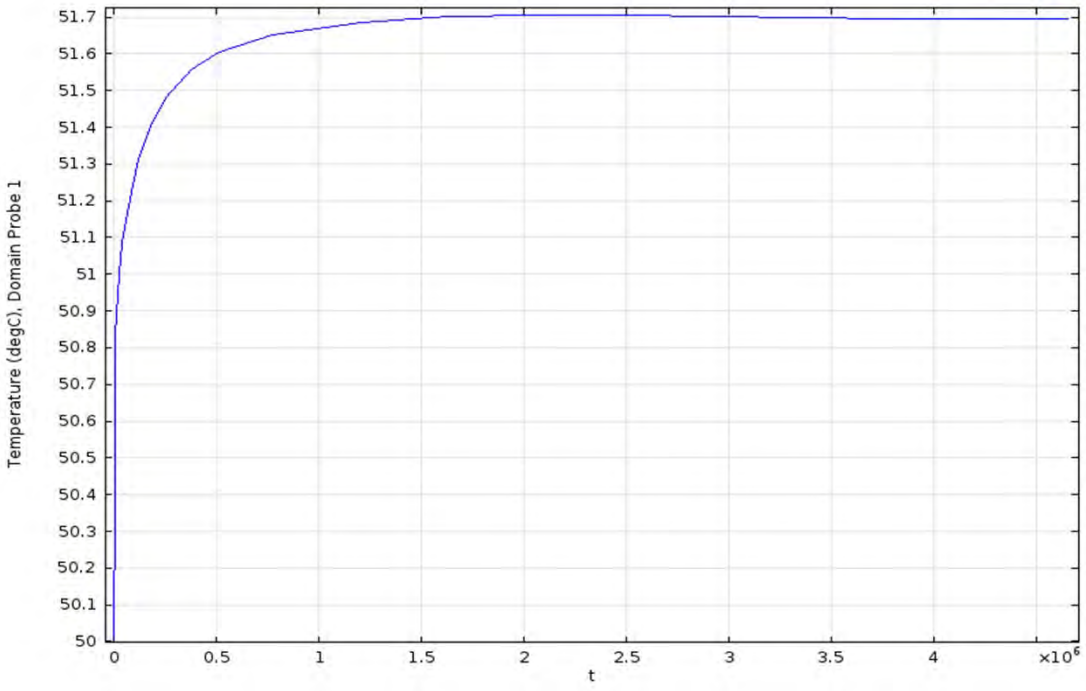

1/8 inch paste thickness
4 inch cradle thickness
3X Uranium rate:

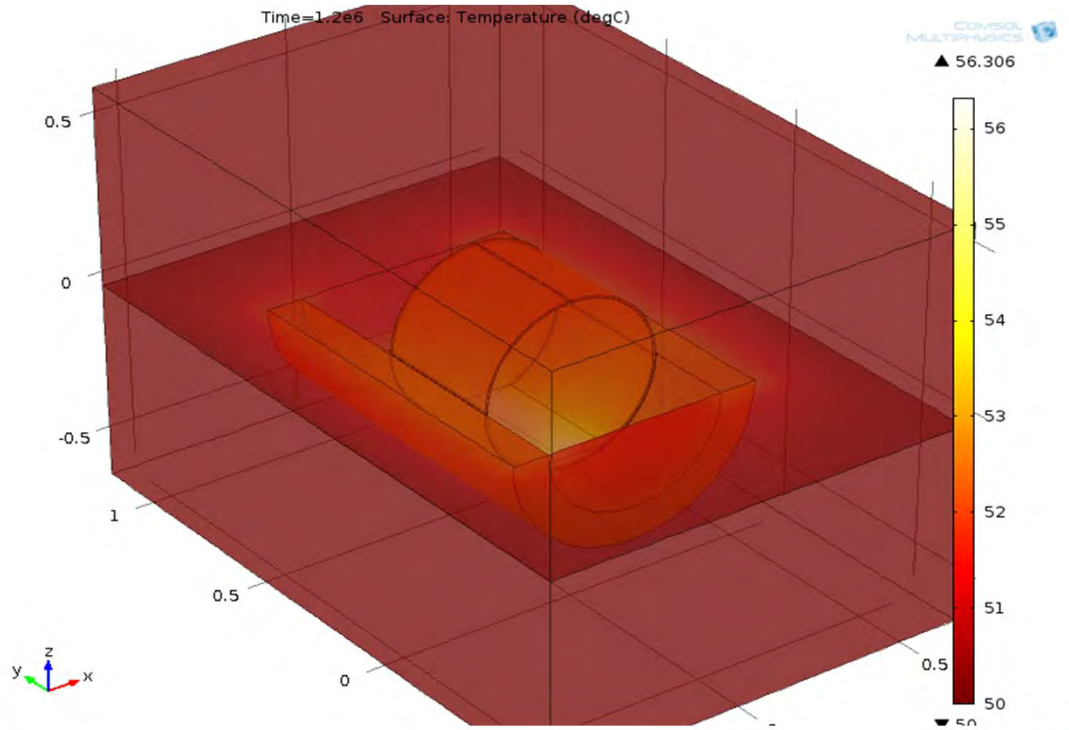

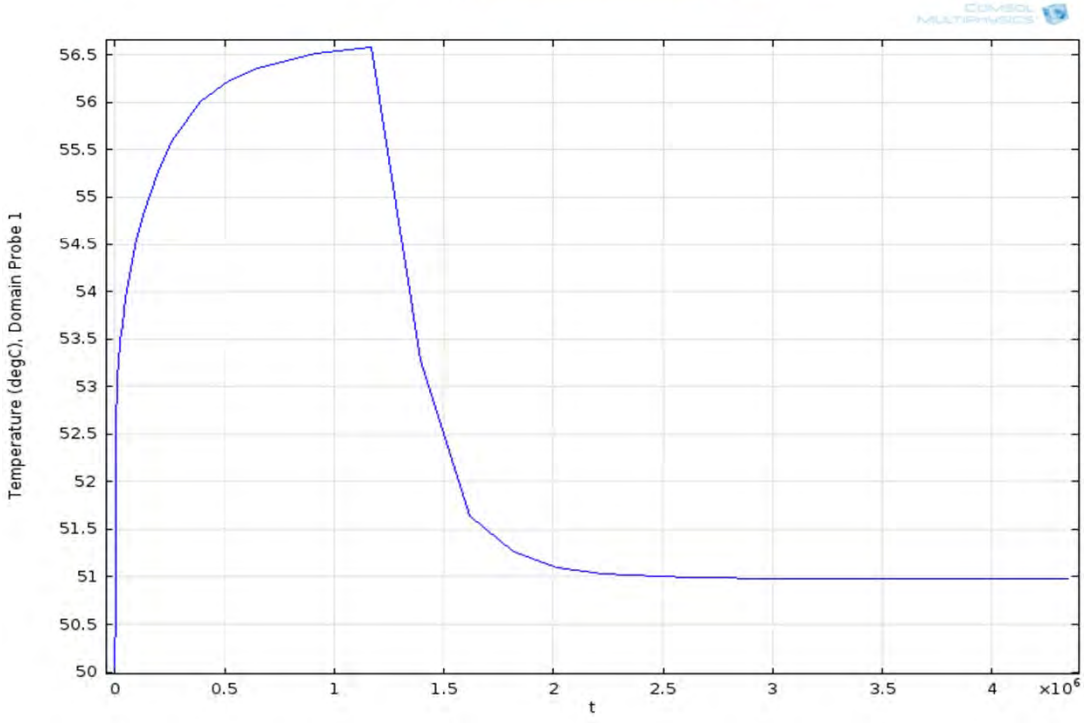

1/8 inch paste thickness
2 inch cradle thickness
1X Uranium rate: is stable

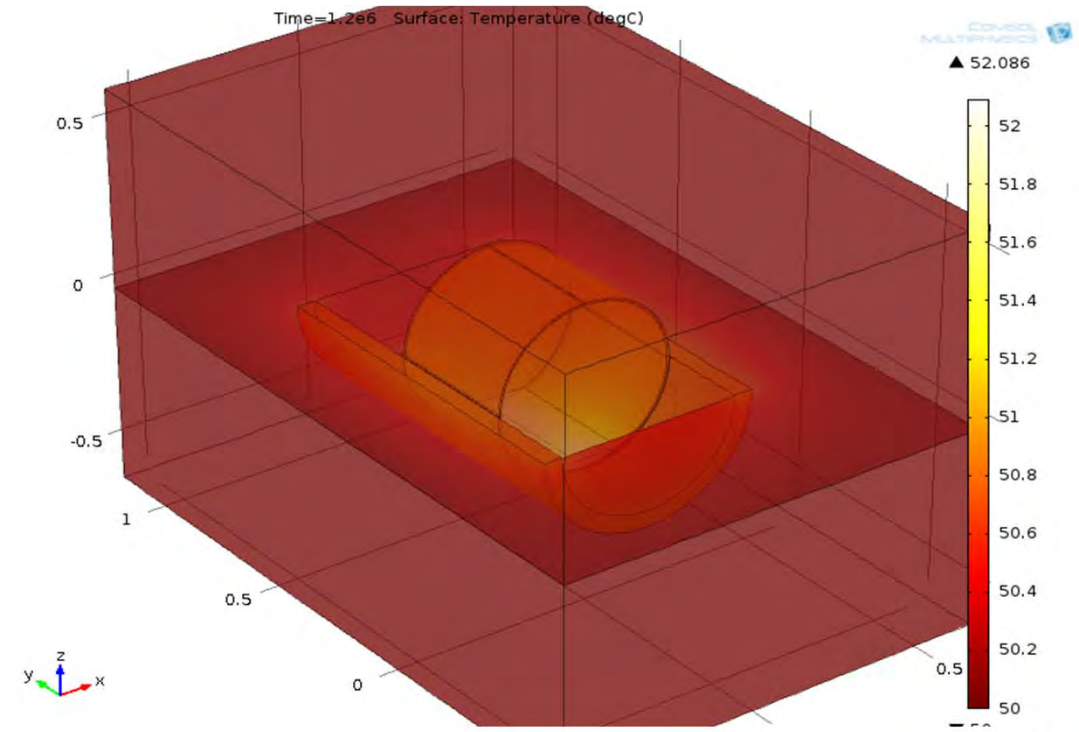

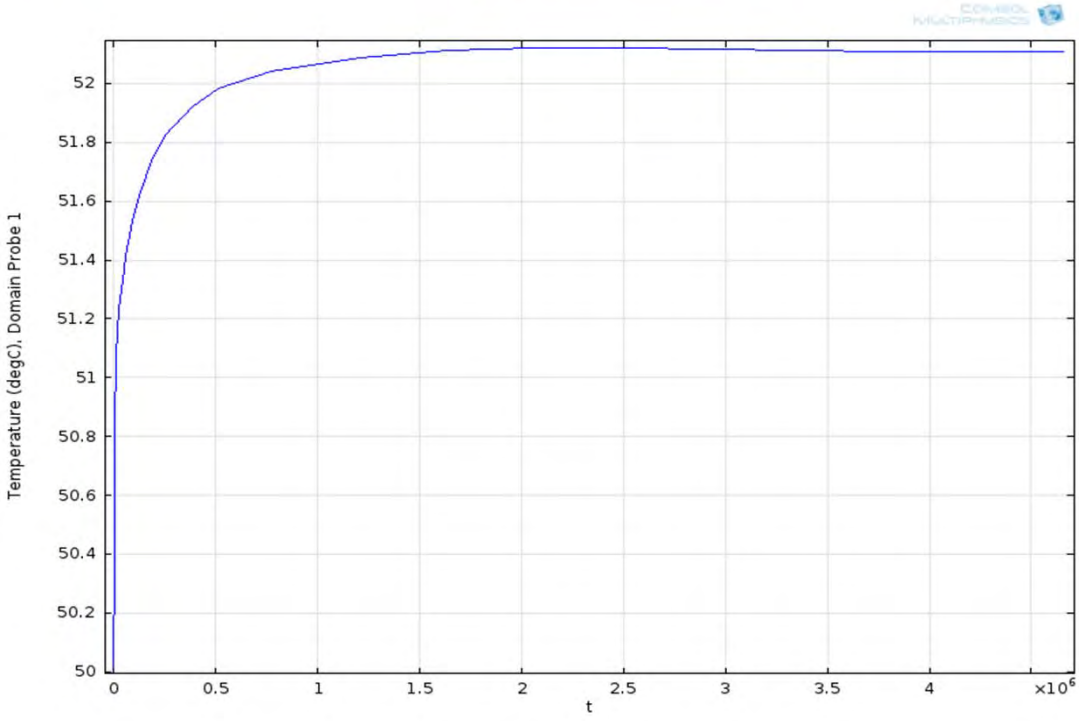

1/8 inch paste thickness
2 inch cradle thickness
3X Uranium rate: is stable

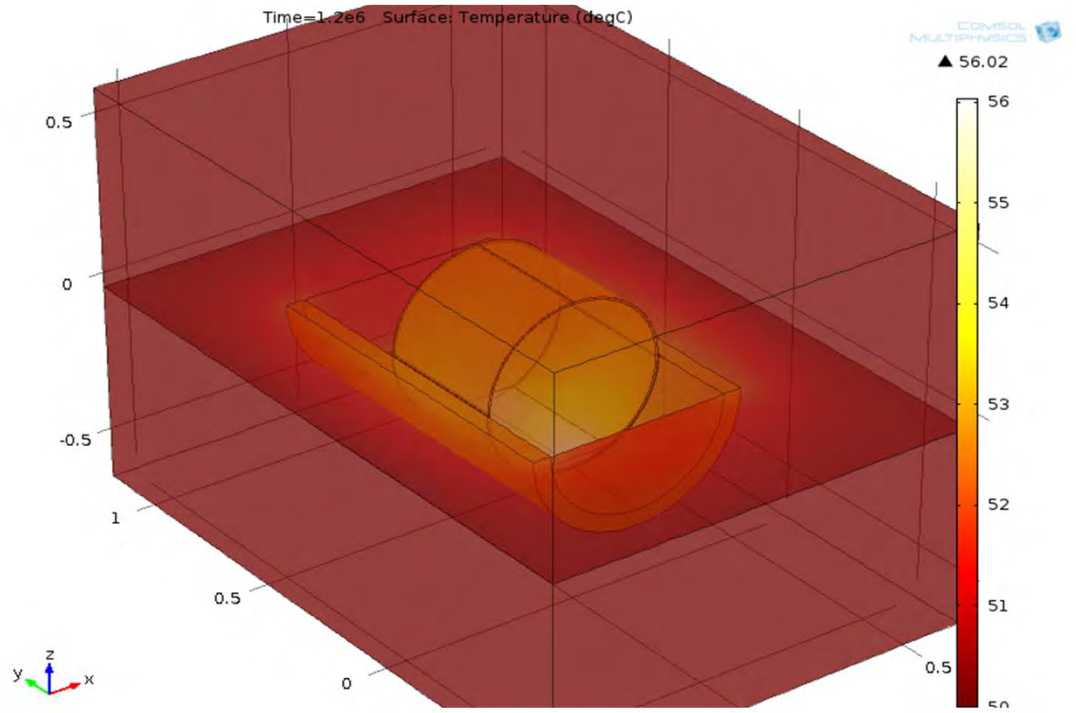

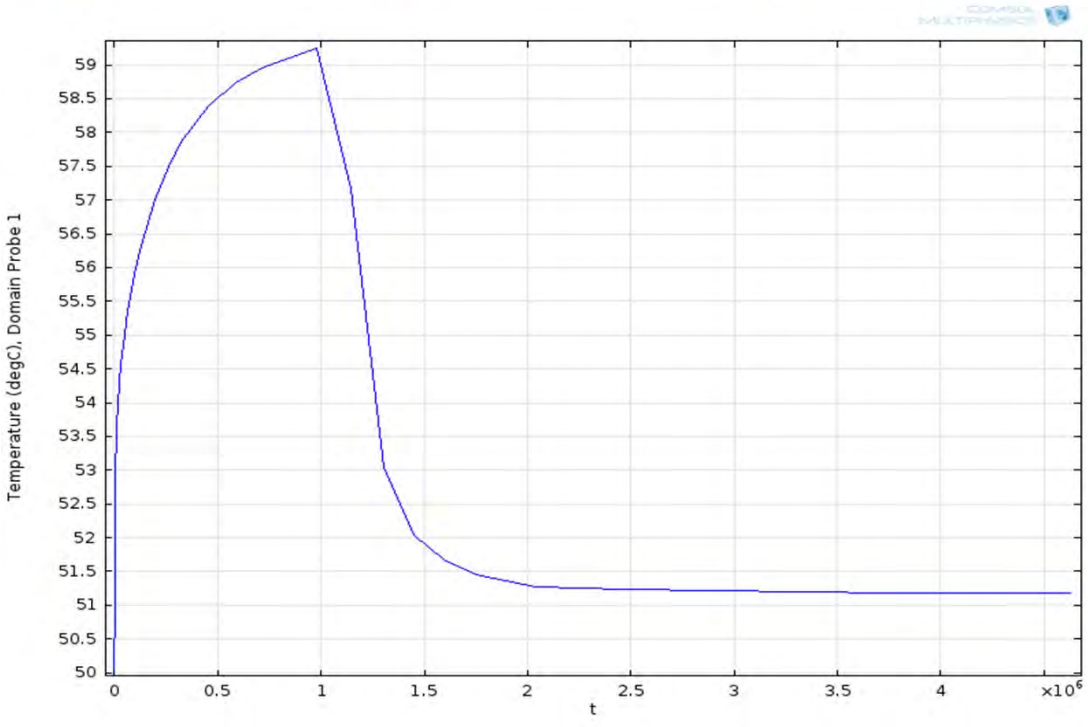

1/8 inch paste thickness
1 inch cradle thickness
1X Uranium rate: is stable

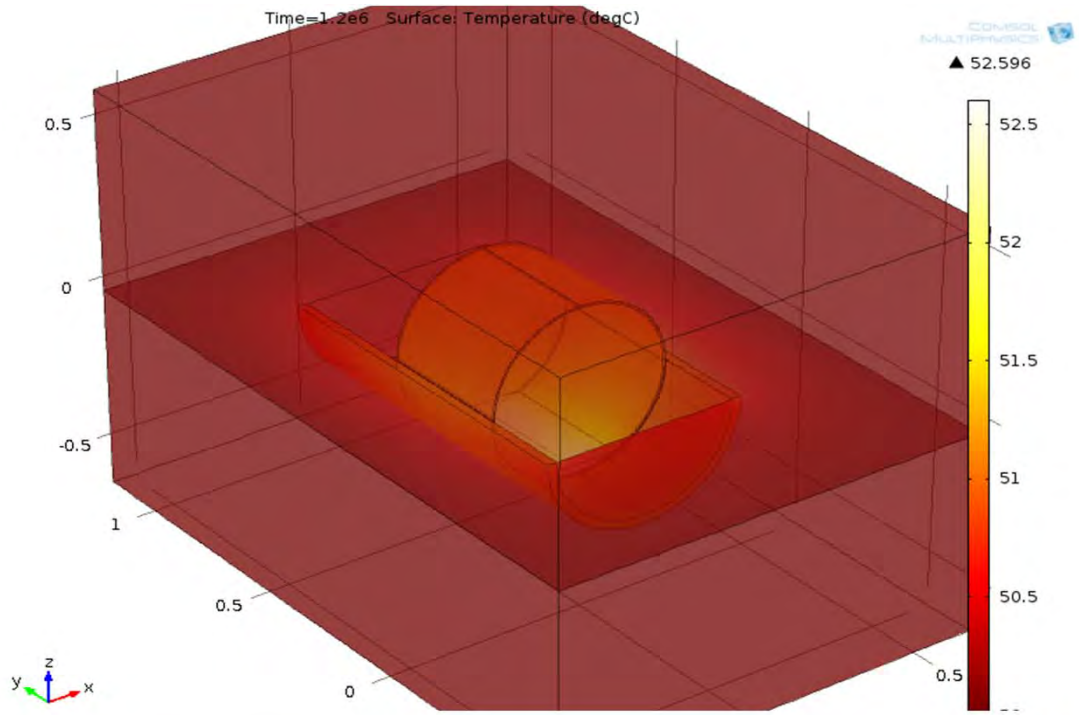

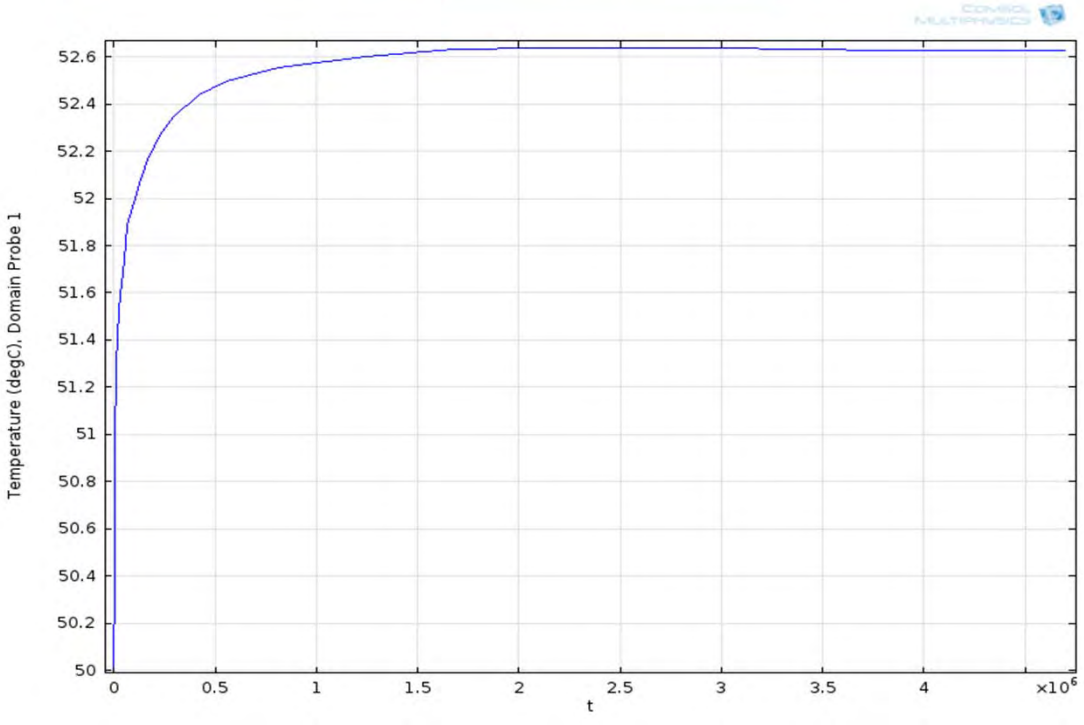

1/8 inch paste thickness
1 inch cradle thickness
3X Uranium rate: is stable

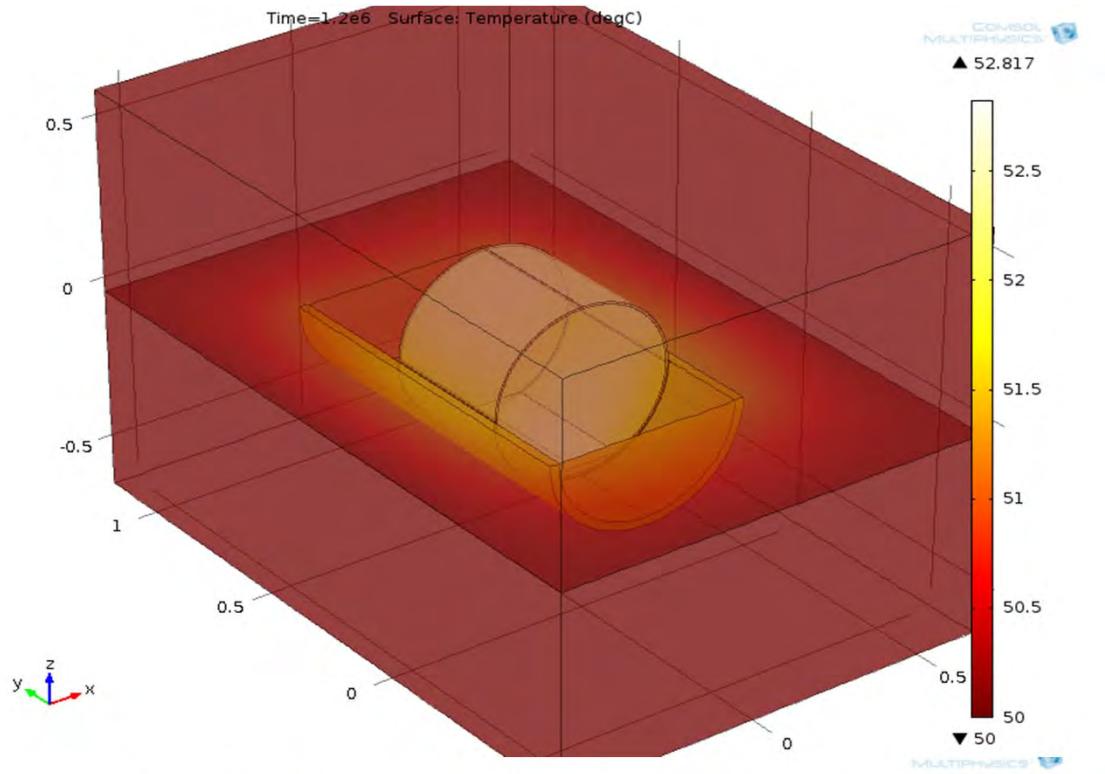

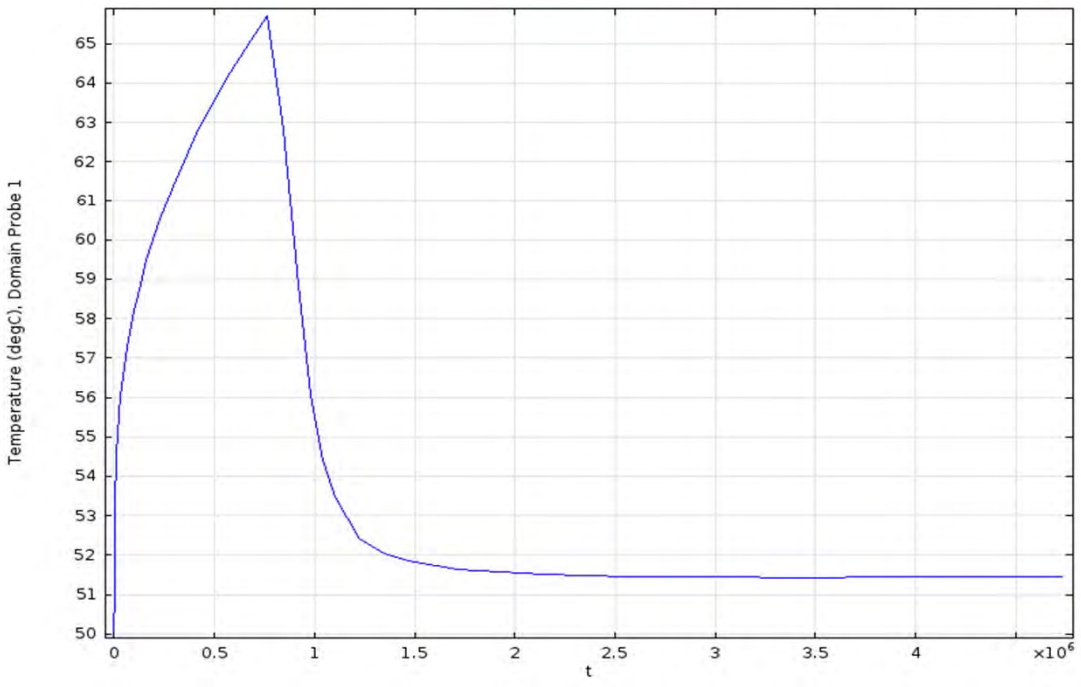

1/8 inch paste thickness
1/2 inch cradle thickness
1X Uranium rate: is stable

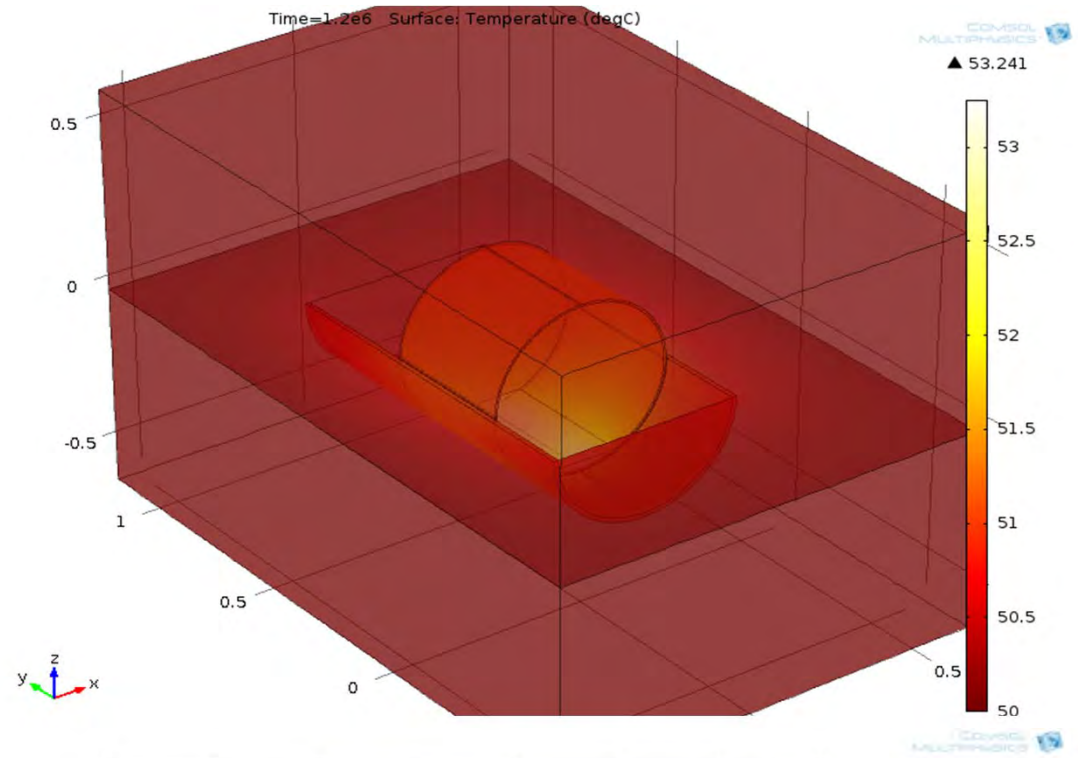

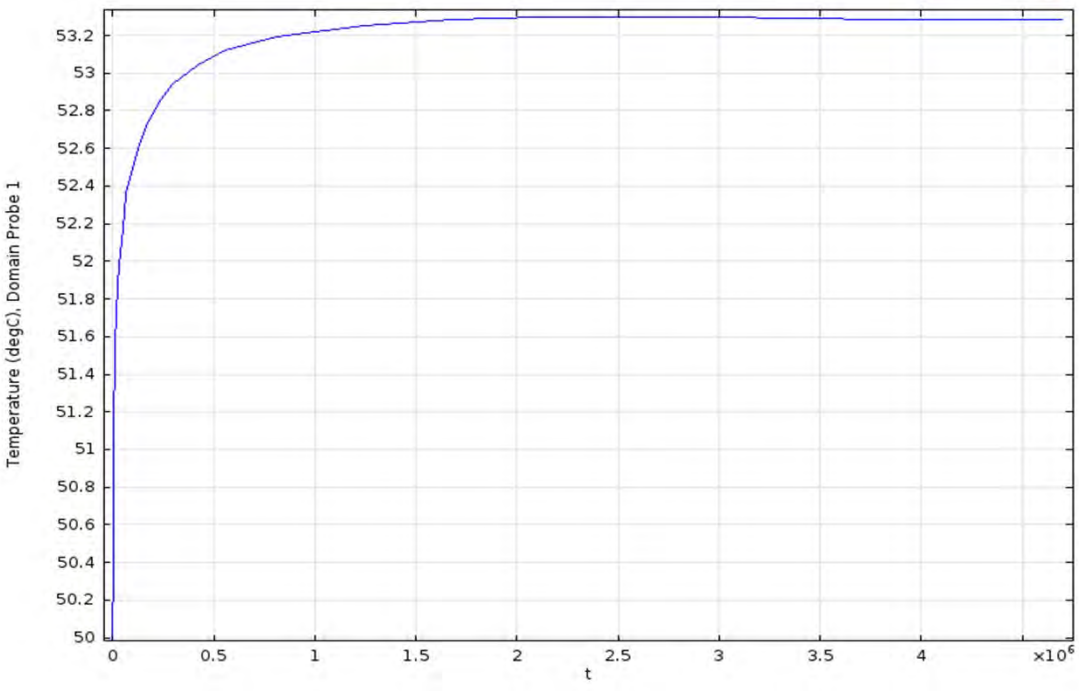

1/8 inch paste thickness
1/2 inch cradle thickness
3X Uranium rate: is unstable

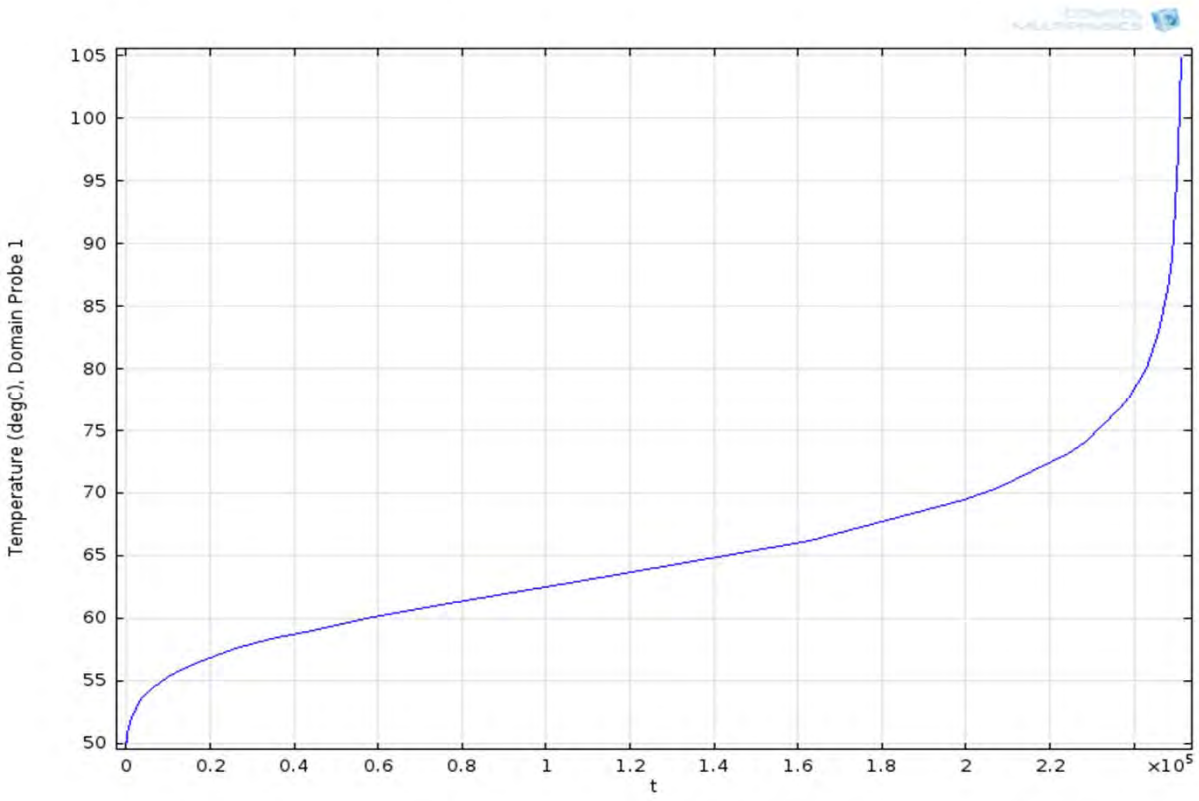

1/8 inch paste thickness
1/4 inch cradle thickness
1X Uranium rate: is stable

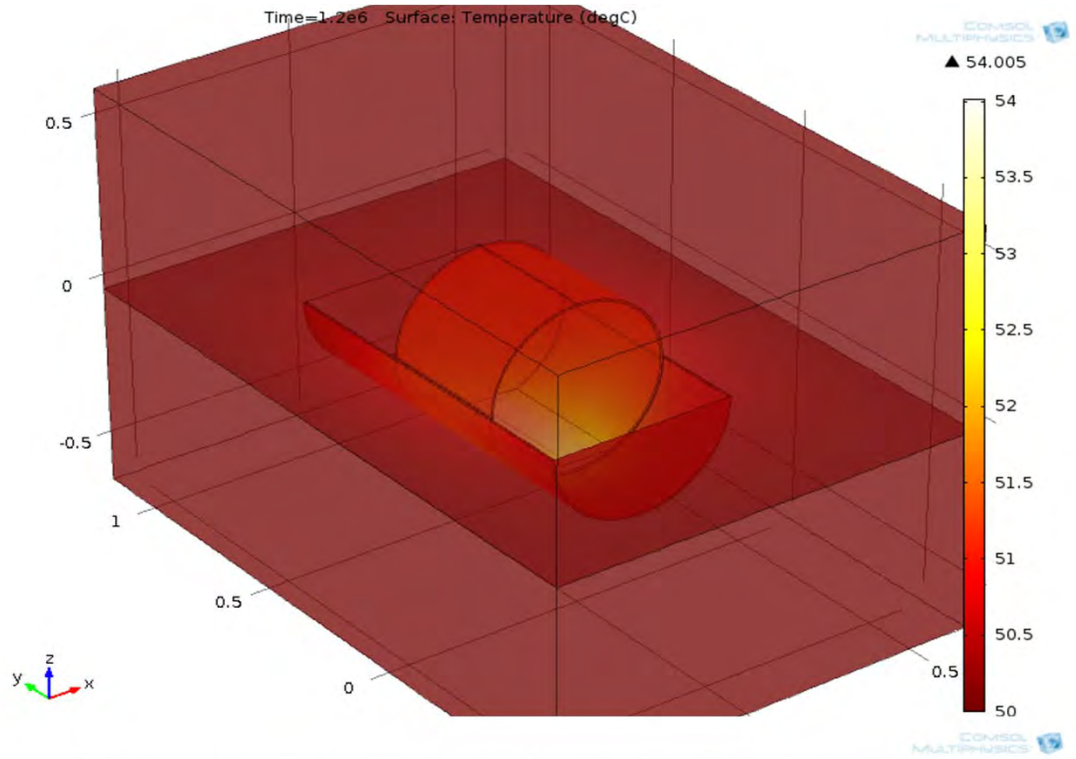

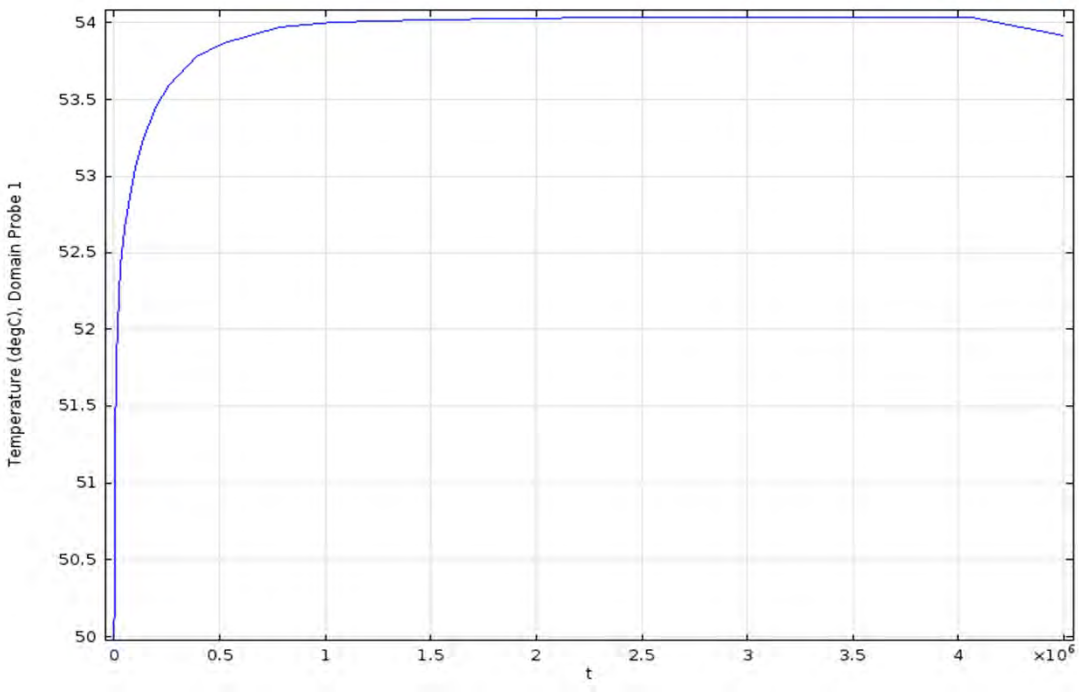

Normal Uranium heating
starting at 50C is stable
dry sand 0.14 W/mK grout the tube cradle is sunk into is at 1 W/mK
cradle walls 1/2 inches 1/8 inch gap
air in gap at a conductivity at 0.0299 W/mK

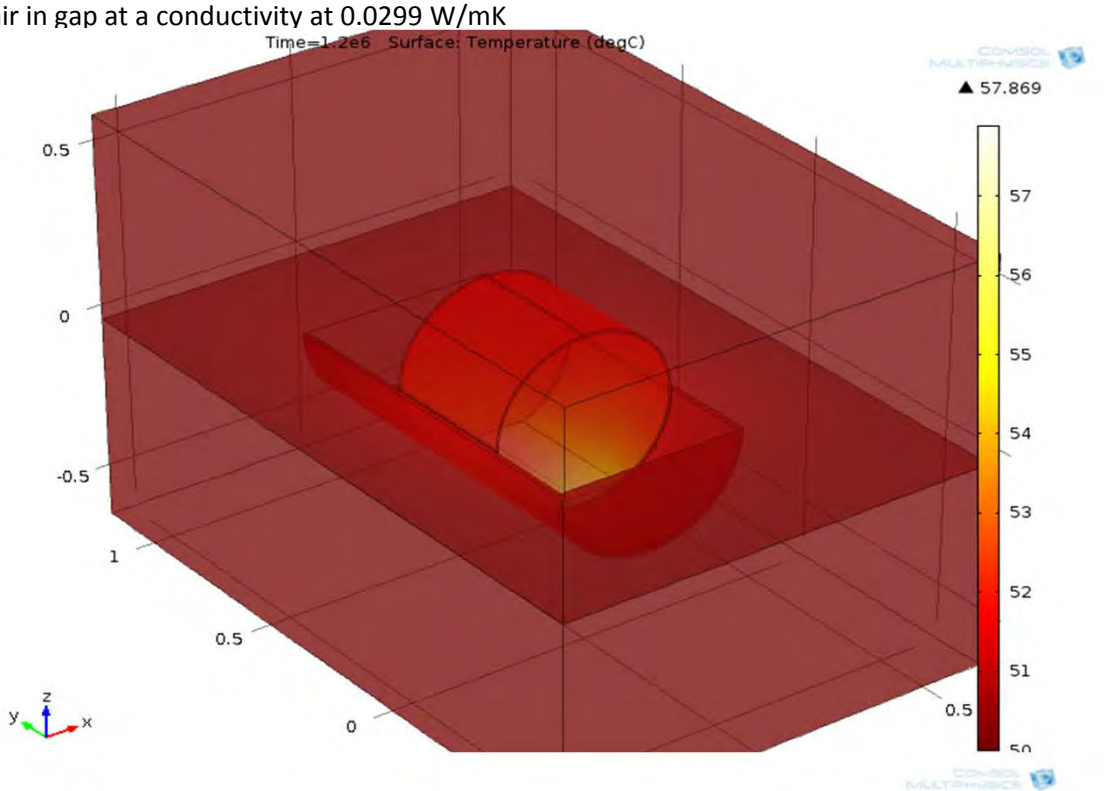

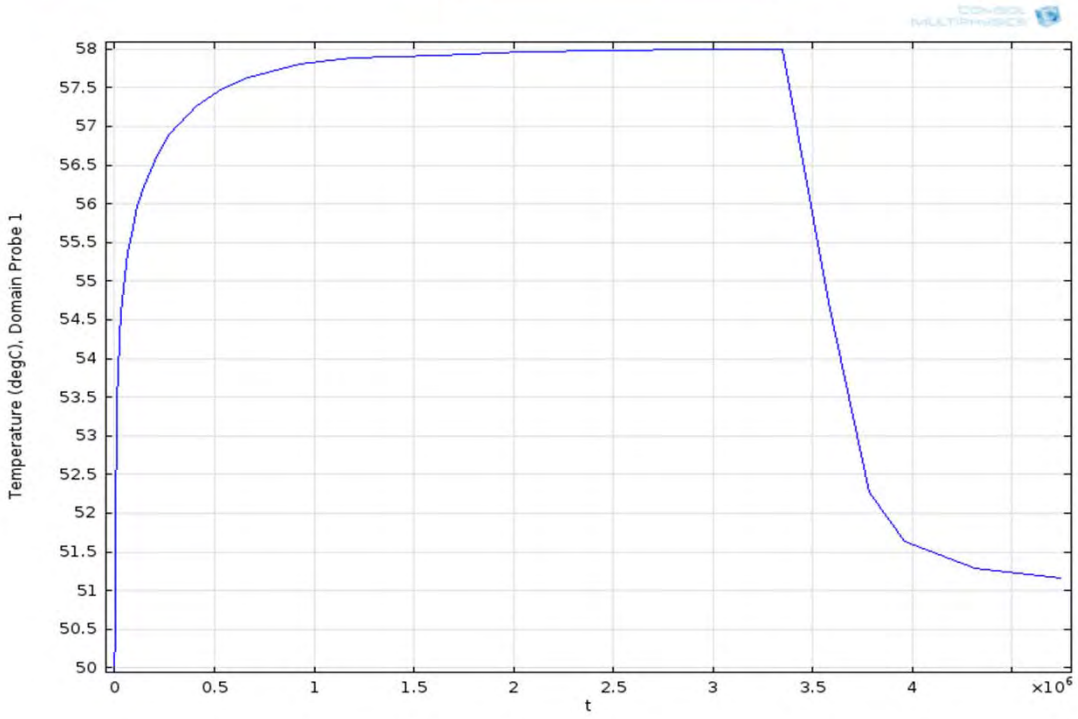

Normal Uranium heating 3X Uranium heating unstable

starting at 50C is stable

dry sand 0.14 W/mK grout the tube cradle is sunk into is at 1 W/mK

cradle walls 1/2 inches 1/16 inch gap

air in gap at a conductivity at 0.0299 W/mK

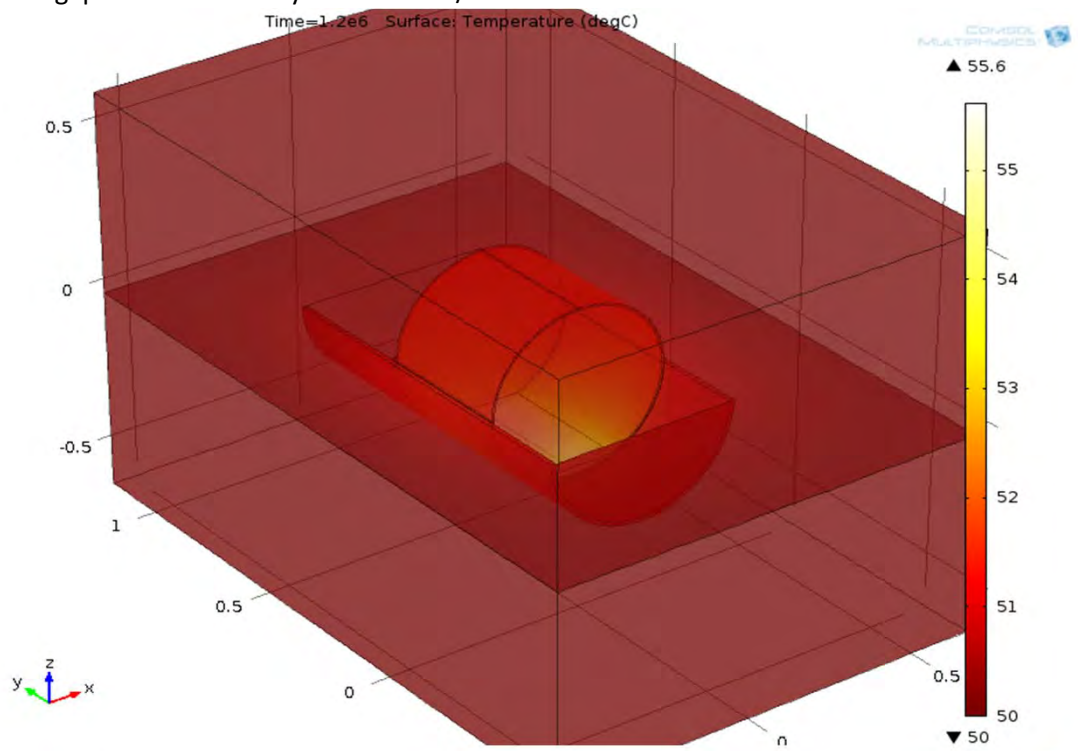

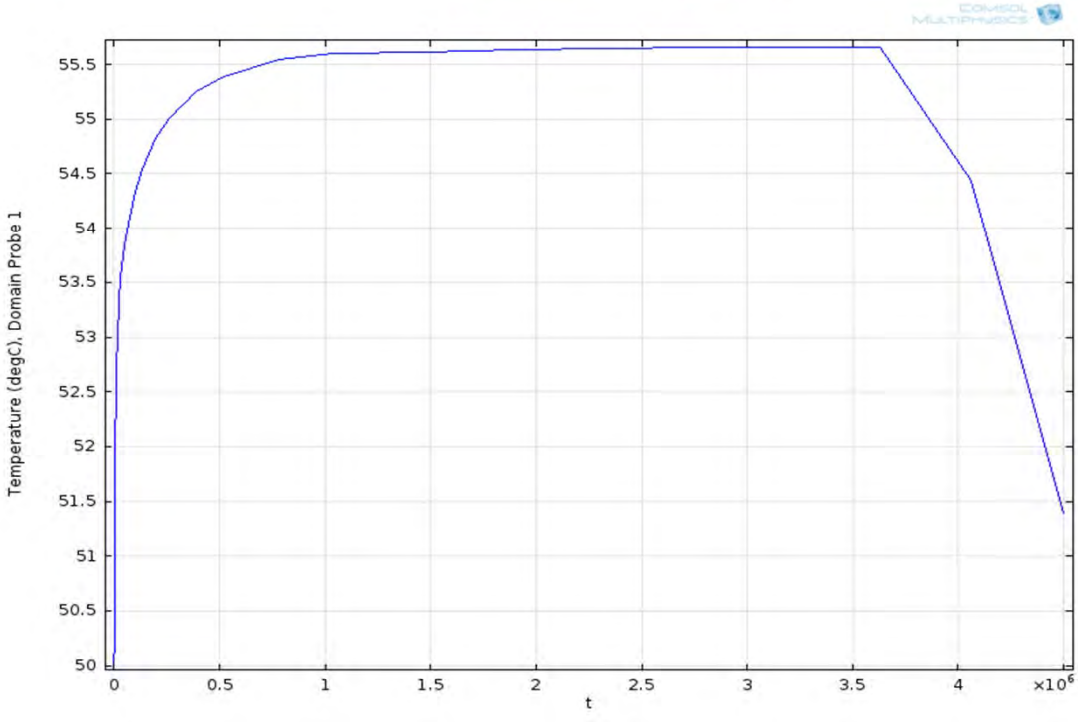

other parameters for the paste are found under base case report

air parameters

Parameters

Name	Expression	Description
radius	0.254	m
wall	6.35E-03	m
depth	0.0223	m
Twall	273.15 + 50	K
ksludge	3.9	[W/(m*K)]
rhosludge	9.60E+03	[kg/m^3]
Cpsludge	290	[J/(kg*K)]
kwall	16.2	[W/(m*K)]
rhowall	8.03E+03	[kg/m^3]
Cpwall	5.00E+02	[J/(kg*K)]
kgrout	0.5	[W/(m*K)]
rhogrout	1.72E+03	[kg/m^3]
Cpgrout	1165	[J/(kg*K)]
tubeLength	0.381	m
BoxWidth	1.219	m
BoxDepth	1.219	m
BoxHeight	1.829	m
ksand	0.5 - .36	[W/(m*K)]
rhosand	1.90E+03	[kg/m^3]
Cpsand	1400	[J/(kg*K)]
qsun	990.541	W/m^2
Tex	Twall[K]	
heattransferco	7.9[W/(m^2*K)]	W/m^2K
heat	2.15E+06	J/kg maximum heat generated by uranium
kshot	30	[W/(m*K)]
rhoshot	rhowall	[kg/m^3]
Cpshot	Cpwall	[J/(kg*K)]
Gap	6.35E-3/4	m
kpaste	0.0299	[W/(m*K)]
rhopaste	1	[kg/m^3]
Cppaste	1009	[J/(kg*K)]
subtract	-0.1	
tubethick	.102/8	
tubedist	1.219 - .219	
kpHighTCgrout	1	[W/(m*K)]
rhoHighTCgrou	2.62E+03	[kg/m^3]
CpHighTCgrout	Cpgrout	[J/(kg*K)]

dry sand k =0.13 W/mK
paste k = 1 W/mK
cut off at 2.145E6 J/kg
1/4 inch paste thickness
2 inch cradle thickness
3X Uranium rate: stable

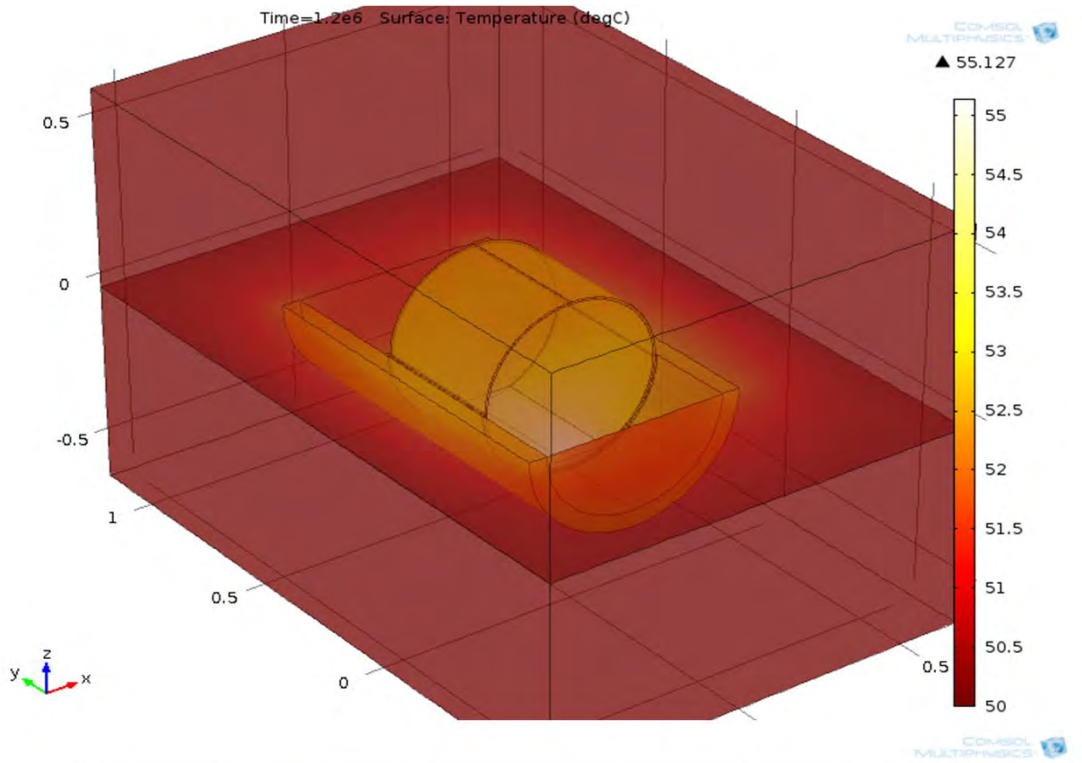

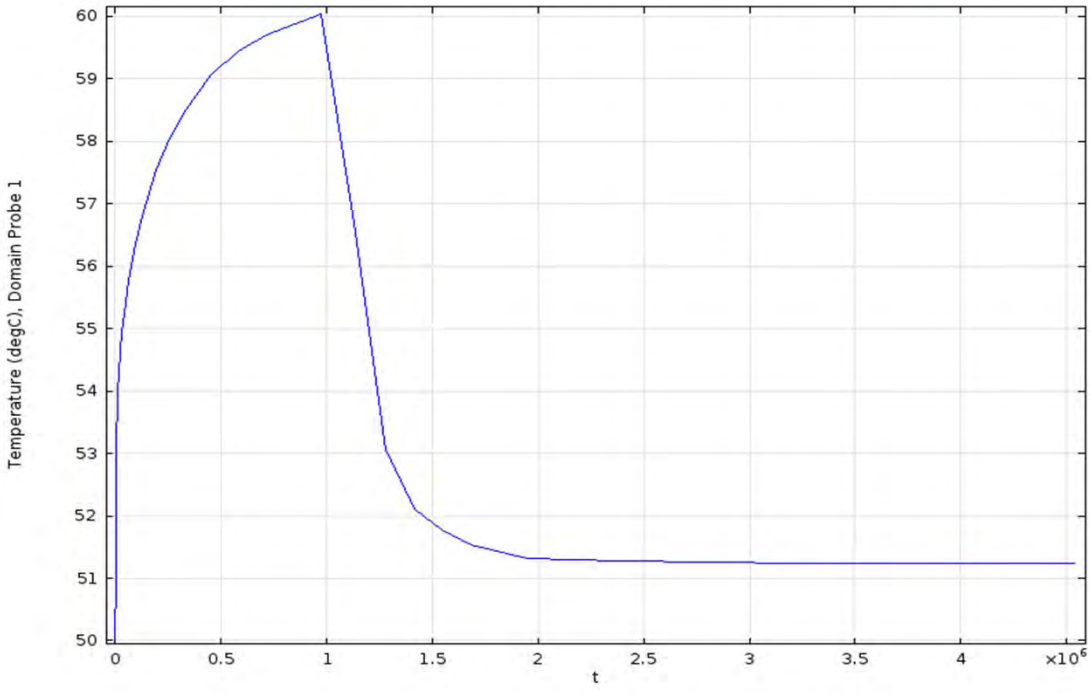

dry sand k =0.13 W/mK
paste k = 1.5 W/mK
cut off at 2.145E6 J/kg
1/4 inch paste thickness
2 inch cradle thickness
3X Uranium rate: stable

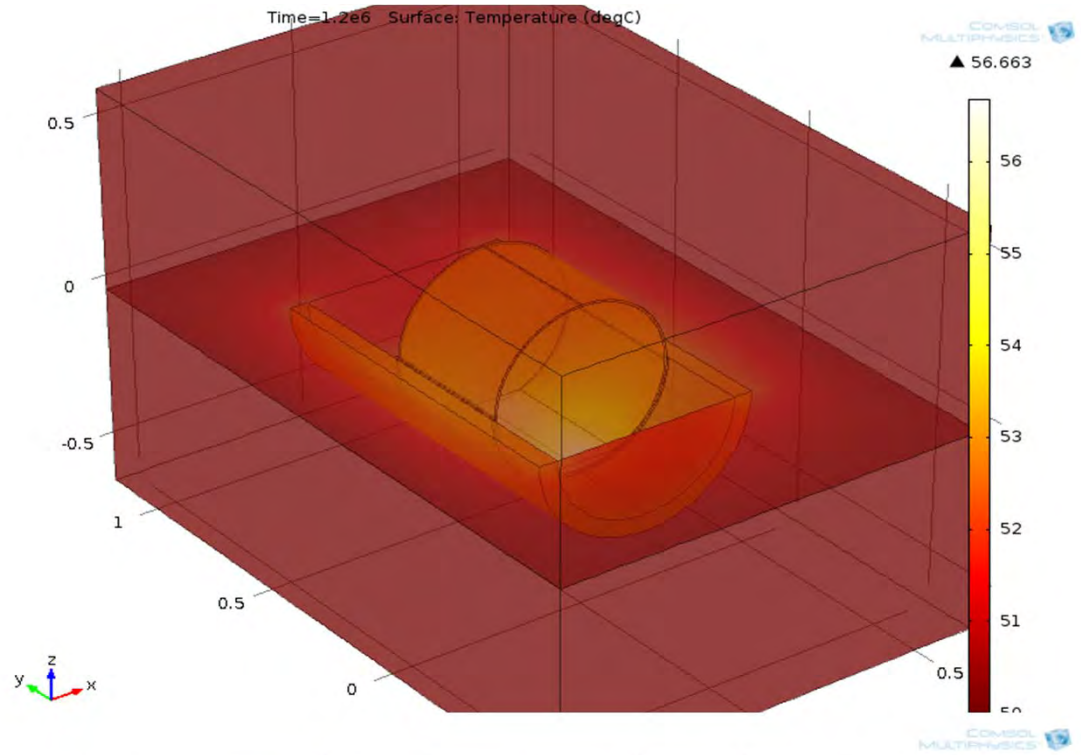

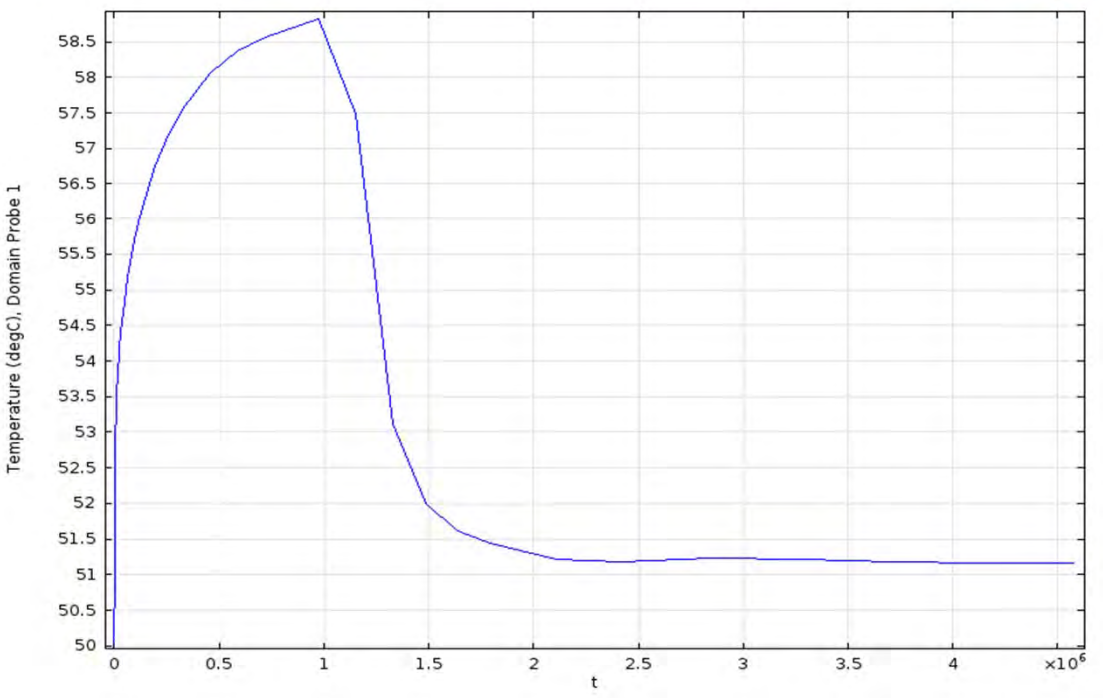

dry sand k =0.13 W/mK
paste k = 2 W/mK
cut off at 2.145E6 J/kg
1/4 inch paste thickness
2 inch cradle thickness
3X Uranium rate: stable

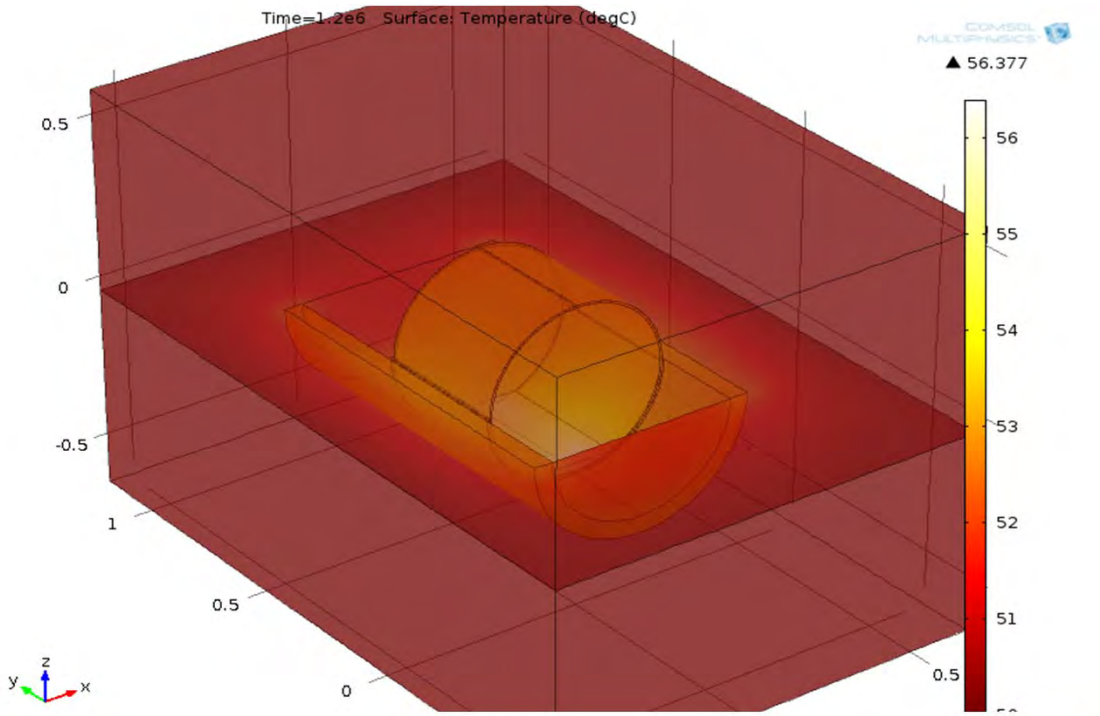

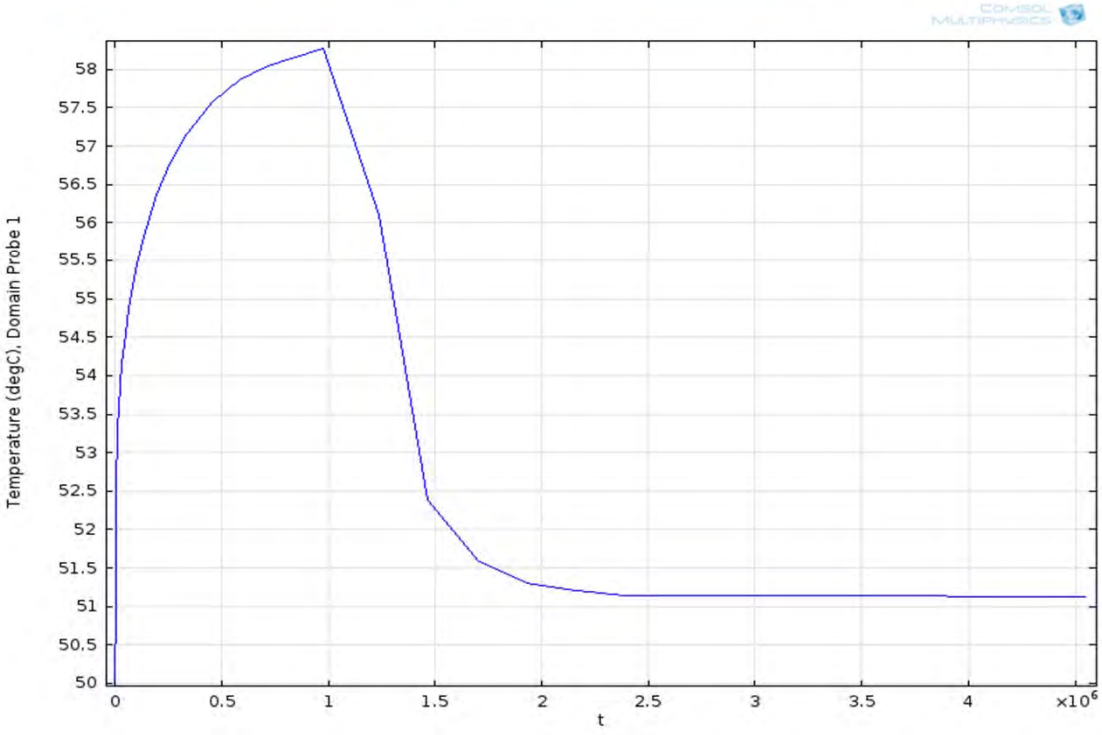

dry sand k =0.13 W/mK
paste k = 0.67 W/mK
cut off at 2.145E6 J/kg
1/4 inch paste thickness
1 inch cradle thickness
3X Uranium rate: unstable

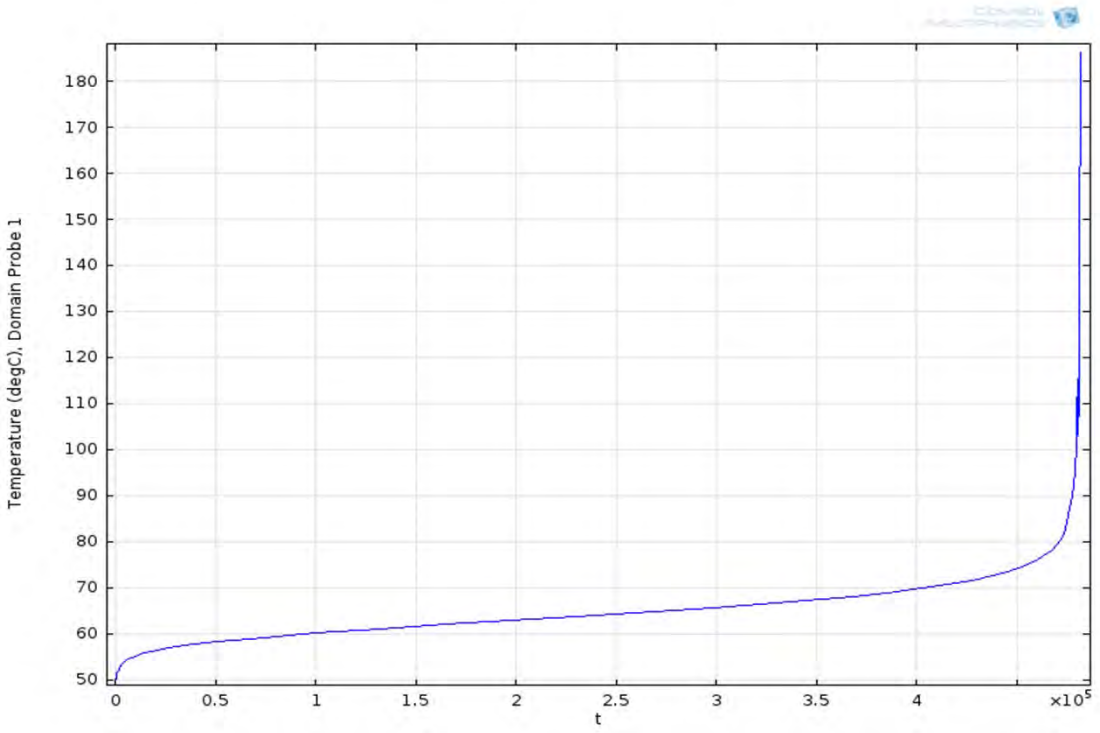

dry sand k =0.13 W/mK
paste k = 1.0 W/mK
cut off at 2.145E6 J/kg
1/4 inch paste thickness
1 inch cradle thickness
3X Uranium rate: stable

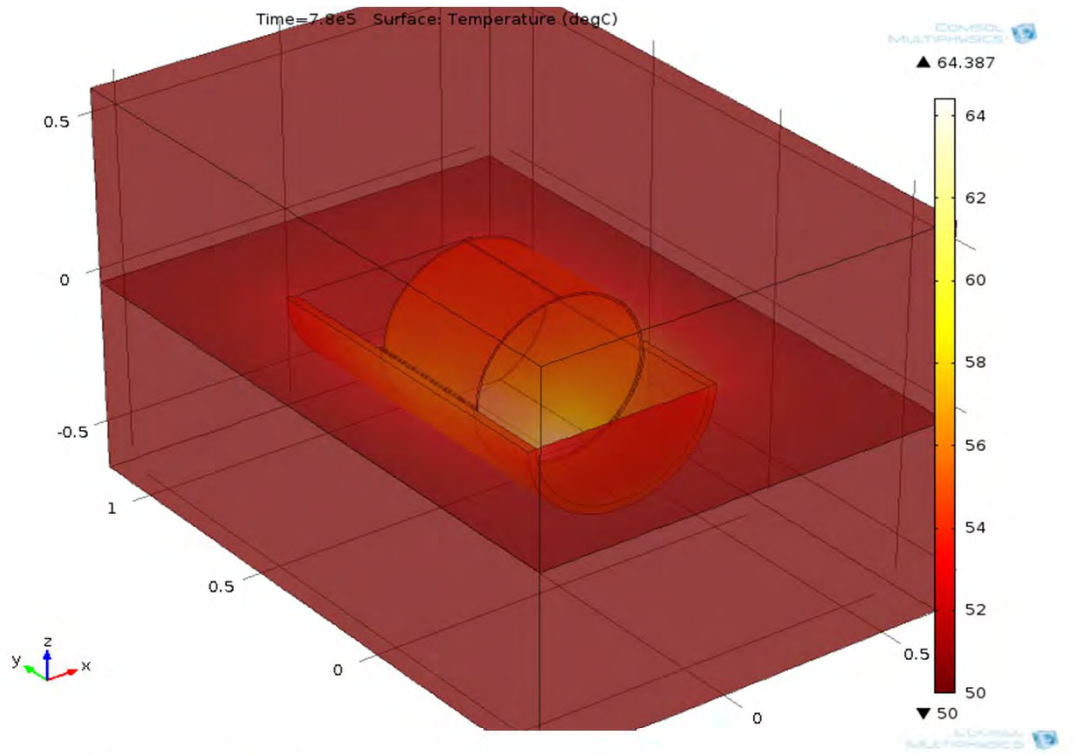

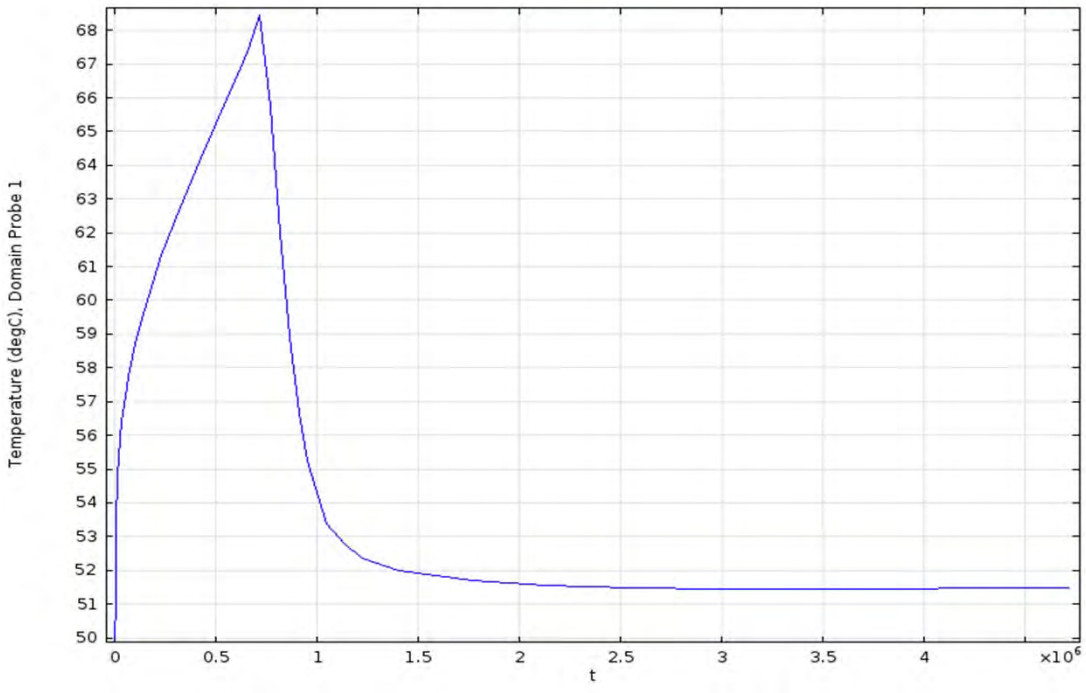

dry sand k =0.13 W/mK
paste k = 1.5 W/mK
cut off at 2.145E6 J/kg
1/4 inch paste thickness
1 inch cradle thickness
3X Uranium rate

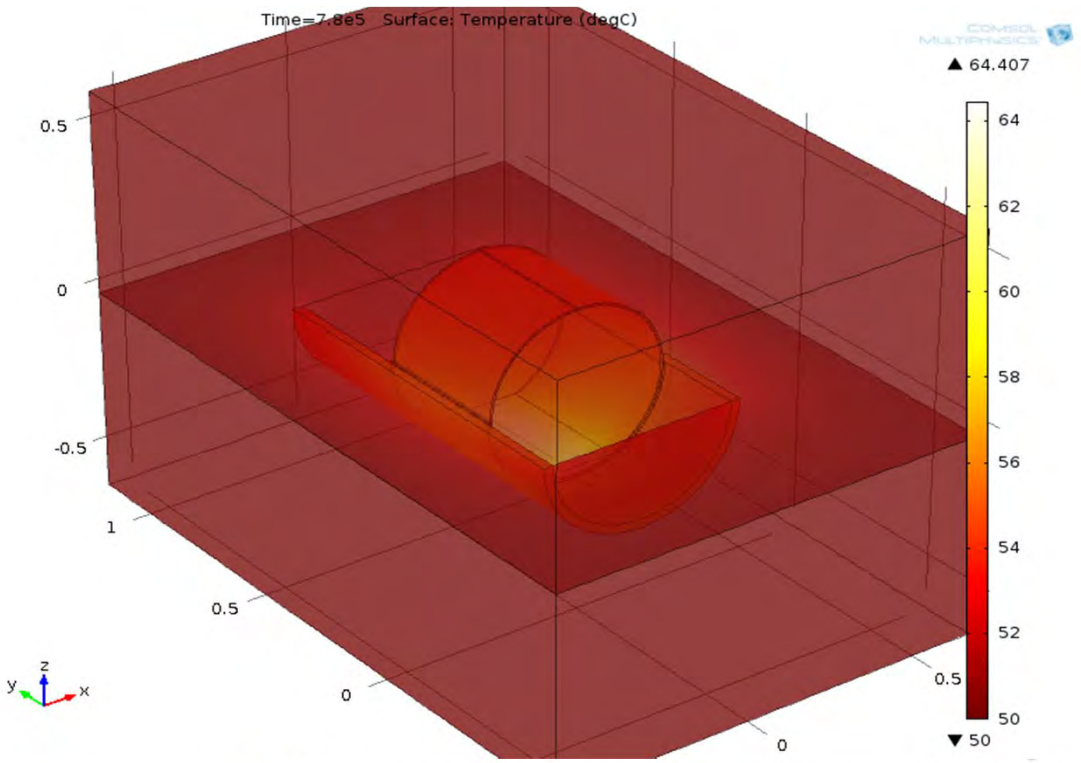

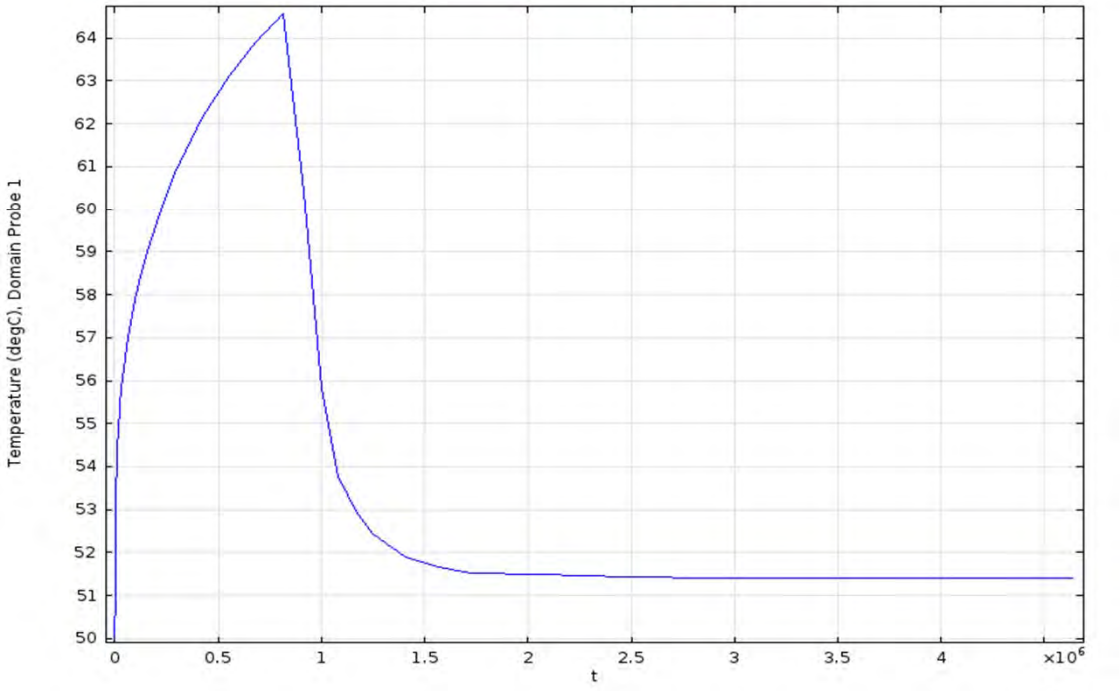

dry sand k =0.13 W/mK
paste k = 2 W/mK
cut off at 2.145E6 J/kg
1/4 inch paste thickness
1 inch cradle thickness
3X Uranium rate

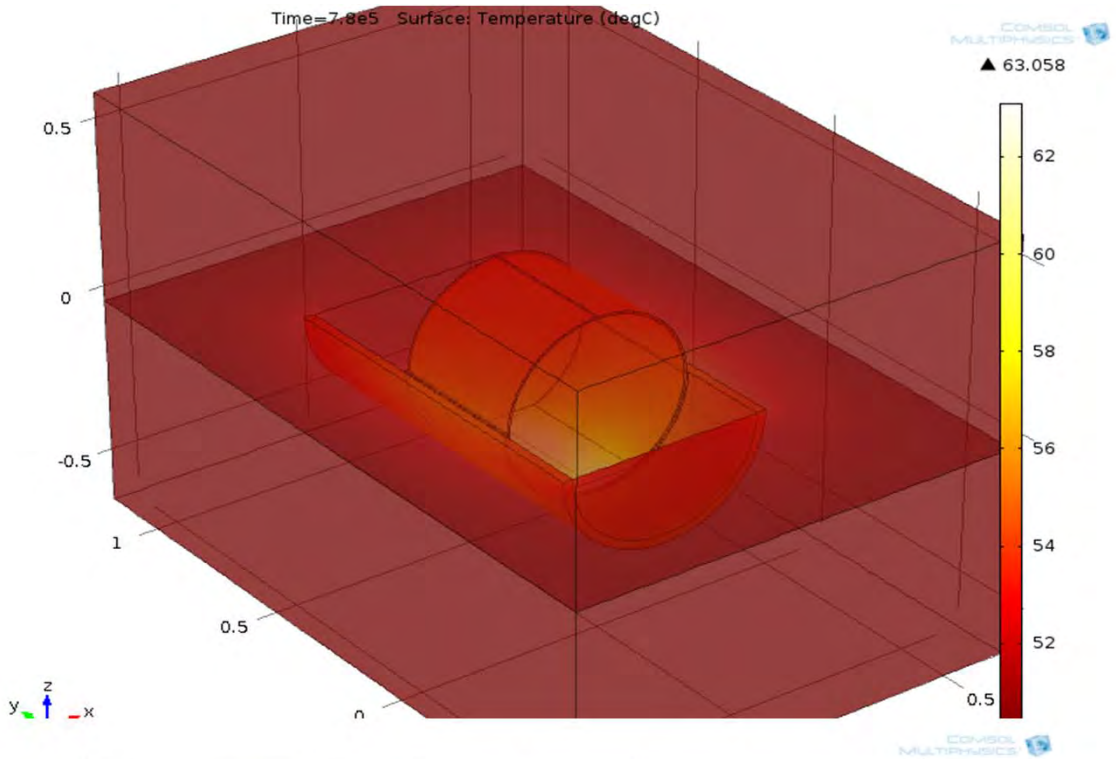

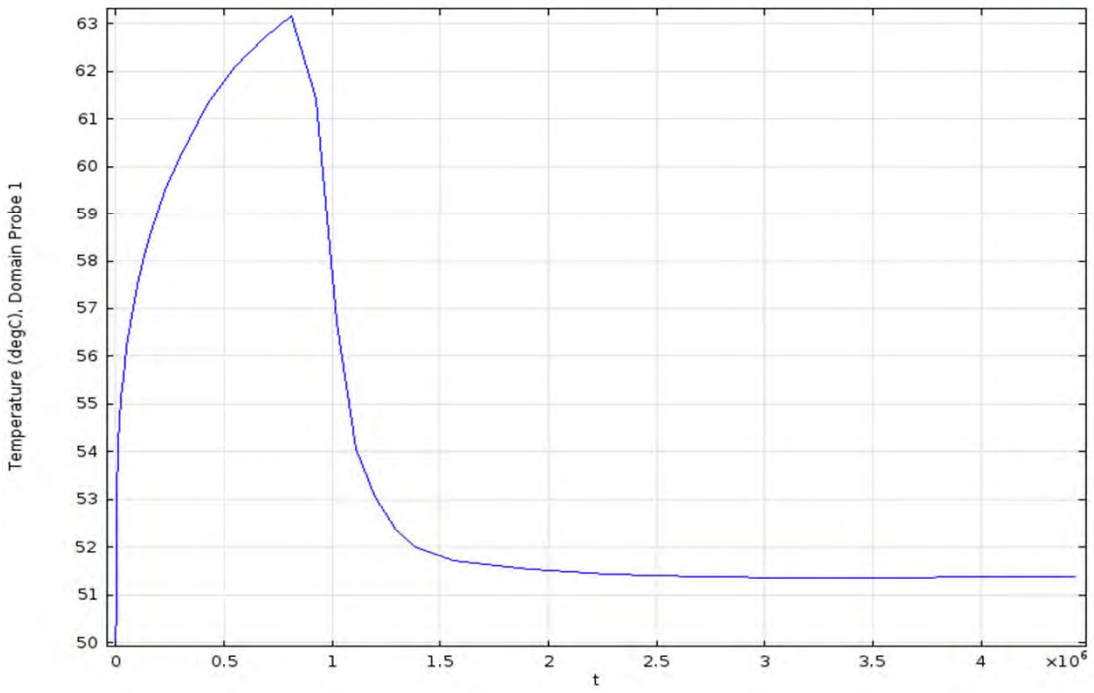

Case 8
file: K basin Box HeatSinkTube Grout in box solar3.mph
file: K basin Box HeatSinkTube Grout in box solar3.docx
dry sand k =0.13 W/mK
paste k = 0.67 W/mK
cut off at 2.145E6 J/kg
1/4 inch paste thickness
2 inch cradle thickness
1X Uranium rate: is stable

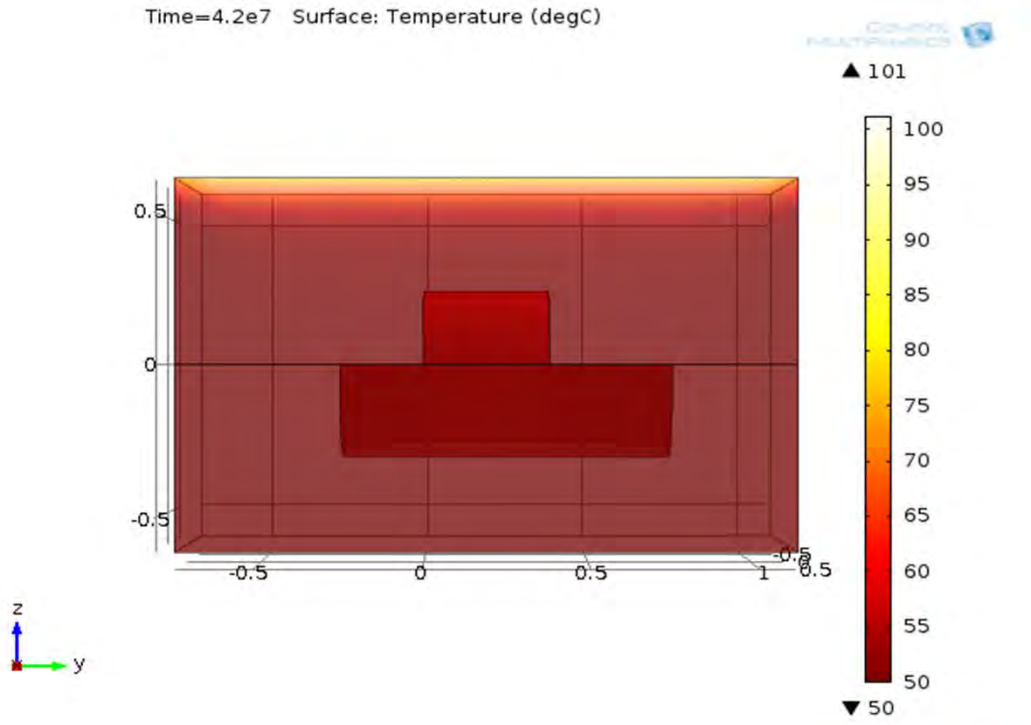

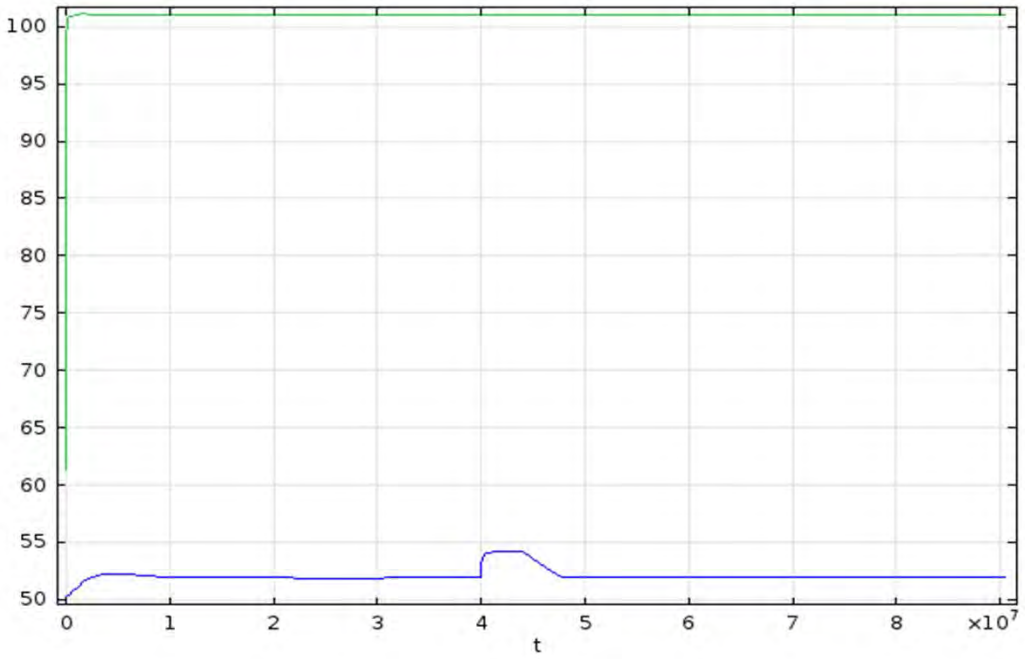

Before uranium sludge temperature dependent heating is turned on

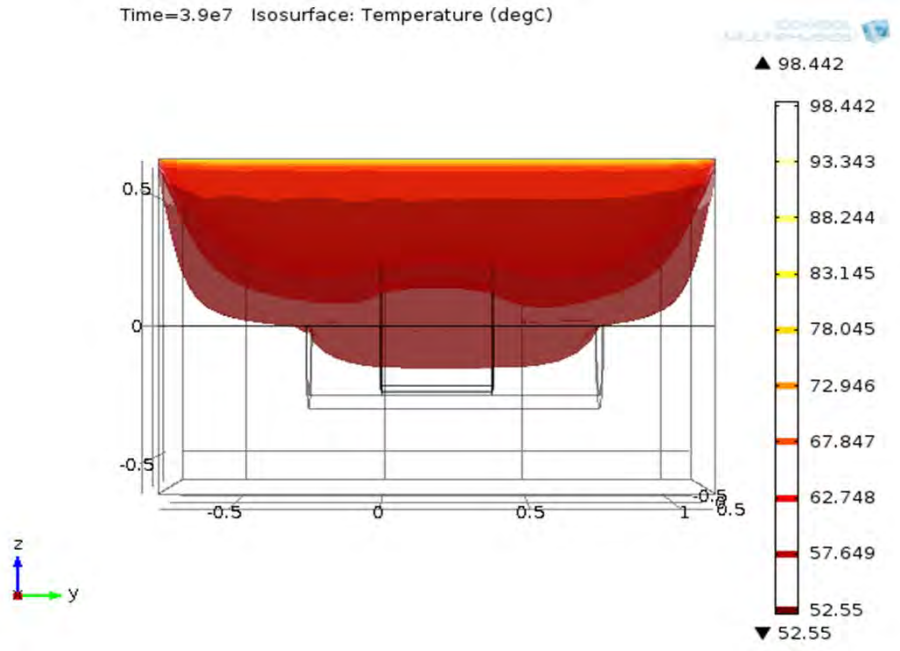

after uranium sludge temperature dependent heating is turned on

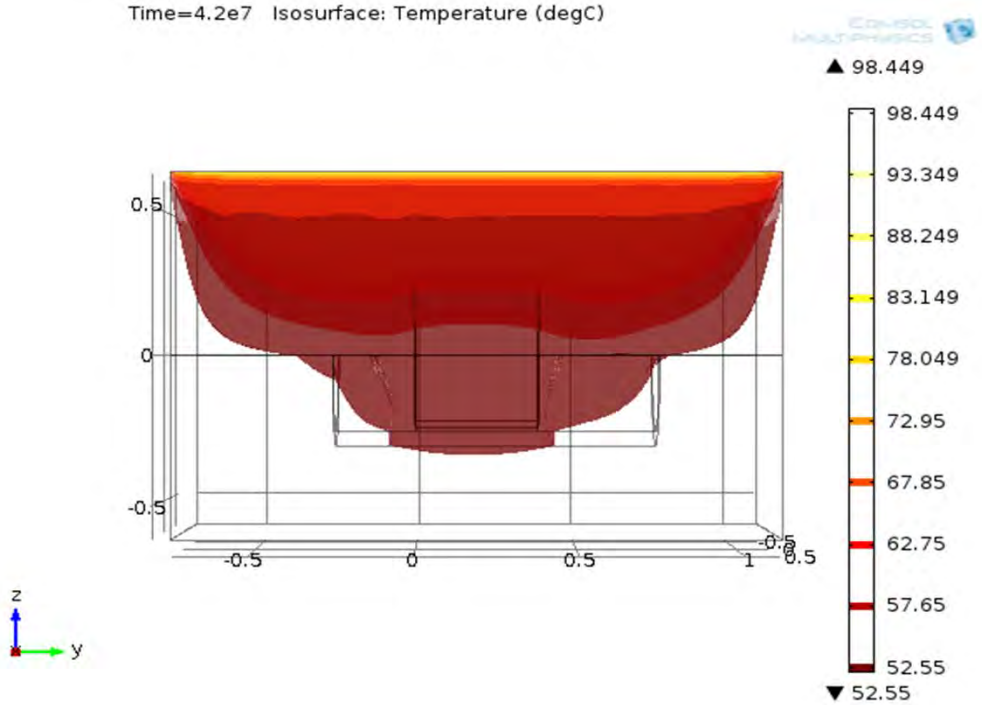

1/4 inch paste thickness
2 inch cradle thickness
3X Uranium rate: is stable

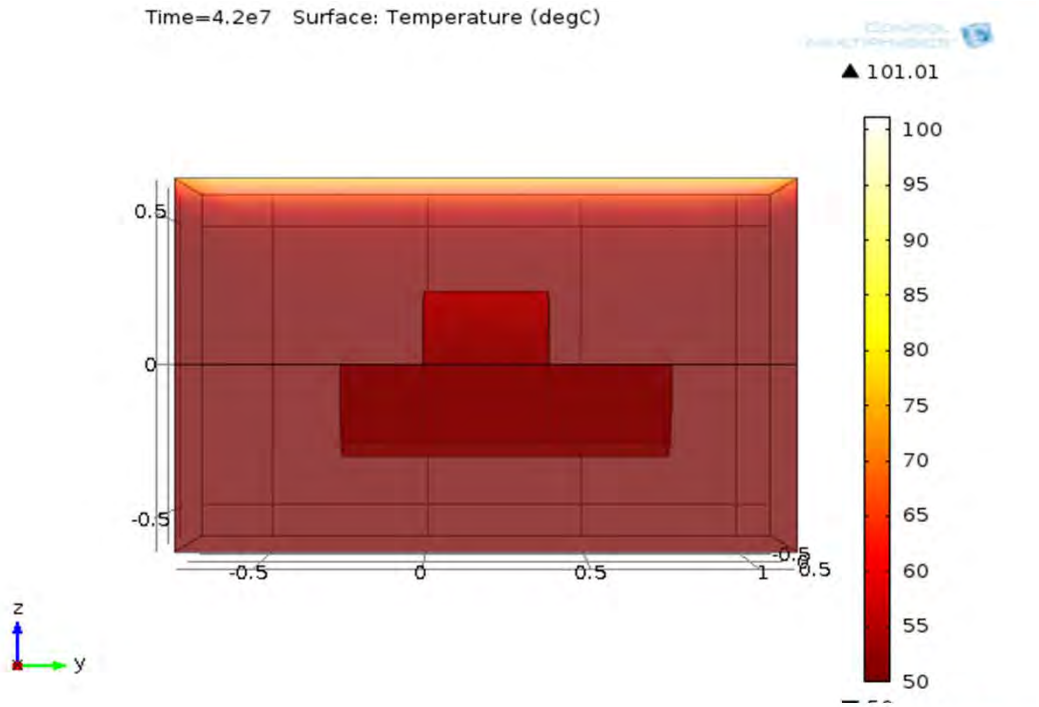

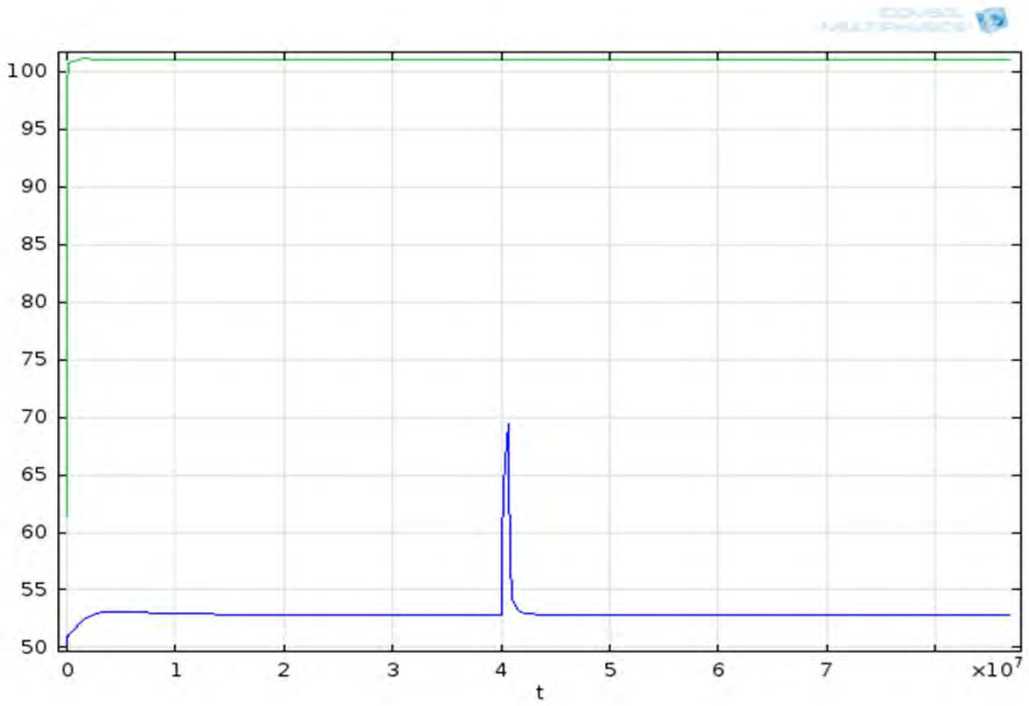

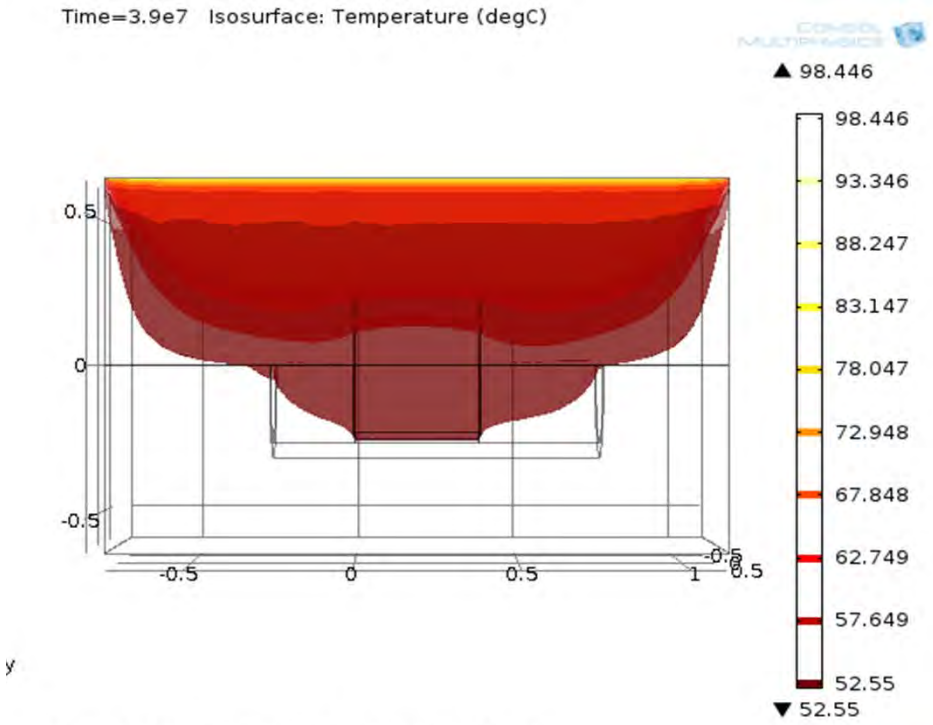
Time=3.9e7 Isosurface: Temperature (degC)
▲ 98.446
98.446
93.346
88.247
83.147
78.047
72.948
67.848
62.749
57.649
52.55
▼ 52.55
0.5
0
-0.5
-0.5
0
0.5
1
-0.5
0.5

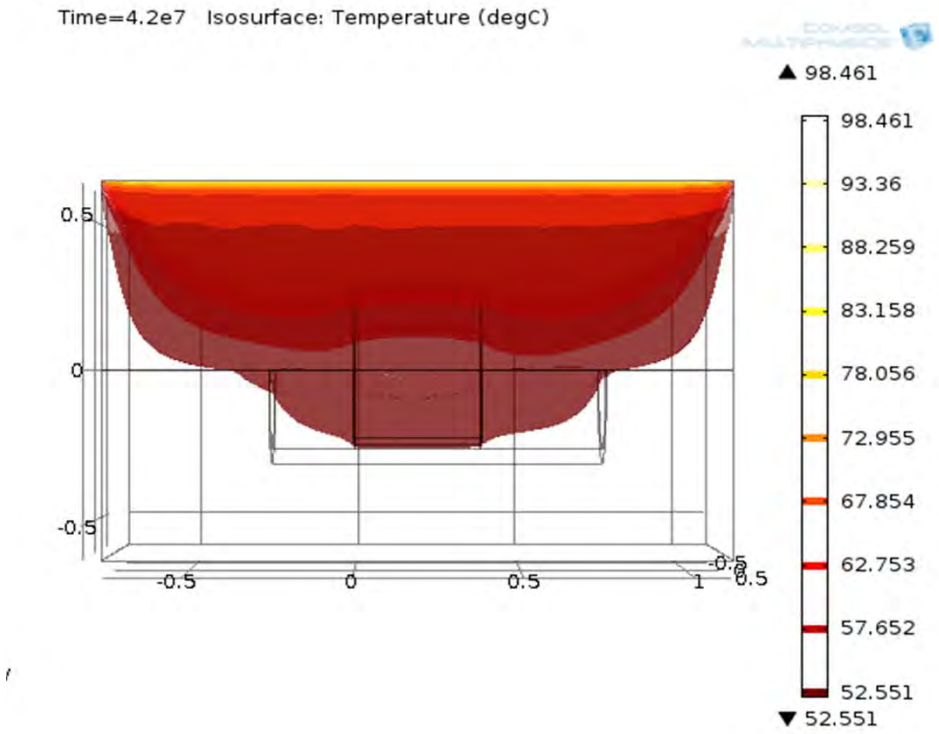
Time=4.2e7 Isosurface: Temperature (degC)
▲ 98.461
98.461
93.36
88.259
83.158
78.056
72.955
67.854
62.753
57.652
52.551
▼ 52.551
0.5
0
-0.5
-0.5
0
0.5
1
-0.5
0.5

1/4 inch paste thickness
1 inch cradle thickness
1X Uranium rate: is stable

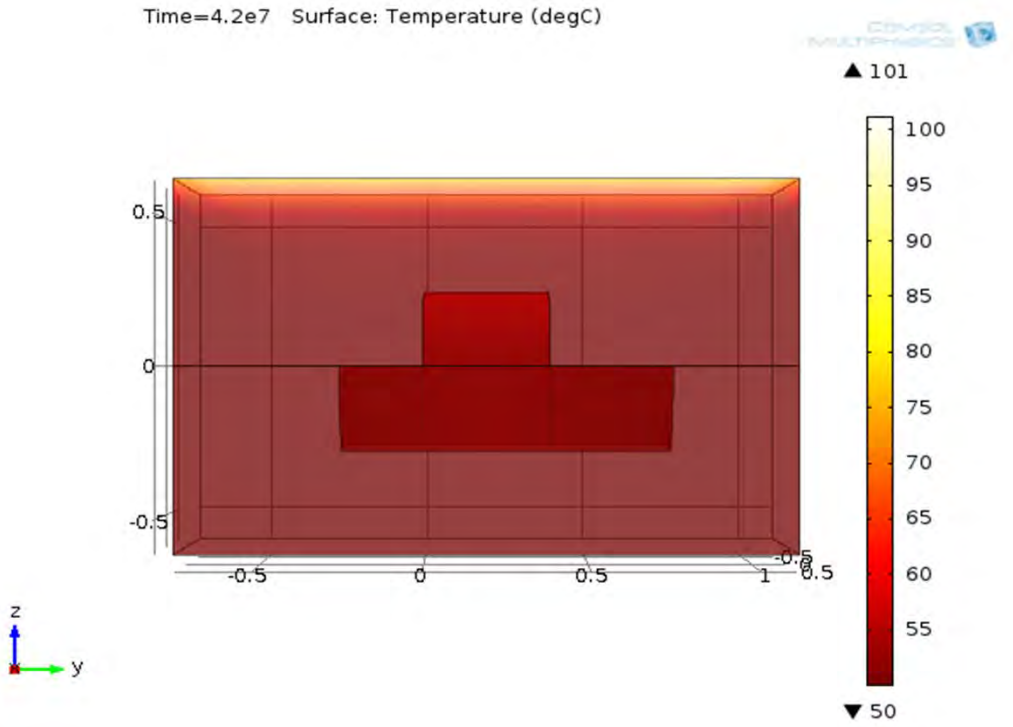

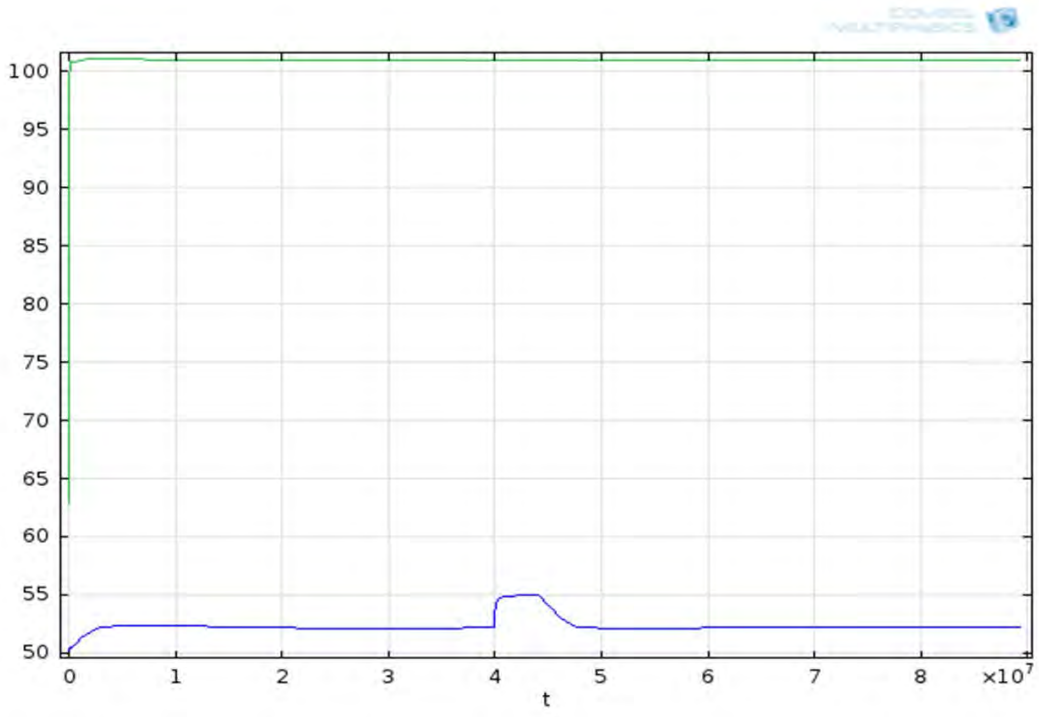

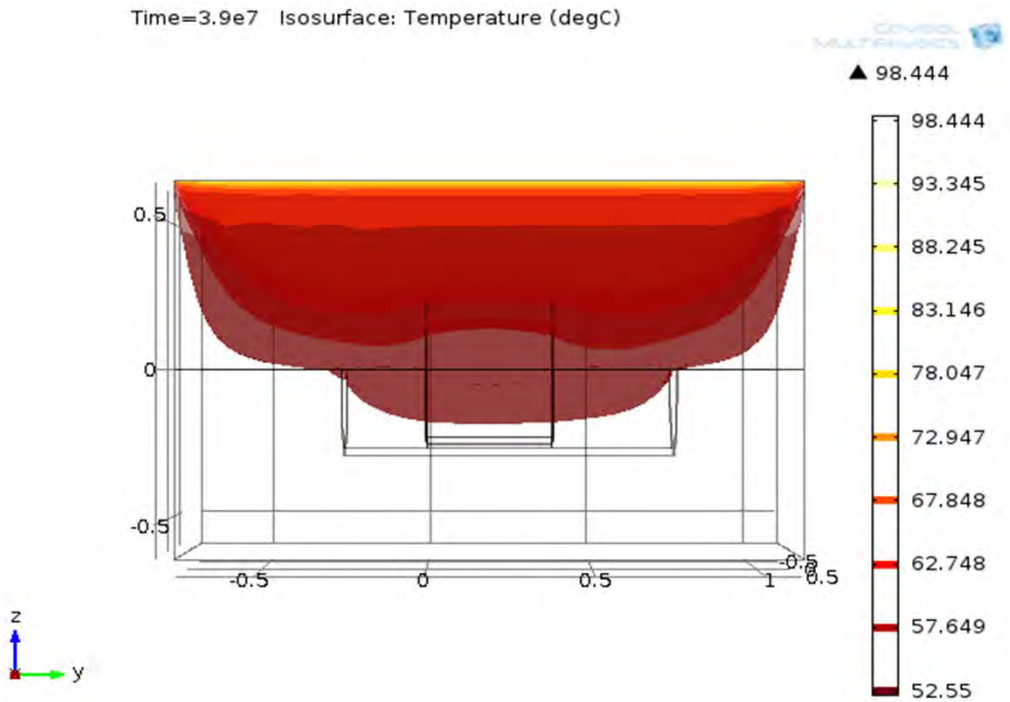
Time=3.9e7 Isosurface: Temperature (degC)
▲ 98.444
98.444
93.345
88.245
83.146
78.047
72.947
67.848
62.748
57.649
52.55
▼ 52.55
0.5
0
-0.5
-0.5
0
0.5
1
-0.5
0.5
z
y

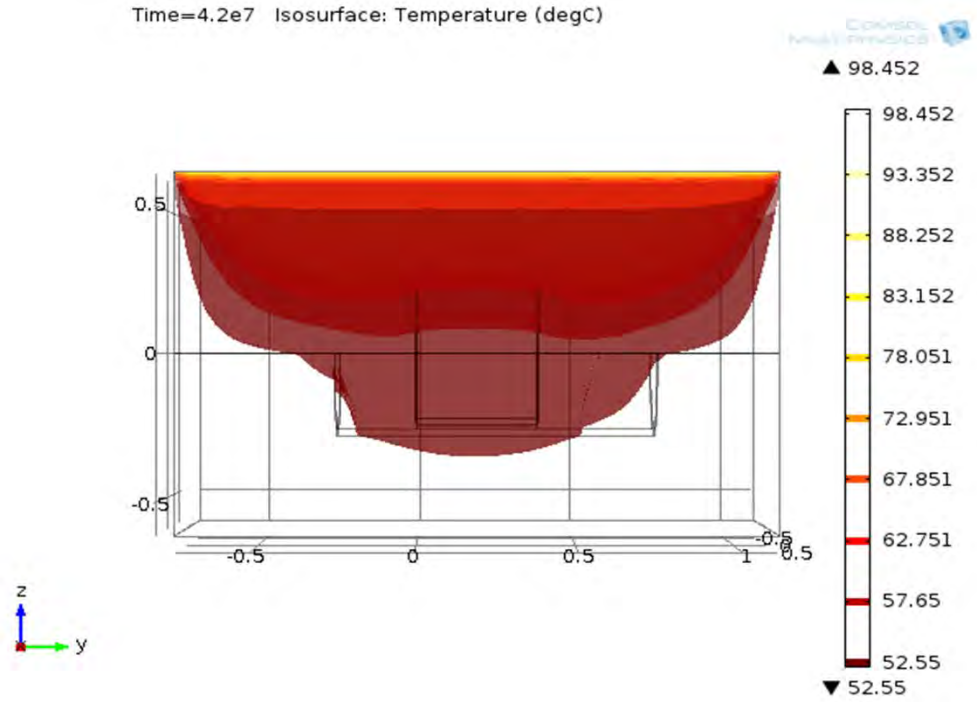
Time=4.2e7 Isosurface: Temperature (degC)
▲ 98.452
98.452
93.352
88.252
83.152
78.051
72.951
67.851
62.751
57.65
52.55
▼ 52.55
0.5
0
-0.5
-0.5
0
0.5
1
-0.5
0.5
z
y

1/8 inch paste thickness
1 inch cradle thickness
3X Uranium rate: is stable

went to lower paste thickness because 1/4th inch case was not stable in case 7 with 3X Uranium rate and 1 inch cradle thickness

This simulation proved to be unstable with .67 W/mK paste conductivity

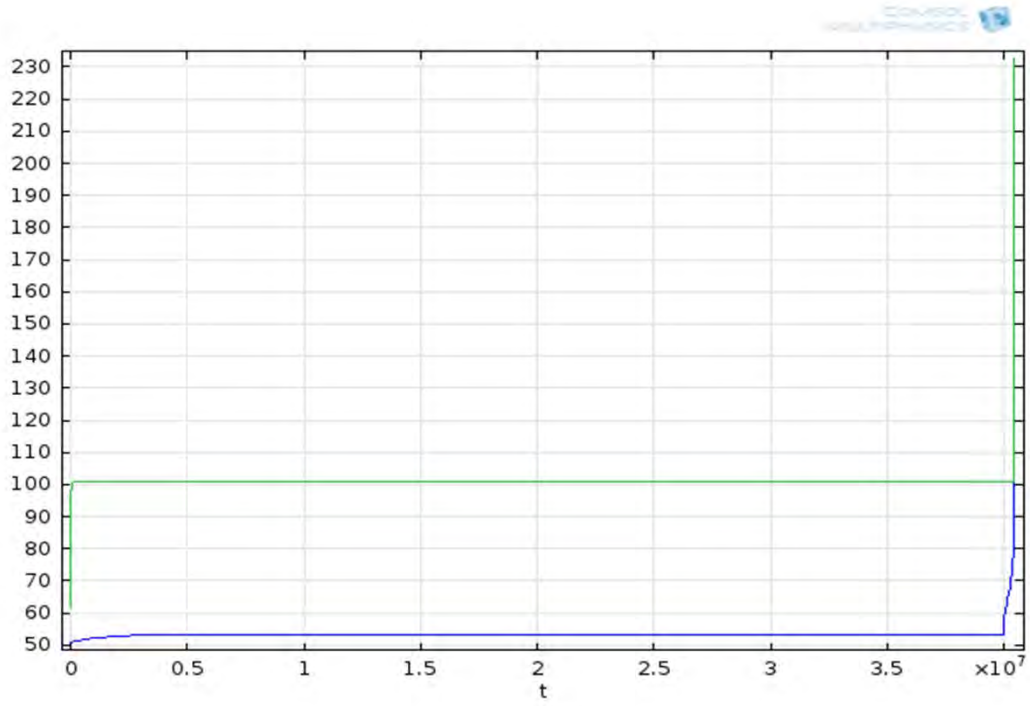

changing the paste conductivity to 2 W/mK causes a stable solution

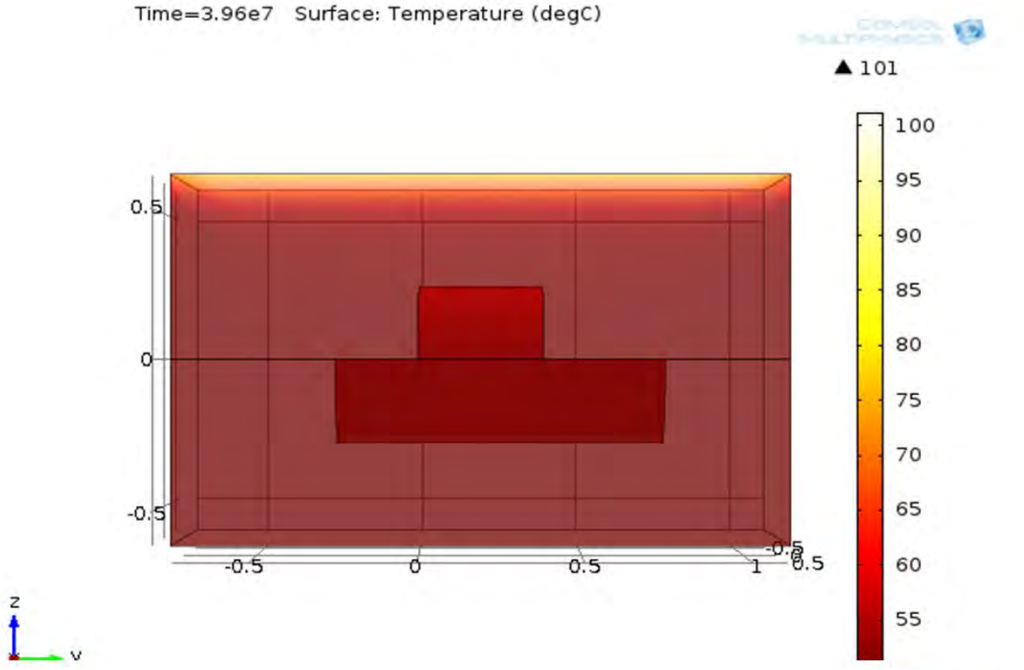

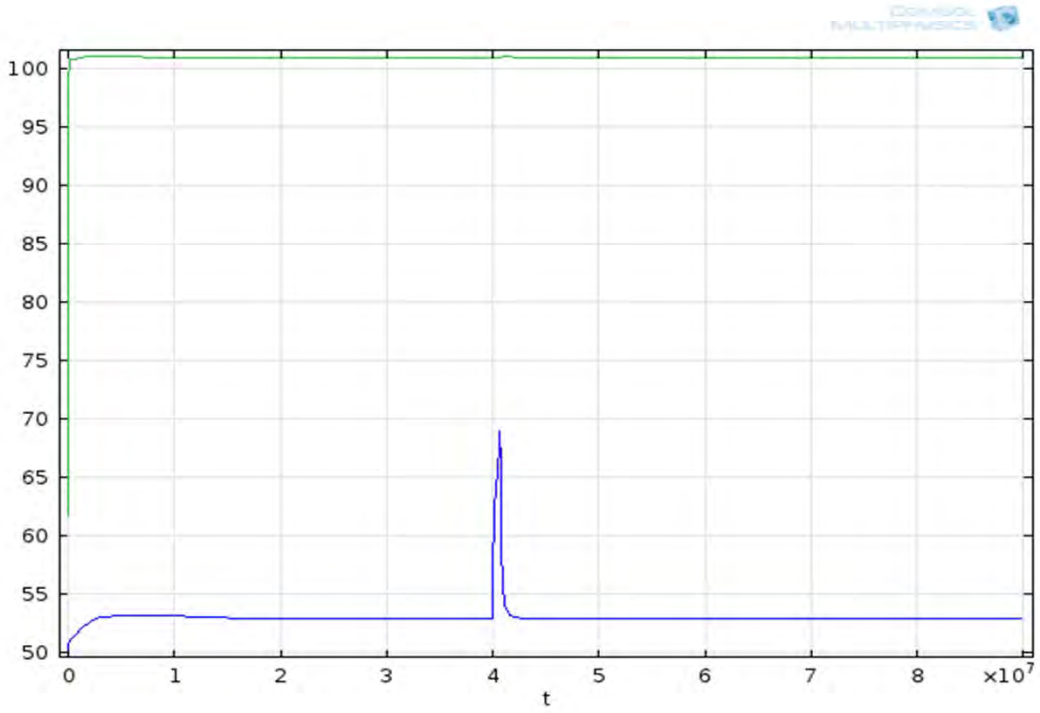

changing the paste conductivity to 1 W/mK also causes a stable solution

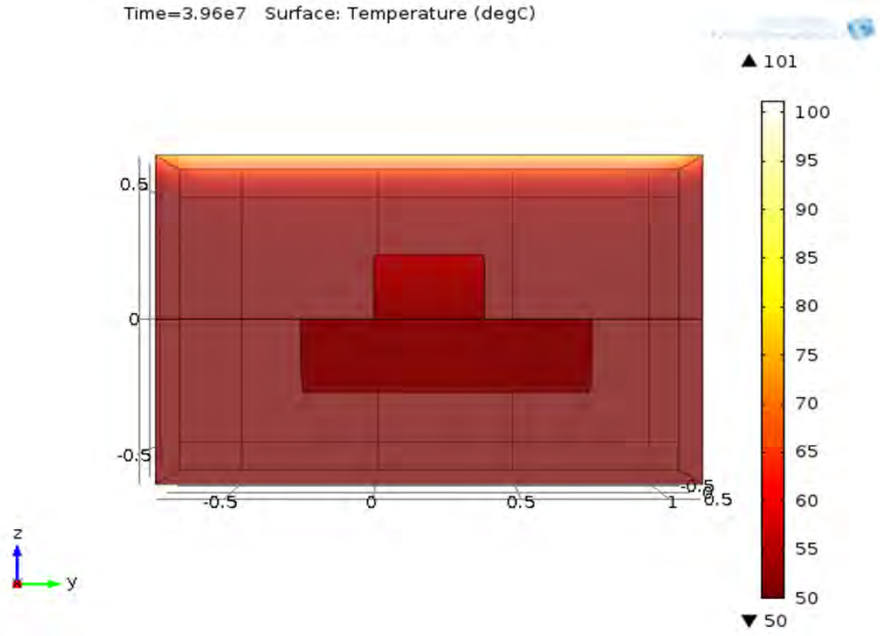

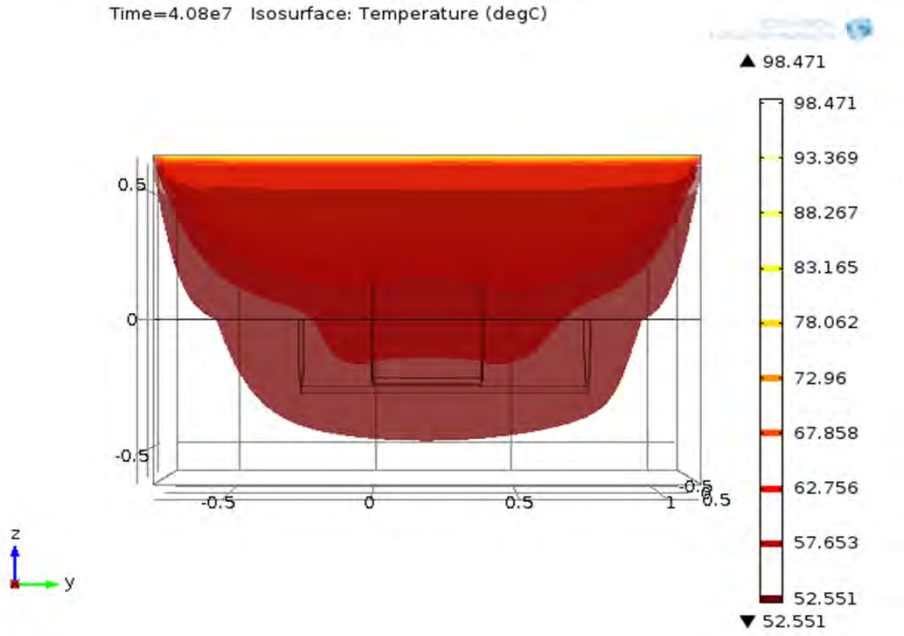

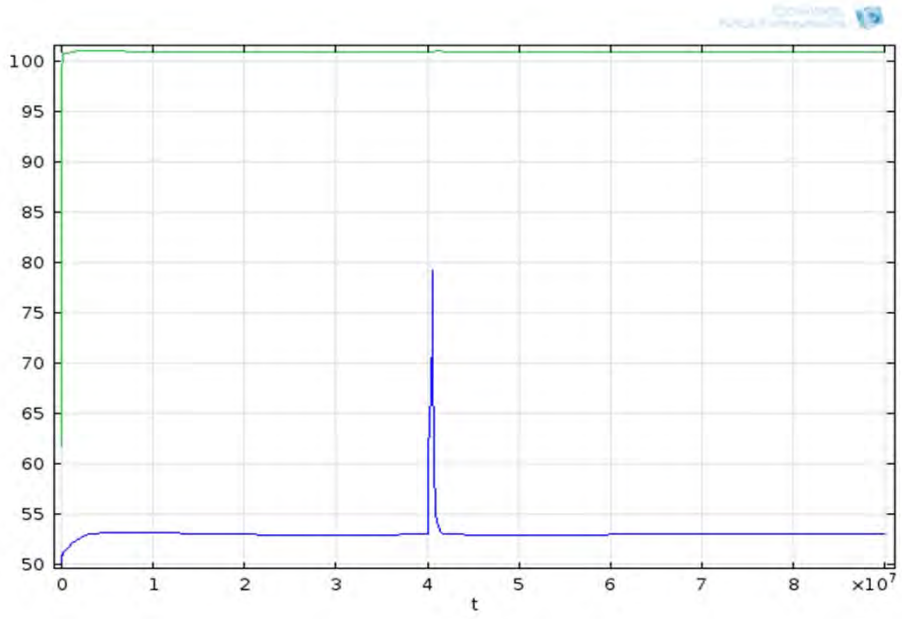
100
95
90
85
80
75
70
65
60
55
50
0
1
2
3
4
5
6
7
8
×10^7
t

Parameters

Name	Expression	Description
radius	0.254	m
wall	6.35E-03	m
depth	0.0223	m
Twall	273.15 + 5(	K
ksludge	3.9	[W/(m*K)]
rhosludge	9.60E+03	[kg/m^3]
Cpsludge	290	[J/(kg*K)]
kwall	16.2	[W/(m*K)]
rhowall	8.03E+03	[kg/m^3]
Cpwall	5.00E+02	[J/(kg*K)]
kgrout	0.5	[W/(m*K)]
rhogrout	1.72E+03	[kg/m^3]
Cpgrout	1165	[J/(kg*K)]
tubeLength	0.381	m
BoxWidth	1.219	m
BoxDepth	1.219	m
BoxHeight	1.829	m
ksand	0.5 - .36	[W/(m*K)]
rhosand	1.90E+03	[kg/m^3]
Cpsand	1400	[J/(kg*K)]
qsun	990.541	W/m^2
Tex	Twall[K]	
heattransfe	7.9[W/(m^	W/m^2K
heat	2.16E+06	J/kg maximum heat generated by uranium
kshot	30	[W/(m*K)]
rhoshot	rhowall	[kg/m^3]
Cpshot	Cpwall	[J/(kg*K)]
Gap	6.35E-03	m
kpaste	0.67	[W/(m*K)]
rhopaste	2100	[kg/m^3]
Cppaste	1000	[J/(kg*K)]
subtract	-0.1	
tubethick	.102/2	
tubedist	1.219 - .219	
kpHighTCg	1	[W/(m*K)]
rhoHighTC	2.62E+03	[kg/m^3]
CpHighTCg	Cpgrout	[J/(kg*K)]
emis	0.84	picked and emisivity of 0.84

picked a lowish heat transfer coefficent (see heattransfercoefficent parameter)
http://www.engineeringtoolbox.com/overall-heat-transfer-coefficients-d_284.html
heat transfer coefficients are generally between 10 to 100 W/m^2*K for air to metal
http://www.engineeringtoolbox.com/overall-heat-transfer-coefficient-d_434.html

Case 9
file: K basin time dependent4 with convective cooling.mph
file: K basin time dependent4 with convective cooling.docx

	Stability Limit Temperature			
	r=f(Temp)	r=f(Temp)	r=3*f(Temp)	r=3*f(Temp)
U Thermal Conductivity	Baseline U depth	2X Baseline U depth	2X Baseline U depth	Baseline U depth
3.9	55	43	25	39
1.8	54	41	23	38
0.5	53	39	20	36
0.3	52	37	18	35

heattransfercoefficent = 7.9 [W/m^2*K]
Basline U depth is 2.23 cm

Convective boundary with ambiant temperatures at 25 C

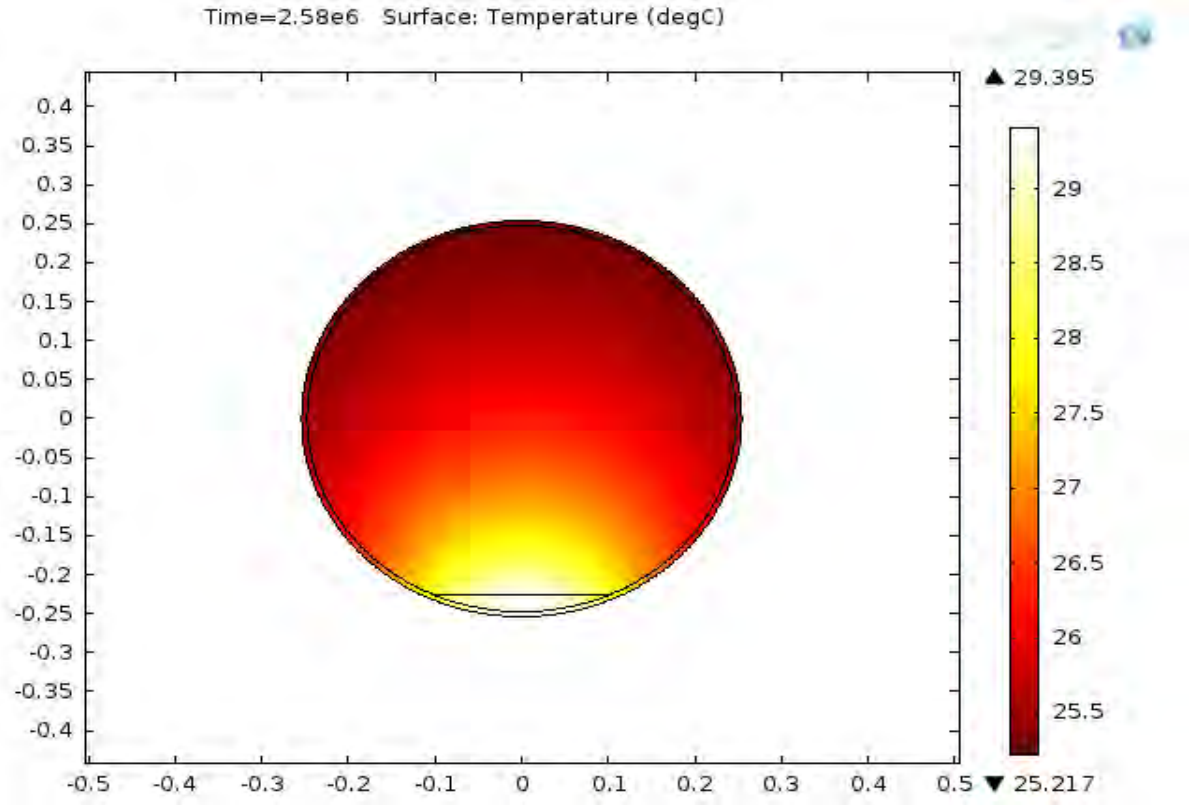

heating rate equation

q(T)= (10^(9.9752-3565.8/T))*(65*2156.3/3600)*1000

qtotal = q(T)+.9E3 W/m^3

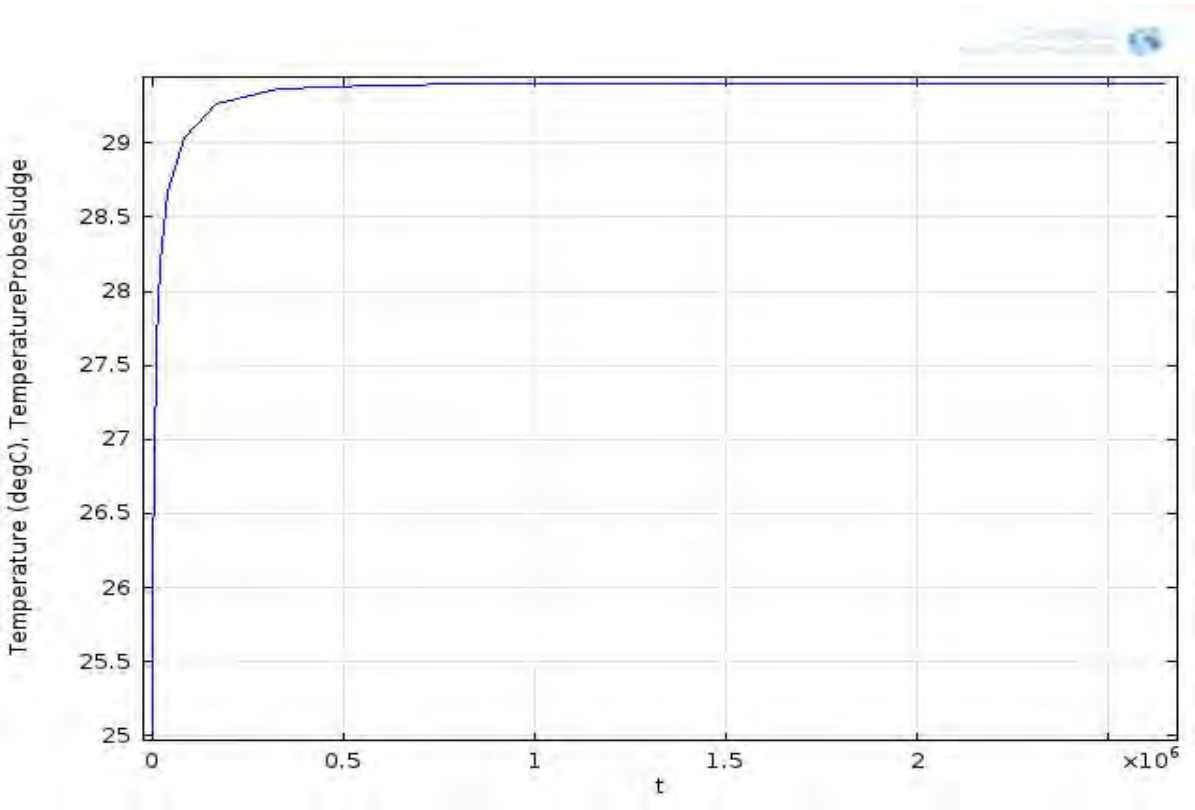

	Stability Limit Temperature			
	r=f(Temp)	r=f(Temp)	r=3*f(Temp)	r=3*f(Temp)
U Thermal Conductivity	Baseline U depth	2X Baseline U depth	2X Baseline U depth	Baseline U depth
3.9	46	33	12	29
1.8	46	32	11	29
0.5	45	31	9	28
0.3	45	30	8	27

heattransfercoefficent = 3 [W/m^2*K]

Case 10

file: K basin Box HeatSinkTube Grout in box solar long tube and cradle.mph

file: K basin Box HeatSinkTube Grout in box solar long tube and cradle.docx

cut off at 2.145E6 J/kg

1/4 inch paste thickness

1 inch cradle thickness

dry sand k =0.13 W/mK

paste k = 0.67 W/mK

1X Uranium rate: is stable

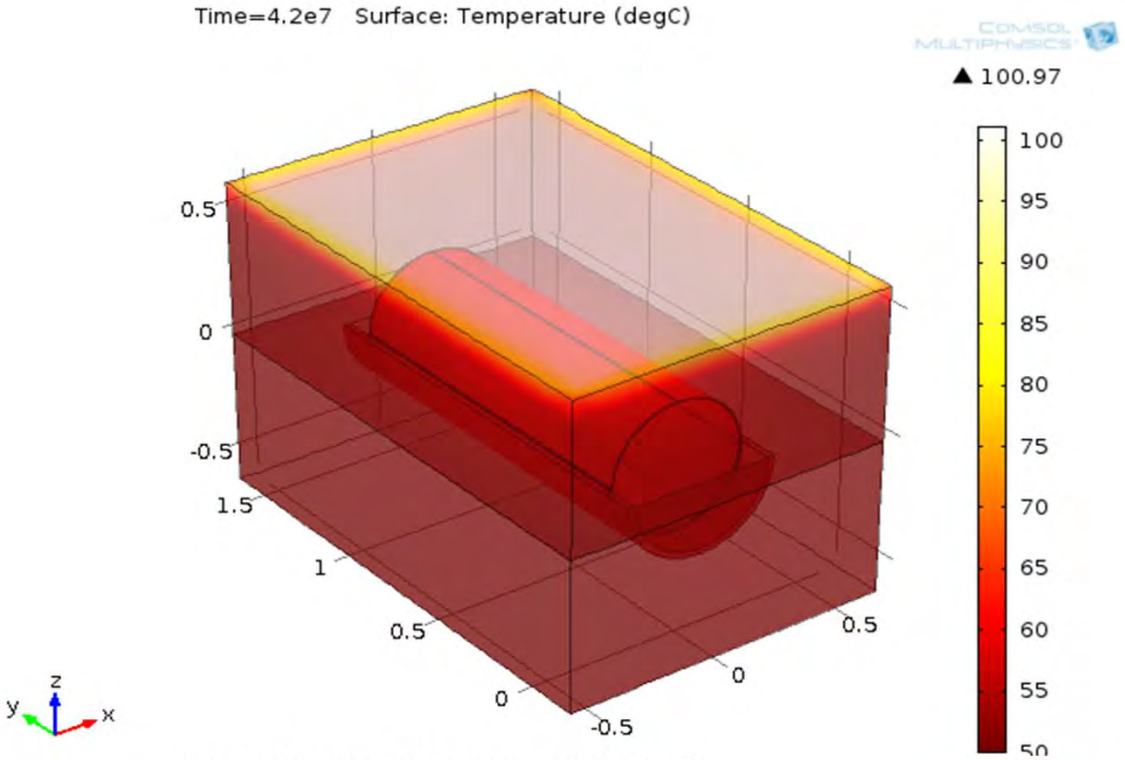

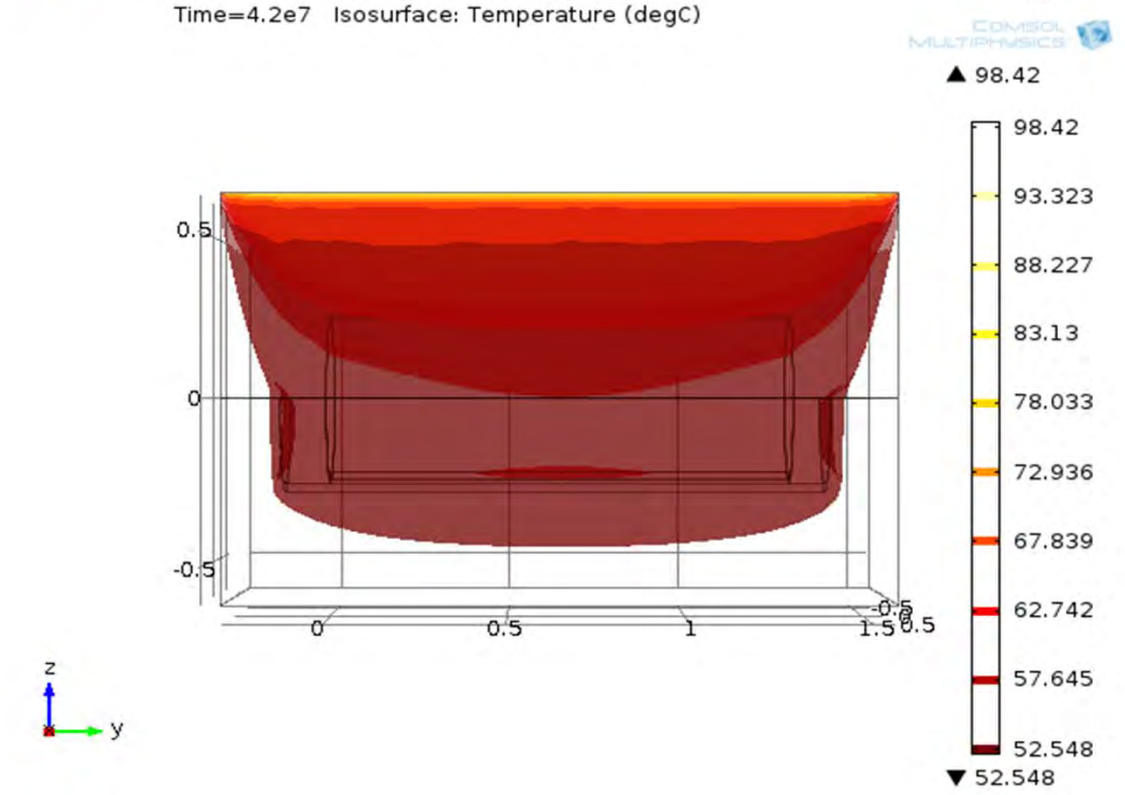

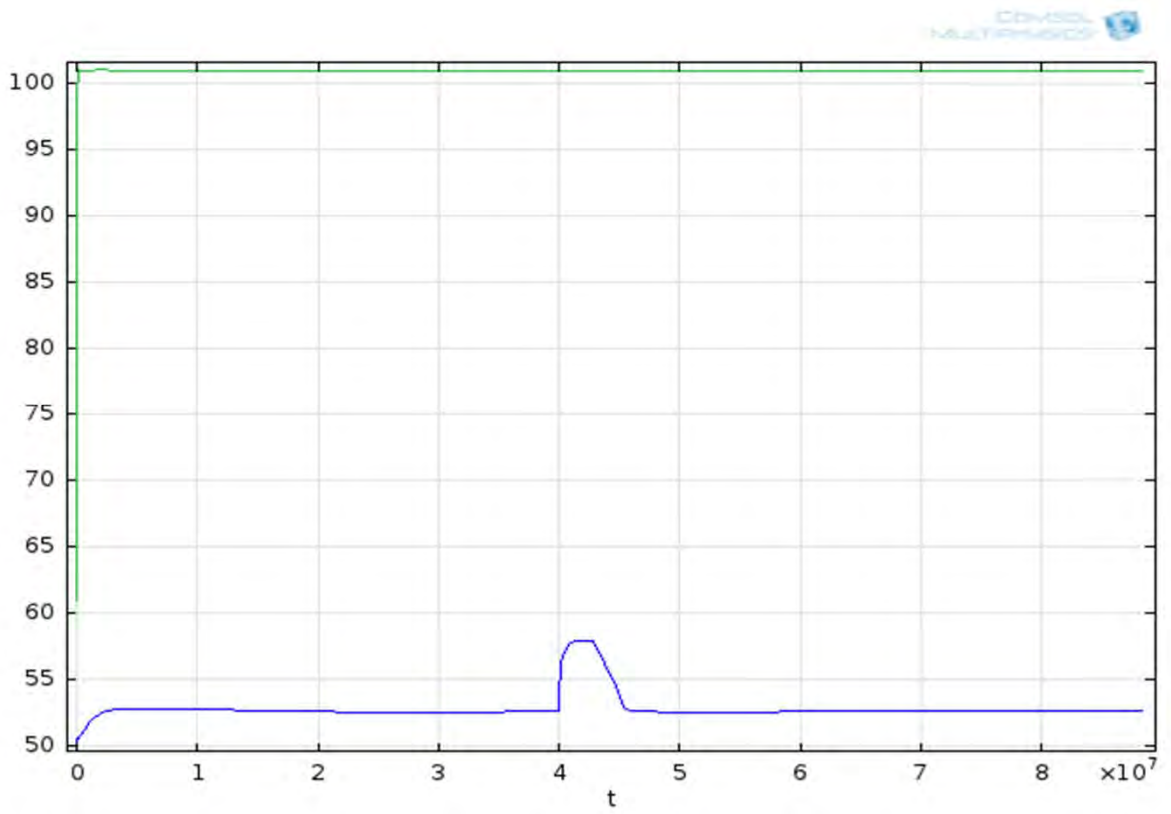
100
95
90
85
80
75
70
65
60
55
50
0
1
2
3
4
5
6
7
8
×10^7
t

cut off at 2.145E6 J/kg
1/4 inch paste thickness
2 inch cradle thickness

dry sand k =0.13 W/mK
paste k = 0.67 W/mK
3X Uranium rate: unstable

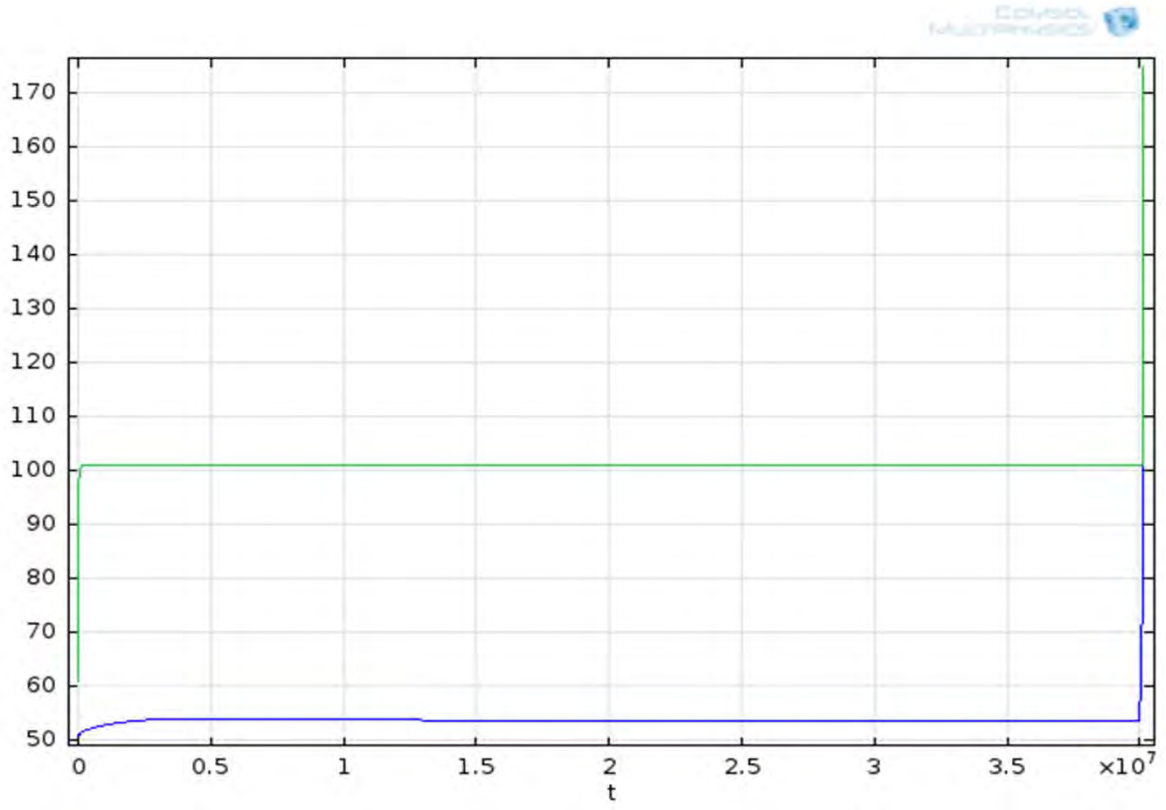

cut off at 2.145E6 J/kg
1/8 inch paste thickness
2 inch cradle thickness

dry sand k =0.13 W/mK
paste k = 0.67 W/mK
3X Uranium rate: unstable

cut off at 2.145E6 J/kg
1/8 inch paste thickness
2 inch cradle thickness

dry sand k =0.13 W/mK
paste k = 1 W/mK
3X Uranium rate: simulation crashed

cut off at 2.145E6 J/kg
1/8 inch paste thickness
2 inch cradle thickness

dry sand k =0.13 W/mK
paste k = 1.5 W/mK
3X Uranium rate: unstable

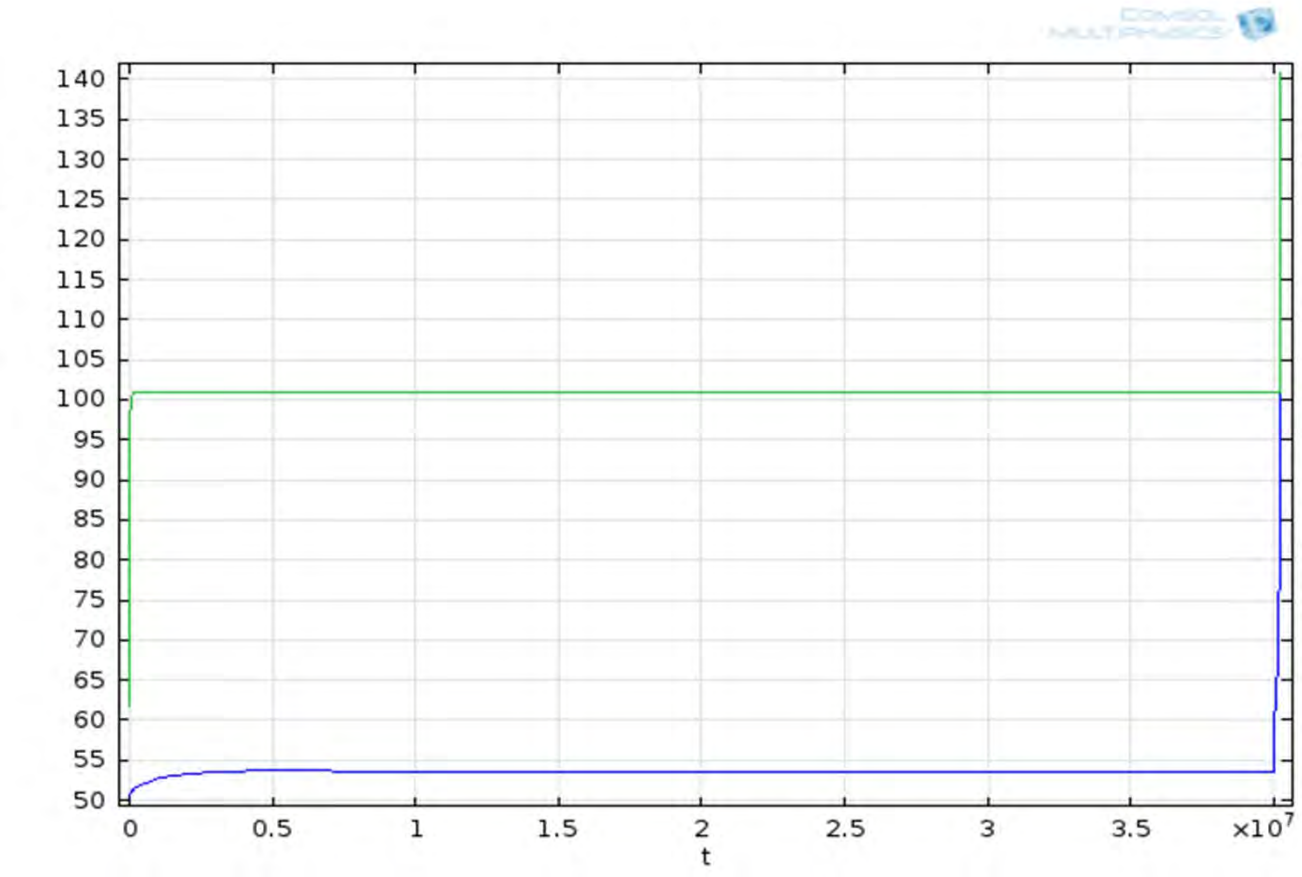

cut off at 2.145E6 J/kg	dry sand k =0.13 W/mK
1/8 inch paste thickness	paste k = 1 W/mK
4 inch cradle thickness	3X Uranium rate: simulation crashed

cut off at 2.145E6 J/kg	dry sand k =0.13 W/mK
1/8 inch paste thickness	paste k = 1.5 W/mK
4 inch cradle thickness	3X Uranium rate: simulation crashed

cut off at 2.145E6 J/kg
1/8 inch paste thickness
4 inch cradle thickness

dry sand k =0.13 W/mK
paste k = 0.67 W/mK
1X Uranium rate: is stable

Time=4.02e7 Surface: Temperature (degC)

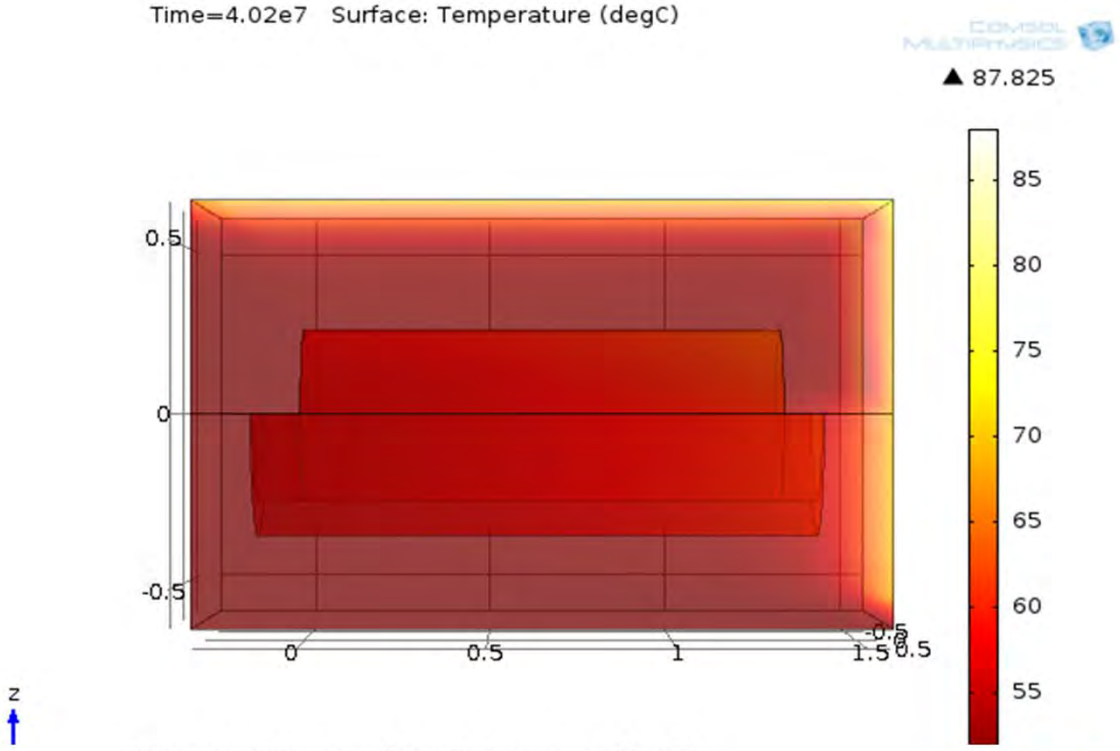

Time=4.02e7 Isosurface: Temperature (degC)

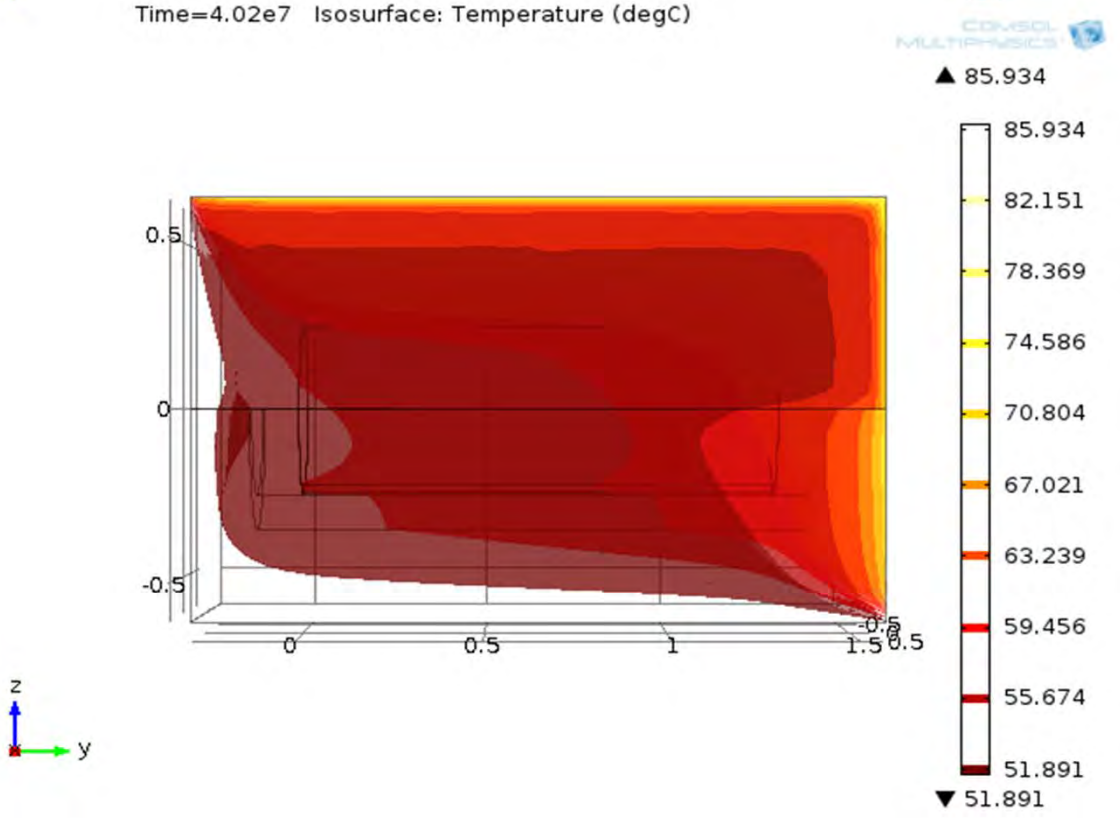

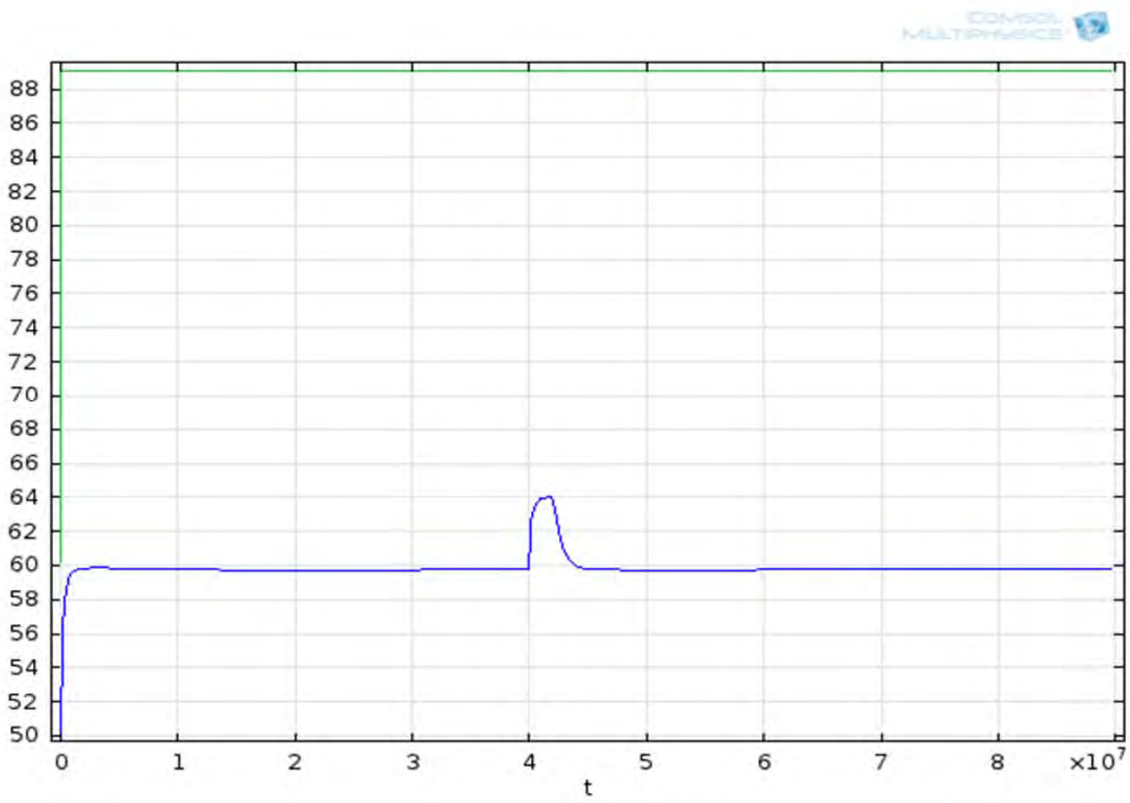
88
86
84
82
80
78
76
74
72
70
68
66
64
62
60
58
56
54
52
50
0
1
2
3
4
5
6
7
8
x10^7
t

-0.5 z direction

-0.5 y direction

cut off at 2.145E6 J/kg

1/4 inch paste thickness

1 inch cradle thickness

dry sand k =0.13 W/mK

paste k = 0.67 W/mK

1X Uranium rate: is stable

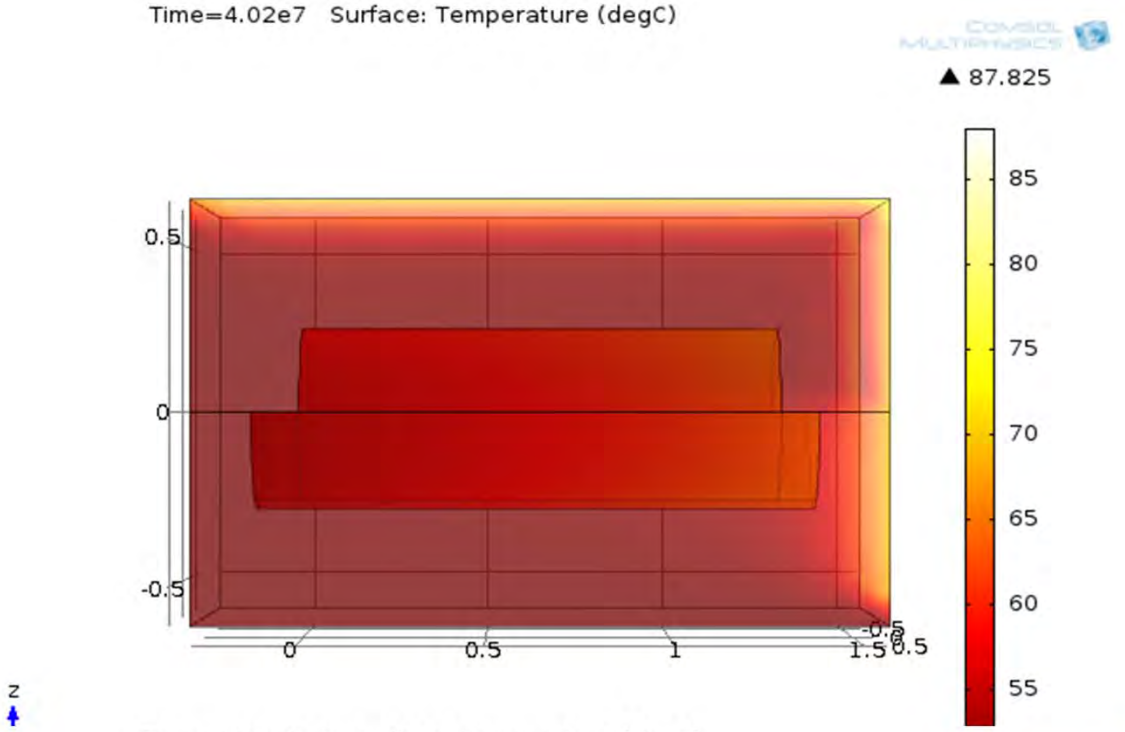

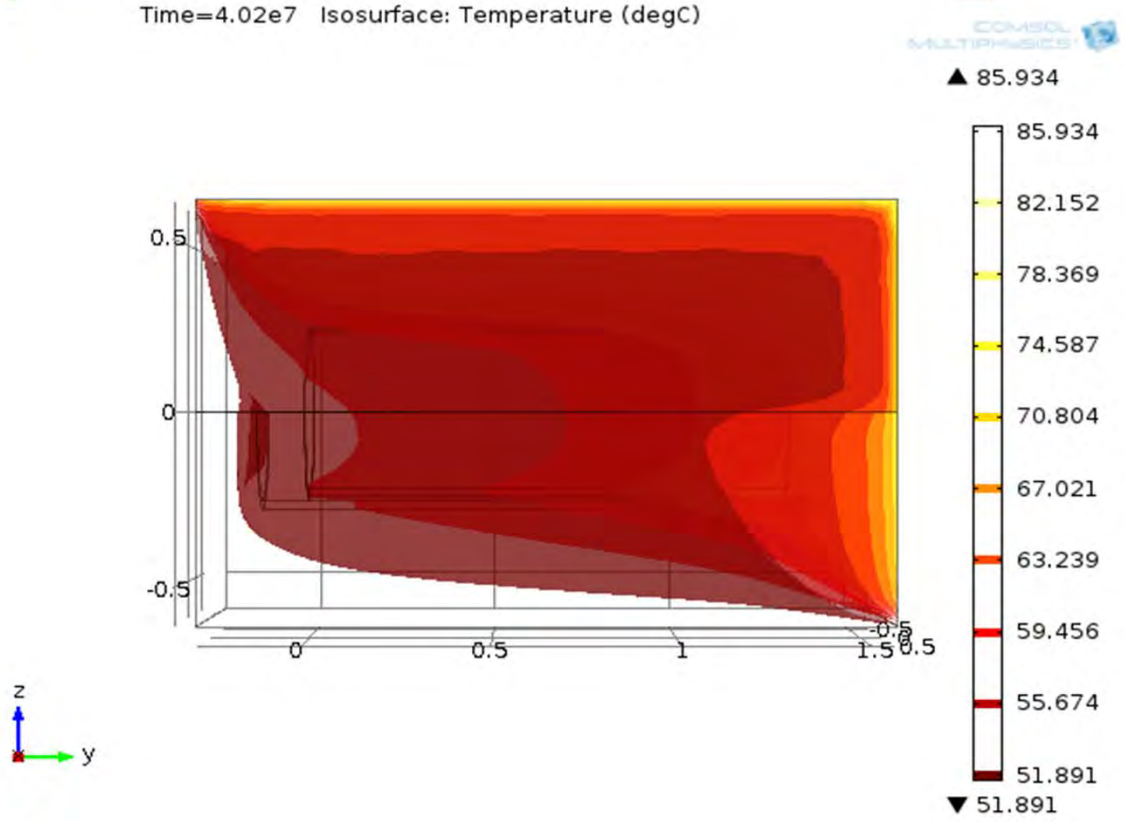

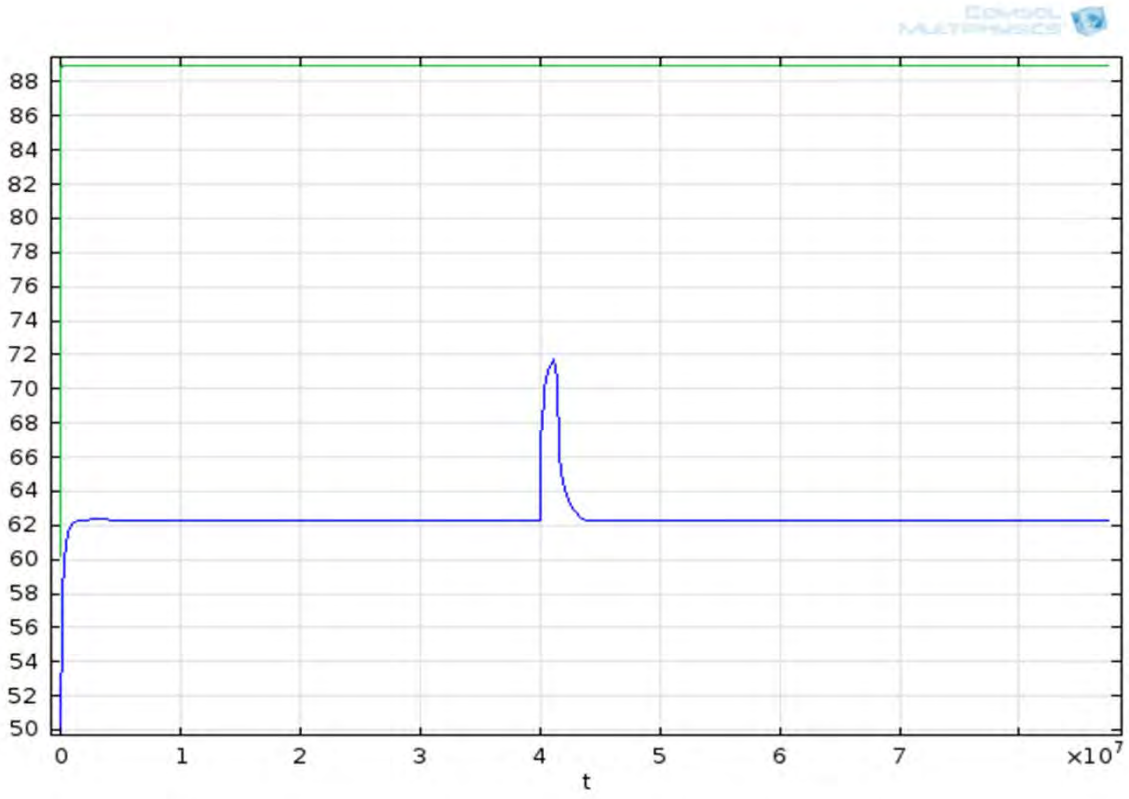
88
86
84
82
80
78
76
74
72
70
68
66
64
62
60
58
56
54
52
50
0
1
2
3
4
5
6
7
×10^7
t

-1 z direction

-0.5 y direction

cut off at 2.145E6 J/kg

1/4 inch paste thickness

1 inch cradle thickness

dry sand k =0.13 W/mK

paste k = 0.67 W/mK

1X Uranium rate: is stable

Time=4.02e7 Surface: Temperature (degC)

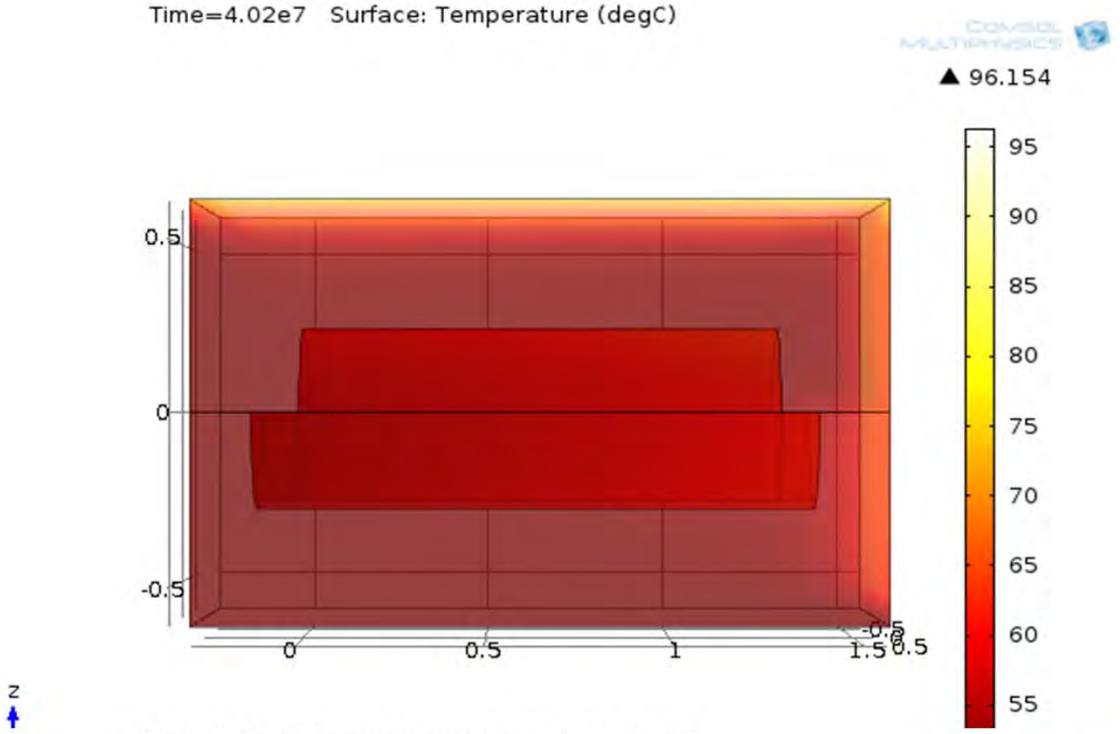

Time=4.02e7 Isosurface: Temperature (degC)

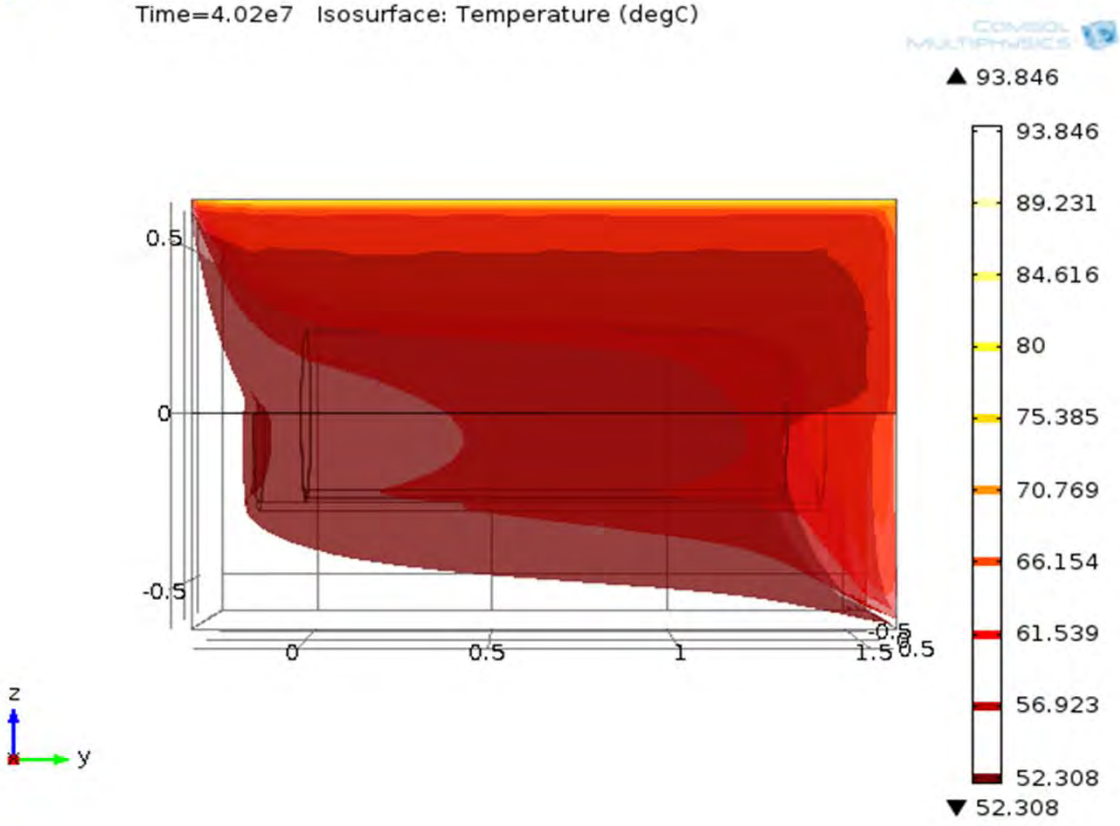

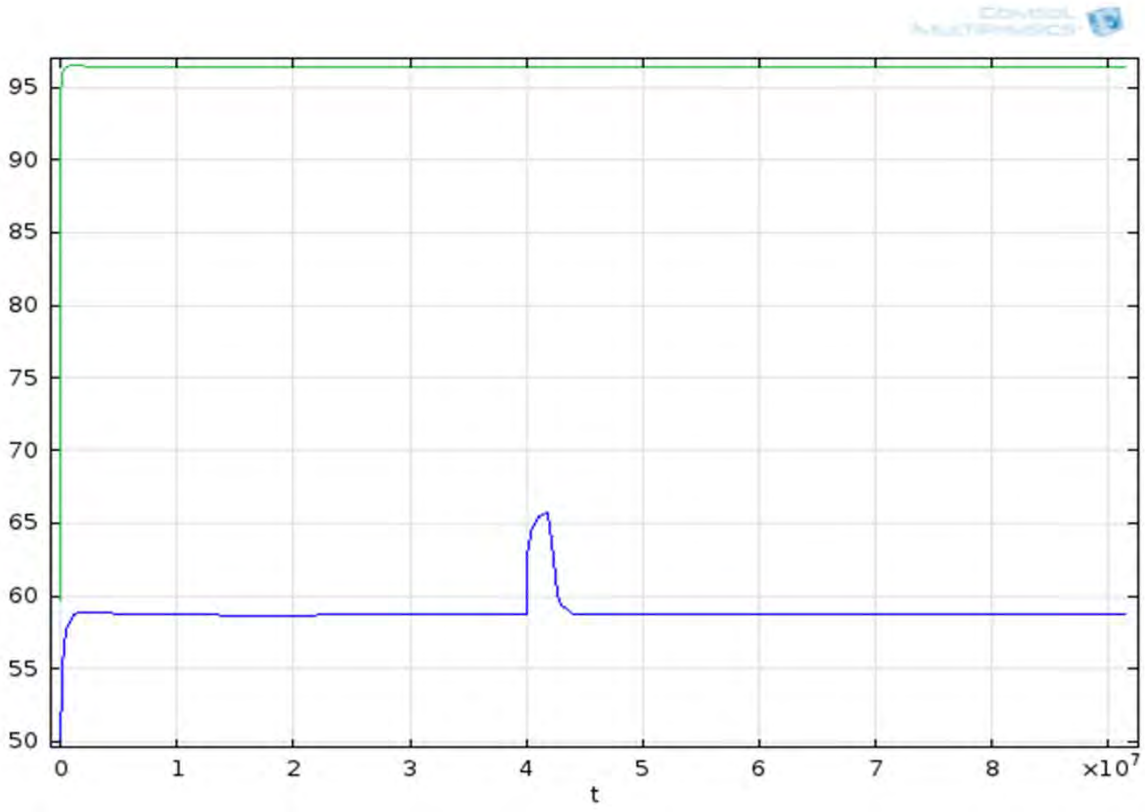
95
90
85
80
75
70
65
60
55
50
0
1
2
3
4
5
6
7
8
x10^7
t

Appendix B

Report Review Documentation

Appendix B

Report Review Documentation

1	Software Quality Assurance Plan for Uses of Console
2	Technical Review of COMSOL Modeling – Paul Humble
3	Technical Review of Report and Spreadsheets – Sergey Sinkov
4	Technical Review of Parameter Selection – Calvin H. Delegard

Software Quality Assurance Plan for Use of COMSOL Multiphysics in Project 64078

Revision History

Rev. #	Effective Date	Description of Change
0	March 25, 2015	Initial release.

Approvals

Name and Title	Approval Signature	Date
David E. Stephenson, Analyst	David Stephenson	3/23/15
Andrew J. Schmidt, Project Manager	Andrew J. Schmidt	3/23/15
William C. Dey, Project Quality Engineer	William C. Dey	3/24/15
Kary M. Cook, Software Subject Matter Expert		3/24/15
Steve N. Schlahta, Project Management Office Director, Nuclear Science and Legacy Waste	Steve Schlahta	3/25/15

1 Software Quality Assurance Plan for Use of COMSOL Multiphysics in Project 64078

This section documents the rigor determination for PNNL software quality assurance (SQA) requirements, per the HDI Use or Develop Software workflow. The purpose is to provide adequate confidence that a software process has been identified and that the use, modification, and/or development of software will meet established requirements, as applicable.

Table 1 - Software Risk & Classification Determination

Software Risk & Classification Determination			
EPR Software Risk Source (rating): High/Medium/Low: Medium – Project 64078			
Completed By:	Schmidt, Andrew J	**Date:**	01/26/2015
Section 1: Software Activity			
Select your software work activity, per the HDI Use or Develop Software workflow (Check all that apply): ☒ Use or Develop Software for Analysis (EPR Software Risk: MEDIUM) ☐ Develop Software for Delivery (EPR Software Risk: MEDIUM) ☐ Develop Prototype (EPR Software Risk: LOW)			
Section 2: Safety Software Determination			
☒ *Not* Safety Software (go to Section 3) ☐ Safety Software (per DOE Order 414.1D) (EPR Software Risk: HIGH): *For Safety Software, the following is required:* **Grade**: ☐ A ☐ B ☐ C **Category**: ☐ Safety System Software ☐ Hazard Analysis and Design Software ☐ Management and Administrative Controls Software **SQP Name**: (last name, first name, middle initial) *A Software Quality Practitioner (SQP-H) is required* (go to Section 4)			
Section 3: High Assurance (non-Safety) Software Determination			
☒ *Not* High Assurance Software ☐ High Assurance Software (EPR Software Risk: HIGH): **SQP Name**: (last name, first name, middle initial) *A Software Quality Practitioner (SQP-H) is required*			
Section 4: Software Description The following software will be used/modified/developed on this project:			

Software Name	Version	Description and Intended Use	Software Use or Development?
COMSOL Multiphysics	4.3b	**Description:** COMSOL Multiphysics is a finite element analysis, solver, and simulation software / finite	Use

		element analysis (FEA) software package for various physics and engineering applications, especially coupled phenomena, or multiphysics. The software is cross-platform (Windows, Mac, Linux). In addition to conventional physics-based user interfaces, COMSOL Multiphysics also allows for entering coupled systems of partial differential equations (PDEs). The PDEs can be entered directly or using the so-called weak form. In this case, heat transport equations came from the heat transfer module, which has preprogramed boundary and transport equations. **Intended use of software/analysis/results**: Model various scenarios in the solidification and subsequent handling of the KW Basin settler tube material to investigate thermal stability. From the client ME Johnson, Senior Technical Adviser (CHPRC), (1/19/2015): *I believe the COMSOL model will be used for "Key input to decision making (qualitative)" and for Waste Management. The model output is not being used for Nuclear Safety decisions which have been addressed through separate analyses.*	
COMSOL Heat Transfer Module	5	Version includes the full heat transfer module which among other things, allow efficient handling of heat transfer via convection and radiation. **Intended Use**: Same as above, but allowing for greater complexity of heat transfer modeling.	Use

1.1 Use or Develop Software for Analysis

The table below specifies how software quality requirements will be met:

Table 2 - Use or Develop Software for Analysis; Software Quality Requirements

Planning ***HDI Activities: Evaluate and Plan for Development of Software; Collaborate on Planning the Use or Development of Software***
Describe if software needs to be acquired and/or developed for the analysis. Response: Licensed COMSOL software is available at PNNL; procurement was not required.
Software Features/Functions ***HDI Activity: Implement Project: Use or Develop Software for Analysis***
Document what the software is supposed to do and how well it's supposed to do it (features/functions. Don't describe the intended use as described above in Table 1). For our application, a model is set up to represent the geometry of the scenario being investigated. Boundary conditions are set by the user. Thermal properties are set by the user (density, thermal conductivity, heat capacity). Heat generation sources, exothermic reactions, and radioactivity decay heats are input into the model. The model is then used to determine temperature of the system as a function of time and location. To compensate for uncertainties in how well thermal properties are known, bounding conditions for the properties and heat sources are evaluated during modeling. The goal is to understand conditions that lead to a temperature greater than 100 °C in the uranium sludge layer. If 100 °C is reached, the configuration is considered thermally unstable. The model must give reliable predictions within established bounding conditions (example: for uranium reaction rate, the bounding condition is 3× the nominal rate).
Control and Maintain Work (Configuration Management) ***HDI Activity: Implement Project: Use or Develop Software for Analysis***
Explain how you will control and version your items (evidence) such as tests, test plans, reports, publications, software versions (use and/or development) so that the work is reproducible and no one else can inadvertently make changes to your data, etc. • *How will you version or uniquely identify items?:* All work with COMSOL for this project is being performed by a single analyst (David E. Stephenson) on two workstations). Code version is specified as 4.3b and 4.3b with heat transport module. • *Documentation, to include data:* A complete model report that documents model definitions, geometry, heat transport equations, meshing, study configurations, and results will be preserved as a project QA record for each scenario evaluated. Input parameters for each series of cases evaluated will be preserved as a project QA record. • *Will you use any tools to control your items (e.g., will you use SharePoint, date/time stamp, CVS, or a controlled file share)?* Each complete model report will have time/date stamp.
Test / Verification

HDI Activities: Implement Project: Use or Develop Software for Analysis; Review Use or Development of Software for Analysis for Validation

Describe how you intend to verify your work (analysis). This may be verified by reviews (see Reviews section below); if so, state that here.

COMSOL Multiphysics provides "A Model Library Manual, Heat Transfer Module, 5.0 COMSOL". This library contains numerous solved benchmark COMSOL Cases. To verify correct functioning and installation of COMSOL, the analyst programmed and evaluated the case, "Heat Conduction in a Cylinder" (which was taken from a NAFEMS benchmark collection and shows an axisymmetric steady-state thermal analysis). Results: David Stephenson obtained a result of 332.957 K, which matches the results stated in the benchmark case of 332.957 K at the same location of r= 0.04 m and z = 0.04 m. David used 557 elements, which was slightly more than the 540 elements in the benchmark simulation. The 557 elements is the standard finer mesh in the 4.3b version used here, vs. the benchmark use of the 5.0 version. The test against the benchmark will be included in the project QA records.

The same bench mark was set up an executed on the second workstation. Results were exactly the same.

Reviews

HDI Activities: Implement Project: Use or Develop Software for Analysis; Review Use or Development of Software for Analysis for Validation; Disposition Results of the Review of Software Use or the Development for Analysis

Describe how you intend to review the analysis which is produced by the software (e.g., independent review, technical review, etc.).

Paul Humble, a senior analyst/engineer in the Thermal and Reaction System Group, who is also the lead of the PNNL COMSOL users group, will perform and document an independent technical review of the COMSOL modeling performed by David Stephenson.

Cal Delegard (Staff Scientist) and Andy Schmidt (Chief Engineer), both with more 10 years of experience on the K Basin Sludge Treatment Project, will provide independent technical review of input parameters to the model.

Signed independent technical review forms will be included in the project QA records.

Delivery of Results/Analysis
HDI Activity: Need to Deliver Information Product

Summary-level results of the COMSOL modeling will be delivered to the client in a formal PNNL report. This report will also describe the development of the model input parameters. The formal report will be reviewed by the client (CHPRC), the project QE (William Dey), independent peer review (Sergey Sinkov or Randle Scheele), and the PMOD (Steven Schlahta). The software quality assurance management plan, as documented here, will be reviewed by the PNNL Software Quantity Assurance Subject Matter Expert, Kary Cook.

Report Checklist for Project 53451 – RPT21 Rev 0.

Document Title: "Evaluation of Settler Tank Thermal Stability during Solidification and Disposition to ERDF" 53451-RPT-21 Rev 0.	Page 1 of 1

Independent Technical Reviewer: Paul Humble

Paul Humble — Signature

Mar 26, 2015 — Date

Scope of Review: COMSOL models used for 10 cases described in 53451-RPT-21 Rev 0; benchmark case "Heat Conduction in a Cylinder" used to verify correct functioning and installation of COMSOL; - and Sections 8.3 of 53451-RPT-21 Rev. 0. This section of report prepared by DE Stephenson and AJ Schmidt.

If correct: initial and date	Criteria
3/26/15 PH	Are the heat transfer models set up correctly, with appropriate equations and boundary conditions?
3/24/15 PH	Using the model parameters described in the report, are the report results reproducible?
3/26/15 PH	Are the model results consistent with the analysis and conclusions in the report?

Comments: My review included opening a copy of each finite element (COMSOL) model described in the report. I checked how each model was set up insuring that the heat transfer equations and boundary conditions were implemented as intended. I went through the parameters used in the heat transfer equations for the different material domains to make sure there were no transcription errors. I also examined the parameter values including the thermal conductivities and heat rates, by solving the model with the parameters used for select cases described in the report and comparing the solution to the reported results.

Figures 8.12 and 8.16, show some discontinuity in the slope of the temperature profile with time at longer times. This is a numerical artifact due to automatic time stepping procedure used by COMSOL. Using a shorter time step would remove these discontinuities in the maximum temperature profiles. However, these discrepancies do not impact the conclusions of the report.

Document Title: Evaluation of Settler Tank Thermal Stability during Solidification and Disposition to ERDF" 53451-RPT-21 Rev 0.

Scope of Review: Detailed review of Sections 1 – 7 of 53451-RPT-21 Rev. 0 and supporting excel calculations. High level review of Section 8.

Excel Workbook Titles: Grout Heat Rate Model; Portland Cement Setting Activation Energy; Settler Tank Sludge Volume.

Please: attach spreadsheet review for from the three workbooks.

Item	If correct, initial and date	Criteria
G1	SIS 03/30/2015	Reported results are traceable to and consistent with recorded data spreadsheets, literature?
G2	SIS 03/30/2015	Results from Test Instructions, LRBs, calculations, and other sources have been correctly transcribed.
G3	SIS 03/30/2015	Data from Test Instructions, LRBs, calculations, and other sources have been correctly transcribed.
G4	SIS 03/30/2015	Data reduction has been accomplished correctly.
G5	SIS 03/30/2015	Calculations are complete, and evidence is available that they have been checked.
G6	SIS 03/30/2015	Data are traceable to their origins and reported results.
G7	SIS 03/30/2015	The deliverable is consistent internally and with other reports.

Comments:

NO COMMENTS

Document Title: Evaluation of Settler Tank Thermal Stability during Solidification and Disposition to ERDF" 53451-RPT-21 Rev 0.

Technical: Inferences and Conclusions

Item	If correct, initial and date	Criteria
C1	SIS 03/30/2015	Inferences and conclusions are soundly based and are supported by the data in the report and references.
C2	SIS 03/30/2015	All activities are reported and if some activities were not performed, the omission is discussed.
C3	SIS 03/30/2015	The deliverable satisfies the project objectives.

Comments:

NO COMMENTS

Independent Technical Reviewer:

SERGEY SINKOV 03/30/2015

Printed Name and Signature Date

Calculation Review Sheet

Reviewer Name: Sergey Sinkov
Reviewer Title: Scientist
Review Date: 03/27/2015

Title of Spreadsheet Calculation Reviewed: Settler Tank Sludge Volume.xlsx
Revision Number: 0
Date Prepared: 3-Feb-2015

Scope of Spreadsheet Review: (Check one or more of the following)

- [√] General Validation Review: (General review & spot checks) For Tab "Depth Calc."
- [ ] Review of updated spreadsheet/calc (Revised portion only)
- [√] 100% Verification Review (Verification of all cells/calculations) For Tab "Depth from Dose Distr."
- [ ] Independent calculation check (With hand calcs or independent spreadsheet)
- [ ] Other:

CHECK LIST

Spreadsheet/Calculation Identification	**Yes**	**No**	**NA**
Spreadsheet/Calculation Title:	√		
Revision Number:	√		
Date Prepared	√		
Prepared by:	√		
General Statement of Purpose:	√		
General Description of Approach (note: specific approaches may be described for each section/subsection of spreadsheet/calculation)	√		

Comments:

Assumptions	**Yes**	**No**	**NA**
Are assumptions clearly stated?	√		
Are assumptions supported/justified?	√		
Are assumptions reasonable?	√		

Comments:

Input Values	**Yes**	**No**	**NA**
Are input parameters correct (verified with source?)	√		
Are parameter units consistent?	√		
Are input values properly referenced?	√		

Comments:

Equations/Approach	**Yes**	**No**	**NA**
Are equations adequately defined?	√		
Are equations properly referenced?	√		
Are limitations of approach/equations identified?	√		
Are equations appropriate?	√		
Are units consistent?	√		

Comments:

Results/Conclusions	**Yes**	**No**	**NA**
Are formulas consistent in spreadsheet cells?	√		
Are calculations correct?	√		
Are conclusions consistent with results?	√		
Are conclusions consistent with applicable limits?	√		

Comments:

Reviewer Sign/Date: Sergey Sinkov March 27, 2015

Calculation Review Sheet

Reviewer Name: Sergey Sinkov
Reviewer Title: Scientist
Review Date: 03/27/2015

Title of Spreadsheet Calculation Reviewed: Portland Cement Setting Activation Energy.xlsx
Revision Number: 0
Date Prepared: 3-Feb-2015

Scope of Spreadsheet Review: (Check one or more of the following)

	General Validation Review: (General review & spot checks)
	Review of updated spreadsheet/calc (Revised portion only)
√	100% Verification Review (Verification of all cells/calculations)
	Independent calculation check (With hand calcs or independent spreadsheet)
	Other:

CHECK LIST

Spreadsheet/Calculation Identification	**Yes**	**No**	**NA**
Spreadsheet/Calculation Title:	√		
Revision Number:	√		
Date Prepared	√		
Prepared by:	√		
General Statement of Purpose:	√		
General Description of Approach (note: specific approaches may be described for each section/subsection of spreadsheet/calculation)	√		

Comments:

Assumptions	**Yes**	**No**	**NA**
Are assumptions clearly stated?	√		
Are assumptions supported/justified?	√		
Are assumptions reasonable?	√		

Comments:

Input Values	**Yes**	**No**	**NA**
Are input parameters correct (verified with source?)	√		
Are parameter units consistent?	√		
Are input values properly referenced?	√		

Comments:

Equations/Approach	**Yes**	**No**	**NA**
Are equations adequately defined?	√		
Are equations properly referenced?	√		
Are limitations of approach/equations identified?	√		
Are equations appropriate?	√		
Are units consistent?	√		

Comments:

Results/Conclusions	**Yes**	**No**	**NA**
Are formulas consistent in spreadsheet cells?	√		
Are calculations correct?	√		
Are conclusions consistent with results?	√		
Are conclusions consistent with applicable limits?	√		

Comments:

Reviewer Sign/Date: Sergey Sinkov March 27, 2015

Calculation Review Sheet

Reviewer Name: Sergey Sinkov
Reviewer Title: Scientist
Review Date: 03/27/2015

Title of Spreadsheet Calculation Reviewed: Grout Heat Rate Model.xlsx
Revision Number: 0
Date Prepared: 3-Feb-2015

Scope of Spreadsheet Review: (Check one or more of the following)

- [V] General Validation Review: (General review & spot checks) For Tab "Model Enth. Check"
- [ ] Review of updated spreadsheet/calc (Revised portion only)
- [V] 100% Verification Review (Verification of all cells/calculations) For Tab "Hyd Enth Data and Model"
- [ ] Independent calculation check (With hand calcs or independent spreadsheet)
- [ ] Other:

CHECK LIST

Spreadsheet/Calculation Identification	**Yes**	**No**	**NA**
Spreadsheet/Calculation Title:	✓		
Revision Number:	✓		
Date Prepared	✓		
Prepared by:	✓		
General Statement of Purpose:	✓		
General Description of Approach (note: specific approaches may be described for each section/subsection of spreadsheet/calculation)	✓		

Comments:

Assumptions	**Yes**	**No**	**NA**
Are assumptions clearly stated?	✓		
Are assumptions supported/justified?	✓		
Are assumptions reasonable?	✓		

Comments:

Input Values	**Yes**	**No**	**NA**
Are input parameters correct (verified with source?)	✓		
Are parameter units consistent?	✓		
Are input values properly referenced?	✓		

Comments:

Equations/Approach	**Yes**	**No**	**NA**
Are equations adequately defined?	✓		
Are equations properly referenced?	✓		
Are limitations of approach/equations identified?	✓		
Are equations appropriate?	✓		
Are units consistent?	✓		

Comments:

Results/Conclusions	**Yes**	**No**	**NA**
Are formulas consistent in spreadsheet cells?	✓		
Are calculations correct?	✓		
Are conclusions consistent with results?	✓		
Are conclusions consistent with applicable limits?	✓		

Comments:

Reviewer Sign/Date: Sergey Sinkov March 27, 2015

Document Title: Evaluation of Settler Tank Thermal Stability during Solidification and Disposition to ERDF" 53451-RPT-21 Rev 0.

Scope of Review: Sections 8.1 and 8.2 of 53451-RPT-21 Rev. 0. This section of report prepared by AJ Schmidt.

Item	If correct, initial and date	Criteria
G1	CHD 26 March 2015	Reported results are traceable to and consistent with recorded data spreadsheets, literature?
G2	CHD 26 March 2015	Results from Test Instructions, LRBs, calculations, and other sources have been correctly transcribed.
G3	CHD 26 March 2015	Data from Test Instructions, LRBs, calculations, and other sources have been correctly transcribed.
G4	CHD 26 March 2015	Data reduction has been accomplished correctly.
G5	CHD 26 March 2015	Calculations are complete, and evidence is available that they have been checked.
G6	CHD 26 March 2015	Data are traceable to their origins and reported results.
G7	CHD 26 March 2015	The deliverable is consistent internally and with other reports.

Comments: The explanatory text following Table 8.5 is very CHD useful as it explains origins of ranges of values.

Document Title: Evaluation of Settler Tank Thermal Stability during Solidification and Disposition to ERDF" 53451-RPT-21 Rev 0.

Technical: Inferences and Conclusions

Item	If correct, initial and date	Criteria
C1	CAD 26 March 2015	Inferences and conclusions are soundly based and are supported by the data in the report and references.
C2	CAD 26 March 2015	All activities are reported and if some activities were not performed, the omission is discussed.
C3	CAD 26 March 2015	The deliverable satisfies the project objectives.

Comments:

Independent Technical Reviewer:

CAL DELEGARD — 26 March 2015

Printed Name and Signature — Date

Distribution

No. of Copies

12 **Pacific Northwest National Laboratory**
(Electronic Distribution)
CH Delegard
WC Dey
C Freeman
SK Fiskum
P Humble
RO Orth
AJ Schmidt
SN Schlahta
SI Sinkov
DE Stephenson
Information Release
Project Files

5 **CH2MHill Plataeau Remediation Company**
(**Electronic Distribution)**
GM Davis
ME Johnson
MW Johnson
UE Wajeeh
STP Project File (FE Wickstrand, MS R1-29)

Pacific Northwest
NATIONAL LABORATORY

Proudly Operated by **Battelle** *Since 1965*

U.S. DEPARTMENT OF
ENERGY

902 Battelle Boulevard
P.O. Box 999
Richland, WA 99352
1-888-375-PNNL (7665)

www.pnnl.gov